A Novel Peptide Hydrogel for an Antimicrobial Bandage Contact Lens

Thesis submitted in accordance with the requirements of the
University of Liverpool for the degree of
Doctor in Philosophy

By

Andrew Gerard Gallagher

October 2017

ABSTRACT

A Novel Peptide Hydrogel for an Antimicrobial Bandage Contact Lens by Andrew Gerard Gallagher

Introduction:

Corneal bandage lenses could have an important role to play in the treatment of corneal infection and disease. The application of bandage contact lenses for corneal ulcers are of interest as current treatment involves the topical administration of antibiotics, of which only 1 - 7% is absorbed to the site of infection. This inefficiency allows a lot of scope to improve the delivery of drugs to the surface of the eye. This study aimed to investigate the natural antimicrobial activity of a novel hydrogel as well as observing differences in activity when compounds such as additional poly-ε-lysine (pεK), penicillin G and amphotericin B were covalently or ionically coupled to the hydrogel. The ability to detect microbial keratitis pathogens was also investigated with the association of bacteria-identifying peptides to the hydrogel.

Methods:

Peptide hydrogels were synthesised from pεK cross-linked with octanedioic acid to densities of 0.067 - 0.1 g cm^{-3} and 45 - 80% cross-linking. The hydrogels were evaluated with a range of mechanical and physical tests. The hydrogels were also modified to bind additional pεK or the ionic association of penicillin G, amphotericin B or fluorescently labelled antimicrobial peptides. Hydrogel samples were incubated with *E. coli*, *S. aureus* or *C. albicans* and metabolic activity assays, plate counts and immunofluorescence techniques used to determine antimicrobial activity and the ability to identify microbes. Cytotoxicity of the hydrogels towards a human corneal epithelial cell line was monitored via a CCK-8 assay, scratch assay and antibody staining.

Results:

High water content (> 70%) hydrogels with comparable mechanical and physical properties to commercial contact lens materials were developed. A significant difference in antimicrobial activity was obtained by altering the surface properties of the hydrogel with either additional pεK or penicillin G compared to the LB agar control. Similar results for *E. coli* were observed. Hydrogels loaded with amphotericin B retained an antifungal activity against *C. albicans* under both normal conditions and in the presence of horse serum. The hydrogel demonstrated a drug release profile which was maintained above therapeutic levels for 72 h whilst amphotericin B stability was maintained for at least 48 h. The sorption of fluorescently labelled antimicrobial peptides to the hydrogel resulted in the successful labelling of both *S. aureus* and *E. coli* with no cytotoxicity towards HCE-T cells.

Conclusion:

Cross-linked pεK hydrogels with mechanical and physical properties comparable to commercial lens materials were developed. These alone were not antimicrobial towards *E. coli*, *S. aureus* or *C. albicans*, however, associating known antimicrobials with the free amine groups on the cross-linked hydrogel caused a significant antimicrobial effect. Furthermore, the association of fluorescently labelled antimicrobial peptides enabled the hydrogel to label bacteria. These modified hydrogels could have a role as bandage contact lenses in the diagnosis and treatment of corneal ulcers.

CONTENTS

ACKNOWLEDGEMENTS

This work was funded by SpheriTech Ltd.

Firstly, I would like to thank my academic supervisors Professor Rachel Williams and Professor Ahmed Elsheikh for their continued support and direction over the last four years. Rachel, for your wide-ranging knowledge of biomaterials and their potential application within ophthalmology, your mentorship and for continuously challenging me to reach my potential.

A special thanks to Dr Mal Horsburgh, Dr Heather Allison, Dr Jamal Alorabi and Mr Paul Loughnane for their expertise and guidance through the antimicrobial analysis of the materials developed during this thesis.

I would like to thank my colleagues at SpheriTech Ltd. for their continued support, guidance and friendship since I started there in January 2012. Dr Don Wellings as my industrial supervisor has played a pivotal role in mentoring me. Mr Ian Thomas and Mr Dean Simpkin for helping me to develop peptide, polymer and analytical chemistry skills with their expertise.

Thanks also to all my colleagues within the Department of Eye and Vision Science (IACD) at the University of Liverpool for their support, advice and friendship. Special thanks to Drs Victoria Kearns, Stephnie Kennedy, Atikah Haneef, Aruni Makuloluwa, Rebecca Lace and Keri McLean for their help and support with aspects of cell biology, microscopy, porcine eye dissection, antifungal activity and assistance in the use of the Linkam tensile tester and DSA 10 equipment.

I also gratefully acknowledge the love, encouragement and support from my wife Laura and our two children, Andrew and Caoimhe throughout the highs and lows of the last four years. My sisters Lucinda and Shaunagh for continually testing my explanatory skills and providing encouragement throughout. Finally, but by no means least I would like to thank my parents Gerard and Jacinta to whom I am extremely grateful. Without their love, support and belief in me, this thesis would not have been possible.

Go raibh míle maith agaibh gach duine! Tá mé an-bhuíoch.

LIST OF ABBREVIATIONS AND SYMBOLS

AMP - Antimicrobial peptide

AmpB - Amphotericin B

APMA - N-(3-Aminopropyl) methacrylamide

Boc-Lys(Fmoc)-OH - N-α-t-Butyloxycarbonyl-N-ε-(9-fluorenylmethyloxycarbonyl)-L-lysine

BSA - Bovine serum albumin

CCK-8 - Cell counting kit-8

DAPI - 4',6-Diamidino-2-phenylindole

DIC - N,N-Diisopropylcarbodiimide

Dk - Oxygen permeability

DMA - N,N-Dimethylacrylamide

DMAP - N,N-Dimethylaminopyridine

DMEM/F12 - Dulbecco's Modified Eagle's Medium / Ham's F12

DMF - N,N-Dimethyl formamide

DMSO - Dimethyl sulfoxide

EDCI - 1-Ethyl-3-(3-dimethylaminopropyl) carbodiimide

EMA - Ethyl methacrylate

EWC - Equilibrium water content

FCS - Fetal calf serum

FDA - Food and Drug Administration

FITC - Fluorescein isothiocyanate

Fmoc - Fluorenylmethyloxycarbonyl

GMA - Glycidyl methacrylate

GRAS - Generally regarded as safe

GUK - Guanylate kinase domain

HCE-T - Human corneal epithelial cell line

HMPA - 4-(Hydroxmethyl) phenoxyacetic acid

HOBt - 1-Hydroxybenzotriazole

HPLC - High Performance Liquid Chromatography

IL - Interleukin

ISO - International Organisation for Standardisation

LB - Luria-Bertani

LPS - Lipopolysaccharide

MAA - Methacrylic acid

MMA - Methyl methacrylate

MMP - Matrix metalloproteinase

MIC - Minimum inhibitory concentration

MIC_{90} - Lowest MIC to kill 90% of an organism

MRC - Medical research council

$NaClO_4 \cdot H_2O$ - Sodium perchlorate

NaH_2PO_4 - Sodium dihydrogen phosphate

NBD - Nitrobenzodiazole

NHS - N-Hydroxysuccinimide

NMM - N-Methylmorpholine

NVP - N-Vinyl pyrollidone

PBS - Phosphate buffered saline

PC - 2-Methacryloxyethyl phosphorylcholine

PCR - Polymerase chain reaction

PD - Potato dextrose

PI - Propidium iodide

pαK - Poly-α-lysine

pεK - Poly-ε-lysine

PFA - Perfluoroalkoxy

PLGA - Poly-(lactic-*co*-glycolic acid)

pHEMA - Poly-(2-hydroxyethylmethacrylate)

pMMA - Poly-(methylmethacrylate)

PTFE - Poly-(tetrafluoroethylene)

PVA - Poly-(vinylalcohol)

PVC - Poly-(vinylchloride)

PVP - Poly-(vinylpyrrolidone)

QC - Quality control

RP-HPLC - Reversed-phase high-performance liquid chromatography

SD - Standard deviation

SEM - Scanning electron microscope

SOP - Standard operating procedure

TC - Tissue culture

TFA - Trifluoroacetic acid

TFLL - Tear film lipid layer

TNF - Tumour necrosis factor

TPVC - 3-[Tris(trimethylsiloxy)silyl] propyl vinyl carbamate

TRIS - 3-[Tris(trimethylsiloxy)silyl] propyl methacrylate

TRITC - Tetramethylrhodamine isothiocyanate

UV - Ultraviolet

ZO-1 - Zonal occludens-1

LIST OF FIGURES

LIST OF TABLES

PUBLICATIONS FROM THE FOLLOWING THESIS

Published papers:

Gallagher, A. G., Alorabi, J. A., Wellings, D. A., Lace, R., Horsburgh, M. J. and Williams, R. L. (2016) 'A novel peptide hydrogel for an antimicrobial bandage contact lens', *Advanced Healthcare Materials*, 5(16), pp. 2013-2018.

Gallagher, A.G., McLean, K., Stewart, R.M.K., Wellings, D.A., Allison, H.E. and Williams, R.L. (2017) 'Development of a poly-ε-lysine contact lens as a drug delivery device for the treatment of fungal keratitis', *Investigative Ophthalmology and Visual Science*, 58(11), pp. 4499-4505.

Published abstracts:

Gallagher, A.G. (2015) 'A novel macroporous scaffold with potential applications in tissue engineering', *Journal of Tissue Science and Engineering,* 6(2), pp. 118.

Williams, R.L., Gallagher, A.G., Elsheikh, A. and Wellings, D.A. (2015) 'Design of peptide gels for bandage contact lenses', *Investigative Ophthalmology & Vision Sciences,* 56(7), pp. 6081.

Pending publications:

Gallagher, A.G., Wellings, D.A., Megia-Fernandez, A., Portal, C., Bradley, M. and Williams, R.L. 'The attachment of optical molecular sensing peptides to a hydrogel carrier to detect and Identify microbial keratitis'

1. INTRODUCTION

1.1 The Cornea

The cornea is a transparent, avascular tissue composed of five layers and situated in the anterior segment of the eye (Figure 1.1). It is responsible for the refraction of light necessary for vision. The smooth surface of the anterior cornea is the refractive surface of the eye and coupled with corneal transparency allows light to pass through to the lens and onto the retina for photoreceptor activation (Gheorghe *et al.*, 2016). The cornea is the part of the eye most exposed to injury from external risk factors but is surrounded by a trilayer coating called the tear film that acts as a protective mechanism. The cornea, in turn, provides a protective barrier against disease and trauma to the rest of the eye tissue.

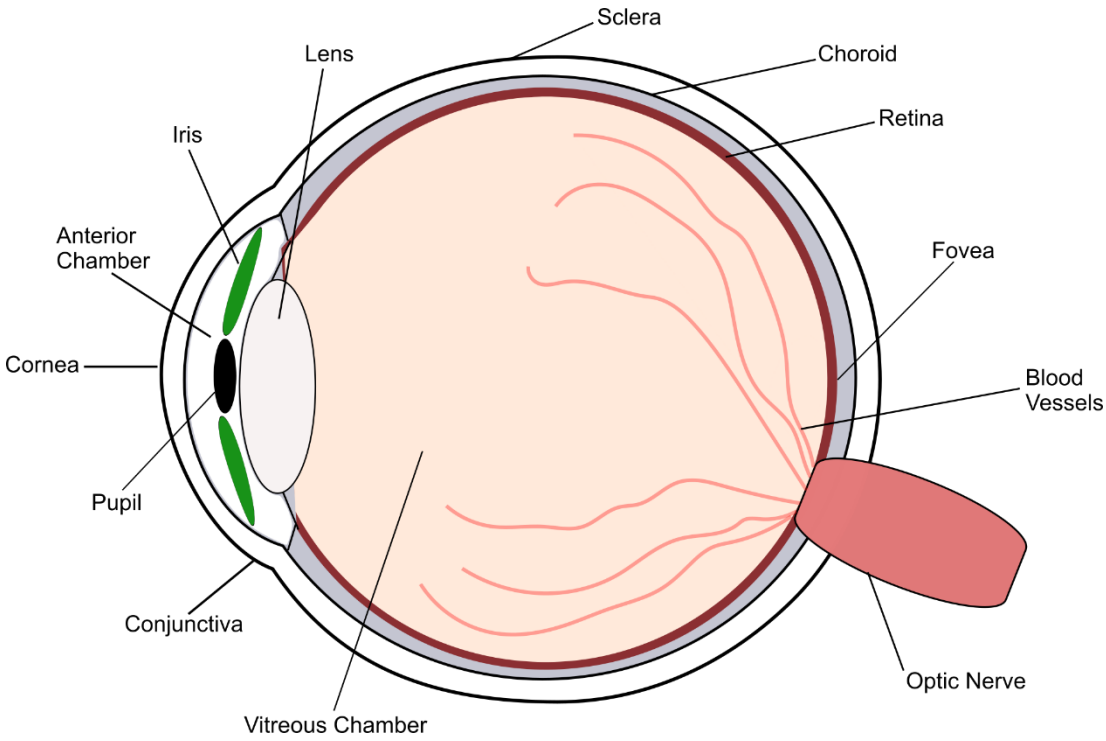

Figure 1.1: An illustration of the eye highlighting the position of the cornea at the anterior region.

1.1.1 Structure and function of the cornea:

The five layers of the cornea (Figure 1.2) the epithelium, Bowman's layer, the stroma, Descemet's membrane and the endothelium form the 550 µm thick corneal tissue (Shah *et al.*, 1999). As well as providing a barrier to injury and infection to the posterior of the eye the cornea also provides approximately three quarters of the eyes total refractive power. This is mainly attributed to the cornea having a refractive index of 1.38 and a 7.8 mm radius of curvature (Eghrari, A.O., Riazuddin, S.A. and Gottsch, 2015; Kim *et al.*, 2004).

The corneal epithelium is a non-keratinised stratified squamous epithelium, approximately 50 µm thick and consists of 5 - 7 layers of epithelial cells. The main function of the corneal epithelium is to act as a physical barrier to intrusions from the external environment whilst preventing a loss of fluid from the underlying stroma and maintaining ocular transparency (Szliter-Berger and Hazlett, 2010). The posterior layer of the corneal epithelium consists of basal epithelial cells that anchor the epithelium to bowman's layer by way of a basement membrane complex, a complex mesh of type VI and VII collagen (Forrester *et al.*, 2008). Hemidesmosomes form tight adhesions between the basal epithelial cells and the basement membrane and play an important role in both cell renewal and the formation of a protective barrier (Stepp, 2010). Gap junctions and desmosomes organise the cell-cell barrier function between basal epithelial cells and the suprabasal wing-like cells that align themselves above the columnar basal cells (Hamrah and Sahin, 2013). The outermost cell type in the corneal epithelium is the superficial cells that contain microvilli that interact with and stabilise the surrounding tear film. Tight junctions are formed between superficial cells via zonula occludens to provide the most effective barrier at the anterior surface where the epithelium interacts with the tear film. The continuous renewal of the epithelium to maintain transparency begins with the proliferation of basal epithelial cells that migrate towards the anterior of the epithelium and ultimately result in the shedding of superficial cells from the surface (Lu, Reinach and Kao, 2001). In response to injury limbal epithelial stem cells located at the limbus begin rapid division resulting in their differentiation to early transient amplifying cells which in turn differentiate into transient amplifying cells before replacing

basal epithelial cells (Hamrah and Sahin, 2013). This continuous renewal of corneal epithelial cells allows for maintenance of the integrity of the epithelium allowing it to continually function as an effective barrier and maintain transparency.

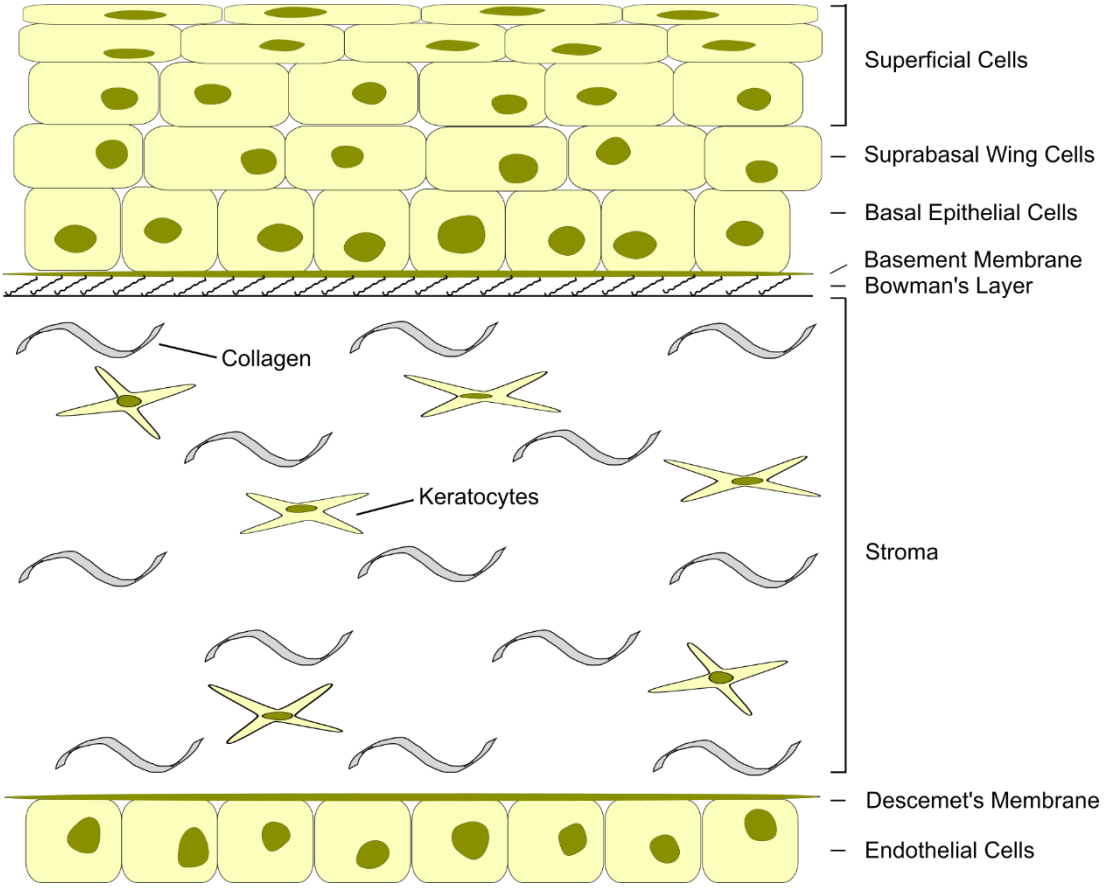

Figure 1.2: The five layers of the cornea with their primary cell types. Diagram is not to scale.

Bowman's layer is an acellular region that separates the epithelial basement membrane from the anterior corneal stroma. It is between 8 - 14 µm thick and formed by fine, densely packed collagen (types I, III, V and VI) (Forrester *et al.*, 2008; Lagali, Germundsson and Fagerholm, 2009). Collagen IV fibrils are also present and act as an anchoring mechanism to the epithelium above (Wilson and Hong, 2000). The collagen fibrils associated with Bowman's layer are randomly ordered compared to the aligned fibrils that make up the lamellae of the corneal stroma (Lagali, Germundsson and Fagerholm, 2009).

The precise function of Bowman's layer is unknown; however, nerve axons pass through Bowman's layer to provide innervation to the epithelium. It has been suggested that Bowman's layer facilitates wound healing of the cornea by acting as a physical barrier to the underlying stroma, allowing for accelerated restoration of transparency whilst protecting the nerve plexus underlying the epithelium. The physical, acellular barrier can also prevent the passing of viruses through the epithelium to the posterior of the cornea (Gandhi and Jain, 2015; Lagali, Germundsson and Fagerholm, 2009).

The stroma is a centrally located, avascular layer of the cornea and is approximately 500 µm thick (Chen, Mienaltowski and Birk, 2015). The stroma consists of 200 - 250 layers of 2 µm thick lamellae which are mostly composed of collagen (types I, V and VI) and proteoglycans that interact with collagen fibrils to form an ordered, closely packed network that ensures the transparency of the corneal tissue (Forrester *et al.*, 2008; Meek and Boote, 2004). Type I collagen is the most abundant type of collagen contained within the fibrils followed by type V collagen which along with proteoglycans help to regulate the gaps between fibrils which is vital to maintaining transparency (Forrester *et al.*, 2008). Type VI collagen forms 100 nm thick filaments that may also play a role in regulating fibril arrangement (Meek and Boote, 2004). Keratocytes, differentiated mesenchymal fibroblasts with a dendritic morphology, are the primary cell type within the stroma and are responsible for the deposition of the collagenous matrix as well as other extracellular matrix macromolecules and proteins such as laminin and fibronectin (Gandhi and Jain, 2015). The stratification of keratocytes reduces the surface area of the cell exposed to light thereby minimising light scattering and maintaining transparency. Keratocytes are interconnected within the stroma by filopodia with gap-junctions mediating cell-cell contact (Chen, Mienaltowski and Birk, 2015). The anterior and the posterior of the stroma differ in their composition. The posterior is more ordered, hydrated and has a lower refractive index than the anterior with changes in keratocyte number and morphology evident (Bron, 2001; Meek *et al.*, 2003). Part of the anterior stroma lamellae interweaves into Bowman's layer resulting in increased mechanical stability of the anterior cornea (Meek and Boote, 2004).

Descemet's membrane separates the stroma from the posterior endothelium layer of the cornea. At birth, the membrane is 3 µm thick and gradually increases to 10 µm in adults due to deposition of extracellular matrix macromolecules from the underlying corneal endothelial cells (Pavelka and Roth, 2010). Similarly to Bowman's layer and other basement membranes of the body, Descemet's membrane contains collagen IV. Types V and VI collagen are found at the anterior of Descemet's membrane and most likely part of an adherence mechanism linking it with the stroma (Forrester *et al.*, 2008). Type VIII collagen is present in high concentrations in Descemet's membrane but is rarely seen in other parts of the body. It forms lattice type networks and is most prevalent in the anterior segment of the membrane (Pavelka and Roth, 2010). Descemet's membrane is a basement membrane for the underlying endothelial cells and assists in maintaining corneal dehydration (Eghrari, A.O., Riazuddin, S.A. and Gottsch, 2015).

The posterior segment of the cornea is the endothelium and is composed of a monolayer of endothelial cells. The cells are approximately 6 µm thick and rest on Descemet's membrane upon which they excrete extracellular matrix proteins and molecules (Forrester *et al.*, 2008). The main function of the endothelium is to provide a barrier and regulate deturgescence to maintain transparency. This is achieved by way of tight and adherens junctions and an ionic pump function associated with bicarbonate dependant Mg^{2+} -ATPase and Na^{+}/K^{+} -ATPase (Joyce, 2012; Eghrari, A.O., Riazuddin, S.A. and Gottsch, 2015; Ali and Murphy, 2016). Corneal endothelial cells are non-regenerative in vivo reducing from 6,000 cells mm^{-2} at birth to 2300 cells mm^{-2} at 85 years of age with an average rate of loss of 0.6% per year (Bourne, 2003; Joyce, 2012). During a lifetime, endothelial cell surface area increases to maintain the endothelial barrier and maintain function as loss of cells to disease and trauma are not replaced (Bourne and McLaren, 2004). Trauma to this area of the cornea can result in serious complications most notably if the ion pump capacity is compromised as this may result in a loss of visual acuity and lead to more serious conditions such as bullous keratopathy (Parekh *et al.*, 2013).

1.1.2 The tear film:

The tear film is a physical barrier that protects the outermost mucosal tissue of the eye from microorganisms and organic matter whilst retaining a stable fluid that complements the rest of the cornea ensuring transparency is maintained (McCulley and Shine, 2001; Craig, Tomlinson and McCann, 2010). The tear film is composed of three layers (Figure 1.3) and is approximately 4 - 8 µm thick. The posterior layer consists of mucins secreted from the underlying corneal and conjunctival epithelium followed by an aqueous layer that is coated with the tear film lipid layer (TFLL). More specifically, goblet cells of the conjunctiva play a pivotal role in mucin secretion (Johnson and Murphy, 2004; Cwiklik, 2016).

The underlying mucous layer of the tear film is approximately 3 - 5 µm thick and is secreted by epithelial cells to provide a hydrophilic surface to stabilise and aid spreading of the aqueous portion of the tear film during the blink cycle (Cwiklik, 2016; Craig, Tomlinson and McCann, 2010). Mucins have a protein rich backbone coupled with an O-linked carbohydrate side chain that accounts for 70% of their mass. To date, 21 mucin genes have been identified in humans and these can be classed as membrane spanning or secretory mucins with the former sub categorised into large gel forming and non-gel forming (Johnson and Murphy, 2004; Hodges and Dartt, 2013). Membrane spanning mucins (MUC1, -3A, -3B, -4, -12, -13, -15, -16, -17, -20 and -21) have a short C-terminal cytoplasmic tail and a hydrophobic domain that allows the mucin to span the conjunctival and corneal epithelial cell membranes and help form the ocular surface glycocalyx. This is followed by a threonine/serine rich extracellular region that provide sites for O-glycosylation (Dartt, 2004; Hodges and Dartt, 2013). Some of these extracellular regions can be up to 500 nm long protruding into the aqueous portion of the tear film (Govindarajan and Gipson, 2010). The main function of membrane spanning mucins is to provide a protective barrier to the ocular surface with hydrophilic O-glycans binding water to provide a rigid, gel like structure. This mechanism can prevent microbial and viral entry to the epithelium as O-glycans are known to prevent viruses from binding to cells and mucins can express decoy ligands for bacterial attachment via complex

carbohydrates (Guzman-Aranguez and Argüeso, 2010; Hodges and Dartt, 2013). Membrane bound mucins also provide lubrication and anti-adhesive properties to the epithelial cells of the cornea and conjunctiva during blinking (Gipson, 2004).

Secretory mucins can be either small soluble mucins (MUC7 and -8) or larger gel forming mucins (MUC2, -5AC, -5B, -6 and -19). They are generally stored in secretory granules until an appropriate stimulus triggers their release (Hodges and Dartt, 2013; Uchino and Tsubota, 2010). MUC5AC is produced by goblet cells in the conjunctiva and is important in lubrication and hydration of the ocular surface, whereas, MUC7 is produced by the acinar cells of the lacrimal gland and the conjunctiva and is thought to play a role in preventing pathogens from binding to the ocular surface (Johnson and Murphy, 2004; Paulsen and Berry, 2006).

The mid layer of the tear film is an aqueous layer of approximately 4 µm thick and it originates from the lacrimal and the accessory glands of Wolfring and Krause. Mucin concentration gradually decreases from the posterior to the anterior of this layer. The aqueous layer contains an abundance of proteins, peptides, electrolytes and other small molecules (Uchino and Tsubota, 2010; Cwiklik, 2016). Lipocalin and lysozyme are two of the most abundant proteins in the aqueous phase and have specific roles in the spreading of tears and antimicrobial activity respectively (McDermott, 2013). Fleming and Allison were the first to report the bactericidal activity of lysozyme in 1922 (Fleiszig, Kwong and Evans, 2003). Sodium, calcium, potassium and phosphate ions help to control osmolality of tears whilst maintaining a constant pH (Johnson and Murphy, 2004). Other molecules in the aqueous portion of the tear film include lactoferrin which works in synergy with lysozyme by binding to bacterial lipoteichoic acids to allow lysozyme access to peptidoglycan and IgA which may have an immunological role (Forrester *et al.*, 2008). The aqueous phase is secreted continuously by the lacrimal glands at a rate of 1.2 mm^3 min^{-1} with extra tear production induced by psychophysical or mechanical stimuli (Forrester *et al.*, 2008; Dartt and Willcox, 2013; Cwiklik, 2016).

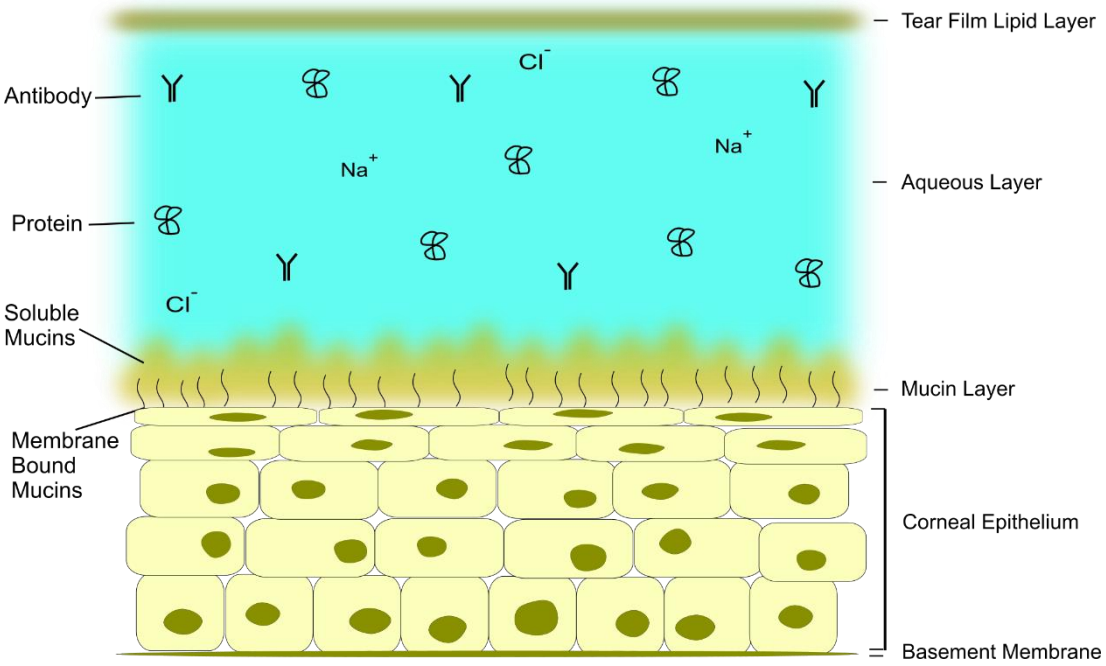

Figure 1.3: The layers of the tear film with some associated components and its interaction with the corneal epithelium. Diagram is not to scale.

The TFLL is the anterior portion of the tear film and is between 50 - 100 nm thick (Hodges and Dartt, 2013; Craig, Tomlinson and McCann, 2010). The posterior tear film is composed of polar lipids (e.g. phospholipids) separating the aqueous phase and the external environment followed by layers of non-polar lipids (wax esters, sterol esters and triglycerides) on the outermost surface of the TFLL. The lipids are thought to be secreted by meibomian glands; however, this has been challenged recently. Proteins are also thought to form part of the TFLL but again this is still unknown (Millar and Schuett, 2015; Cwiklik, 2016). The main function of the TFLL is to prevent evaporation from the aqueous layer of the tear film and prevent any spill over of tears whilst providing a clear optical medium. The TFLL also plays a role in preventing sebaceous lipids from the skin migrating onto the ocular surface (Forrester *et al.*, 2008; Johnson and Murphy, 2004).

1.2 Ulcerative Keratitis

There are many conditions that affect the surface of the eye and they range from dry eye disease to corneal ulcers. Corneal diseases, in general, are a leading cause of blindness worldwide but incidences vary depending on location. Approximately 75,000 Americans contract corneal ulcers annually but the condition is much more prevalent and still under reported in developing countries where up to 1,500,000 people contract the condition annually (Whitcher, Srinivasan and Upadhyay, 2002; Amescua, Miller and Alfonso, 2012). In the western world microbial infection or herpes simplex virus present complications from which opaqueness of the cornea can occur and ultimately lead to vision loss (Williams and Wong, 2009). Many of the incidences of corneal ulceration in the developing world result in blindness mainly due to the expensive cost of antimicrobials, proximity to treatment centres and drug resistance (Whitcher, Srinivasan and Upadhyay, 2001). The most prevalent causes of corneal ulcers include contact lens wear, ocular trauma, ocular surface disease (keratitis) and systemic diseases such as rheumatoid arthritis and HIV (Lee and Manche, 2016). Of the infectious cases, there is a global divide with fungal keratitis most prevalent in the developing world primarily due to manual labourers working in optimal environments for fungal pathogens. In the developed world bacterial keratitis is the most common cause of corneal ulcers and is most often contracted by improper use of contact lenses and their associated lens care solutions (Upadhyay, Srinivasan and Whitcher, 2007).

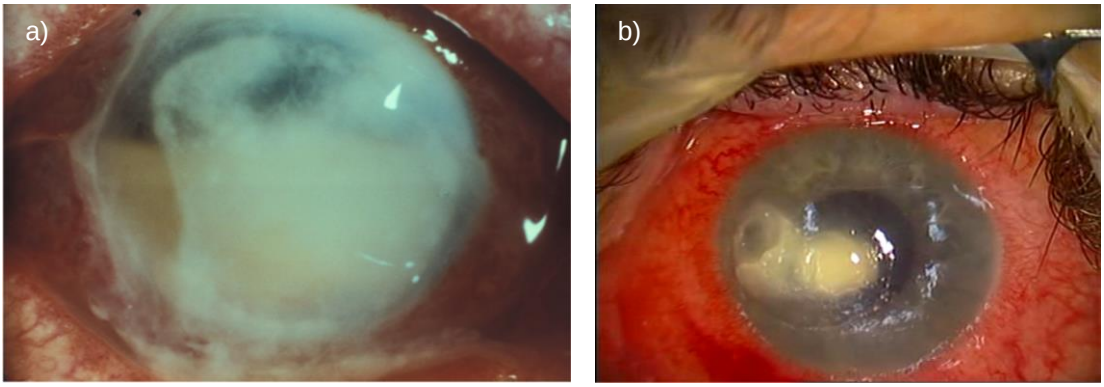

Figure 1.4: a) *Pseudomonas* keratitis, b) fungal keratitis. Images provided courtesy of Professor S.B. Kaye (St Paul's Eye Unit, Liverpool).

1.2.1 Bacterial keratitis:

Bacterial keratitis (Figure 1.4a) is one of the most threatening ocular infections to visual integrity primarily due to complications that may arise and the rate of pathogenesis (Schaefer *et al.*, 2001). Treatment is normally commenced following culture retrieval from the site of infection and it usually takes the form of administration of a single or a combination of antimicrobials in drop form to provide a range of activity against both Gram-positive and Gram-negative organisms. Once the isolate from the cultures is identified then a more tailored treatment is applied (Kaye *et al.*, 2010). One of the major challenges for an ophthalmologist is distinguishing bacterial keratitis from other ulcer causative conditions and then further identifying the correct species of microbial pathogen to administer the correct first-line antibiotic (O'Brien, 2003). Any delays in treatment especially with bacterial keratitis can result in severe complications due to the rate of pathogenicity with corneal perforations occurring in less than 24 h from *Pseudomonas aeruginosa* and *Staphylococcus aureus* infections (Schaefer *et al.*, 2001). Some of the major risk factors include ocular trauma, post-ocular surgery and systemic disease such as diabetes mellitus. Bacterial keratitis associated with contact lens wear is now the most prevalent risk factor in the developed world. Individuals who wear contact lenses are 10 - 20 times more susceptible to bacterial keratitis mainly due to extended wear of lenses or contamination due to increased bioburden as a result of unhygienic practices (Bourcier *et al.*, 2003; Stapleton and Carnt, 2012). Other predisposing factors implicated in the

onset of contact lens associated bacterial keratitis include smoking and mechanical epithelial trauma from the contact lens itself due to increased rigidity of some silicone hydrogel contact lenses. Smoking may increase toxins and result in changes to mucous membranes whilst contact lens materials have already been implicated in other mechanical complications to the cornea such as subepithelial arcuate lesions (Szczotka-Flynn *et al.*, 2010). It should be noted that microbial invasion of a healthy cornea by ocular pathogens is extremely rare as the host response is sufficient to maintain ocular surface integrity. A compromised epithelium is required to allow pathogens to invade the cornea and in turn cause microbial keratitis (Schaefer *et al.*, 2001; Keay *et al.*, 2006).

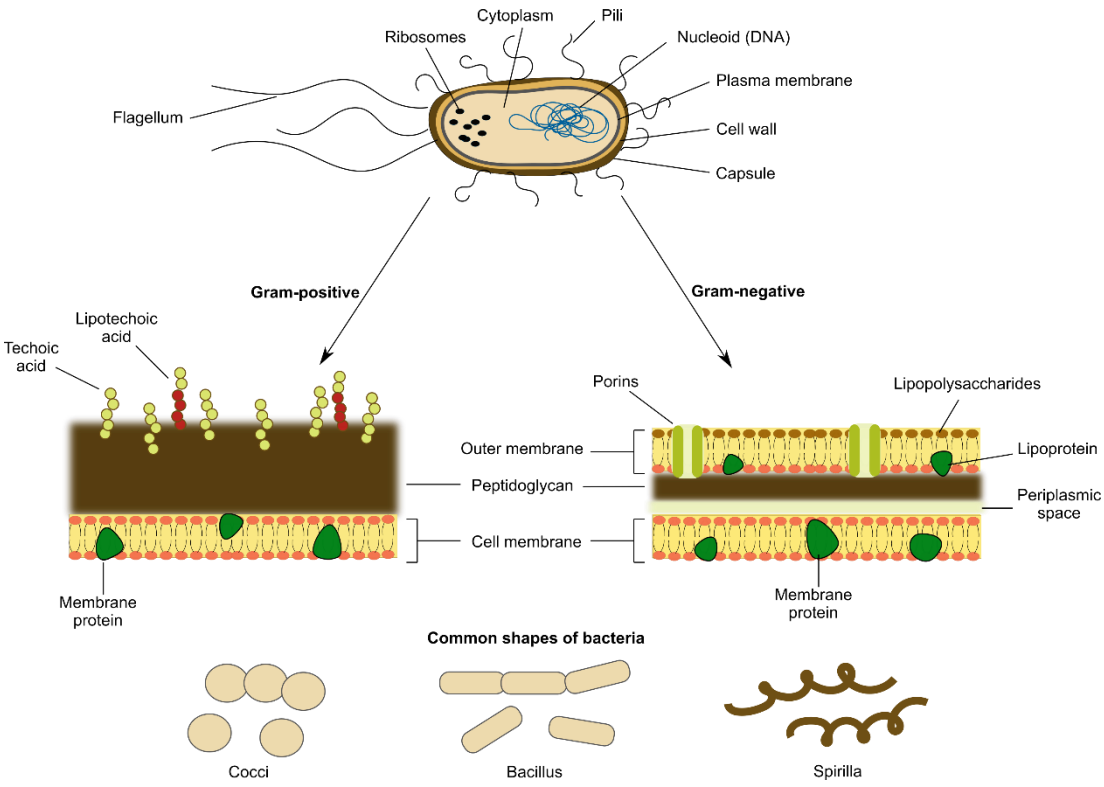

Figure 1.5: Bacterial cell and outer membrane composition followed by some common bacterial shapes.

Both Gram-negative and Gram-positive bacteria are implicated in bacterial keratitis (Figure 1.5). Some of the most common isolates are *Staphylococcus* spp., *Streptococcus* spp., *P. aeruginosa* and *Escherichia coli* however numbers tend to vary depending on, for example, the geographical region or risk factor involved (Green, Apel and Stapleton, 2008; Lichtinger *et al.*, 2012; Hong *et al.*, 2013). *Streptococcus pneumoniae* is most associated with permanent damage of the ocular surface and *P. aeruginosa* infections progress rapidly (Karsten, Watson and Foster, 2012).

P. aeruginosa in particular is associated with contact lens wear and is the most prevalent isolate of bacterial keratitis in tropical climates such as Brisbane (71%), Singapore (79%) and Miami (78%) whereas Gram-positive cocci are more commonly reported in non-contact lens associated keratitis (Green, Apel and Stapleton, 2008; Saraswathi and Beuerman, 2015). Invasive isolates of *P. aeruginosa* rely on adhesion to the epithelium via flagella, pili, membrane proteins and lipopolysaccharide (LPS) and an endocytosis-like approach to internalising itself within the corneal epithelial cells (Fleiszig, 2006). Once inside epithelial cells the organism is protected from extracellular host defences such as antibodies and complement and in turn gain access to the cytoplasm where it can replicate at rates of 10-fold per hour (Fleiszig and Evans, 2002; Fleiszig, 2006). However, there are isolates of *P. aeruginosa* known to cause cytotoxicity extracellularly via an ExoU dependant mechanism. ExoU is a toxin that is injected into epithelial cells via ‘needles’ protruding from the microbe (Fleiszig, Kwong and Evans, 2003). LPS is an important virulence factor in *P. aeruginosa* infection as well as allowing the pathogen to adhere to the corneal epithelium and surfaces such as contact lenses it also imparts resistance to the antimicrobial protein complement and allows the bacteria to accumulate in the tear film (Fleiszig and Evans, 2002).

In most cases of non-contact lens related bacterial keratitis the pathogen usually has a route through a damaged epithelium into the stroma. The epithelium can be compromised by factors such as disease and trauma. Once in the stroma the pathogen can damage the structured order that

allows for maintenance of transparency as well as prompting a host immune response that can result in tissue degradation (Fleiszig, 2006). Other bacterial pathogens such as *Neisseria gonorrhoeae*, *Neisseria meningitides*, *Shigella* and *Listeria* can penetrate the corneal epithelium via a complex array of enzymes and virulence factors to enter the stroma. *S. aureus* adheres to host tissue via collagen and fibronectin unlike *P. aeruginosa* that adheres to tissue without fibronectin present (O'Brien, 2003). The collagen binding adhesin is an important virulence factor in *S. aureus* keratitis and allows it to penetrate the wounded epithelium of the cornea (Rhem *et al.*, 2000).

In cases of contact lens associated bacterial keratitis biofilm forming bacteria are usually associated. Biofilms present a greater challenge when it comes to eradicating the pathogen as microbes within biofilms can be between 10- to 1000-fold more resistant to antibiotics than their planktonic forms (Zegans, Shanks and O'Toole, 2005). Biofilm formation on contact lenses and contact lens cases has been well established (McLaughlin-Borlace *et al.*, 1998) and they provide a microbial environment for organisms to survive repeated cleaning regimes until an opportunity presents itself (e.g. ocular injury) to commence infiltration of compromised tissue (Zegans *et al.*, 2002). Organisms such as *P. aeruginosa* have an array of genes that allow it to adapt to changes within their environment (Bispo, Haas and Gilmore, 2015).

1.2.2 Fungal keratitis:

Fungal infections of the cornea (fungal keratitis) are challenging to treat. The first sign of fungal keratitis (Figure 1.4b) is a granular infiltration of the corneal epithelium and the stroma, however, this is also the case for bacterial keratitis (Dóczi *et al.*, 2004). Initial diagnosis may take several days before results of corneal scrapes or biopsies become available. However, a presumptive diagnosis may be made by examining corneal scrapings directly under a microscope followed by an appropriate staining procedure (Gram or Giemsa method, periodic acid Schiff or Gomori methenamine silver) and administration of a first-line antibiotic until the specific organism is identified (Thomas, 2003). Despite intensive antifungal therapy (typically hourly eye

drops including through the night, combined with oral medication) it is not uncommon for emergency corneal grafts to be necessitated. The associated severe inflammation and scarring often leads to some permanent loss of vision (Whitcher, Srinivasan and Upadhyay, 2001). If the infection is not controlled, it may spread throughout the eye resulting in endophthalmitis. Even when the infection is controlled, a recurrence rate of 5 - 14% is typical but this can be as high as 31%. These recurrence rates are greater than recurrence rates for bacterial keratitis and result in the need for keratoplasty more often (Lalitha *et al.*, 2006; Shi *et al.*, 2010). Furthermore, fungi are the leading cause of ocular infections in tropical and subtropical regions, which cover most developing countries where access to healthcare may be limited (Ou and Acharya, 2007).

There are two types of fungi that cause keratitis; filamentous fungi such as *Fusarium* and *Aspergillus* spp., and yeast-like fungi such as *Candida albicans* (Figure 1.6). Filamentous fungal keratitis tends to occur as a result of trauma involving vegetative matter and is more prevalent in tropical climates (Thomas and Kaliamurthy, 2013). *Candida* infections are more common in those with pre-existing ocular surface disease such as insufficient tear production or poor eyelid closure, topical steroid use, post-surgery or with other systemic risk factors (such as diabetes or immunosuppression) and is more prevalent in temperate climates (Sun, Jones and Wilhelmus, 2007). Historically fungal keratitis accounts for ≤ 5% of the total microbial keratitis cases, however, this appears to be increasing with estimates of up to 52% in the early part of the 21st century (Sengupta *et al.*, 2012). From 2005 - 2007 more than 300 cases of *Fusarium* keratitis were identified from patients who used contact lenses and ReNu with Moistureloc lens cleaning solution (Bausch and Lomb, Rochester, NY). Many of the patients required some form of keratoplasty resulting in the lens cleaning solution being withdrawn from the market (Gower *et al.*, 2010; Mukherjee *et al.*, 2012). A review of keratitis cases at Bascom Palmer Eye Institute in Florida, USA from 2001 - 2007 found that fungal pathogens were identified in 20.8% of keratitis cases. *Fusarium* (54.1%) and *Candida* (28%) were two of the most common fungal

isolates. Of the total fungi recovered 10.7% were implicated in contact lens related keratitis (Alfonso *et al.*, 2006).

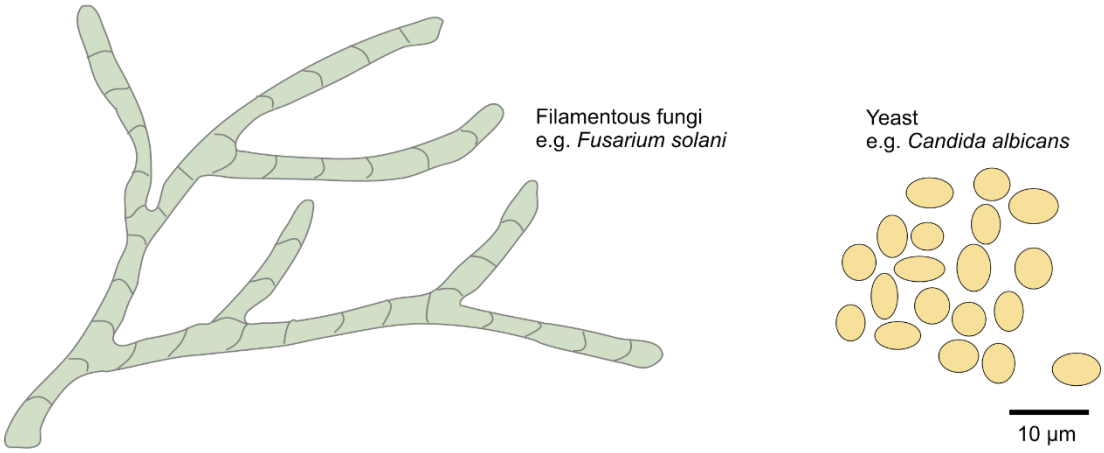

Figure 1.6: Filamentous and yeast-like fungi are causative organisms in fungal keratitis.

The pathogenesis of fungal keratitis is lesser understood on a molecular level than bacterial keratitis and the efficacy of anti-mycotic therapy is low. These reasons may contribute to lower clinical success rates for fungal keratitis. The key mechanisms involved in fungal pathogenesis include adherence, invasiveness, toxigenicity and morphogenesis (Ananthi *et al.*, 2008). Virulence factors such as toxins and proteases enable hyphal invasion of the corneal tissue (Leal *et al.*, 2010). *Aspergillus* and *Fusarium* are ubiquitous in the environment with up to 200 conidia inhaled by individuals per day. In the presence of a disrupted corneal epithelium *Aspergillus fumigatus* conidia or conidiaphores can easily inoculate the wound. *Aspergillus* conidia are smaller than *Fusarium* conidia and can therefore penetrate deeper into tissue (Leal *et al.*, 2010; Pearlman *et al.*, 2010). *Candida* infects the cornea initially in the yeast stage prior to germination and the formation of pseudohyphae which then penetrate the stroma. Phospholipases and in particular phospholipase B play a pivotal role in facilitating *Candida* invasion via tissue destruction. It has been suggested that genes regulating hyphal formation as opposed to adherence determine *C. albicans* virulence (Pearlman *et al.*, 2010). Morphogenesis such as the presence of hypha in hyphae, intrahyphal

hyphae and a thickened cell wall provide protective mechanisms to the host immune response and antifungal drugs. Mycotoxins such as fumonisin B_1, moniliformin and fusaric acid from *Fusarium* spp. are also thought to play a role in pathogenesis (Naiker and Odhav, 2004).

1.2.3 The role of biofilms in microbial keratitis:

The first mention of biofilms came in the 17th century when Anthony van Leeuwenhoek took scrapings from his teeth and observed them under an early microscope. He identified small living microbes in the plaque samples and described how the plaque may have helped the microbes to survive the vinegar washes he used to clean his mouth (Bispo, Haas and Gilmore, 2015). A more modern description of biofilms is that they consist of multiple layers of sessile microbial cells attached to a surface and surrounded by a complex extracellular matrix. The sessile cells are morphologically and phenotypically distinct from their planktonic equivalents (Acker, Dijck and Coenye, 2014). The overlying matrix with thicknesses up to 50 µm provides a barrier that protects the microbial community from external factors such as antibiotics, chemical detergents and increases resistance to a host immune response. In some cases a 1000-fold increase in antibiotic resistance has been observed from biofilm communities (Høiby *et al.*, 2010; Saraswathi and Beuerman, 2015).

Bacterial biofilm formation is initiated when bacteria attach to a surface. Adherence may be aided by the presence of a protein layer that promotes increased hydrophobic or electrostatic interactions. Irreversible binding followed by the emergence of microcolonies promote the production of biofilm extracellular matrix (Høiby *et al.*, 2010). Small water channels are formed between the microcolonies that provide a flow of nutrients, waste products and communication molecules such as quoromones (Pratt and Kolter, 1998; Davies, 2003). A study of bacterial biofilm formation on contact lenses revealed that *P. aeruginosa* could adhere to and form biofilms on etafilcon A, balafilcon A and poly-(2-hydroxyethyl methacrylate) (pHEMA) lens materials with most attachment observed on balafilcon A lenses (Willcox

et al., 2001). Other studies identified a 3 - 9 times greater risk of microbial keratitis following extended wear of lotrafilcon A lenses (Willcox, 2013).

Fungal biofilms begin in much the same way as bacterial biofilms. Biofilm formation begins when yeast cells attach to a surface followed by deposition of an extracellular matrix primarily composed of β-glucan. Other components of the matrix include carbohydrates, proteins, hexosamines and phosphorus. Filamentous cells produce a hyphal network within the matrix that helps increase resistance to many antifungal drugs (Sardi *et al.*, 2013; Zhang *et al.*, 2017). The presence of bacteria can help regulate fungal biofilm formation and vice-versa. *S. aureus* has shown decreased susceptibility to vancomycin when present in a co-culture of *C. albicans* (Desai, Mitchell and Andes, 2014). An in vitro model of fungal biofilm formation on contact lenses demonstrated the ease at which both *Fusarium* spp. and *C. albicans* could form biofilms on lens materials such as etafilcon A, lotrafilcon A and balafilcon A (Imamura *et al.*, 2008). In cases of microbial keratitis the formation of a biofilm is considered an important developmental characteristic (Zhang *et al.*, 2017).

1.2.4 Host response to microbial keratitis:

The first defensive mechanism microbial pathogens encounter at the ocular surface is the tear film and the many proteins and molecules associated with it (Figure 1.7). These factors combine with the blinking mechanism and the continued renewal of the tear film to successfully limit the numbers of microbial pathogens in close proximity to the ocular surface by removing them towards the nasolacrimal duct (Gipson and Argüeso, 2003). Lysozyme was one of the first characterised antimicrobial components of the tear film, whilst the iron binding lactoferrin, mucins, antibodies, complement proteins, short cationic β-defensin peptides and secretory phospholipase A_2 have also been identified as important antimicrobial factors (Fleiszig and Evans, 2002; Fleiszig, Kwong and Evans, 2003). Lipocalin binds to fungal siderophores and lactoferrin is a divalent cation scavenger which in turn inhibit iron uptake by fungi (Shoham, 2015). Many microbes can be inhibited by the host antimicrobials but others have evolved virulence factors that can directly

inhibit them. Some Gram-negative bacteria are resistant to secretory phospholipase A_2 but have been shown to be susceptible to β-defensins (Fleiszig, Kwong and Evans, 2003). β-defensins are produced when the presence of bacterial LPS is detected (Fleiszig and Evans, 2002). Mucins play a role in preventing microbes from adhering to the surface of the epithelium by binding to them via decoy ligands or via a barrier mechanism (Hodges and Dartt, 2013). The virulence mechanisms of invasive and cytotoxic *P. aeruginosa* isolates are inhibited by mucins.

The epithelium has mechanisms of protection that identify and inhibit microbes that penetrate the tear film. Tight junctions between cells via zonula occludens in an uncompromised cornea provide a closed barrier to microbial penetration through the epithelium. The sloughing mechanism by superficial cells of the anterior cornea can remove bacteria that have managed to invade these outermost cells. It is thought that the shedding of cells on the outermost surfaces of the body is a mechanism of removing pathogens that have invaded them (Fleiszig, 2006). However, ocular trauma, surgery, disease and other factors that may compromise the epithelium bypass this barrier function and open up the deeper stromal tissue to microbial infection (Fleiszig and Evans, 2002).

The corneal epithelium also responds to microbial invasion by recruiting neutrophils and other cells involved in the immune response. Corneal epithelial cells express receptors to LPS such as TLR4 and CD14 that upregulates cytokines. This in turn promotes an inflammatory response (cytokines and antimicrobial peptides (AMPs)) and the recruitment of lymphocytes and macrophages followed by neutrophil infiltration (Fleiszig and Evans, 2002; O'Brien, 2003). TLRs can recognise specific pathogens such as *S. aureus* (TLR2) and *P. aeruginosa* (TLR4). TLRs along with leukocytes and keratocytes recognise fungi such as *F. solani* and *A. fumigatus* (Yuan and Wilhelmus, 2010). It is thought that this enhanced immune response plays a pathogenic role in keratitis as an upregulation in matrix metalloproteinase (MMPs) and other inflammatory factors released

from neutrophils and macrophages can lead to stromal necrosis and corneal edema (Hazlett, 2010; Shoham, 2015).

In particular it is thought that increased levels of MMP-9 and neutrophil infiltration leads to invasion of the stroma by fungi as it changes from yeast to hyphae (Mitchell and Wilhelmus, 2005). Epithelial and stromal cells also release cytokine IL-1α after their cell membranes are compromised. IL-1α and tumour necrosis factor (TNF-α) combine to promote keratocyte synthesis of IL-6 and β-defensins. The neuropeptides substance P and calcitonin are released when pain is detected by corneal nerves and then bind to corneal epithelial cells to promote IL-8 synthesis which in turn promotes neutrophil infiltration (Akpek and Gottsch, 2003). Bowman's layer is thought to provide a barrier to the stromal layer of the cornea. The pores of the membrane are much smaller than 2 µm and therefore should prevent bacteria from penetrating it (Fleiszig, 2006).

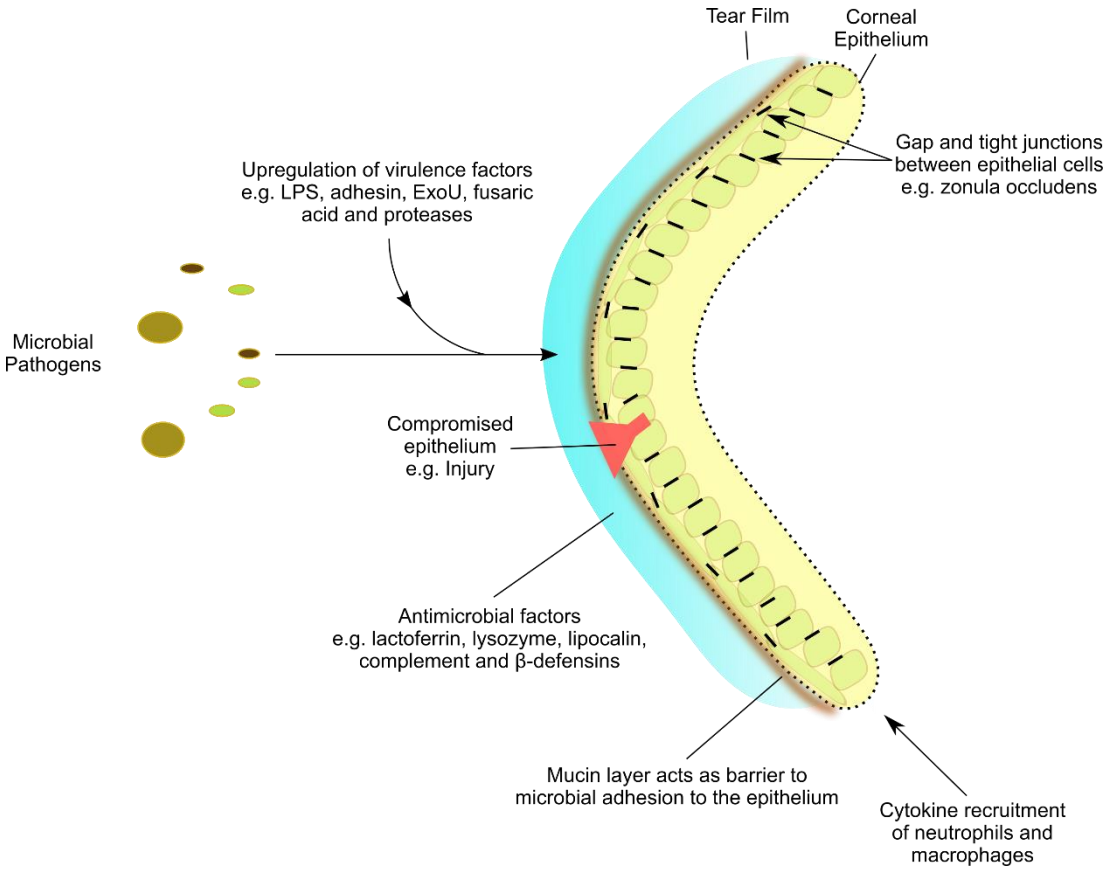

Figure 1.7: Factors involved in host response to microbial invasion of the cornea.

1.2.5 Current treatments for microbial keratitis:

In all cases of microbial keratitis, the first action is to identify the pathogen involved in infection. As stated previously (section 1.2.1) this involves retrieval of the pathogen from the cornea via a corneal scrape usually after the application of local anaesthetic to help relieve discomfort. The scrapes are sent for culture and susceptibility testing but can take several days to weeks to determine the pathogen involved resulting in diagnosis at the later stages of the condition (Akram *et al.*, 2015; Leck, 2015). Direct microscopic observation of the scrape followed by specific staining procedures can yield more accurate determinations of the pathogen involved and identify the correct class of antibiotic to administer. However, this approach is not as accurate and may lead to inefficient treatment regimens that can result in unresponsive keratitis. Antibiotics are usually administered topically via drops or ointments due to the avascular nature of the cornea and a blood-aqueous barrier rendering systemically delivered antibiotics mostly ineffective (Garhwal *et al.*, 2012). In vitro susceptibility testing of microorganisms obtained from corneal scrapes are also not representative of the concentrations required to eradicate organisms using antibiotic drops. The breakpoints used in vitro are generally for systemic concentrations as opposed to those required for ocular topical administration. Several other methods have been deployed to speed up diagnosis times including antibody based detection systems, polymerase chain reaction (PCR) and AMPs (Wang *et al.*, 2014). Antibody based detection systems are powerful tools, however, they have limited stability under harsh environmental conditions, lack of batch to batch consistency and can be expensive to produce. PCR is another powerful tool but requires an extraction step and with a lack of portability may hinder its use in the field (Kulagina *et al.*, 2005; Mannoor *et al.*, 2010). AMPs with their natural affinity towards microbes have been modified structurally to identify specific organisms or classes of organisms via fluorescent based detection systems. AMPs are more stable than normal proteins with some maintaining antimicrobial activity after autoclaving or in the presence of chemical denaturants (Mannoor *et al.*, 2010). Cationic AMPs such as magainin I and fragments of ubiquicidin are currently being investigated as they have a broad binding spectrum to microbes, are highly

stable and can be produced at a comparably low cost via well-established peptide synthesis procedures (Kulagina *et al.*, 2005; Akram *et al.*, 2015). The stability of AMPs coupled with a fluorescent detection system should allow for a greater deal of portability for use in the field.

1.2.5.1 Bacterial keratitis:

After initially ruling out fungi as the causative organism in microbial keratitis, bacteria are the main suspect. This is especially true in temperate climates where they are the most prevalent organism implicated in microbial keratitis. Empirical broad-spectrum antibiotic treatment usually in the form of eye drops or an ointment is then administered until the culture and susceptibility data of the pathogen becomes available. The choice of antibiotic (Figure 1.8) is usually determined by the geographic location and associated antibiotic susceptibility data to known pathogens (Orlans, Hornby and Bowler, 2011; Shalchi *et al.*, 2011).

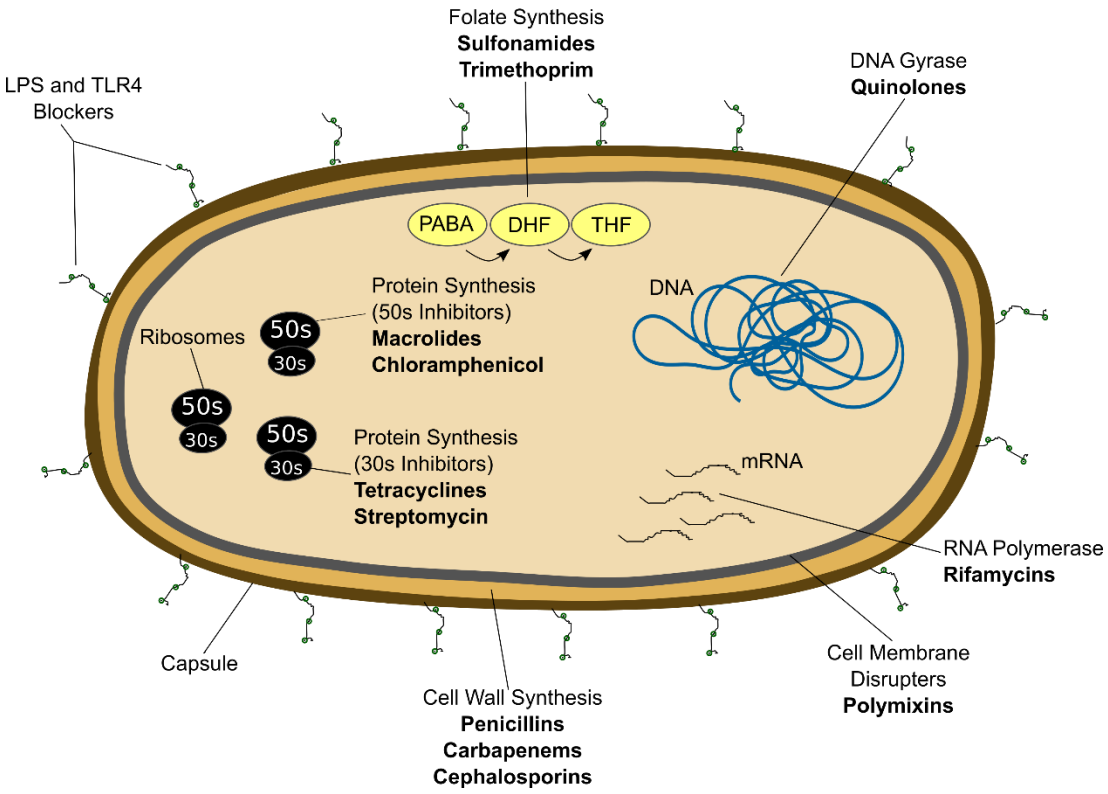

Figure 1.8: Mechanism of action of common antibiotics against bacteria.

The current first-line therapy treatment for bacterial keratitis has been shaped by decades of global antibiotic resistance patterns. Resistance started to become a problem in the 1960s when *S. aureus* resistance to penicillin became common and resulted in the introduction of cephalosporins followed by gentamycin in the 1970s mainly due to the rise of contact lens related keratitis caused by *P. aeruginosa* (Sueke *et al.*, 2010). Until the early 1990s the choice of first-line therapy was a fortified antibiotic formulation of gentamycin (1.5%) and cefuroxime (5%) that covered a broad-spectrum of Gram-positive and Gram-negative organisms. The main issue with this treatment was toxicity to the corneal epithelium and the limited stability of the fortified antibiotics at room temperature (Tuft and Matheson, 2000). Gentamycin also had a poor bioavailability after topical application due to poor corneal penetration resulting in a lack of detection of the antibiotic on the ocular surface 10 min after drop administration and 40 min after ointment application (Schaefer *et al.*, 2001). First and second generation fluoroquinolones were introduced in the early 1990s as a monotherapy for bacterial keratitis with reduced corneal toxicity and broad-spectrum activity against Gram-positive and Gram-negative organisms. However, recent reports from India and the United States have identified resistance to both ciprofloxacin and ofloxacin in cases of bacterial keratitis with *S. aureus* resistance rising from 5.8% in 1993 to 35% in 1997 but by 2000 the resistance rate had risen as high as 82% (Tuft and Matheson, 2000; Schaefer *et al.*, 2001; Shalchi *et al.*, 2011). Third (levofloxacin) and fourth (moxifloxacin, gatifloxacin and tobramycin-cefazolin) generation fluoroquinolones were introduced for ophthalmic applications to combat this resistance in the early 2000s (Mather *et al.*, 2002). Fourth generation fluoroquinolones have better efficacy against Gram-positive organisms than earlier generation fluoroquinolones and maintain broad spectrum susceptibility when administered against Gram-negative organisms. However, ciprofloxacin is still more effective against Gram-negative organisms. A recent study in Britain found that Gram-positive fluoroquinolone resistance had not increased over the previous 10 years and highlighted the upward trend of Gram-negative infection rates with *P. aeruginosa* as the predominant organism. This lead to the recommendation that ciprofloxacin

remained the first-line antibiotic therapy in Britain for bacterial keratitis (Shalchi *et al.*, 2011; Wong *et al.*, 2012). A similar study was carried out on clinical isolates in Toronto between 2000 and 2010 with the recommendation that dual therapy of vancomycin and tobramycin be administered. Gram-negative organisms were more sensitive to tobramycin (98.2%) than ciprofloxacin (97.4%) and all Gram-positive organisms were sensitive to vancomycin. Coagulase negative *Staphylococcus* was the predominant organism isolated followed by *P. aeruginosa* and *S. aureus* with methicillin-resistant *S. aureus* making up 1.3% of the isolates with again no upward trends in resistance identified (Lichtinger *et al.*, 2012). Although ciprofloxacin is still the first-line antibiotic therapy research is continuing to identify future antibiotics and stay a step ahead of bacterial resistance. Multi-drug resistance is becoming an increasing problem to conventional treatments for microbial keratitis. A study at the Prasad Eye Institute in India from 2007 - 2014 found that approximately 25% of all cases of *Pseudomonas* keratitis were caused by a multi-drug resistant strain of the pathogen. The main risk factors identified were the use of a preservative free ointment, a compromised epithelium and the use of bandage contact lenses. Clinical outcomes were generally worse for patients with keratitis from multi-drug resistant strains of *Pseudomonas* compared to those infected with responsive strains (Vazirani, Wurity and Ali, 2015). New research is investigating carbapenems as potential candidates for ocular infections. These β-lactams are resistant to hydrolysis via β-lactamases and as a result overcome a common pathogen resistance mechanism. Carbapenems are usually described as ‘antibiotics of last resort’ as they maintain the greatest potency and broadest spectrum against both Gram-negative and Gram-positive organisms (Papp-Wallace *et al.*, 2011). Meropenem is currently being investigated as a treatment for bacterial keratitis and is already approved by the Food and Drug Administration (FDA) to treat skin infections and bacterial meningitis. A study was conducted on bacterial keratitis clinical isolates to determine the minimum inhibitory concentration at which 90% of isolates died (MIC_{90}) for a range of antibiotics including ciprofloxacin, moxifloxacin and meropenem. The MIC_{90} of meropenem was found to be lower than all the other antibiotics tested against coagulase negative

Staphylococcus, P. aeruginosa, E. coli and S. aureus (Sueke *et al.*, 2010). Further work determined that meropenem had a low toxicity in vitro towards primary human keratocytes and a human corneal epithelial cell line (HCE-T). Furthermore, good corneal penetration achieved MIC_{90} levels of meropenem in the anterior chamber (Sueke *et al.*, 2015).

1.2.5.2 Fungal keratitis:

Once fungal keratitis is confirmed and the pathogen identified an hourly treatment for 24 - 48 h of antifungal drops is administered with prolonged treatment for 6 weeks not uncommon or 12 weeks in severe cases involving filamentous fungi that have extended into the stroma. Current treatment for fungal keratitis is still inadequate mainly due to poor drug bioavailability as is the case for antibacterial drops. However, other reasons more specific to fungal keratitis include narrow spectrum of drug activity, high recurrence rates, ocular toxicity and increased cost due to the common practice of systemic use of the same antifungal that is topically administered (Thomas, 2003; Neoh *et al.*, 2014). Antifungal agents (Figure 1.9) can be classified into six groups: polyenes (natamycin and amphotericin B) that increase cell permeability; pyrimidines; imidazoles (miconazole) and triazoles (fluconazole and voriconazole) that inhibit fungal ergosterol biosynthesis; allylamines and echinocandins (Achiron and Hamiel, 2014; Neoh *et al.*, 2014).

Natamycin (5%) or amphotericin B (0.15%) are the current first-line therapy for cases of fungal keratitis caused by filamentous or yeast pathogens respectively. This may be followed by sub-conjunctival miconazole or oral administration of fluconazole if lesions are seen (Thomas, 2003; Dóczi *et al.*, 2004). As mentioned previously in section 1.2.2, recurrence is a greater issue with fungal keratitis than bacterial keratitis and can necessitate the need for keratoplasty. In some instances the recurrence rate can be as high as 31% (Lalitha *et al.*, 2006). Generally recurrent keratitis will be given another chance to respond to treatment prior to keratoplasty with an example treatment regimen being the addition of fluconazole eye drops (0.5%) every 30 min coupled with either amphotericin B (0.15%) or natamycin (5%) eye drops every 2 h and intravenous fluconazole (200 mg) once a day for 5 - 7

days. If the keratitis does not respond to the treatment then keratoplasty is initiated (Shi *et al.*, 2010).

Resistant strains of *Fusarium* implicated in keratitis have been identified and although resistance is rare compared to bacterial keratitis the end result could be more devastating (Edelstein *et al.*, 2012). The cost associated with treatment of bacterial keratitis is already almost twice as costly to treat than non-infectious keratitis with costs of treatment for fungal keratitis almost 7 times greater (Keay *et al.*, 2006). These costs do not consider an increase in resistance and the more extensive treatment that this entails.

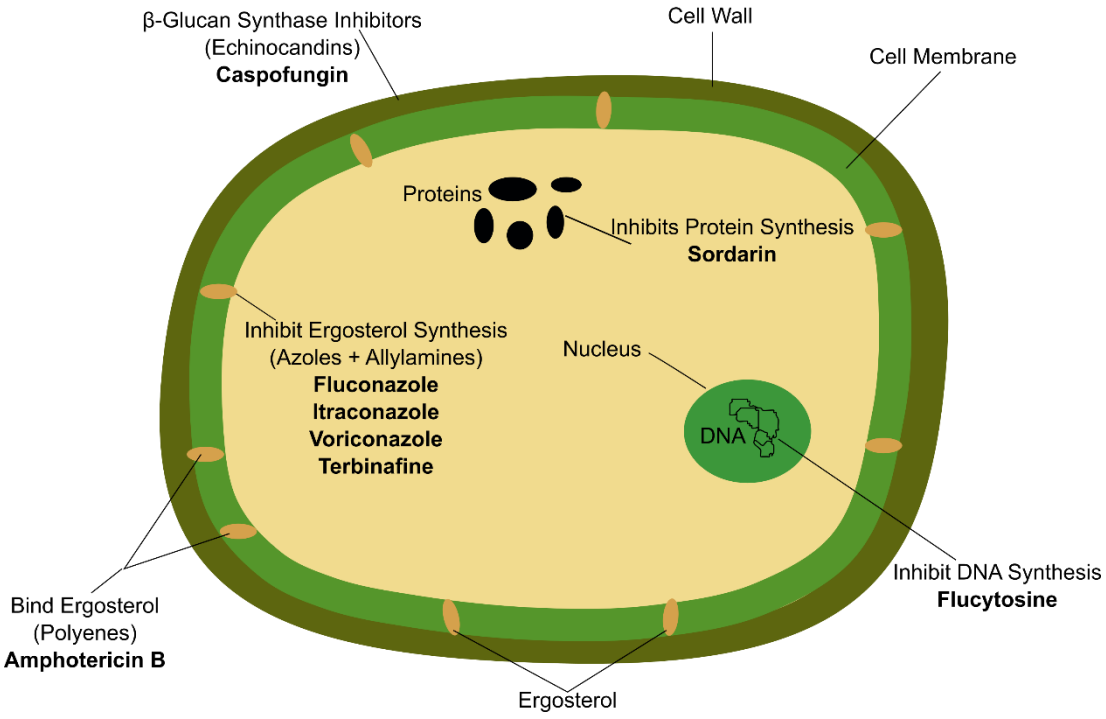

Figure 1.9: Mechanism of action of common antifungals.

Voriconazole has a broader spectrum and better bioavailability than most antifungal agents, with fewer side effects and a comparable efficacy to standard antifungal agents with some signs that a synergy approach between

a polyene and an azole may be beneficial as a future antifungal treatment (Bunya *et al.*, 2007; Prajna *et al.*, 2013).

1.2.6 Limitations to current microbial keratitis treatments:

Initial diagnosis requires application of local anaesthetic followed by several corneal scrapes to inoculate a range of nutrient agar. A lack of patient compliance can present problems with retrieval and handling of culture plates outside a controlled laboratory environment increases the risk of contamination. In less equipped eye care centres, particularly those in remote regions of the developed world, the full range of nutrient agar may not be available and may impede pathogen identification (Kaye *et al.*, 2003).

The mainstay of treatment for microbial keratitis is topical antibiotic drops or ointments with drops accounting for 90% of the administration routes. Antibiotic drops enable high local concentrations of drugs with minimal systemic side effects. The efficacy is, however, limited by a series of clearance mechanisms that usually protect the eye from foreign debris and infection (Ciolino, 2009; Morrison and Khutoryanskiy, 2014).

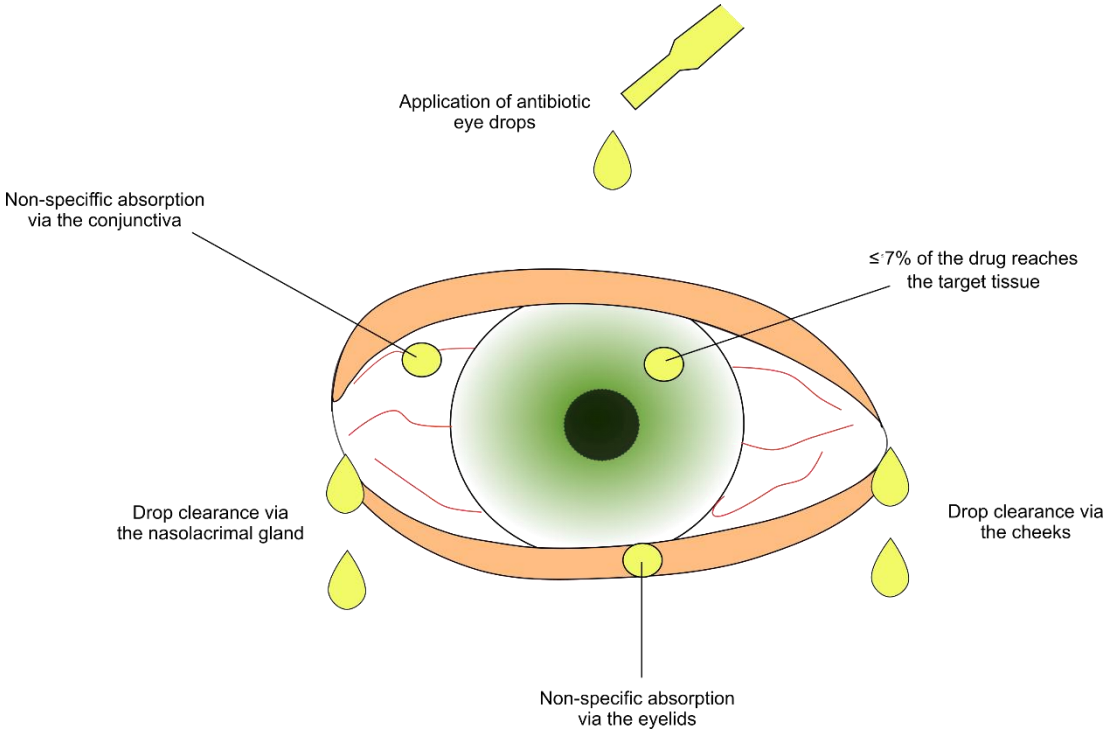

Figure 1.10: Common limitations with antibiotic eye drop administration.

The majority of the drop either immediately drains down the cheek, is cleared down the nasolacrimal duct away from the eye or is absorbed through non-target tissue such as the highly vascular conjunctiva or the eyelids (Figure 1.10). The remainder is subject to non-specific absorption, continuous dilution by the tear film and reflex tearing or dispersed by blinking (Shell, 1982; Ghate and Edelhauser, 2008; Tashakori-Sabzevar and Mohajeri, 2015). As a result, only 1 - 7% of the drug reaches the target tissue and only a fraction of the dose will penetrate the deep layers of the corneal stroma where infections, particularly in cases of fungal keratitis, may extend (O'Day *et al.*, 1984; Järvinen, Järvinen and Urtti, 1995; Manzouri, Vafidis and Wyse, 2001; Ghate and Edelhauser, 2008).

To overcome these limitations, prolong contact time with the cornea and achieve therapeutic drug concentrations, regular (hourly or half-hourly) instillation of drops is required (O'Day *et al.*, 1984). Initially this includes throughout the night for patients with severe keratitis often requiring hospital admission. Although drop frequency decreases as the infection improves, regimes typically last for months (Johns and O'Day, 1988; Thomas and Kaliamurthy, 2013). Unsurprisingly, patient compliance is problematic (Yoltan, 2001). A drug release system which delivers sufficient quantities of drug to the cornea whilst increasing the contact time would improve drug efficacy and patient compliance. It may also have benefits in developing countries where access to healthcare may be limited or where lack of supervision of patients can lead to inadequate drop administration.

1.3 Bandage Lenses

Corneal bandages have been considered as epithelial wound healing devices for decades. Over time they have developed from standard contact lens materials such as poly-(methyl methacrylate) (pMMA) to more advanced polymers such as pHEMA in 1954 (Willoughby, Batterbury and Kaye, 2002; Alvarez-Lorenzo, Yanez and Concheiro, 2010). There were many drawbacks to the use of early contact lenses as bandage contact lenses ranging from a

poor ocular compatibility with the corneal epithelium to incompatibility with the tear film due to the hydrophobicity of the lenses. These complications often led to conditions such as allergic and infective conjunctivitis, corneal thinning and protein fouling of lenses (Hadassah *et al.*, 2008). Modern corneal bandage materials include collagen shields; amniotic membrane derived materials and advanced hydrogel polymers containing silicone monomers or pHEMA hydrogels with additional hydrophilic monomers such as N-vinyl pyrollidone (NVP) and methacrylic acid (MAA) (Willoughby, Batterbury and Kaye, 2002; Saw *et al.*, 2007; Alvarez-Lorenzo, Yanez and Concheiro, 2010; Dell *et al.*, 2011). The purpose of a corneal bandage was originally to protect a post-operative wound on the surface of the eye and relieve discomfort caused by eyelid movement to the highly innervated cornea (Dell *et al.*, 2011). However, research has now focussed on utilising bandage lenses as drug delivery devices for transporting and controlling the release of ocular drugs.

1.3.1 Collagen shields:

Collagen was first introduced for the management of wounds in the 1970s specifically as a wound healing device in the treatment of burns and skin ulcers. It was not until the 1980s that collagen was utilised in ophthalmic applications. In 1984, Fyodorov developed collagen shields as devices to protect post-operative wounds following photorefractive surgery and radial keratotomy (Willoughby, Batterbury and Kaye, 2002; Hadassah *et al.*, 2008).

Collagen is a readily available, natural material that is thought to have good biocompatibility with the corneal epithelium. It also possesses wound healing properties and can provide a good mechanical support for the healing epithelium (Hadassah *et al.*, 2008; Chak, Kumar and Visht, 2013). Collagen shields (Figure 1.11a) have been studied as drug delivery devices whereby the shield is soaked in an appropriate drug solution. The collagen shield then performs as a drug reservoir after applying it to the cornea. The drug releases as the collagen shield degrades thereby providing a limited slow release mechanism that enables prolonged drug-contact time with greater bioavailability (Panda and Sudan, 2003; Kearns and Williams, 2009).

Figure 1.11: a) Collagen bandage lens, reproduced with permission from Elsevier, b) amniotic membrane bandage lens. Image taken from www.biotissue.com, c) size comparison of a hydrogel contact lens and a hydrogel bandage lens. Image taken from www.focalpointeyecare.com.

In some animal studies, high corneal and anterior chamber concentrations of gentamycin, vancomycin, heparin and pilocarpine were obtained after delivery via collagen corneal shields. Minimum inhibitory concentration (MIC) concentrations of tobramycin were obtained in the anterior chamber for 4 - 6 h when delivered via collagen shields (Kleinmann *et al.*, 2006). Another study found MIC concentrations of both gatifloxacin (2.3 μg cm^{-3}) and moxifloxacin (3.1 μg cm^{-3}) in the aqueous humor 3 h after application of antibiotic laden collagen bandages (Kleinmann *et al.*, 2006). One example of a commercial collagen ophthalmic device is Soft Shield® collagen shields (Oasis Medical Inc., San Dimas, CA, USA). They are derived from bovine or porcine collagen and range in dissolution rates from 12 - 72 h. The dissolution rate is controlled via the degree of UV irradiation applied during the cross-linking process (Greenwald and Kleinmann, 2008; Dell *et al.*, 2011). Although collagen shields have been trialled for drug delivery they are expensive, dissolve rapidly and have risks of xenogeneic disease transfer (Willoughby, Batterbury and Kaye, 2002). Visual acuity is also reduced to approximately 6/60 which is less desirable in patients with early stage or milder keratitis who may otherwise maintain near normal vision (Friedberg, Pleyer and Mondino, 1991; Wedge and Rootman, 1992). Additionally, this opacity requires the shield to be removed so the clinician can assess the cornea to monitor disease progression. Other drawbacks for collagen shields include the impermissible use of bovine and porcine collagen to patients of certain religious groups, biological incompatibility for individuals with specific allergies as well as concerns of initial discomfort upon insertion, foreign body

sensation and irritation due to the acidic pH of collagen (Dell *et al.*, 2011; Guzman-Aranguez, Colligris and Pintor, 2013).

1.3.2 Amniotic membrane:

The use of amniotic membrane as a suitable substrate for transplantation was first described by Davies in 1910 as a skin graft. A surge in publications describing its use as a substrate for transplantation followed with applications such as a bandage for dressing burns or non-healing skin ulcers as well as a substrate in hernia repair and prevention of tissue adhesion following surgery (Dua *et al.*, 2004). However, it was not until de Rötth followed by Sorsby and Symons in the 1940s that amniotic membrane transplantation was described in ophthalmic applications. It was primarily described as a substrate for conjunctival plastic surgery and as a bandage for ocular chemical burns with some initial success, however, for unknown reasons further research was limited over the next five decades (Kruse, Rohrschneider and Völcker, 1999; Dua *et al.*, 2004). Following conception, the amniotic membrane along with the placenta derives from the outer cell mass whilst the foetus develops from the inner cell mass. It consists of an epithelial layer in contact with a basement membrane and an avascular stromal layer with a varying thickness of between 20 µm and 500 µm (Azuara-Blanco, Pillai and Dua, 1999; Dua *et al.*, 2004; Liu, Sheha and Fu, 2010). Several characteristics that make the amniotic membrane a suitable candidate for transplantation include anti-inflammatory, bacteriostatic and anti-scarring properties, pain reduction and wound healing properties followed by a lack of immunogenicity (Azuara-Blanco, Pillai and Dua, 1999; Fish and Davidson, 2010; Gheorghe *et al.*, 2016).

Amniotic membrane transplantation was re-introduced by Kim and Tseng in 1995 as a treatment for epithelial defects from corneal ulcers. They also further developed a method of preservation and storage that has established its role as a membrane for ophthalmic applications (Kruse, Rohrschneider and Völcker, 1999; Dua *et al.*, 2004; Thatte, 2011). Amniotic membrane has since been developed as both a bandage lens material to reduce inflammation and as a sutured graft to replace a damaged ocular surface and

promote wound healing (Hanada *et al.*, 2001). ProKera® (Bio-Tissue Inc., Doral, FL, USA) (Figure 1.11b) is one such commercial amniotic membrane device and was approved by the FDA in 2003 as a medical device in the treatment of bacterial keratitis, chemical injuries and Stevens-Johnson syndrome (Suri *et al.*, 2013). The device is an amniotic graft surrounded by a 16 mm polycarbonate ring that is placed on the surface of the eye by inserting between the upper and lower eye lids (Trattler, 2012). ProKera® can be applied as a sutureless bandage which reduces surgery time and costs, allows for topical anaesthesia and eradicates inflammation caused by the insertion of sutures (Liu, Sheha and Fu, 2010). In one study ProKera® relieved discomfort and reduced inflammation within 96 h of application in three cases of severe microbial keratitis followed by healing of the corneal ulcer (Sheha *et al.*, 2009). However, in a more recent study where ProKera® was applied to eyes with microbial keratitis only 44% of those healed with partial or complete success (Suri *et al.*, 2013). This variation in clinical success is thought to be due to the varying biologic composition of amniotic membrane and methods used in storage of amniotic membranes prior to procedures. The possibility of transmissible infections and tissue variability are two prominent reasons for the reduced availability of amniotic tissue for transplantation (Pratoomsoot *et al.*, 2008).

1.3.3 Hydrogel bandage contact lenses:

Most of the drawbacks attributed to collagen shields and amniotic membrane as ocular bandage lens materials have been resolved with the development of advanced hydrogel lenses. These hydrogels are composed of non-animal derived materials with an improved visual acuity, coupled with greater comfort and oxygen permeability due to their increased water content (Dell *et al.*, 2011). The idea that soft contact lenses could be used in a therapeutic setting as bandage lenses was conceived by Kaufman in the 1970s and were mainly used for the protection of corneal wounds. He discovered that diseased and damaged corneas would heal faster if a soft contact lens was applied (Stein, 2008; Mohammadpour *et al.*, 2015). Present day use of hydrogel bandage contact lenses (Figure 1.11c) include but are not limited to pain management, provision of a barrier function to protect a wound from the

natural blinking mechanism and the external environment, promotion of re-epithelialisation and most recently in the elution of ocular drugs (McMahon and Zadnik, 2000).

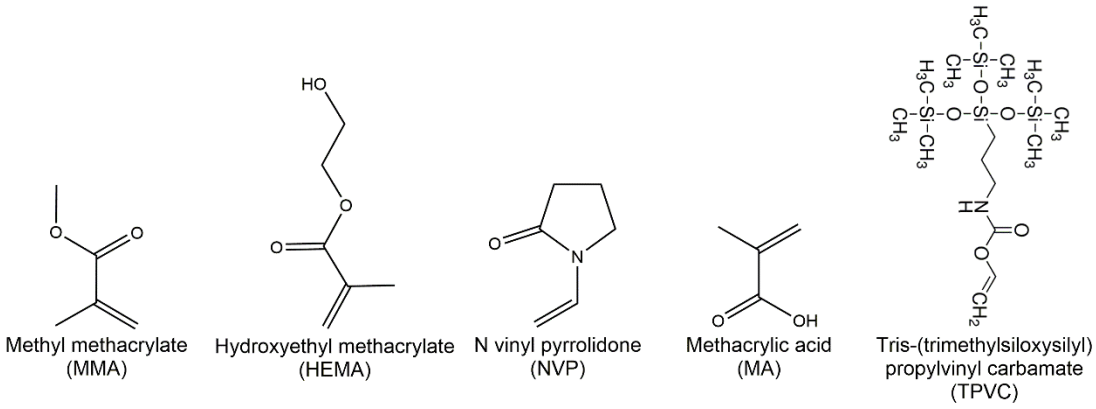

Figure 1.12: Some of the most common hydrogel contact lens monomers.

Modern day hydrogel bandage contact lenses are either conventional HEMA or silicone-based hydrogels that conform to the surface of the eye (Figure 1.12). Conventional hydrogel lenses are usually high water content polymers with oxygen transmissibility (Dk) corresponding to the water content. Unfortunately, no hydrogels meet the 87 Barrer Dk value required for a lens to be recommended for overnight wear. A typical high water content (74%) hydrogel has a Dk of 36 Barrer (Blackmore, 2010; Tashakori-Sabzevar and Mohajeri, 2015). Despite not meeting the recommendation for extended use, conventional hydrogel lenses remain the most common lenses used as bandage contact lenses (Grentzelos *et al.*, 2009; Mohammadpour *et al.*, 2015). The introduction of hydrophobic silicone monomers into hydrogel lenses greatly enhanced the oxygen permeability. Once incorporated, the amorphous silicone bulk material creates space between the hydrogel's polymer chains allowing for smaller molecules such as oxygen to pass through more freely (Nicolson and Vogt, 2008). Therefore, silicone hydrogel lenses have a greater oxygen transmissibility that allows more oxygen to

reach the cornea resulting in less hypoxia and the potential for longer term wear (Blackmore, 2010). Lotrafilcon A has been FDA approved for 30 day continuous wear whilst a more recent iteration lotrafilcon B has gained FDA approval for 6 days of continuous wear (Grentzelos *et al.*, 2009). Silicone hydrogel lenses also provide a greater mechanical protection; however, the increased elastic modulus provides less comfort than lower elastic moduli conventional hydrogel lenses. In the decade following the introduction of silicone hydrogel lenses, new generation silicone hydrogel lenses (senofilcon A and comfilcon A) are addressing this issue with lower elastic moduli and increased water contents whilst maintaining a similar degree of oxygen transmissibility as older generation silicone hydrogel materials (lotrafilcon A and balafilcon A) (Table 1.1).

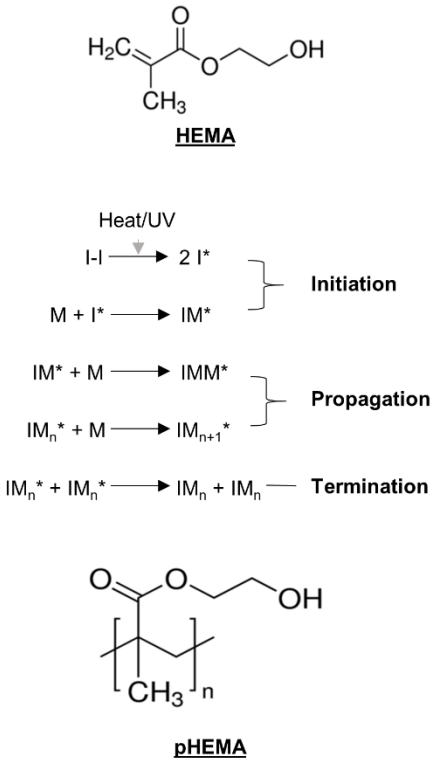

Figure 1.13: Addition polymerisation process used to make pHEMA hydrogels. Other monomers such as those in Figure 1.12 are usually added and result in co-polymers. I - Initiator, I* - free radical, M - monomer, M* - monomer free radical.

These new generation silicone hydrogels allow for greater comfort and less disruption of the tear film and cornea via hydrophobic interactions (Blackmore, 2010; Baenninger, 2014). This was mainly achieved with the incorporation of hydrophilic monomers such as PVP within the polymer matrix (senofilcon A) as opposed to plasma treatment (lotrafilcon A and balafilcon A) in improving wettability. Structural changes such as the addition of longer chain monomers (comfilcon A) has also helped to achieve lower moduli (Nicolson and Vogt, 2008; Tighe, 2013).

Polymers in general are chemically synthesised by either addition or condensation polymerisation. However, in the case of hydrogel lens materials, addition polymerisation is the predominant method and occurs between vinyl groups (C = C) of monomers. This route requires heat or a UV source to form free radicals from a decomposed chemical initiator that in turn combines with monomers to form free radical monomers that react with other monomer units to form part of a growing polymer chain (Figure 1.13). The reaction components are usually contained within a solvent mixture to maintain solubility. The choice of initiator and reaction parameters are usually dictated by the method used to cast a lens which is either spin casting, lathing or the most widely used method, cast moulding. Lathed lenses are cut from solid dehydrated hydrogel buttons that have long polymerisation times. Thermal initiators with low activation energies are used so reaction temperatures can be set lower. Buttons are usually much greater in volume than the final lathed lens so they allow for any surface imperfections to be removed during processing. Spin casting normally involves short polymerisation times (≤ 1 h), however a diluent is required to ensure efficient mixing of monomers during polymerisation and the reaction is often purged with nitrogen to provide anaerobic conditions. Cast moulded lenses also involve relatively short polymerisation times whereby monomers are polymerised between two moulds with a rapid rise in temperature required during the curing process. Cast moulding is the current method of choice for disposable lens manufacture (Maldonado-Codina and Efron, 2003; Winterton and Su, 2005; Maldonado-Codina, 2017).

Hydrogel bandage contact lens use as a primary treatment for corneal abrasions was first described in the 1980s (Acheson, Joseph and Spalton, 1987) with quicker healing times and most patients reporting less discomfort. Hydrogel bandage contact lenses have also been used to treat corneal abrasions on soldiers in a battlefield situation and in most cases this allowed them to remain on full duty due to retention of visual acuity and a reduction in pain. These factors could prove vital in a combat situation (Buglisi *et al.*, 2007). Recurrent corneal erosion is another condition that has been treated with hydrogel bandage contact lenses. It is usually characterised by repeated breakdown of the corneal epithelium and may progress from episodes of corneal abrasion and trauma. In one study 9 of 12 patients treated with a hydrogel bandage contact lens reported no recurrent corneal erosion 1 year later with only 1 of 12 patients reporting a recurrence of the condition (Fraunfelder and Cabezas, 2011).

Hydrogel	Monomers	Name	Water Content (%)	Dk (Barrer)	Elastic Modulus (MPa)
Conventional Hydrogel					
Omafilcon A	HEMA, 2-Methacryloxyethyl phosphorylcholine **(**PC)	Proclear (Coopervision)	62	27	0.49
Lidofilcon A	MMA, NVP	Omniflex (Coopervision)	70	32	0.31
Silicone Hydrogel					
Lotrafilcon A	TRIS, fluoroether macromer, dimethylacrylamide (DMA)	AIROPTIX Night and Day (CIBA Vision)	24	140	1.4
Balafilcon A	3-[Tris(trimethylsiloxy)silyl] propyl vinyl carbamate (TPVC), NVP	PureVision (Bausch & Lomb)	36	99	1.1
Senofilcon A	Modified 3-[Tris(trimethylsiloxy)silyl] propyl methacrylate (TRIS), Poly-(vinylpyrrolidone) (PVP)	Acuvue OASYS (Vistakon)	38	103	0.73
Comfilcon A	Long-chain siloxane macromer	Biofinity (Coopervision)	48	128	0.75
Lotrafilcon B	TRIS, fluoroether macromer, DMA	O_2Optix (CIBA Vision)	33	110	1.2

Table 1.1: Comparison of mechanical and physical properties of conventional and silicone contact lens materials. Adapted from (Maldonado-Codina and Efron, 2003; Blackmore, 2010; Mohammadpour *et al.*, 2015; Bhamra and Tighe, 2017).

Another area where hydrogel bandage contact lenses are used is post-surgery and in particular after photorefractive keratectomy. In a study of 44 patients, re-epithelialisation was reported to be complete 3 days after surgery in 75% (lotrafilcon A) and 72.7% (lotrafilcon B) of cases (Grentzelos *et al.*, 2009).

The most common complication reported following the application of hydrogel bandage contact lenses in the treatment of ocular conditions is microbial keratitis. The increased risk comes from extended wear silicone hydrogel bandage contact lenses which comes as no surprise as the same trend is noted with extended wear vision correction silicone hydrogel lenses. An increase of 4.1 to 13.3 times risk of microbial keratitis has been observed for extended wear over daily wear lenses (Saini *et al.*, 2013). In one study, pain reduction and better post-operative results were observed from patients wearing a lotrafilcon A silicone hydrogel bandage lens compared to those wearing the conventional hydrogel lens omafilcon A. However, less corneal infiltrates were observed in those patients wearing omafilcon A bandage lenses (Edwards *et al.*, 2008). In another study the combined approach of antibiotics and the application of a silicone hydrogel bandage contact lens could not prevent the occurrence of microbial keratitis (Saini *et al.*, 2013). Conventional hydrogel bandage lenses have also been implicated in cases of microbial keratitis and in one study 13% of patients were treated for microbial keratitis following the application of conventional hydrogel bandage lenses to treat corneal abrasions (Buglisi *et al.*, 2007).

1.4 Recent work around drug eluting bandage lenses

Recently, studies have intensified into controlling the release of drugs from bandage lens materials to directly promote wound healing and lower the microbial burden at the site of an ocular wound. Several different methods of drug attachment to bandage lenses have been described including covalent attachment and ionic interaction of drugs to functional groups within the hydrogel bandage lens matrix, molecular imprinting, absorption of drugs into

the hydrogel or addition of drug loaded nanoparticles into the hydrogel matrix (Figure 1.14) (Ciolino *et al.*, 2009; Garhwal *et al.*, 2012; Guzman-Aranguez, Colligris and Pintor, 2013; Kakisu *et al.*, 2013). The incorporation of drugs should not compromise the mechanical or optical properties of bandage contact lenses whilst also remaining non-toxic to the corneal epithelium after application of the lens (Ciolino, 2009).

1.4.1 Absorption of drugs within a hydrogel matrix:

Absorption of drugs into hydrogel networks is the simplest, conventional and most cost-effective method of hydrogel drug incorporation. It usually involves soaking of a hydrogel contact lens material in a solution of the drug of choice for a period of time to allow drug saturation of the lens (Maulvi, Soni and Shah, 2016). Drug concentration is usually dependant on and limited by the water content of the hydrogel as the absorption of the drug is a simple equilibrium of the drug concentration in the soaking solution and the concentration within the hydrogel. After application of the hydrogel to the eye the drug releases via simple diffusion from the hydrogel into the post-lens tear film (Filipe *et al.*, 2016; Maulvi, Soni and Shah, 2016). This is aided by the blink cycle, as the anterior surface of the lens becomes dry immediately after blinking this allows for the diffusion of up to 5 times greater amounts of drugs to the post-lens tear film than to the replenished lachrymal fluid at the anterior surface of the lens (Alvarez-Lorenzo, Yanez and Concheiro, 2010). The hydrogel performs like a drug reservoir ensuring greater drug contact time with the tear film and cornea allowing for greater concentrations to be achieved.

Absorption of drugs via a soaking method has been tested for decades. Ruben and Watkins (1975) described the elution of pilocarpine from soft contact lenses and in more recent times Maulvi *et al.* (2015) described the release of hyaluronic acid from hydrogel contact lenses for the treatment of dry eye syndrome. Other examples include the loading and elution of the antimicrobial cationic peptide melimine. Willcox *et al.* (2008) reported an 80% reduction in viable *P. aeruginosa* and *S. aureus* when cultured in the presence of an etafilcon A lens loaded with melimine.

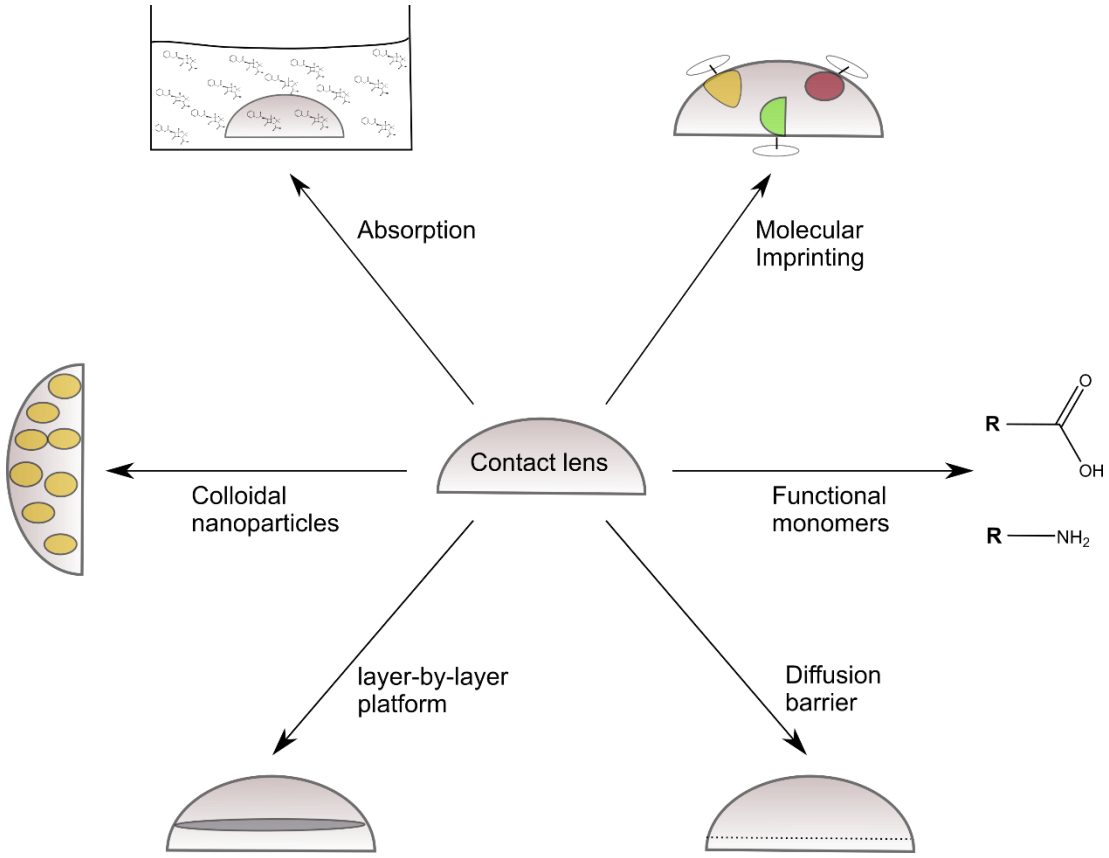

Figure 1.14: Methods currently used for incorporation of drugs and their controlled release from contact lens materials.

Some of the limitations associated with this method of drug incorporation include a limited drug loading capacity determined by the water content and thickness of the lens combined with the drug soaking time, a short release time of usually < 2 h coupled with a 'burst' release profile that sees much of the drug released almost immediately after application of the hydrogel followed by a slower release of much lower concentrations of the drug. These initial high concentrations of drugs can cause toxicity to the corneal epithelium. Current research is focussing on drug release that follows 'zero-order' kinetics i.e. a slower release of drugs at constant concentrations (Xinming *et al.*, 2008; Ciolino, 2009; Chauhan, 2015). Another limitation is that high molecular weight and hydrophobic drugs cannot penetrate the aqueous portion of the hydrogels and tend to remain on the surface thereby limiting their uptake (Maulvi, Soni and Shah, 2016).

1.4.2 Attachment of drugs to functional groups in a hydrogel:

Another method of drug loading involves attachment of ionic drugs to functional groups within the hydrogel matrix. This is similar to the soaking method but a stronger bond is formed either ionically or with additional cross-linking chemistry resulting in a more permanent covalent bond between drug molecule and hydrogel. Ionic attachment of drugs to a hydrogel results in an anionic/cationic drug-hydrogel complex. Drug release is facilitated by ionic components within the tear film such as sodium and chloride that gradually displace the drug from the hydrogel over time (Chauhan, 2015). Covalent attachment of drugs to hydrogels result in a more local drug concentration as it remains attached to the hydrogel for longer than ionic binding allows. Cleavage of attached biomolecules is initiated by hydrolytic enzymes and can result in a slower release profile (Filipe *et al.*, 2016).

Some examples of drug adsorption to hydrogels include a pHEMA-co-MAA hydrogel with a relatively low water content (38%) and an elastic modulus within the range of commercial lens materials (0.76 MPa). A high loading of gatofloxacin was obtained (11.78 μg mg^{-1}) and was released slowly over 24 h without an initial burst release profile. The drug loading was threefold greater than that obtained from a pHEMA only and a commercial pHEMA based hydrogel that included NVP, ethyl methacrylate (EMA) and glycidyl methacrylate (GMA) (Shi *et al.*, 2013). Melimine has also been covalently attached to etafilcon A lenses (152 μg $lens^{-1}$) and the antimicrobial activity measured. A reduction in both *P. aeruginosa* (3.1 log) and *S. aureus* (3.9 log) was observed as well as a 2 log reduction in multi-drug resistant strains of the same organisms. A significant reduction in adhesion of viable organisms was also observed compared to the non-melimine coated control (Dutta *et al.*, 2013).

The drug attachment approach has similar limitations to drug absorption (section 1.4.1) in that associated drugs have a short release profile but this may be prolonged with the addition of covalently attached drugs or the addition of functional monomers to the hydrogel to add a much higher loading of the drug of choice. In one case a pHEMA lens with NVP and aminopropyl

methacrylamide (APMA) functional monomers increased loading of ibuprofen and diclofenac by 10- and 20-fold followed by a release that lasted 24 h and 1 week respectively (Andrade-Vivero *et al.*, 2007). Any additional molecules must not modify the optical, physical or mechanical properties of the lens. Another limitation that can be rectified with the addition of further ionic monomers is the swell and contraction of the hydrogel network after disassociation of the drug and association of various salts such as chlorides from the surrounding tear film (Xinming *et al.*, 2008).

1.4.3 Colloidal nanoparticles:

The incorporation of drug-laden colloidal systems such as nanoparticles, micro-emulsions, micelles and liposomes into hydrogels during polymerisation are aimed at increasing the overall drug loading capacity and control of the release time (Maulvi, Soni and Shah, 2016). Upon insertion on the eye the drug diffuses away from the colloidal nanoparticles and towards the post-lens tear film. This diffusion is slowed due to the drug having to diffuse through nanoparticles into the lens and then from the lens into the tear film and in turn providing a continuous release for extended periods of time (Xinming *et al.*, 2008). Encapsulating the drug in colloidal nanoparticles protects the drug from the initial polymerisation of the hydrogel but once inserted on the eye it can prevent enzymatic degradation from lysozymes and other enzymes in the tear film (Maulvi, Soni and Shah, 2016). The choice of colloidal nanoparticle system can also greatly enhance drug delivery by overcoming the effective barriers of the corneal epithelium and stroma that inhibit hydrophilic and hydrophobic drugs, respectively. The corneal epithelium mucosa is negatively charged and therefore cationic molecules are more permeable at physiological pH. To overcome this, cationic liposomes have been found to be more effective at delivering drugs such as penicillin G and tropicamide than anionic and neutral liposomes (Gaudana *et al.*, 2010).

Silica based nanoparticles laden with the hydrophobic drug lidocaine have been polymerised inside a pHEMA hydrogel. The introduction of the nanoparticles reduced the light transmittance of the hydrogel to 78%

compared to an 88% transmittance through a pHEMA hydrogel without nanoparticles incorporated. An initial drug loading of 0.23 mg g^{-1} was obtained and a release of lidocaine was observed over an 8 day period (Gulsen and Chauhan, 2004). Polycaprolactone nanospheres have been formulated to contain ciprofloxacin prior to incorporation into pHEMA lenses. Of the total amount of ciprofloxacin released (274.9 µg) from the hydrogels the majority (255.9 µg) was released in the first 24 h. This was sufficient to prevent proliferation of both *P. aeruginosa* and *S. aureus* for 3 days after application of the lens (Garhwal *et al.*, 2012).

Several limitations are associated with this method of drug loading including a decrease in water content, lower refractive index and an increase in elastic modulus due to the introduction of particles within the hydrogel matrix (Maulvi, Soni and Shah, 2016). This may result in undesirable properties such as an increase in discomfort of the lens, decreased oxygen permeability and a loss of visual acuity. Another limitation may the instability of the drug within the colloidal nanoparticles during storage and transportation resulting in diffusion into the hydrogel matrix. This would effectively nullify any slow, continuous release properties from the colloidal nanoparticles and rely solely on diffusion of the drug through the hydrogel (Xinming *et al.*, 2008).

1.4.4 Molecular imprinting:

Molecular imprinting technology was first developed in 1972; however, it is a relatively new method in the controlled release of drugs from hydrogel bandage contact lenses (Wulff, 1995; Tashakori-Sabzevar and Mohajeri, 2015). Molecular imprinting seeks to optimise the spatial distribution of functional monomers to increase the efficiency of the interactions between the hydrogel and the drug. This is achieved by mixing functional monomers and the drug together to form self-assembled complexes that are then polymerised within the hydrogel. The drug is then removed to leave imprinted cavities and bonding preferences that allow a greater affinity for a specific drug (Xinming *et al.*, 2008; Chauhan, 2015). There are two approaches to molecular imprinting either covalent or ionic interaction of the target molecule-functional monomer matrix. Ionic interaction is preferred in drug -

polymer situations as this allows faster binding and release properties (Alvarez-Lorenzo, Yanez and Concheiro, 2010; Tashakori-Sabzevar and Mohajeri, 2015). A reported two- to threefold increase in drug loading capacity compared to absorption alone has been reported via this method (Kearns and Williams, 2009).

Numerous studies have identified molecular imprinting technology as having greater loading and slower drug release capacities than absorption or the chemical attachment of drugs alone. A 4- to 50-fold greater mean residence time of ketotifen was observed from imprinted pHEMA lenses compared to a non-imprinted control (Tieppo *et al.*, 2012). Other studies have noted smaller increases of two- to threefold greater concentrations of timolol in the tear fluid from imprinted lenses compared to their non-imprinted lens controls (Hiratani *et al.*, 2005). High molecular weight molecules such as hyaluronic acid have also been molecularly imprinted and the release controlled from poly-(vinyl alcohol) (PVA) lenses. The ratio of functional monomers was increased to prolong the release of the hyaluronic acid from the lenses. Hyaluronic acid was released at a rate of 6 μg h^{-1} over a 24 h period (Ali and Byrne, 2009).

A few limitations have been noted with molecular imprinting technology for ophthalmic applications including swelling and contraction of the hydrogel network due to interactions with the tear film. This distorts the imprinted cavities which thereby inhibits the drugs affinity to these areas within the hydrogel (Alvarez-Lorenzo, Yanez and Concheiro, 2010). The water content may also be reduced due to the swelling and contraction resulting in increased discomfort and reduced oxygen permeability (Maulvi, Soni and Shah, 2016). Drug loading is dependent on the functional monomers and the target molecules that have been used to imprint the cavities and it is difficult to control drug release (Xinming *et al.*, 2008).

1.4.5 Layer-by-layer platforms:

A less widespread technique to control drug release from hydrogel contact lenses involves the incorporation of poly-(lactic-*co*-glycolic acid) (PLGA) films coated with a drug into contact lenses. Drug elution is determined by the ratio

of drug - PLGA which can be easily altered prior to incorporation (Maulvi, Soni and Shah, 2016). Ciolino and co-workers have developed pHEMA hydrogels with drug covered PLGA layers incorporated into the matrix. In one instance, they incorporated econozole into PLGA films prior to forming a pHEMA hydrogel with results indicating fungicidal activity towards *C. albicans* in vitro. In another instance the glaucoma drug, latanoprost, was incorporated in the same way and results showed an early burst release followed by a slow release of the drug for a further month (Ciolino *et al.*, 2009, 2011, 2014). Several limitations with this layer-by-layer method are yet to be addressed including a lack of transparency due to the drug - PLGA films, alterations to the mechanical properties of the pHEMA hydrogels, reduced oxygen permeability and an increase in protein fouling of the lens (Maulvi, Soni and Shah, 2016).

1.4.6 Diffusion barriers:

The inclusion of diffusion barriers is another lesser known method of regulating drug elution from hydrogels. The most common diffusion barrier is the hydrophobic molecule vitamin E. The hydrophobic nature of the barrier minimises the rapid diffusion of drug molecules from within the hydrogel to the external solution. Contact lenses loaded with 30% vitamin E were able to extend elution time of dexamethasone by 7 - 9 days from hydrogel contact lenses which is a 9- to 16-fold increase over hydrogels without vitamin E added (Filipe *et al.*, 2016). The inclusion of diffusion barriers still have some limitations to overcome including reduced mechanical properties and oxygen permeability as well as increased protein fouling and reduced water content due to the hydrophobicity of vitamin E (Maulvi, Soni and Shah, 2016).

1.5 SpheriTech Ltd. hydrogels

The peptide based polymer in this study has previously been developed in macroporous form as a wound dressing and a 3-D scaffold for tissue engineering applications (Wellings and Gallagher, 2012) (Figure 1.15). The polymer is based on poly-ε-lysine (pεK) cross-linked with bis-carboxylic acids.

A feature which makes this hydrogel unique is the incorporation of two naturally occurring non-animal derived components, pεK and short to medium chain bis-carboxylic acids. PεK is an edible, non-toxic, cationic homo-poly-amino acid composed mostly of 25 - 35 lysine residues with an amide linkage between the α-carboxyl and the ε-amino groups. It is currently used as an emulsifier and preservative in foodstuffs and has been classified as 'generally regarded as safe' (GRAS) by the FDA since 2004 (Nishikawa and Ogawa, 2006; Shih, Shen and Van, 2006; Hyldgaard *et al.*, 2014). PεK was first isolated by Shima and Sakai (1977) from the soil bacterium *Streptomyces albulus* 346 during screening for Dragendorff positive substances (Bankar and Singhal, 2013).

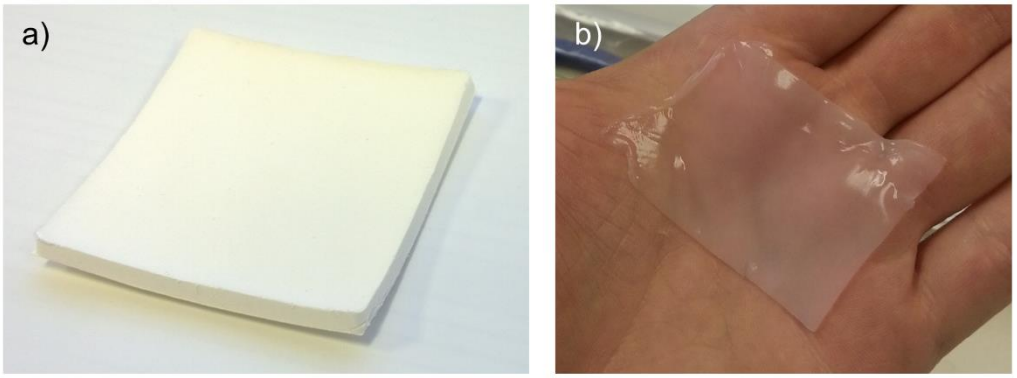

Figure 1.15: a) Macroporous pεK/tridecanedioic acid 10 cm^2 wound dressing, b) early prototype pεK/decanoic acid hydrogel.

The pεK molecule is highly soluble in aqueous media and stable at high temperatures including after autoclaving at 120 °C for 20 min (Shih, Shen and Van, 2006; Li *et al.*, 2014). PεK is antimicrobial against a broad spectrum of Gram-positive and Gram-negative bacteria, yeasts and mould with MICs of < 100 μg cm^{-3} for most organisms tested including *E. coli* (8 μg cm^{-3}), *S. aureus* (16 μg cm^{-3}) and *C. albicans* (54 μg cm^{-3}) (Zhou *et al.*, 2011; Ye *et al.*, 2013). Furthermore, the natural pεK has been found to be less toxic and more antimicrobial than the synthetic poly-α-lysine (pαK) which has been used more commonly for biological applications (Shima *et al.*, 1984; Shih,

Shen and Van, 2006). Short to medium chain bis-carboxylic acids are found in both plants and animals. In the latter they are products of the ω-oxidative degradation of longer chain mono-carboxy fatty acids (Passi *et al.*, 1983; Volkman, 2006). Medium chain bis-carboxylic acids have greater water solubility than their mono-carboxy fatty acid equivalents due to the carboxylic functional groups at each end of the molecule (Grego and Mingrone, 1995). Short to medium chain bis-carboxylic acids have been administered as treatments for several disorders including melisma, toxic melanoderma, acne and in killing malignant melanocytes in humans without having cytotoxic effects on normal healthy cells (Passi *et al.*, 1983). Furthermore, they are β-oxidised by the mitochondria and peroxisomes to acetyl-CoA, malonyl-CoA and succinyl-CoA to become substrates for lipogenesis and gluconeogenesis (Kølvraa and Gregersen, 1986; Grego and Mingrone, 1995; Houten *et al.*, 2012).

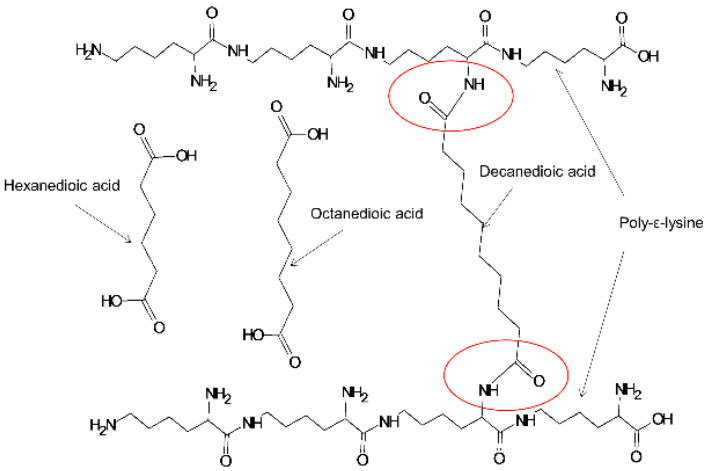

Figure 1.16: Proposed nature of the cross-linking between pεK and bis-carboxylic acids.

The proposed nature of the cross-linking involved in the polymerisation of the pεK/bis-carboxylic acid polymer has been detailed (Figure 1.16). The α-amino group of the lysine residues of pεK are cross-linked to form an amide bond with either end of a bis-carboxylic acid residue via condensation polymerisation (Figure 1.17). The cross-linking is mediated by 1-Ethyl-3-(3-

dimethylaminopropyl) carbodiimide (EDCI)/ N-hydroxysuccinimide (NHS) to introduce a zero-length cross-link between the pεK and bis-carboxylic acid under aqueous conditions (Grabarek and Gergely, 1990). This method of cross-linking is well established as carbodiimides were identified over 100 years ago followed by NHS esters in the 1960s and have since been used in peptide synthesis and bioconjugation techniques (Wilchek and Miron, 1987; Nakajima and Ikada, 1995). EDCI in the presence of a carboxylic acid will form an intermediate O-acylisourea which subsequently reacts with NHS to form the more stable NHS ester of the carboxylic acid. The ester upon reaction with a primary amine forms an amide bond with reconstituted NHS and isourea as the by-products (Hermanson, 2013b).

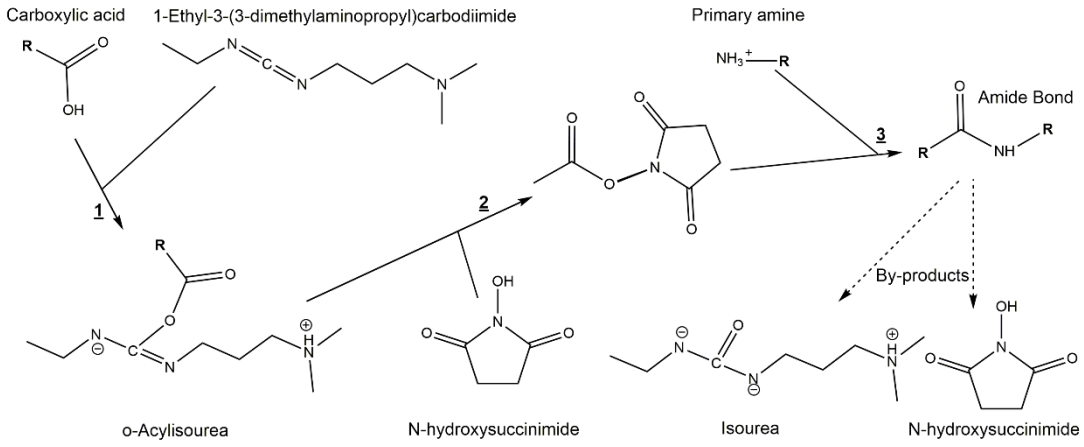

Figure 1.17: Cross-linking chemistry used to form an amide bond between pεK and bis-carboxylic acids.

The very nature and degree of the cross-linking that results in the formation of a hydrogel allows for the potential attachment of other biomolecules to the polymer backbone. A possibility is to attach (absorb, ionic, covalent) an array of biomolecules for the diagnosis and treatment of conditions such as microbial keratitis.

A pεK/methacrylamide hydrogel has been previously described that is non-cytotoxic to human primary keratinocytes that has an antimicrobial activity against a broad spectrum of organisms including *P. aeruginosa*, *S. aureus* and *C. albicans*. The hydrogels described had an elastic modulus between 0.1 - 0.2 MPa and suggested as potential antimicrobial coatings for medical devices (Zhou *et al.*, 2011). These previous findings suggest that a viable antimicrobial hydrogel based on pεK may be possible. The elastic modulus of pεK hydrogels has already been described as similar to commercial contact lens materials. Another pεK hydrogel with dextran aldehyde has been described as a non-viral gene carrier for gene therapy with the biodegradability of the polymer identified as a potential for controlling release (Togo *et al.*, 2013). Biodegradable polymersomes composed of decanedioic acid and polyethylene glycol have been investigated with encapsulating calcein and a degradation time of 2 weeks was observed. These polymersomes have been suggested for drug carrier applications (Najafi and Sarbolouki, 2003). Both pεK and bis-carboxylic acids have been included as components of drug carriers for delivery and the slow release of drugs.

1.6 Hypothesis/aims

The hypothesis was that a hydrogel with antimicrobial properties could be produced from a pεK/bis-carboxylic acid polymer and have comparable mechanical and physical properties to commercial contact lens materials.

The aims were:

- To investigate and optimise the mechanical and physical properties (water content, transparency, etc.) of the polymer to attain similar values as those already described for commercial contact lens materials.

- To investigate the natural antimicrobial activity towards Gram-positive and Gram-negative bacteria and further enhance this activity with the addition of antimicrobial biomolecules.

- Determine the antifungal capacity of the hydrogel after the sorption of a model antifungal compound.

- Demonstrate how the sorption of an AMP with environmentally sensitive fluorophores could be used to identify Gram-positive and Gram-negative bacteria.

2. MATERIALS AND METHODS

2.1 Hydrogel Characterisation

The hydrogel variants were manufactured in the laboratories of SpheriTech Ltd. (Runcorn, England). The following materials were used in this part of the study; **N,N-dimethylaminopyridine (DMAP)** A13016, **1,10-decanedioic acid** A14158, **N-methylmorpholine (NMM)** A12158, **sodium octane sulfonate** A11243 and **piperidine** A12442 (Alfa Aesar, Haverhill, MA, USA), **NHS** FH02165, **1-hydroxybenzotriazole (HOBt)** FH02087 and **EDCI** FD05800 (Carbosynth Ltd., Compton, England), **0.45 µm syringe filter** F2502-1 (Crawford Scientific Ltd., Strathaven, Scotland), **trifluoroacetic acid (TFA)** 008708 (Fluorochem Ltd., Hadfield, England), **N,N-diisopropylcarbodiimide (DIC)** 222116 (Manchester Organics, Runcorn, England), **phosphate buffered saline (PBS)** BR0014 (Oxoid Ltd., Hampshire, England), **hexanedioic acid** 02130, **octanedioic acid** S5200, **P_2O_5** 79609, **NaH_2PO_4** 17844, **phosphoric acid** 04107, **N,N-dimethyl formamide (DMF)** 33120 and **diethyl ether** 32203 (Sigma-Aldrich, St Louis, MO, USA), **nonanedioic acid** A1318 and **heptanedioic acid** P0435 (TCI Europe, Zwijndrecht, Belgium), **tween 80** 28830, **$NaClO_4 \cdot H_2O$** 27988, **NaOH** 28244, **HCl** 20252, **high-performance liquid chromatography (HPLC) water** 23595 and **MeCN** 20060 (VWR International Ltd., Lutterworth, England), **pεK** (Zhengzhou Bainafo Bioengineering Co., Ltd., Zhengzhou City, China). All HPLC and peptide synthesis equipment was supplied by SpheriTech Ltd whilst all other equipment and reagents were provided by the University of Liverpool unless otherwise stated.

2.1.1 Poly-ε-lysine characterisation:

A reverse phase HPLC technique modified from Hirohara *et al.* (2007) was used to determine the chain length distribution of each batch of pεK . Samples were run on a SpectraSYSTEM AS3000 (Thermo Scientific, Waltham, MA, USA) with a Luna C18 column, 4.6 x 100 mm, 3 µm particle size (Phenomenex, Torrance, CA, USA), kept at room temperature (Figure 2.1). Solvent A was composed of NaH_2PO_4 (10 mmol dm^{-3}), $NaClO_4 \cdot H_2O$

(100 mmol dm^{-3}) and sodium octane sulfonate (10 mmol dm^{-3}) in HPLC H_2O and solvent B was composed of NaH_2PO_4 (20 mmol dm^{-3}), $NaClO_4 \cdot H_2O$ (200 mmol dm^{-3}), sodium octane sulfonate (20 mmol dm^{-3}) in 50:50 HPLC H_2O:MeCN. Both buffers were adjusted to pH 2.6 with dropwise addition of concentrated phosphoric acid. Each analysis was run over 105 min at a flow rate of 0.6 cm^3 min^{-1} with 70 - 100% solvent B over the first 95 min and 100% solvent B for a further 10 min. A 30 min column wash of 90:10 MeCN:H_2O (solvent C) was added at the end of each run. Samples were detected at 215 nm on a SpectraSYSTEM UV100 detector (Thermo Scientific, Waltham, MA, USA).

The following adjustment was made after the inclusion of a new Luna C18(2) column 4.6 x 100 mm, 3 µm particle size (Phenomenex, Torrance, CA, USA). Each analysis was run over 70 min at a flow rate of 0.6 cm^3 min^{-1} with a solvent program of 50 - 80% solvent B over the first 60 min then 80% solvent B for 10 min followed by 80 - 100% solvent B for 10 min and finally 100% solvent C for a further 20 min.

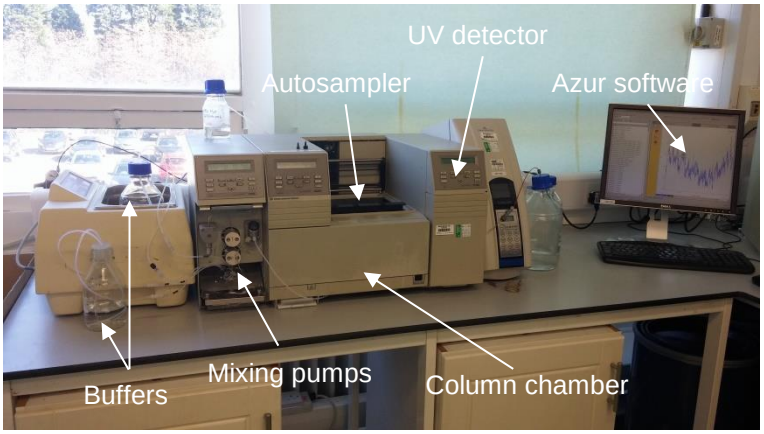

Figure 2.1: HPLC equipment used in experiments.

Analysis of the peak area and percentage of oligomer residues > 20 was carried out using the integration feature on the supplied Azur software (Kromatek Ltd., Great Dunmow, England).

2.1.1.1 Poly-ε-lysine synthetic oligomer synthesis:

Synthetic oligomers of pεK were synthesised via solid phase peptide synthesis using fluorenylmethyloxycarbonyl (Fmoc) chemistry at 5, 10, 15, 20, 25 and 30 residues long as standards to identify the correct chain lengths within each chromatogram (Figure 2.2). A 500 mg aliquot of a 0.8 mmol g^{-1} SpheriTide®™ solid support resin (SpheriTech Ltd., Runcorn, England) was added to a glass Büchner filter funnel with integrated No. 2 glass sinter (Scientific Glass Laboratories Ltd., Stoke-on-Trent, England) and swollen in 50:50 H2O:DMF overnight prior to a 1 h neutralisation with 20 v/v% piperidine in DMF. The resin was washed 10 x DMF. A 4-hydroxymethyl phenoxyacetic acid (HMPA) linker was attached to the resin to provide a carboxylic acid terminal to the oligomers upon cleavage from the resin. HMPA (1.2 mmol, 218 mg) and HOBt (2.4 mmol, 367 mg) were added as solids prior to DIC (1.6 mmol, 252 mm^3). DMF was added until the resin was covered with reaction solution and left for 2 h. A Kaiser test was used to determine reaction completion by comparing with a Kaiser test prior to HMPA attachment with a negative result signalling reaction completion. The first residue of Boc-Lys(Fmoc)-OH (AGTC Bioproducts Ltd, East Riding, England) was double coupled by adding Boc-Lys(Fmoc)-OH (562 mg) and DMAP (5 mg) as solids followed by DIC (186 mm^3). The reaction mixture was covered by adding extra DMF and leaving for 1 h. The reaction components were removed and the resin washed 10 x DMF. The coupling was repeated, the resin washed 10 x DMF and the Fmoc protecting group removed by washing with 20 v/v% piperidine in DMF for 3 min followed by a further 7 min wash. The resin was again washed 10 x DMF followed by a Kaiser test to detect for the presence of amine functional groups from the now de-protected lysine residue. With a positive Kaiser result the reaction continued. A single coupling of Boc-Lys(Fmoc)-OH was repeated a further 29 times with resin removed every 5 residues for cleavage to give the desired oligomer chain lengths.

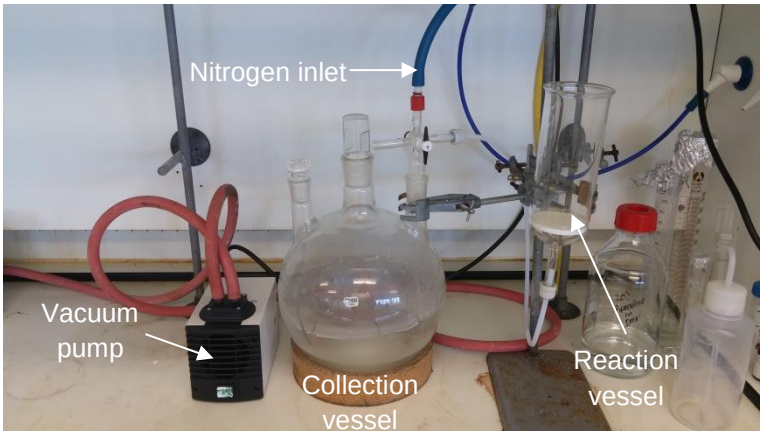

Figure 2.2: Peptide synthesis set up.

2.1.1.2 PεK oligomer work-up:

After every 5 residues of lysine were added a portion of the peptide resin was removed for cleavage from the peptide resin. The resin was added to a glass Büchner filter funnel with integrated No. 2 glass sinter and dried in a step-wise fashion using mixtures of DMF:diethyl ether from 75:25 to 50:50 to 25:75 and finally 100% diethyl ether. A cleavage solution of TFA:H_2O (40 cm^3, 95:5) was added to the dried resin in a round bottom flask and left for 2 h. A glass Büchner filter funnel with integrated No. 2 glass sinter and a collection vessel were set up and washed through with TFA prior to filtering the peptide. The cleavage solution/peptide resin was filtered and the filtrate collected. The retentate was washed 4 x TFA (20 cm^3) to collect as much peptide as possible. The filtrate was rotary evaporated until all liquid had been removed before washing 4 x diethyl ether and decanting each wash. The peptide was left in diethyl ether overnight. Finally, the diethyl ether was decanted and the peptide left to air dry before a final weight and yield was obtained.

2.1.2 Hydrogel design:

The hydrogel material used in this study was composed of pεK cross-linked with a bis-carboxylic acid using an NHS/EDCI mediated cross-linking technique (Figure 1.17). Alterations to the level of cross-linking and the density of the polymer produced different variants of the hydrogel. These alterations were achieved by varying the molar concentrations of either pεK

itself or the bis-carboxylic acid cross-linker. An Excel spreadsheet was prepared to facilitate the calculations and provide the polymer compositions (Appendix 8.1). C, H and N elemental analysis (Butterworth Laboratories Ltd., Teddington, England) was carried out to determine the amine content (mmol g^{-1}) of pεK for this study. The quantity of bis-carboxylic acid added to the polymer mix directly correlated to the percentage of amine groups to be cross-linked. All the polymer compositions for the investigation into the optimal bis-carboxylic acid cross-linker and density are provided below (Tables 2.1 - 2.5).

For a 20 cm^3 final polymer solution pεK was dissolved in water (5 cm^3). The bis-carboxylic acid (500 mmol dm^{-3}) pre-dissolved with a 2:1 molar ratio of NMM, was added to the pεK with 5 v/v% Tween 80 (200 mm^3) and topped up to a final volume (10 cm^3) with water. NHS and EDCI were weighed into a separate tube and topped up with water to a final volume (10 cm^3) and allowed to mix for 5 min. All solutions were filtered to 0.45 µm using a syringe filter. The two solutions were then mixed together to a total volume (20 cm^3) and inverted 5 times before aliquots (10 cm^3) were poured into 10 cm^2 polystyrene weigh boats (175-1414-250, Elkay Laboratory Products Ltd., Basingstoke, England). The polymer was left to polymerise for a minimum of 5 h. The hydrogels were then removed from incubation and washed 10 x in water before storing in water prior to use in experiments.

Reagent	PεK / hexanedioic acid hydrogels			
	60 mol% cross-linked, 0.1 g cm^{-3}	60 mol% cross-linked, 0.067 g cm^{-3}	80 mol% cross-linked, 0.1 g cm^{-3}	80 mol% cross-linked, 0.067 g cm^{-3}
PεK	2.19 g (12.72 mmol)	1.46 g (8.48 mmol)	2.05 g (11.89 mmol)	1.36 g (7.92 mmol)
Hexanedioic acid	0.56 g (3.82 mmol)	0.37 g (2.54 mmol)	0.69 g (4.75 mmol)	0.46 g (3.17 mmol)
NMM	1.39 cm^3	0.93 cm^3	1.30 cm^3	0.87 cm^3
EDCI	3.66 g (19.08 mmol)	2.44 g (12.72 mmol)	4.56 g (23.77 mmol)	3.04 g (15.85 mmol)
NHS	0.73 g (6.36 mmol)	0.49 g (4.24 mmol)	0.68 g (5.94 mmol)	0.46 g (3.96 mmol)

Table 2.1: PεK / hexanedioic acid hydrogel composition.

Reagent	PεK / heptanedioic acid hydrogels			
	60 mol% cross-linked, 0.1 g cm^{-3}	60 mol% cross-linked, 0.067 g cm^{-3}	80 mol% cross-linked, 0.1 g cm^{-3}	80 mol% cross-linked, 0.067 g cm^{-3}
PεK	2.13 g (12.39 mmol)	1.42 g (8.26 mmol)	1.98 g (11.50 mmol)	1.32 g (7.67 mmol)
Heptanedioic acid	0.59 g (3.72 mmol)	0.40 g (2.48 mmol)	0.74 g (4.60 mmol)	0.49 g (3.07 mmol)
NMM	1.36 cm^3	0.91 cm^3	1.60 cm^3	0.84 cm^3
EDCI	3.56 g (18.58 mmol)	2.38 g (12.39 mmol)	4.41 g (23.00 mmol)	2.94 g (15.34 mmol)
NHS	0.71 g (6.19 mmol)	0.48 g (4.13 mmol)	0.66 g (5.75 mmol)	0.44 g (3.83 mmol)

Table 2.2: PεK / heptanedioic acid hydrogel composition.

Reagent	PεK / octanedioic acid hydrogels			
	60 mol% cross-linked, 0.1 g cm^{-3}	60 mol% cross-linked, 0.067 g cm^{-3}	80 mol% cross-linked, 0.1 g cm^{-3}	80 mol% cross-linked, 0.067 g cm^{-3}
PεK	2.08 g (12.07 mmol)	1.39 g (8.05 mmol)	1.92 g (11.14 mmol)	1.28 g (7.43 mmol)
Octanedioic acid	0.63 g (3.62 mmol)	0.42 g (2.41 mmol)	0.78 g (4.46 mmol)	0.52 g (2.97 mmol)
NMM	1.33 cm^3	0.88 cm^3	1.22 cm^3	0.82 cm^3
EDCI	3.47 g (18.11 mmol)	2.31 g (12.07 mmol)	4.27 g (22.29 mmol)	2.85 g (14.86 mmol)
NHS	0.70 g (6.04 mmol)	0.46 g (4.02 mmol)	0.64 g (5.57 mmol)	0.43 g (3.71 mmol)

Table 2.3: PεK / octanedioic acid hydrogel composition.

Reagent	PεK / nonanedioic acid hydrogels			
	60 mol% cross-linked, 0.1 g cm^{-3}	60 mol% cross-linked, 0.067 g cm^{-3}	80 mol% cross-linked, 0.1 g cm^{-3}	80 mol% cross-linked, 0.067 g cm^{-3}
PεK	2.03 g (11.77 mmol)	1.35 g (7.85 mmol)	1.86 g (10.80 mmol)	1.24 g (7.20 mmol)
Nonanedioic acid	0.67 g (3.53 mmol)	0.44 g (2.36 mmol)	0.81 g (4.32 mmol)	0.54 g (2.88 mmol)
NMM	1.29 cm^3	0.86 cm^3	1.19 cm^3	0.79 cm^3
EDCI	3.39 g (17.66 mmol)	2.26 g (11.77 mmol)	4.14 g (21.61 mmol)	2.76 g (14.41 mmol)
NHS	0.68 g (5.89 mmol)	0.45 g (3.92 mmol)	0.62 g (5.40 mmol)	0.42 g (3.60 mmol)

Table 2.4: PεK / nonanedioic acid hydrogel composition.

Reagent	**PεK / decanedioic acid hydrogels**			
	60 mol% cross-linked, 0.1 g cm^{-3}	60 mol% cross-linked, 0.067 g cm^{-3}	80 mol% cross-linked, 0.1 g cm^{-3}	80 mol% cross-linked, 0.067 g cm^{-3}
PεK	1.98 g (11.49 mmol)	1.32 g (7.66 mmol)	1.80 g (10.49 mmol)	1.20 g (6.99 mmol)
Decanedioic acid	0.70 g (3.45 mmol)	0.47 g (2.30 mmol)	0.85 g (4.20 mmol)	0.57 g (2.80 mmol)
NMM	1.26 cm^3	0.84 cm^3	1.15 cm^3	0.77 cm^3
EDCI	3.30 g (17.23 mmol)	2.20 g (11.49 mmol)	4.02 g (20.97 mmol)	2.68 g (13.98 mmol)
NHS	0.66 g (5.74 mmol)	0.44 g (3.83 mmol)	0.60 g (5.24 mmol)	0.40 g (3.50 mmol)

Table 2.5: PεK / decanedioic acid hydrogel composition.

Reagent	**PεK / octanedioic acid hydrogels**			
	60 mol% cross-linked, 0.067 g cm^{-3} **(Su 60 15)**	60 mol% cross-linked, 0.071 g cm^{-3} **(Su 60 14)**	60 mol% cross-linked, 0.077 g cm^{-3} **(Su 60 13)**	65 mol% cross-linked, 0.067 g cm^{-3} **(Su 65 15)**
PεK	1.38 g (8.05 mmol)	1.48 g (8.62 mmol)	1.60 g (9.29 mmol)	1.36 g (7.88 mmol)
Octanedioic acid	0.42 g (2.41 mmol)	0.45 g (2.59 mmol)	0.49 g (2.79 mmol)	0.45 g (2.56 mmol)
NMM	0.88 cm^3	0.95 cm^3	1.02 cm^3	0.87 cm^3
EDCI	2.31 g (12.07 mmol)	2.48 g (12.94 mmol)	2.67 g (13.93 mmol)	2.46 g (12.83 mmol)
NHS	0.46 g (4.02 mmol)	0.50 g (4.34 mmol)	0.53 g (4.60 mmol)	0.45 g (3.91 mmol)

Table 2.6: Su 60 15, Su 60 14, Su 60 13 and Su 65 15 hydrogel compositions.

The hydrogel composition was further modified to investigate variants (Su 60 15, Su 60 14, Su 60 13 and Su 65 15) with octanedioic acid as the bis-caboxylic acid (Table 2.6).

The codes designated to the hydrogels are derived from their composition. For example, Su 60 14 is a pεK/octanedioic acid (Su for suberic acid) hydrogel cross-linked to 60% of the total amine groups available and at a density of 0.07 g cm^{-3} (14 for 14 cm^3 g^{-1} which is the reverse of 0.07 g cm^{-3}).

2.1.3 Mechanical property analysis:

Mechanical properties of the hydrogel variants were measured using a Linkam TST350 tensile tester (Linkam Scientific Instruments Ltd., Tadworth, England). Stress (σ), strain (ε) and elastic modulus (E) were determined for each sample.

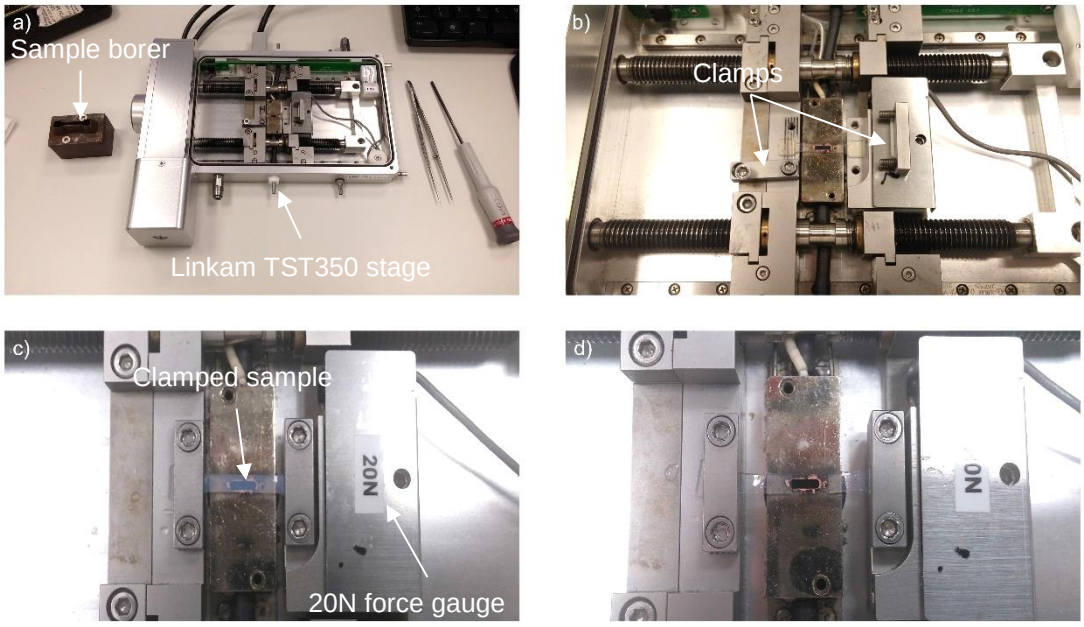

Figure 2.3: Linkam tensile tester. a) Linkam TST stage with some tools commonly used, b) hydrogel loaded onto the stage, c) hydrogel clamped into position immediately prior to test, d) a failed hydrogel after a tensile test.

Hydrogel samples were removed from aqueous storage and cut to a 15 mm long dog bone shaped piece using a borer. The width and thickness of each sample was measured with an Absolute Digimatic caliper (Mitutoyo Ltd., Andover, England) and the readings recorded. The sample was then mounted in the Linkam tensile tester and secured in place with the provided clamps (Figure 2.3). The software was run and each sample was elongated until breakage point. A 20 N load cell was used for all mechanical analysis with a strain rate of 100 μm s^{-1}. Results were recorded and analysed using the supplied Linksys32 software.

2.1.4 Optimum polymerisation time and temperature:

Hydrogel Su 60 14 was polymerised as in section 2.1.2 but with the following modifications. Samples to determine the optimum polymerisation temperature were incubated at three different temperatures (6, 21.5 and 37 °C) for a total of 5 h. Polymerisation was halted by removing the hydrogel from the incubator and washing with water followed by aqueous HCl (0.25 mol dm^{-3}) for 30 min. Each sample was washed a further five times with water before being stored in water prior to mechanical testing.

Samples in the polymerisation time study were incubated at 25 °C for 1, 3, 5 18 and 24 h. The samples were worked up in the same way as for the polymerisation temperature study prior to mechanical testing.

2.1.5 Refractive index measurements:

Refractive index measurements were taken using an AR200 digital refractometer (Reichert Technologies, New York, NY, USA). The refractometer (Figure 2.4) was first calibrated with water. A hydrated sample of each hydrogel was cut (0.50 cm^2) and padded dry on a piece of wet filter paper to remove surface water. The sample was then placed onto the glass prism of the refractometer and a measurement taken. Suitable controls were also used, water as a negative control and etafilcon A and narafilcon A as positive hydrogel controls.

Figure 2.4: Refractometer used in experiments.

2.1.6 Percentage light transmittance:

The percentage of light transmittance through the hydrogel variants was measured via a spectrophotometer at a wavelength within the visible light spectrum (485 nm). Each hydrogel sample was removed from water storage and circular discs (0.36 cm^2) were cut using a 6 mm diameter trephine. The samples were placed in a 96-well plate and 100 mm^3 H_2O added to each well to maintain the hydrogels in their hydrated state. For any hydrogels not sitting flush on the bottom of the well they were gently manoeuvred into position with a pair of forceps. The 96-well plate was read at 485 nm on a FLUOstar Omega microplate reader (BMG LABTECH GmbH, Ortenberg, Germany) with an emission filter of 520 nm. The results were exported to Excel and the following formula was used to convert absorbance values to percentage light transmission:

% Transmittance = (10^(-1*Abs))*100

2.1.7 Percentage water content:

Percentage water content of the hydrogel variants was determined following a gravimetric method. Each sample was removed from water storage and cut to approximately 1 cm^2. The samples were padded dry on a piece of wet filter paper to remove surface water. A wet weight reading was recorded before the samples were placed in a desiccator overnight with P_2O_5 to expedite the

removal of water. A reading was taken the next day to determine the dry weight of each sample. The following formula was used to determine the percentage water content of all the hydrogels tested:

$$\frac{\textbf{wet weight - dry weight}}{\textbf{wet weight}} \textbf{ X 100}$$

Other methods used to determine water content included the conversion of data obtained from the refractive index experiments (nD and Brix TC) using the refractometer in section 2.1.5.

2.1.8 Dk values:

Oxygen permeability (Dk) values were obtained for the hydrogels based on their equilibrium water content (EWC). A formula described by Morgan and Efron (1998) was used to convert the EWC to Dk:

$$\mathbf{Dk = 1.67e^{0.0397EWC}}$$

2.1.9 Contact angle analysis:

The wettability of the hydrogels was determined by measuring the contact angle of a small water bead at the surface/liquid interface using a DSA 100 (KRÜSS GmbH, Hamburg, Germany) (Figure 2.5). This technique is known as the sessile drop technique and it measures the static contact angle. Hydrogel samples were cut to size (7 cm^2) and the surface dried by dabbing with a paper towel. The hydrogels were placed on a flat piece of glass on the stage of the DSA 100. The software was calibrated prior to imaging each sample. A drop of water (2 mm^3) was dispensed from a syringe and an image captured by a goniometer. Four points per sample were measured and this was completed in triplicate for each hydrogel variant. A circle profile function was fitted to all water droplets. The contact angle was determined by

measuring the angle of intersection between the baseline (surface of sample) and the circle profile. Poly-(tetrafluoroethylene) (PTFE) and glass were used as material controls.

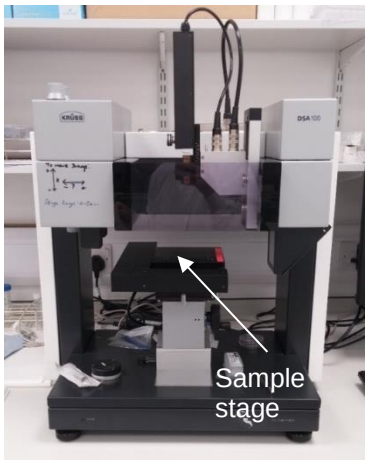

Figure 2.5: Krüss DSA100 contact angle equipment.

2.1.10 Degradation:

The degradation of the hydrogel variants was investigated in different solvents over a 12 month period. Hydrogels Su 60 15, Su 60 14, Su 60 13 and Su 65 15 were polymerised as described in section 2.1.2.

Incubation solutions (10 cm^3) of trypsin (1 mg cm^{-3}), NaOH (0.25 M) and PBS were prepared. Hydrogel discs were cut (0.785 cm^2) and incubated at 5 discs in a 7 cm^3 vial with each incubation solution (5 cm^3) at 37 °C for set time-points of 1 week, 1, 6 and 12 months over 1 year. At each time-point samples were removed, padded dry on a piece of wet filter paper and a wet weight recorded to monitor weight loss. The samples were then placed in small vials (7 cm^3) and covered with parafilm. The samples were frozen at -20 °C overnight, then placed on an Edwards Super Modulyo freeze dryer shelf (Edwards Ltd., West Sussex, England) at -35 °C. The vacuum was applied and the samples freeze dried for at least 4 h at 26 °C. The dried samples were mounted onto carbon tabs (Agar Scientific Ltd., Stansted, England) on a scanning electron microscope (SEM) specimen stub. Finally, the samples

were observed using a Tabletop SEM TM3030 (Hitachi High-Technologies Europe GmbH, Berkshire, England) following the manufacturer's protocol.

2.1.11 Lens manufacture:

Several techniques were investigated to try and make a lens shaped prototype of the pεK/bis-carboxylic acid hydrogel. Spin casting, immiscible solvents and various moulds were investigated as potential methods.

2.1.11.1 Spin casting:

Spin cast moulds (Figure 2.6a) were custom designed for SpheriTech Ltd. from a range of materials including polyoxymethylene, PVC, PTFE, PFA and glass. Polymer solution for hydrogel Su 60 14 was made up as described in section 2.1.2. Before adding the polymer mix to the moulds they were individually mounted onto an overhead stirrer that had been turned upside down. The moulds were rotated at between 400 - 900 RPM. Immediately after mixing the polymer solution it was pipetted into moulds with various volumes ranging from 60 - 120 mm^3. The moulds were spun for 1 h before stopping and observing the mould for signs of a cast lens material.

2.1.11.2 Immiscible solvent:

Boiling tubes were secured upright and different volumes of polymer solution were added. Polymer solution for hydrogel Su 60 14 was made up as already described in section 2.1.2. Toluene (2.5 cm^3) was added to the boiling tube after the polymer solution. The less dense immiscible solvent covers the polymer solution. The polymer was then left to set overnight before observing the cast lens material.

2.1.11.3 Contact lens moulds:

Contact lens moulds were custom designed for SpheriTech Ltd. for spin casting (Figure 2.6a) and in a male/female format (Figure 2.6b). Polymer solution for hydrogel Su 60 14 was made up as described in section 2.1.2. It was added at various volumes (40 - 100 mm^3) to the female mould before placing the male mould on top and snapping into place. The polymer polymerised overnight before observing the cast lens material.

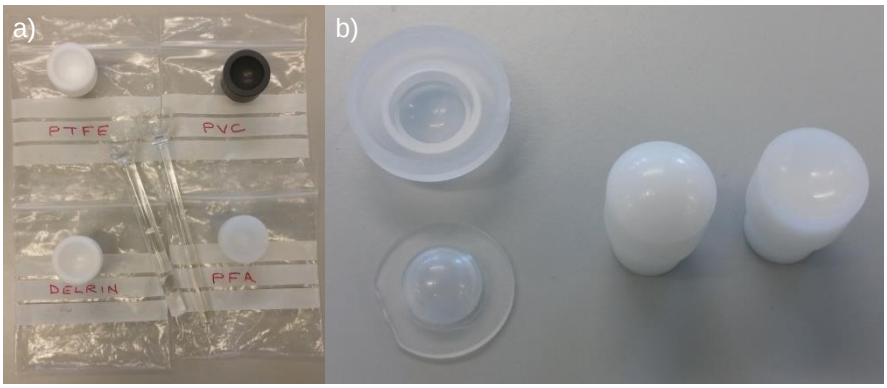

Figure 2.6: a) Spin cast moulds, b) male/female moulds.

2.2 HCE-T Cell Culture

The following materials were also used in this part of the study; **CCK-8 cell viability kit** (Dojindo Laboratories, Kumamoto, Japan), **PBS** BR0014 (Oxoid Ltd., Hampshire, England), **amphotericin B** A2942, **goat serum** G9023, **penicillin-streptomycin** P4333, **dimethyl sulfoxide (DMSO)** D2650, **fetal calf serum (FCS)** F7524, **Dulbecco's Modified Eagle's Medium/Ham's F12 (DMEM/F12)** D8062, **trypsin-EDTA** T3924, **tryphan blue** T8154, **bovine serum albumin (BSA)** and **tween 20** P9416 (Sigma Aldrich, St Louis, USA), **ethanol** (SpheriTech Ltd., Runcorn, England), **live/dead cell staining kit** L3224, **Hoechst 33342** H3570, **4',6-diamidino-2-phenylindole (DAPI)** D1306, **methanol** and **Mr Frosty™** (Thermo Fisher Scientific, Waltham, MA, USA). **HCE-T cells** donated by Kaoru Araki-Sasaki, Japan (Araki-sasaki *et al.*, 1995). All other equipment and reagents were provided by the University of Liverpool unless stated.

2.2.1 Hydrogel design:

The base hydrogel used in this part of the study was Su 60 14 and the polymerisation protocol was followed from section 2.1.2.

2.2.1.1 Hydrogel sterilisation:

Hydrogel Su 60 14 was unsterile post-polymerisation so a suitable sterilisation protocol was required prior to cell culture. The aqueous storage media was decanted from the hydrogel material and replaced with a 70 v/v% aqueous ethanol solution. The hydrogels were soaked in the ethanol solution for 3 h. The vial containing the hydrogels was transitioned to the cell culture cabinet. The ethanol was decanted and replaced with sterile PBS and allowed to soak for 30 min. The PBS wash was repeated a further 2 times before the hydrogels were added to an appropriate tissue culture vessel and incubated with cell culture media overnight under standard cell culture conditions. The media was inspected for infection after decantation and prior to utilising the hydrogel in cell culture studies.

2.2.2 Cell recovery:

After retrieval of the appropriate cryovial from liquid nitrogen storage it was placed in a water bath at 37 °C until only a small amount of frozen suspension remained in the tube. This was to ensure minimal toxicity from DMSO upon cell revival. During incubation, the cap of the cryovial was partially opened to allow any trapped nitrogen to escape without an explosive risk. The content of the cryovial was transferred to a centrifuge tube (15 cm^3) and centrifuged with a Heraeus Multifuge X1 centrifuge (Thermo Fisher Scientific, Waltham, MA, USA) at 185 x g for 5 min. A pipette was used to remove the supernatant before replacing it with cell culture media (2 cm^3). The cell pellet was suspended by aspirating with a pipette. The cell suspension was used to seed a T75 flask with an appropriate volume of DMEM/F12 (8 cm^3) media containing 5% FCS with amphotericin B and penicillin - streptomycin. The flask was incubated at 37 °C with 5% CO_2 prior to any cell culture experiments.

2.2.3 Feeding cells:

Fresh cell culture media (DMEM/F12 media containing 5% FCS with amphotericin B and penicillin - streptomycin) was pre-warmed to 37 °C in a water bath. HCE-T cells were transferred from the incubator to the tissue culture hood. A pipette was used to remove 80% of the spent media prior to replacing it with pre-warmed fresh media. The remaining 20% of spent media was left in the culture vessel to retain some of the macromolecules (i.e. growth factors) in the environment. Immediately prior to placing the HCE-T cells back in the incubator they were observed under a light microscope for confluency, morphology and any obvious signs of distress. If no other action was required, the cells were placed back in the incubator. The above process was carried out twice a week when cells were in culture.

2.2.4 Passaging cells:

When HCE-T cells reached approximately 75% confluency as determined by a visual check with a light microscope they were passaged. PBS, cell culture media and 10 v/v% trypsin-EDTA were pre-warmed to 37 °C in a water bath. HCE-T cells were transferred from the incubator to the tissue culture hood.

All the spent media was removed from the T75 flask containing the cells and replaced with pre-warmed PBS (4 cm^3) that was swirled around the flask to remove any loose cells. The PBS was removed and immediately replaced with 10 v/v% trypsin-EDTA in PBS (4 cm^3). The trypsin solution was swirled around the flask to cover the cell monolayer and placed back into the incubator at 37 °C for 3 - 4 min. The cells were then removed from the incubator and observed under a light microscope to ensure the majority had detached from the tissue culture plastic. If the cells had not detached they were incubated at 37 °C for a further 1 min before again checking for detachment. After most cells had detached from the flask they were transferred again to the tissue culture hood. A pipette was used to swirl the trypsin solution around the flask to detach any remaining cells before adding cell culture media (8 cm^3) to inhibit the action of trypsin. The HCE-T cell suspension was removed from the flask and transferred to a centrifuge tube (15 cm^3) before being centrifuged with a Heraeus Multifuge X1 centrifuge (Thermo Fisher Scientific, Waltham, MA, USA) at 185 x g for 5 min. A pipette was used to remove the supernatant without disturbing the cell pellet. The pellet was suspended in fresh cell culture media (4 cm^3) and at this point the HCE-T cells were counted using a haemocytometer prior to seeding for experiments. To passage, the cell suspension (1 cm^3) was transferred to a new, labelled T75 flask along with fresh cell culture media (9 cm^3) and placed back in the incubator. The above process was carried out approximately once a week when cells were in culture.

2.2.5 Cell freezing:

The storage of cells followed the same procedure as in section 2.2.4 up to the point where a cell pellet was obtained. DMSO (10 v/v%) in cell culture media (6 cm^3) was added to the cell pellet to suspend it. Aliquots of the cell suspension (1 cm^3) were transferred to labelled cryovials before being added to a Mr Frosty™ container with isopropanol. The Mr Frosty™ was transferred to a -80 °C freezer overnight to control the cell freezing at -1 °C min^{-1}. The next morning the cryovials were transferred to liquid nitrogen for long term storage at -196 °C. The above process was carried out in a timely manner to minimise the toxic effects of DMSO on the cells prior to freezing.

2.2.6 Tryphan blue cell viability:

Prior to seeding cells in experiments or after a CCK-8 assay a test of their viability was undertaken. The dye tryphan blue was used and cells that excluded the dye remained viable whereas cells that stained with tryphan blue were non-viable as their compromised membrane allows the dye to pass through. An aliquot (100 mm^3) of 0.4 v/v% tryphan blue in PBS was added to a similar volume of cell suspension. Aliquots (10 mm^3) of the tryphan blue/cell suspension were added to a haemocytometer and a count of viable and non-viable cells was undertaken to determine the percentage of cell viability.

% cell viability = [1.00 - (non-viable cells / total cell number)] x 100

2.2.7 Monitoring hydrogel Su 60 14 Cytotoxicity:

HCE-T cells were cultured under standard tissue culture conditions of 37 °C and 5% CO_2. DMEM/F12 media containing 5% FCS with amphotericin B and penicillin - streptomycin supplementation was used.

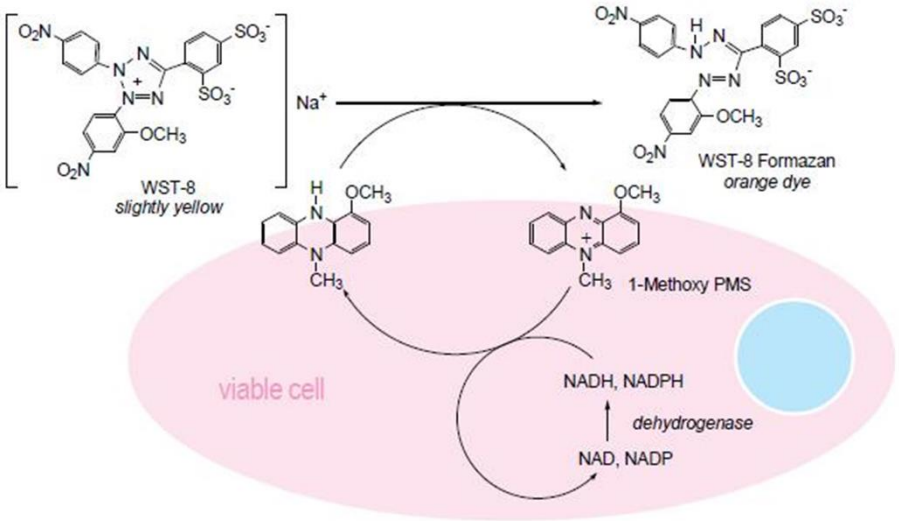

Figure 2.7: Conversion of WST-8 forms the basis of the colorimetric CCK-8 assay. Reproduced with permission from Dojindo Laboratories, Kumamoto, Japan.

A CCK-8 assay (Figure 2.7) was used to monitor cell proliferation at various time-points during an 8 day cell culture period. A standard curve to determine cell number was carried out following the manufacturer's guidelines. HCE-T cells were counted following the passaging protocol (section 2.2.4). An aliquot of the cell suspension was added to each well to achieve the appropriate cell number (Figure 2.8). Each well was filled to a total volume of 500 mm^3 with media before adding CCK-8 solution (50 mm^3) and incubating under standard culture conditions for 2 h. An aliquot (3 x 100 mm^3) of solution from each well was pipetted into labelled wells in a 96-well plate. Suitable controls included media and CCK-8 with no cells or media with cells and no CCK-8. The absorbance was read at 485 nm using a FLUOstar Optima plate reader (BMG Labtech, Ortenberg, Germany) with a background reading at 600 nm and the results recorded. A standard curve was plotted and used to determine HCE-T cell number in the cytotoxicity assays.

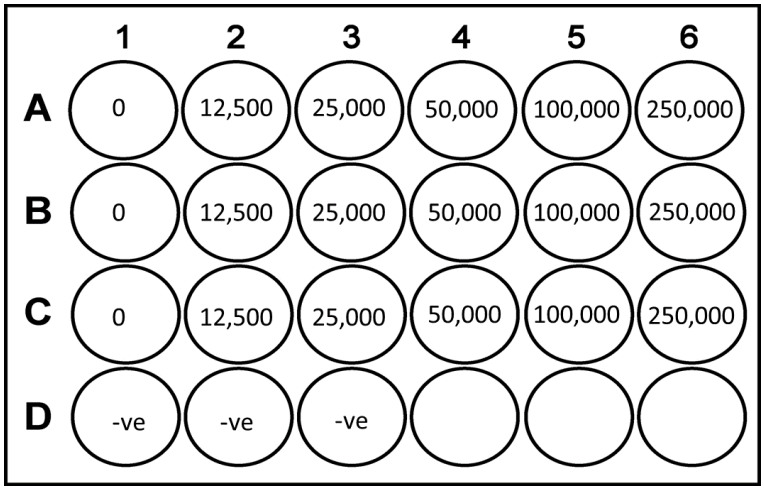

Figure 2.8: CCK-8 standard curve plate layout.

To setup the cytotoxicity study an aliquot of DMEM/F12 media was incubated with hydrogel Su 60 14 and another aliquot was incubated without the hydrogel for 3 days. The incubated media aliquots were used to culture the HCE-T cells. The cells were incubated under standard culture conditions for 4, 24, 48, 96, and 192 h after seeding with an initial density of 5 x 10^4 cells (Figure 2.9). At each time-point CCK-8 solution (50 mm^3) was added to the

media (500 mm^3) in each well. The cells were incubated under standard culture conditions for a further 2 h. An aliquot (3 x 100 mm^3) of solution from each well was pipetted into labelled wells in a 96-well plate. Suitable controls included media and CCK-8 with no cells or media with cells and no CCK-8 and hydrogel controls included media with no hydrogel incubation and media incubated with hydrogel Su 60 14 PO_4. The absorbance was read at 485 nm using a FLUOstar Optima plate reader (BMG Labtech, Ortenberg, Germany) with a background reading at 600 nm and the results recorded.

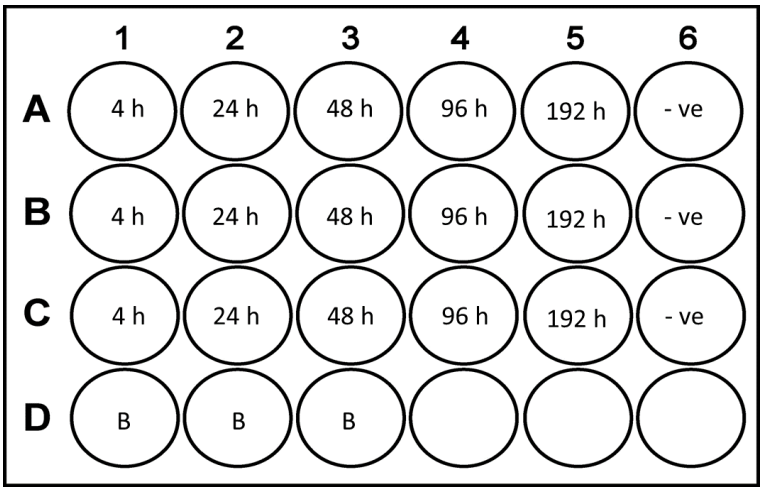

Figure 2.9: Cytotoxicity assay plate layout.

2.2.8 Live/dead and Hoechst cell staining and imaging:

A live/dead cell staining kit was used to determine cell viability and morphology. The cells were counterstained with Hoechst 33342. A stock solution of Hoechst 1:1000 (2 cm^3) was made in PBS. An aliquot (500 mm^3) of the stock solution was added to PBS (1486 mm^3) with ethidium (10 mm^3) and calcein (4 mm^3). HCE-T cells were prepared for staining by removing media and washing with PBS (2 x 1 cm^3) to remove any debris. An aliquot (250 mm^3) of the staining solution was added to each well and the cells were incubated under standard culture conditions for 30 min. Controls used included cells cultured on tissue culture plastic and cells treated with 2% virkon for 5 min. The cells were imaged under dark conditions using a NIKON Eclipse TI-E inverted microscope (Nikon, Tokyo, Japan).

2.2.9 Scratch assay:

A scratch assay (Figure 2.10) was used to determine any effect that leachables from Su 60 14 may have on HCE-T cell re-epithelialisation. A confluent monolayer was obtained by seeding 2.5 x 10^4 cells in a 24-well plate and culturing for 3 - 4 days at which point all media was removed. A straight-lined scratch using a 200 mm^3 pipette tip was made through the cell monolayer in each well. The cells were washed with culture media (2 x 1 cm^3). Hydrogel Su 60 14 was added to all the non-control wells before 750 mm^3 of media was removed to gently bring the hydrogel in direct contact with the cell monolayer. All wells contained culture media (250 mm^3) which was replenished after 12 h if necessary. Controls used were a scratch with no hydrogel present and a no scratch control. Images were taken over a 23 h period at time-points 0, 5 and 23 h. TScratch software was used to determine the rate at which the HCE-T cells closed the scratch (Gebäck *et al.,* 2008).

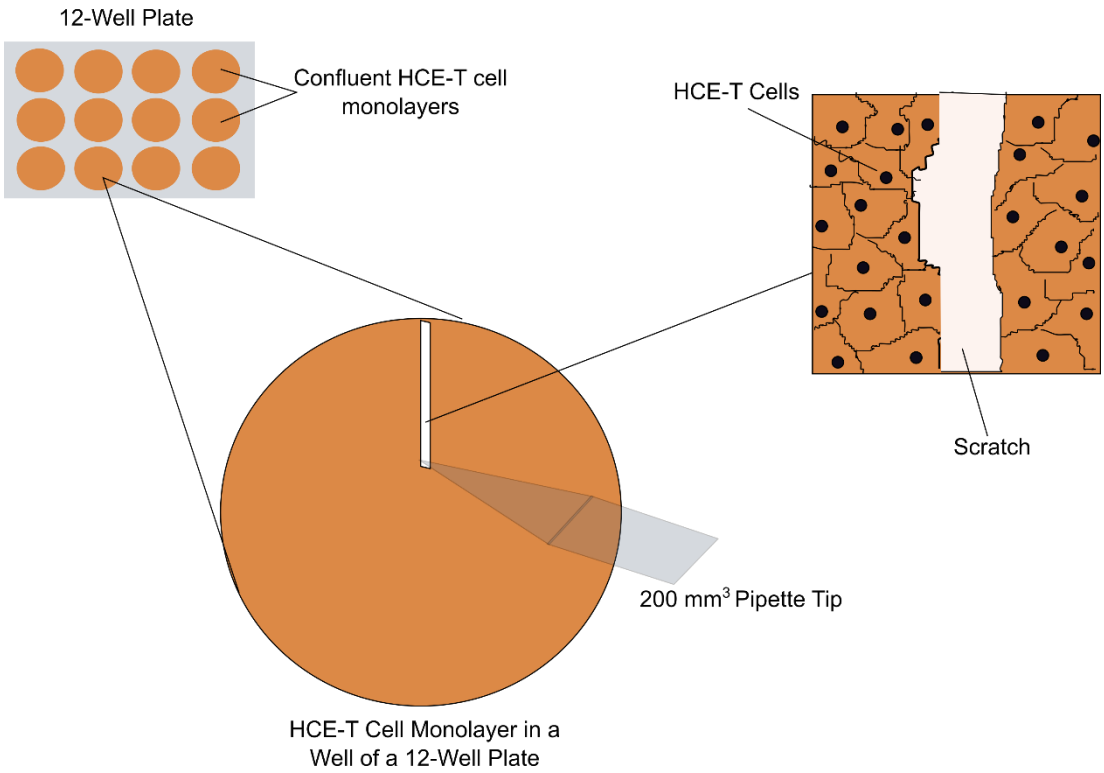

Figure 2.10: Illustration of the scratch assay protocol.

2.2.10 Immunofluorescence staining:

After the scratch assay the HCE-T cells were washed 3 x PBS before being incubated at -20 °C for 10 min with 100% methanol (500 mm^3 per well).

	Primary Antibody	Concentration	2nd Primary Antibody	Concentration	Secondary Antibody	Concentration
1	ZO-1 (Invitrogen 40-2200)	2.5 µg cm^{-3}	/	/	GαR 488	4 µg cm^3
2	ZO-1 (Invitrogen 40-2200)	2.5 µg cm^{-3}	Pan cytokeratin (Abcam ab52460)	1 µg cm^{-3}	GαM 488 GαR 568	4 µg cm^3 4 µg cm^3
3	Occludin (Abcam ab31721)	1 µg cm^{-3}	Cytokeratin MNF116 (Abcam ab756)	1 µg cm^{-3}	GαM 488 GαR 568	4 µg cm^3 4 µg cm^3

Table 2.7: Antibodies used in immunofluorescence studies.

For antibodies 1-3 (Table 2.7): Each well was washed 3 x 0.1 v/v% Tween 20 in PBS before a 5 min PBS wash. A blocking agent containing 1 v/v% goat serum in PBS was applied to each well overnight (500 mm^3). The following morning the blocking agent was removed and each well washed 3 x 0.1 v/v% Tween 20 in PBS. Primary antibody was made at a dilution of 1:100 in 1 v/v% BSA in PBS before being added to each well (200 mm^3) and incubated at 37 °C for 1 h. The primary antibody solution was removed and each well washed 3 x 0.1 v/v% Tween 20 in PBS. Secondary antibody Alexa Fluor was added to 1% BSA in PBS at a dilution of 1:500. It was then added to each well (200 mm^3) and incubated under dark conditions for 1 h at room temperature. The secondary antibody was removed and each well washed 3 x PBS. Controls used were no primary antibody and A19 cells or IgG instead of the primary antibody. Each sample was counter-stained with DAPI (200 mm^3 of 1:30,000 in PBS per well) for 5 min and imaged using a Nikon Ti-E fluorescent microscope (Nikon, Tokyo, Japan).

2.2.11 Microscopy

All microscopy was carried out at the University of Liverpool using an in-house Nikon Eclipse TiE inverted microscope and all images analysed with the associated NIS-Elements software (Nikon, Tokyo, Japan).

2.2.11.1 Phase contrast light microscopy:

Phase contrast imaging allowed for the real-time observation of cells without the need for staining procedures and was most useful for occasional health checks during cell culture and for imaging at set time-points during scratch assays. Microscope slides or tissue culture vessels containing cells were placed on the microscope stage and the various controls within the NIS-Elements software or on the microscope itself were used to observe samples and/or take images.

2.2.11.2 Fluorescence microscopy:

The same principle was used for imaging fixed and stained mammalian and microbial cells via immunofluorescence. Prepared samples on microscope slides or in tissue culture vessels were placed on the microscope stage and the various controls within the NIS-Elements software or on the microscope itself were used to observe samples and/or take images. Filter sets with emission/excitation wavelengths of 360/460 nm (DAPI), 480/535 nm (FITC, fluorescein isothiocyanate) and 540/605 nm (TRITC, tetramethylrhodamine isothiocyanate) were used for all immunofluorescence with x10, x20 and x40 objectives.

2.3 Antibacterial Activity

The following materials were used in this part of the study; **methyl orange** A17604 and **penicillin G** F20Z009 (Alfa Aesar, Haverhill, MA, USA), **Luria-Bertani (LB)-Agar** 110283 and **LB broth** 71753 (Merck Millipore Ltd., Watford, England), **PBS** BR0014 (Oxoid Ltd., Hampshire, England), **acetic anhydride** 320102 and **resazurin** R7017 (Sigma Aldrich, St Louis, MO, USA), **pεK** (Zhengzhou Bainafo Bioengineering Co., Ltd., Zhengzhou City, China). ***S. aureus* Newman** and ***E. coli* MC1061** were supplied by the Institute of Integrated Biology, University of Liverpool. All other equipment and reagents were provided by the University of Liverpool unless otherwise stated.

2.3.1 Bacterial cell culture:

S. aureus Newman and *E. coli* MC1061 were revived from -80 °C storage and streaked using an inoculating loop onto an LB-Agar plate before incubating at 37 °C overnight. A single colony from the relevant streak plate was added to LB broth (10 cm^3) in a 50 cm^{-3} Falcon tube and incubated at 37 °C in a dark room with agitation (300 RPM) on an Innova 2300 platform shaker (Eppendorf GmbH, Hamburg, Germany) overnight. An aliquot of each culture (0.5 cm^3) was added to fresh LB broth (10 cm^3) and cultured again at 37 °C until an OD_{600} of 0.5 - 0.6, measured using a Jenway 6705 UV/Vis Spectrophotometer (Bibby Scientific Ltd., Stone, England), was obtained. This was the working stock solution of bacteria for the subsequent assays.

2.3.2 Hydrogel design:

Several different hydrogel variations were investigated in this part of the study. These included Su 60 14, some cross-link variants Su 45 14 and Su 75 14 (Table 2.8) as well as an acetylated variant of Su 60 14 and Su 60 14 with biomolecules attached and Su PεK PO_4. The polymerisation protocol was followed from section 2.1.2.

Reagent	PεK / octanedioic acid hydrogels		
	45 mol% cross-linked, 0.071 g cm^{-3} **(Su 45 14)**	60 mol% cross-linked, 0.071 g cm^{-3} **(Su 60 14)**	75 mol% cross-linked, 0.071 g cm^{-3} **(Su 75 14)**
PεK	1.58 g (9.20 mmol)	1.48 g (8.62 mmol)	1.40 g (8.12 mmol)
Octanedioic acid	0.36 g (2.07 mmol)	0.45 g (2.59 mmol)	0.53 g (3.04 mmol)
NMM	1.01 cm^3	0.95 cm^3	0.89 cm^3
EDCI	1.98 g (10.33 mmol)	2.48 g (12.94 mmol)	2.92 g (15.23 mmol)
NHS	0.53 g (4.60 mmol)	0.50 g (4.34 mmol)	0.47 g (4.08 mmol)

Table 2.8: Su 45 14, Su 60 14 and Su 75 14 hydrogel compositions.

2.3.2.1 Acetylation of Su 60 14:

Acetylation of the amine groups of hydrogel Su 60 14 was undertaken to investigate any effects on antimicrobial activity. The hydrogel was completely washed after polymerisation and drained of the final wash. A 10 v/v% acetic acid in DMF (50 cm^3) solution was added to 1.5 Molar equivalents of NMM (8.15 cm^3). The mixture was poured onto Su 60 14 and left for 2.5 h. The mixture was then decanted and the hydrogel sheet washed 5 x H_2O.

2.3.2.2 Biomolecule attachment:

Biomolecule attachment (Figure 2.11) for antimicrobial analysis was either ionic interaction (penicillin G) or covalent coupling (pεK). In both instances, the biomolecules were attached post-polymerisation. Prior to attachment the hydrogel was washed 5 x 10 v/v% aqueous NMM (50 cm^3) at 15 min per wash. This was followed by 5 x H_2O (50 cm^3) at 15 min per wash. Penicillin G was attached by soaking the hydrogel in an ionic solution (25 cm^3 of 12.5

mmol dm^{-3} penicillin G in water) of the antibiotic for 3 h. The hydrogel was washed 2 x H_2O for 5 min before being stored in H_2O prior to sterilisation.

PεK (3 g) was attached to hydrogels by dissolving in H_2O (20 cm^3) and adding to NHS (96 mg) and EDCI (610 mg) pre-dissolved in H_2O (5 cm^3). The solution was mixed and added to the hydrogel and incubated for 3 h. The hydrogel was then washed in H_2O followed by 5 x 10 v/v% NMM (50 cm^3) at 15 min per wash followed by 5 x H_2O (50 cm^3) at 15 min per wash before finally storing in H_2O prior to sterilisation.

A positive control hydrogel was designed (for all subsequent assays) as a derivative of Su PεK with phosphate associated with the amine groups (Su PεK PO_4). Su PεK was incubated in PBS (20 cm^3, 10X concentration) for 1 h before being washed in 2 x H_2O (20 cm^3). The hydrogel was stored in H_2O until required in the cytotoxicity assays.

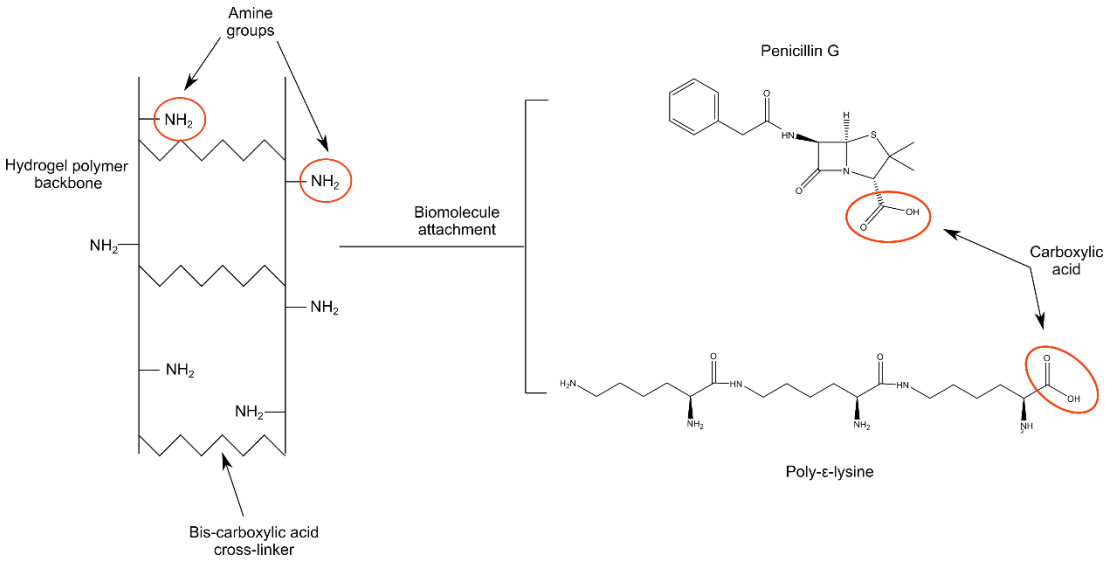

Figure 2.11: Schematic illustrating proposed biomolecule attachment to the hydrogel matrix.

2.3.2.3 Methyl orange amine quantification:

The following method of amine quantification using methyl orange dye (Figure 2.12) was adapted from the original protocol (Itzhaki, 1972). A standard curve of methyl orange concentration against absorbance was produced using known pεK concentrations as standards. A 2 mM methyl orange solution was made up by dissolving (32.7 mg) in H_2O (50 cm^3). A 1.6 mM pεK stock solution was also made up by dissolving (13.2 mg) in H_2O (50 cm^3). This was then serial diluted with water to 800, 400, 200, 100 and 50 µM concentrations. The methyl orange stock (500 mm^3) was added to each of the pεK concentrations (500 mm^3) in a 1.5 cm^3 centrifuge tube. These were mixed by adding them to a 50 cm^3 Falcon tube and placing them on a roller for 30 min. Each 1.5 cm^3 tube was centrifuged with a Heraeus Biofuge Pico at 5345 x g (Thermo Scientific, Waltham, WA, USA) for 5 min. The tubes were retrieved and an aliquot of the supernatant (150 mm^3) removed and added to H_2O (2.85 cm^3) in a cuvette. The cuvette was inverted 3 times before measuring the absorbance at 465 nm using a Cecil CE292 UV spectrophotometer (Cecil Instruments Ltd., Cambridge, England) against a water blank. A standard curve was compiled and used to calculate the number of amino groups in a sample from the concentration of methyl orange. Each unknown sample was prepared in the same way as for the standards above.

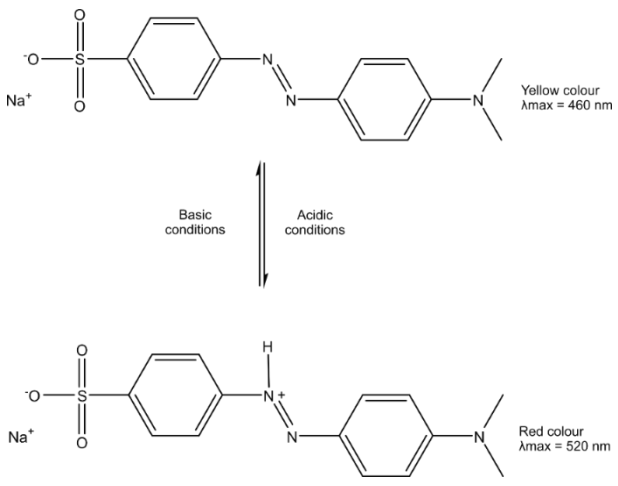

Figure 2.12: Methyl orange colour conversion.

2.3.2.4 Penicillin G elution:

The elution of Penicillin G from the hydrogel prepared in section 2.3.2.2 was monitored with reverse-phase high-performance liquid chromatography (RP-HPLC). Hydrogel discs were cut (0.785 cm^2) and incubated at 3 discs in a 7 cm^3 vial with PBS (1 cm^3) at 37 °C for set time-points of 5, 10, 15, 20, 25, 30, 120, 180 and 260 min over 5 h. At each time-point the supernatant was removed for analysis and replaced with fresh PBS (1 cm^3). Suitable controls included a 0 mg cm^{-3} and 1 mg cm^{-3} solutions of penicillin G in PBS.

RP-HPLC was performed on a SpectraSYSTEM AS3000 (Thermo Scientific, Waltham, MA, USA) with a C18 Vydac column, 4.6 x 250 mm, 5 µm particle size (Hichrom Ltd., Reading, England). The column temperature was set at room temperature and 100 mm^3 was the injection volume at a flow rate of 1 cm^3 min^{-1}. The gradient was set to 20% - 70% B over 20 min with A: 0.1 v/v% TFA in H_2O, B: 0.1 v/v% TFA in MeCN and a detection wavelength of 210 nm.

2.3.3 Antimicrobial activity assay:

A protocol for utilising resazurin to measure bacteria metabolic activity was adapted (Pettit, Weber and Pettit, 2009) and used to determine bacterial burden on different hydrogels. Each sterilised hydrogel variant was placed in individual wells in a 24-well plate before being inoculated with *S. aureus* or *E. coli* inoculum (400 mm^3 with approx. 5 x 10^5 cfu cm^{-3} cells) (Figure 2.13).

	1	2	3	4	5	6	7	8	9	10	11	12
A	Su 60 14									Resazurin only		
B	Su pεK									Reduced resazurin		
C	Su Pen G									LB media only		
D	Su Acetylated									*S. aureus* only		
E	LB agar									*E. coli* only		
F	Process control											
G												
H												

Figure 2.13: Antibacterial assay 96-well plate layout.

Hydrogels were removed at 2, 4 and 18 h time-points and washed in PBS before being placed in a fresh 24-well plate. Resazurin (400 mm^3 at 0.01 mg cm^{-3} in LB broth) was added to each hydrogel and incubated at 37 °C for 45 min. After incubation aliquots (100 mm^3) were removed in triplicate from each well and pipetted into a 96-well plate. Autoclave reduced resazurin (resorufin) served as a positive control whilst stock resazurin prior to assay served as a negative control. Fluorescence intensity of resorufin formed from the reduction of resazurin was measured at 560 nm (excitation) and 592 nm (emission) using a FLUOstar Optima plate reader (BMG Labtech, Ortenberg, Germany) (Figure 2.14).

Planktonic bacteria were measured with resazurin after removal of the hydrogel. The supernatant (360 mm^3) was removed to a fresh 24-well plate and resazurin stock (40 mm^3 of 0.1 mg cm^{-3}) was added to finish with a resazurin concentration of 0.01 mg cm^{-3}. The samples were incubated at 37 °C for 45 min. After incubation aliquots (100 mm^3) were removed in triplicate from each well and pipetted into a 96-well plate. Autoclave reduced resazurin (resorufin) served as a positive control whilst stock resazurin prior to assay served as a negative control. The fluorescence intensity was measured in the same way as for the hydrogels in this section.

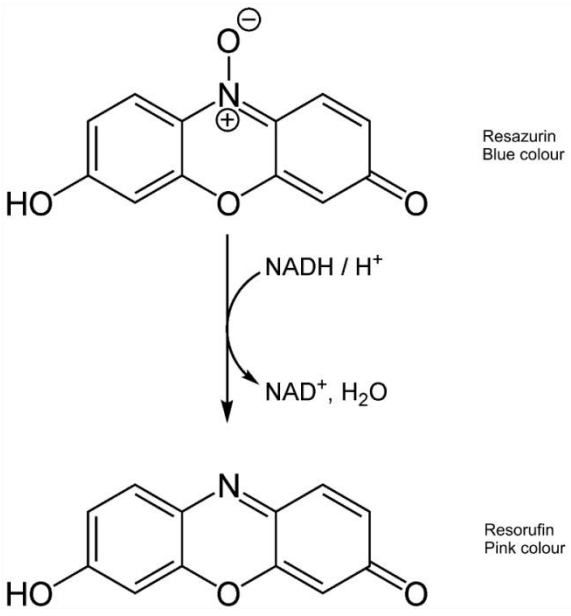

Figure 2.14: Resazurin reduction to resorufin.

2.3.4 Bacteria staining:

Hydrogel variants were inoculated with *S. aureus* (400 mm^3, OD_{600} 0.05) and incubated at 37 °C for 4 h. The hydrogel was then removed and washed in PBS before a 5 min 50% ethanol wash, 10 min 100% ethanol wash and 2 x PBS washes prior to propidium iodide (PI) staining. The supernatant from the incubation was pipetted into 1.5 cm^3 Eppendorf tubes and centrifuged at 13,451 x g with an Eppendorf 5418 R centrifuge (Eppendorf Ltd., Stevenage, England) for 10 min. The supernatant was removed and replaced with LIVE/DEAD® BacLight™ (L7007, Invitrogen, Carlsbad, CA, USA) bacteria viability stain ((300 mm^3 of dye (1.5 mm^3 of SYTO 9 and PI in 1 cm^3)). The pellet was aspirated in the dye and incubated for 15 min at room temperature. Finally, the tube was centrifuged again at 13451 x g for 10 min and the pellet aspirated in sterile water (100 mm^3) before pipetting a sample on a microscope slide and applying a cover slip. The sample was observed using a Zeiss LSM 510 multiphoton confocal microscope (Zeiss, Oberkochen, Germany).

2.3.5 Cytotoxicity of antibacterial hydrogels

The modified hydrogels Su PεK and Su Pen G were investigated for any cytotoxicity towards the HCE-T cell line. Su PεK PO_4 served as a positive control. A CCK 8 viability assay, scratch assay and an investigation of monolayer integrity were carried out as in section 2.2.

2.4 Antifungal Activity

The following materials were also used in this part of the study; **potato dextrose (PD) agar** and **PD broth** (Formedium Ltd., Norfolk, England), **PBS** BR0014 (Oxoid Ltd., Hampshire, England), **amphotericin B** A2942 (Sigma-Aldrich, St Louis, MO, USA). ***Candida albicans* SC5314** was supplied by the Institute of Integrated Biology, University of Liverpool. All other equipment and reagents were provided by the University of Liverpool unless otherwise stated.

2.4.1 Candida albicans cell culture:

Candida albicans SC5314 was revived from -80 °C storage and streaked using an inoculating loop onto a PD-Agar plate before incubating at 37 °C overnight. *C. albicans* was sub-cultured by inoculating a PD-agar streak plate with one colony taken from a previous PD-Agar plate and incubated overnight at 37 °C. Colonies were maintained on PD-Agar stored at 5 °C. Broth cultures were initiated by inoculating PD media (10 cm^3) with one colony of *Candida albicans* taken from a PD Agar plate. Cultures were incubated overnight at 37 °C with constant shaking (100 RPM) on an Innova 2300 platform shaker (Eppendorf GmbH, Hamburg, Germany). These were sub-cultured by taking an aliquot of *C. albicans* broth (500 mm^3) and diluting it in PD (10 cm^3). For experiments, overnight broth culture (500 mm^3) was diluted with PD (10 cm^3) and the OD_{600} was measured hourly with a Jenway 6705 UV/Vis Spectrophotometer (Bibby Scientific Ltd., Stone, England). If an initial OD_{600} measured < 0.5 then it was monitored until an OD_{600} 0.5 - 0.6 was obtained. The broth was diluted 1:1 with PD prior to experiments. To homogenise the culture broth, it was sonicated regularly and for 15 min prior to experiments.

2.4.2 Hydrogel design:

Hydrogel Su 60 15 (30 cm^3) with 60% cross-linking and a polymer density of 0.07 g cm^{-3} was prepared (Table 2.9). The polymerisation protocol was followed from section 2.1.2 with the following exceptions.

- All solutions were filtered in a class II microbiology hood using a 0.2 µm syringe filter.
- An aliquot of the polymer solution (5 cm^3) was pipetted into each 63 cm^2 non-treated tissue culture dish (Greiner Bio-One GmbH, Kremsmünster, Austria).
- Sheets of hydrogel were washed 5 x 10 v/v% aqueous NMM for 5 min followed by 10 x H_2O (5 min per wash) to remove excess NMM. This dissociated the Cl^- ion from the amine groups and these hydrogels were given the code -NH_2.

Reagent	**PεK / octanedioic acid hydrogel** 60 mol% cross-linked, 0.07 g cm^{-3} **(Su 60 15)**
PεK	2.08 g (12.09 mmol)
Octanedioic acid	0.63 g (3.63 mmol)
NMM	1.33 cm^3
EDCI	3.47 g (18.12 mmol)
NHS	0.70 g (6.08 mmol)

Table 2.9: Su 60 15 hydrogel composition.

2.4.3 Biomolecule attachment:

An investigation of the antifungal activity of the hydrogel was undertaken by associating the model antifungal amphotericin B (AmpB) with the hydrogel (Figure 2.15). AmpB (250 µg cm^{-3}) was diluted in sterile PBS to concentrations 30, 25, 20, 15, 10, 5, 3 and 0 µg cm^{-3}. Hydrogels (-NH_2 and -NH_3Cl) were incubated in the various concentrations of AmpB for 1 h before being transferred to 96-well plates and used in the subsequent experiments.

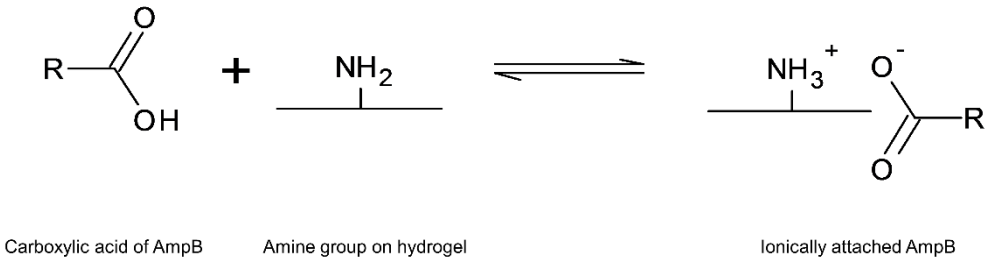

Figure 2.15: Schematic illustrating proposed mechanism of AmpB association with the hydrogel matrix.

2.4.4 Minimum inhibitory concentration (MIC) data:

To establish the fungicidal effect of AmpB and obtain an MIC, AmpB was serially diluted with PD 1:1 from a stock of PD containing 3 µg cm^{-3} AmpB such that each well of the 96-well plate contained 100 mm^3 of solution. Twelve concentrations, ranging from 0 - 3 µg cm^{-3} AmpB, were assessed. Control wells contained PD only and PD with *C. albicans*. *C. albicans* broth (12.5 mm^3) was added before overnight incubation at 37 °C. OD_{600} were measured 18 h later using a FLUOstar Optima plate reader (BMG Labtech, Ortenberg, Germany). Prior to measurement all samples were sonicated for 15 min. The MIC was also analysed for AmpB activity against *C. albicans* in the presence of 10 v/v% horse serum in PD broth following the same protocol but replacing PD broth with 10 v/v% horse serum in PD broth.

2.4.5 Antifungal activity of hydrogel:

AmpB (250 µg cm^{-3}) was diluted in sterile PBS to concentrations 30, 25, 20, 15, 10, 5, 3 and 0 µg cm^{-3}. Hydrogels were incubated in the various concentrations of AmpB for 2 h before being transferred to 96-well microtiter plates. Control wells containing PD only and PD with *C. albicans* were used throughout all these experiments (Figure 2.16). Wells containing PD (100 mm^3) were inoculated with *C. albicans* (12.5 mm^3). Microtiter plates were incubated overnight at 37 °C, and OD_{600} readings were taken after 18 h (Figure 2.17, step 1).

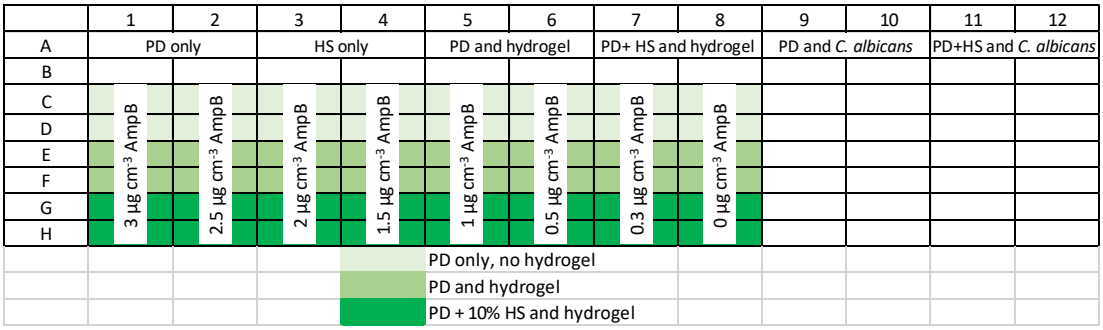

Figure 2.16: Antifungal assay 96-well plate layout.

The above protocol was repeated to include *C. albicans* with the addition of horse serum (10% v/v) to PD broth to promote differentiation and upregulate the expression of virulence genes (Martin, 1978; Blankenship *et al.*, 2003). After the hydrogels were removed from the microtiter plate, they were individually washed in sterile PBS (5 cm^3) to remove any loosely attached fungi and the wash solution collected (Figure 2.17, step 2). The hydrogels were extracted using sterile forceps and placed on PD agar plates to identify the presence of viable fungi. An aliquot of each PBS wash solution (20 mm^3) was also plated (Figure 2.17, step 2). The agar plates were incubated at 37 °C overnight before imaging and counting the colony forming units (Figure 2.17, step 3). After the hydrogels were removed, the plates were incubated at 37 °C for a second night to establish if there was any further growth of *C. albicans*. OD_{600} readings were taken after 24 h (Figure 2.17, step 3).

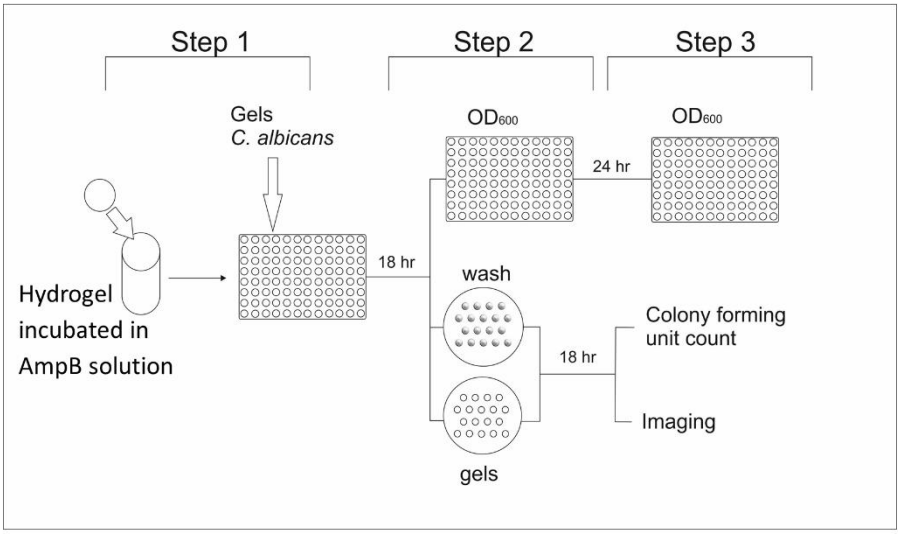

Figure 2.17: Schematic of methods used to monitor antifungal activity. Image provided courtesy of Prof. R.L. Williams (University of Liverpool).

2.4.6 AmpB elution:

Discs of each hydrogel (0.36 cm^2) were incubated in a 30 µg cm^{-3} AmpB solution for 2 h. The hydrogels (-NH_3Cl and -NH_2) were removed and incubated in PBS at 1 hydrogel 100 mm^{-3} for 24, 48, 72 and 96 h. At each time-point the supernatant was removed and used to monitor elution via HPLC. The PBS was replenished and the hydrogel samples were re-incubated. Suitable controls included a 0 mg cm^{-3} and 1 mg cm^{-3} solutions of AmpB in PBS.

RP-HPLC was performed on a SpectraSYSTEM AS3000 (Thermo Scientific, Waltham, MA, USA) with a C18 Vydac column, 4.6 x 250 mm, 5 µm particle size (Hichrom Ltd., Reading, England). The column temperature was set at room temperature and 200 mm^3 was the injection volume at a flow rate of 1 cm^3 min^{-1}. The gradient was set to 40% - 100% B over 15 min with A: 0.1% TFA in H_2O, B: 0.1% TFA in MeCN and a detection wavelength of 380 nm.

2.4.7 AmpB stability attached to the hydrogel:

Discs of the -NH_2 hydrogel (0.36 cm^2) were stored at room temperature for 1, 24 and 48 h after a 2 h incubation with a 30 µg cm^{-3} AmpB solution. The hydrogels were then placed in appropriate wells in a 96-well plate containing PD media (100 mm^3). Incubation solution (12.5 mm^3) was added to separate

wells in the 96-well plate along with PD media (100 mm^3). Each well was inoculated with *C. albicans* (12.5 mm^3) for 18 h and the OD_{600} readings taken and analysed. Suitable controls included a 0 mg cm^{-3} and incubation solutions of AmpB in PBS.

2.4.8 Cytotoxicity of antifungal hydrogels

The modified hydrogel Su 60 15 pre-incubated in 30 µg cm^{-3} AmpB solution was investigated for any cytotoxicity towards the HCE-T cell line. A CCK 8 viability assay was carried out as in section 2.2.7.

2.5 Microbe Detecting Peptide

The following materials were also used in this part of the study; **methyl orange** A17604 (Alfa Aesar, Haverhill, MA, USA), **glutaric anhydride** G3806 (Sigma-Aldrich, St Louis, MO, USA), **sodium bicarbonate** BDH9280 (VWR International Ltd., Lutterworth, England). **BAC ONE** and **BAC TWO** peptides were supplied by the Queens Medical Research Institute (University of Edinburgh, Edinburgh, Scotland). **HCE-T** cells donated (Araki-sasaki *et al.*, 1995) whilst ***E. coli* MC1061** and ***S. aureus* Newman** were supplied by the Institute of Integrated Biology, University of Liverpool. All other equipment and reagents were supplied by the University of Liverpool unless otherwise stated.

2.5.1 Bacteria cell culture:

S. aureus Newman or *E. coli* MC1061 was revived and cultured as in section 2.3.1.

2.5.2 Hydrogel design:

Hydrogel Su 60 14 (50 cm^3) was modified to convert it to a carboxyl moiety (Su 60 14 COOH) with 60% cross-linking and a polymer density of 0.07 g cm^{-3}. Su 60 14 was polymerised as in section 2.1.2 but with the following additional step.

The hydrogels were washed 3 x H_2O followed by 2 x 10 v/v% aqueous NMM (30 min per wash) to neutralise before 3 x H_2O. This was followed by 3 x 0.1 M sodium bicarbonate (5 min per wash). Glutaric anhydride (2 g) was dissolved in 0.1 M sodium bicarbonate (100 cm^3) and aliquoted to each hydrogel (20 cm^3) before a 2 h incubation. The hydrogels were washed 2 x 0.1 M sodium bicarbonate (5 min per wash) prior to repeating the glutaric anhydride coupling. Finally, the hydrogels were washed 5 x H_2O before storing in H_2O prior to use. Immediately before use the hydrogels were sterilised in 70 v/v% aqueous ethanol overnight before washing 5 x sterile PBS and using them for experiments.

2.5.3 Methyl orange amine group determination:

A standard curve of methyl orange concentration against absorbance was produced using known concentrations as standards as in section 2.3.2.3. A 2 mM methyl orange solution was made up by dissolving 32.7 mg in water (50 cm^3). This was serial diluted to 1000, 500, 250 and 125 µM concentrations with water. The methyl orange stock (500 mm^3) was added to a 1.5 cm^3 centrifuge tube. These were mixed by adding them to a 50 cm^3 Falcon tube and placing them on a roller for 30 min. Each 1.5 cm^3 tube was centrifuged with a Heraeus Biofuge Pico at 5345 x g (Thermo Scientific, Waltham, WA, USA) for 5 min. The tubes were retrieved and an aliquot of the supernatant (150 mm^3) removed and added to water (2.85 cm^3) in a cuvette. The cuvette was inverted 3 times before measuring the absorbance at 465 nm using a Cecil CE292 UV spectrophotometer (Cecil Instruments Ltd., Cambridge, England) against a water blank. A standard curve was compiled and used to calculate the number of amino groups in a sample from the concentration of methyl orange. Each unknown sample was prepared in the same way as for the standards above.

2.5.4 Activity of SU 60 14 COOH/BAC peptides against E. coli or *S. aureus:*

The hydrogel samples were cut to fit a well in a 96-well plate (28.26 cm^2) using a 6 mm diameter trephine. A 200 µM stock solution of BAC ONE (5.33 mg) or BAC TWO (1.02 mg) was prepared by dissolving the peptide in water (4 cm^3). The stock was used to prepare incubation concentrations of 40, 20, 10, 5 and 0 µM. Twelve discs of the hydrogel were incubated in each of the incubation concentrations (2 cm^3) for 1 h. Once removed the hydrogels were added to a well in a 96-well plate containing LB media (100 mm^3). The different concentrations of peptide solution were added to separate wells before inoculating them all with the test bacterium (100 mm^3). Suitable controls included media with only bacteria or BAC peptides and media with no cells. Hydrogel controls included hydrogels incubated in 0 µM concentrations and *S. aureus* was used as a control Gram-positive organism in the BAC TWO assay as well as the incubation concentrations of each peptide. The plates (Figure 2.18) were incubated for between 30 min - 4 h prior to reading the fluorescence at 485 nm on a FLUOstar Omega

microplate reader (BMG LABTECH GmbH, Ortenberg, Germany) with an emission filter of 520 nm. The samples were fixed with 70 v/v% aqueous ethanol for 30 min prior to imaging with a FITC fluorescent filter on a Nikon TiE microscope (Nikon, Tokyo, Japan).

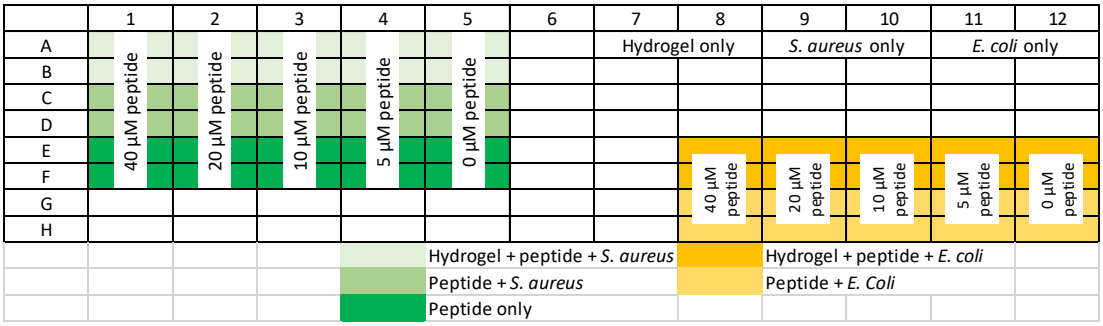

Figure 2.18: Microbial identification assay 96-well plate layout.

2.5.5 Stability of SU 60 14 COOH with either BAC ONE or TWO:

The same BAC ONE or TWO stock solution as in section 2.5.4 was used to prepare incubation concentrations of 40, 20, 10, 5 and 0 µM. Twelve discs of the hydrogel were incubated in each of the incubation concentrations (2 cm^3) for 1 h. Once removed the hydrogels were added to a well in a 96-well plate containing LB media (100 mm^3) prior to inoculating with the test bacterium (100 mm^3). Suitable controls included media with only bacteria or BAC peptides and media with no cells. Hydrogel controls included hydrogels incubated in 0 µM concentrations. Time-points of 0.5, 1, 2, 4 and 21 h were used to monitor fluorescence. At each time-point the fluorescence was read at 485 nm on a FLUOstar Omega microplate reader (BMG LABTECH GmbH, Ortenberg, Germany) with an emission filter of 520 nm.

2.5.6 HCE-T/bacteria co-culture with SU 60 14 COOH/BAC ONE or TWO present:

HCE-T cells were seeded at a density of 2.5 x 10^4 in a 48-well plate and incubated with DMEM/F12 media for 3 days until they were confluent. The same BAC ONE or BAC TWO stock solutions as in section 2.5.4 were used to prepare incubation concentrations of 40 µM. The hydrogel discs (28.26

cm^2) were incubated in the appropriate incubation concentration (2 cm^3) for 1 h prior to a 1 h incubation with HCE-T cells and the test bacterium (100 mm^3). Suitable controls included BAC peptides with only bacteria or BAC peptides with only HCE-T cells. Hydrogel controls included hydrogels incubated in 0 µM concentrations and *S. aureus* was used as a control Gram-positive organism in the BAC TWO assay. The samples were fixed with 70 v/v% aqueous ethanol for 30 min prior to imaging with a FITC fluorescent filter on a Nikon TiE microscope (Nikon, Tokyo, Japan).

2.5.7 Ex vivo bacterial keratitis model:

Porcine eyes were retrieved from the abattoir and prepared for dissection. Each eye was placed in a Petri dish and the eye lids, fatty tissue and muscle were trimmed with surgical scissors (Figure 2.19). The prepared eye was positioned so that an incision could be made with a scalpel to the sclera midway between the optic nerve and the cornea. Surgical scissors were placed in the incision and cut around the sclera until the eye was in two halves. The anterior portion of the eye was positioned with the cornea facing down. It was then cleaned by removing the vitreous humour and the lens using a pair of forceps. The black tissue of the ciliary body and the iris was gently removed from around the cornea by peeling it off with a pair of forceps. The area was gently scraped with a scalpel to further remove all remnants of the ciliary body. The prepared corneas were stored in PBS with penicillin-streptomycin and amphotericin B supplementation.

The corneas were moved to a class II microbiology hood and removed from PBS storage and placed with the anterior portion facing down in a 6-well plate. Autoclaved 2% agar whilst molten was mixed 1:1 with DMEM cell culture media without antibiotic supplementation to finish with a 1% agar solution. The solution was promptly pipetted into the posterior portion of the cornea until it was filled. After 20 min and the agar had completely set the corneas were overturned and immersed with DMEM cell culture media without antibiotic supplementation. The corneas were incubated at 37 °C for 24 h to allow diffusion of antibiotics from the corneal tissue into the media.

The media was removed along with the agar plug. The corneas were washed 2 x PBS and then positioned with the anterior portion facing upwards.

S. aureus Newman or *E. coli* MC1061 were cultured as in section 2.5.1.

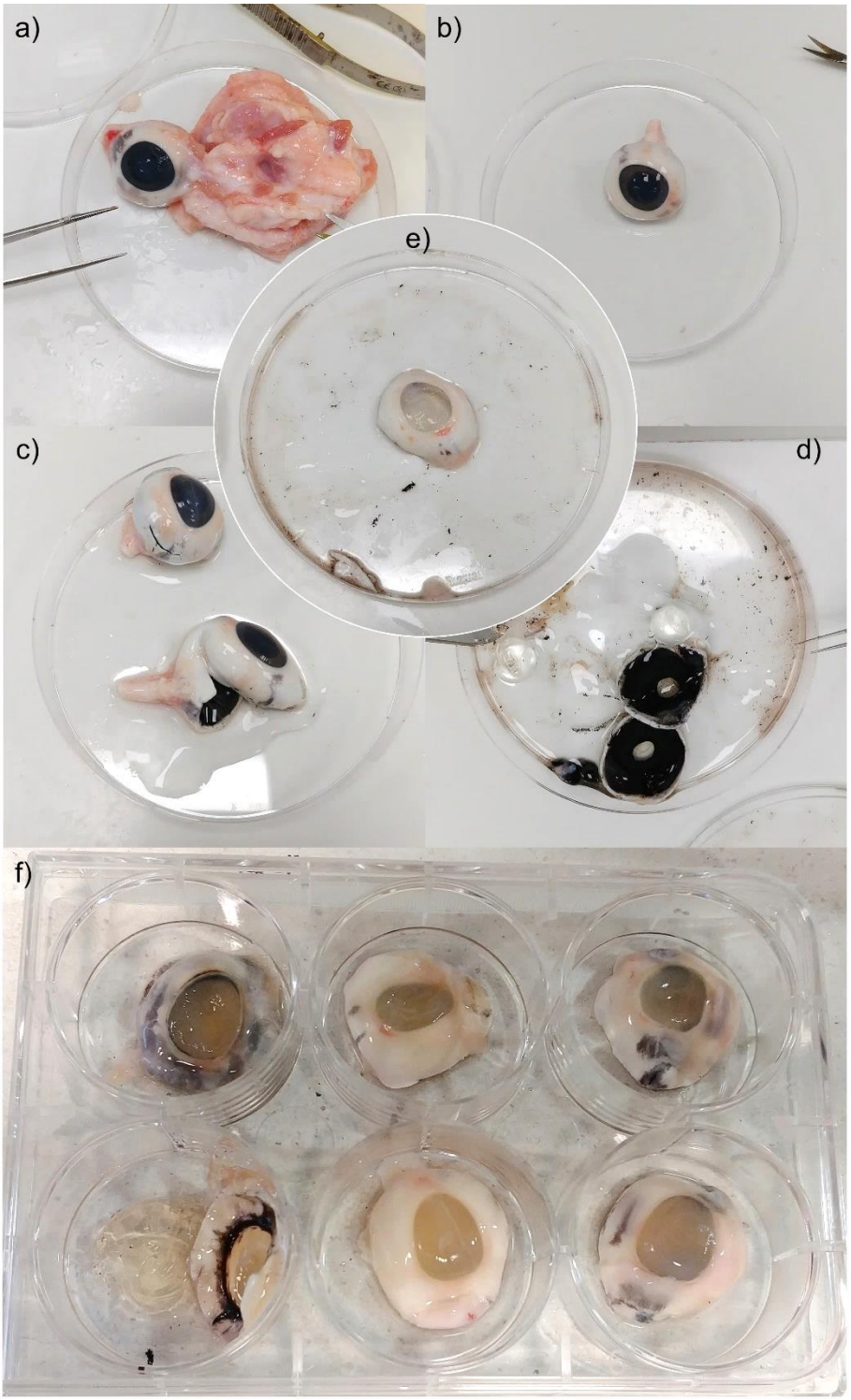

Figure 2.19: Porcine eye dissection, a) removal of muscle and fatty tissue, b) cleaned eye ball and optic nerve, c) incision made and cut around to obtain two halves, d) removal of vitreous humor and lens to expose iris and cilliary body, e) iris and cilliary body removed to leave cornea and some sclera, f) corneas mounted with 1% agar.

The corneas were scored twice vertically and horizontally using a scalpel to represent ocular surface wounds. *S. aureus* or *E. coli* suspension (50 mm^3 of 0.5 OD_{600}) was pipetted directly onto the cornea. DMEM without antibiotic supplementation was added to the well and filled to just below the cornea. The corneas were incubated again at 37 °C for 24 h to allow microbial infection of the ocular tissue to occur.

After incubation, the supernatant was removed from the corneas and they were washed 2 x PBS. Hydrogels were incubated in BAC peptides as in section 2.5.4 at a concentration of 40 μM. The hydrogels were then placed on the infected corneas for 30 min and removed. The samples were fixed with 70 v/v% aqueous ethanol for 30 min prior to imaging with a FITC fluorescent filter on a Nikon TiE microscope (Nikon, Tokyo, Japan).

2.5.8 Cytotoxicity of hydrogels with BAC peptides:

The modified hydrogel Su 60 14 COOH pre-incubated in BAC ONE or BAC TWO solution (40 μM) was investigated for any cytotoxicity towards the HCE-T cell line. A CCK 8 viability assay was carried out as in section 2.2.7 with cell morphology monitored at 24, 120 and 168 h.

2.6 Statistical Analysis

Statistical analysis was performed using GraphPad Prism version 5.03 for Windows (GraphPad Software, San Diego, CA, USA). All statistical data was presented as means with +/- standard deviation of the mean. Statistical data was analysed for equality of variances and significance was measured with two-way ANOVAs followed by Bonferroni post-tests, unless otherwise stated. If required, a log transformation of the data was performed to meet ANOVA assumptions. A p-value of ≤ 0.05 was considered statistically significant.

3. RESULTS

3.1 Hydrogel Characterisation

An investigation of the mechanical and physical characteristics of the pεK/bis-carboxylic acid cross-linked hydrogel was undertaken to characterise the novel polymer. Mechanical properties and transparency were investigated primarily to obtain a hydrogel with similar properties to those of commercial contact lens materials. All other material and physical properties were investigated to further characterise the polymer developed in this project.

3.1.1 Poly-ε-lysine characterisation:

Prior to the beginning of this study three different batches of pεK were supplied, each with a slightly different amine content as determined by C, H and N elemental analysis (Butterworth Laboratories Ltd., Teddington, England). The hypothesis was that pεK with a greater ratio of short chain oligomers would produce a different polymer than pεK with a greater ratio of longer chain oligomers. An HPLC investigation of the pεK batches was followed by mechanical property analysis of hydrogel Su 60 14 polymerised using each of the pεK batches.

A RP-HPLC system was used to characterise the three different batches of pεK. It was found that the ratio of pεK oligomers was different for each of the batches (Figure 3.1). The resulting mechanical analysis of hydrogels synthesised from each of the different batches showed that there was no significant difference in elastic modulus (Figure 3.2). The results show that the oligomer composition of pεK does not influence the mechanical properties of the final hydrogel.

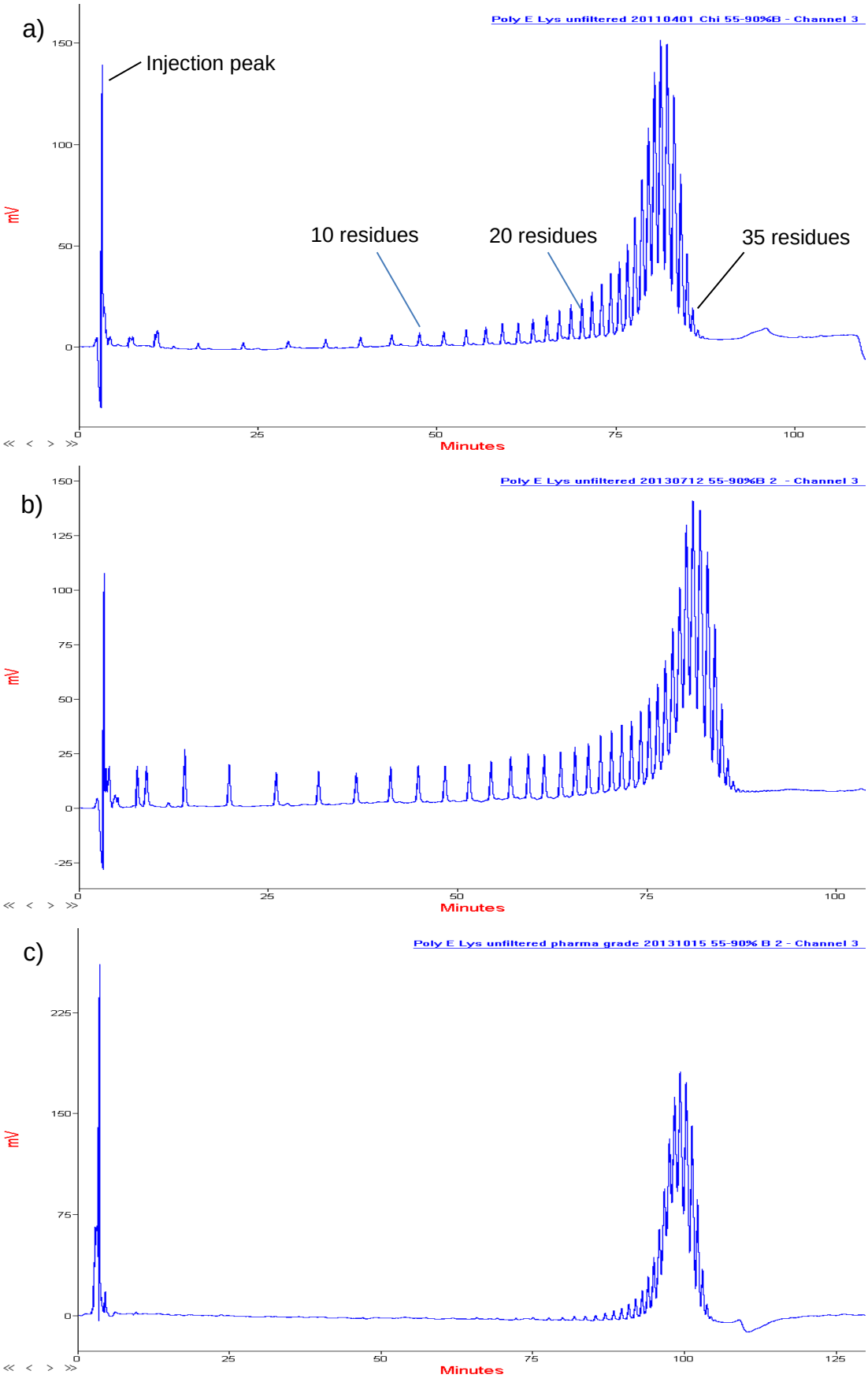

Figure 3.1: RP-HPLC investigation of different pεK batches, a) pεK 5.71 mmol g^{-1} b) pεK 5.81 mmol g^{-1} c) pεK 5.84 mmol g^{-1}.

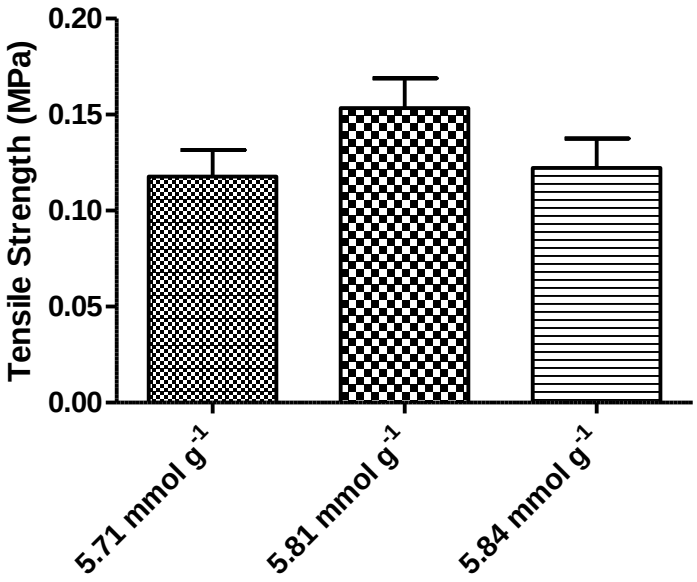

Figure 3.2: Tensile strength comparison of Su 60 14 using different pεK batches. A one-way ANOVA with Tukey post-hoc analysis was performed. Error bars ±SD, *N* = 9.

PεK Batch	Peak Area (mV)	Residues > 20 (%)
20110401 (5.71 mmol g^{-1})	46214 ± 1264	85.7% ± 1.7%
20130712 (5.81 mmol g^{-1})	47024 ± 673	74.1% ± 0.7%
20131015 5.84 mmol g^{-1})	47266 ± 1012	96.2% ± 1.1%

Table 3.1: Peak area calculations for pεK batches. ±SD, *N* = 4.

Peak area calculations confirmed pεK concentrations for each batch tested (Table 3.1). A variation in pεK chain-length distribution (> 20 residues) was noted between the 3 batches (74.1% - 96.2%).

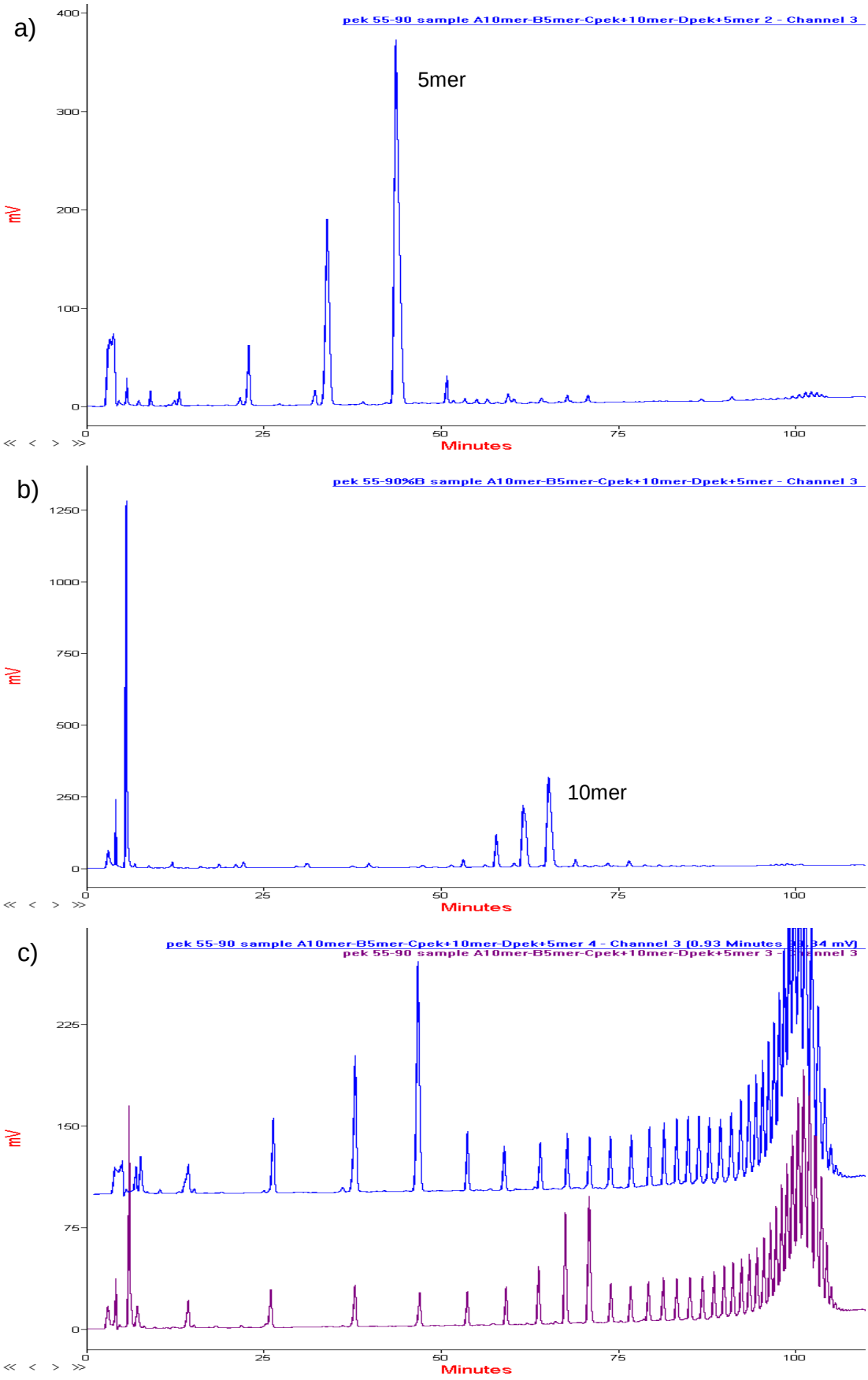

Figure 3.3: Short chain pεK oligomers to identify peak to chain-length residue association, a) pεK 5mer b) pεK 10mer c) pεK 5mer and 10mer overlays spiked with pεK.

Synthetic oligomers of pεK were synthesised in-house and were used as standards to identify the different oligomers in each batch of pεK (Figure 3.3). They confirmed that most pεK oligomers in each batch were between 25 - 35 residues long. The most abundant oligomer of pεK was found to be 30 residues of lysine in length.

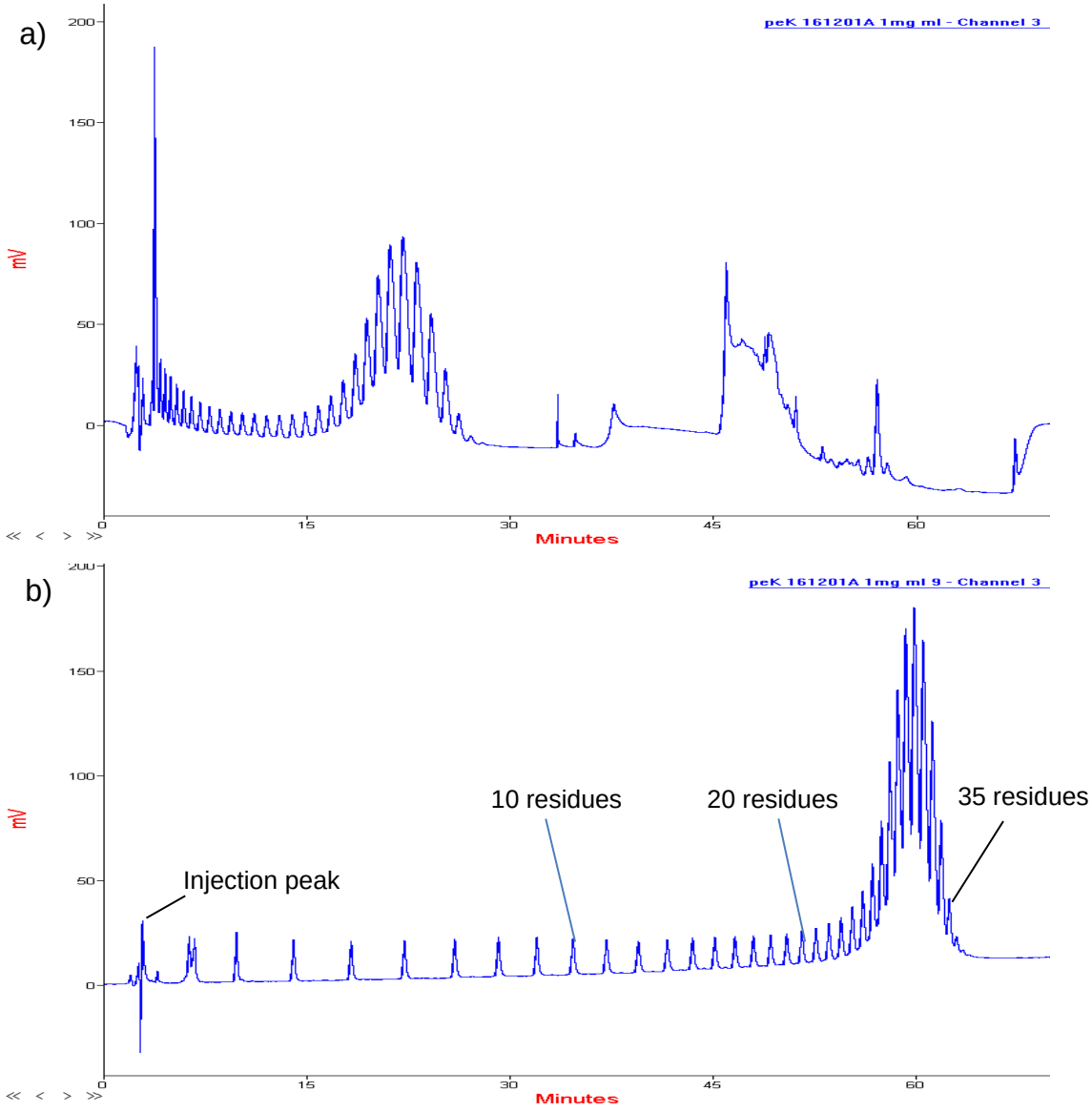

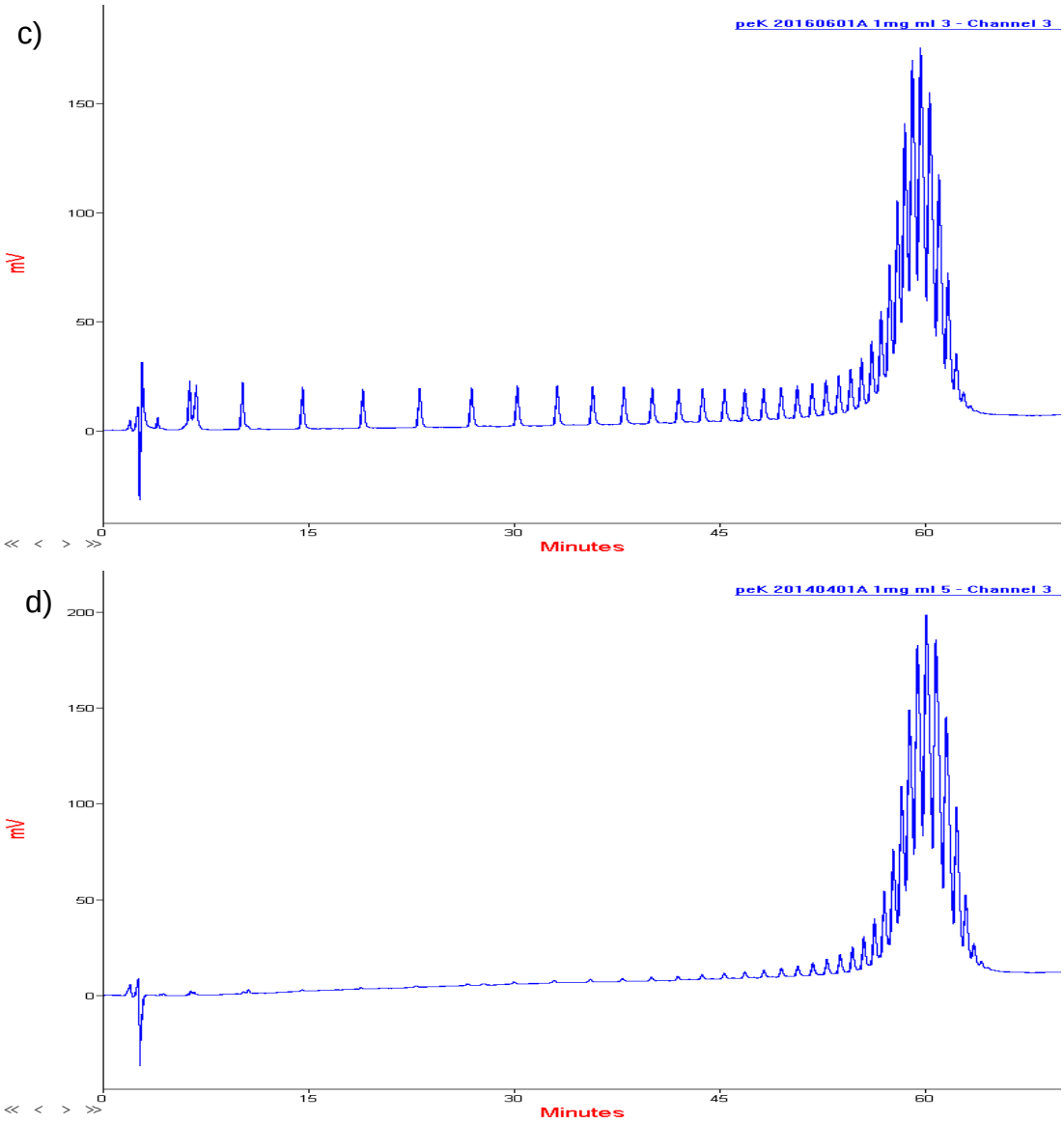

Figure 3.4: Optimisation of pεK HPLC analysis as a quality control SOP, a) old HPLC program on new Luna C18(2) column, b) pεK 161201A, c) pεK 20160601A, d) 20140401A.

PεK Batch	Peak Area (mV)	Residues > 20 (%)
161201A (5.80 mmol g^{-1})	33043 ± 163	85.6% ± 1%
20160601A (5.77 mmol g^{-1})	32870 ± 715	86.0% ± 1%
20140401A (5.81 mmol g^{-1})	33120 ± 509	98.0% ± 0%

Table 3.2: HPLC peak area calculations for pεK batches. ±SD, *N* = 4.

Further optimisation of the pεK characterisation protocol was necessary following a change of HPLC column used in the analysis. This is an important consideration when trying to replicate the protocol on different HPLC systems. The most recent Luna C18(2) column (00D-4251-E0, Phenomenex, Torrance, CA, USA) was used with the same HPLC conditions as in section 2.1.1. The result was a much quicker elution time of < 30 min for pεK (Figure 3.4a). This allowed for a shorter run time to be used for the analysis (75 min). Three new batches of pεK were analysed with the new HPLC conditions (Figure 3.4b-d). Peak area calculations confirmed pεK concentrations for each batch tested (Table 3.2). Only a small variation in pεK concentration (5.77 - 5.81 mmol g^{-1}) and chain-length distribution > 20 residues was observed between the 3 batches (85.6% - 98%).

3.1.2 Bis-carboxylic acid cross-linker, polymer density and degree of cross-linking for the Hydrogel:

An initial study was carried out to determine which short to medium chain bis-carboxylic acid would be best suited as a cross-linker for the hydrogel. Several factors were examined to identify suitability including transparency, solubility and the mechanical properties of the cross-linked hydrogels. The polymer density and degree of cross-linking were also optimised.

The polymer first derived by cross-linking pεK with a bis-carboxylic acid was a fully cross-linked macroporous material. The bis-carboxylic acid cross-linker was decanedioic acid and the polymer density was in the region of 0.04 - 0.05 g cm^{-3}. This polymer provided a starting point for the development of a hydrogel from the same polymer constituents. A preliminary hydrogel was polymerised with 60 mol% cross-linking with decanedioic acid and a polymer density of 0.067 g cm^{-3}. It was noted that the transparency of the hydrogel would not be ideal using decanedioic acid. At this stage, longer chain bis-carboxylic acids (dodecanedioic acid C12 and tridecanedioic acid C13) were discounted due to their long hydrophobic backbone resulting in poorer solubility and lack of transparency when polymerised. A study of four different polymer compositions (60 mol% cross-linked and 0.1 g cm^{-3}, 60 mol% cross-linked and 0.067 g cm^{-3}, 80 mol% cross-linked and 0.1 g cm^{-3}, 80 mol%

cross-linked and 0.067 g cm^{-3}) cross-linked individually with five separate bis-carboxylic acid cross-linkers ranging from hexanedioic acid (C6) up to decanedioic acid (C10) was undertaken. The mechanical properties were obtained for each hydrogel as well as a physical observation for transparency.

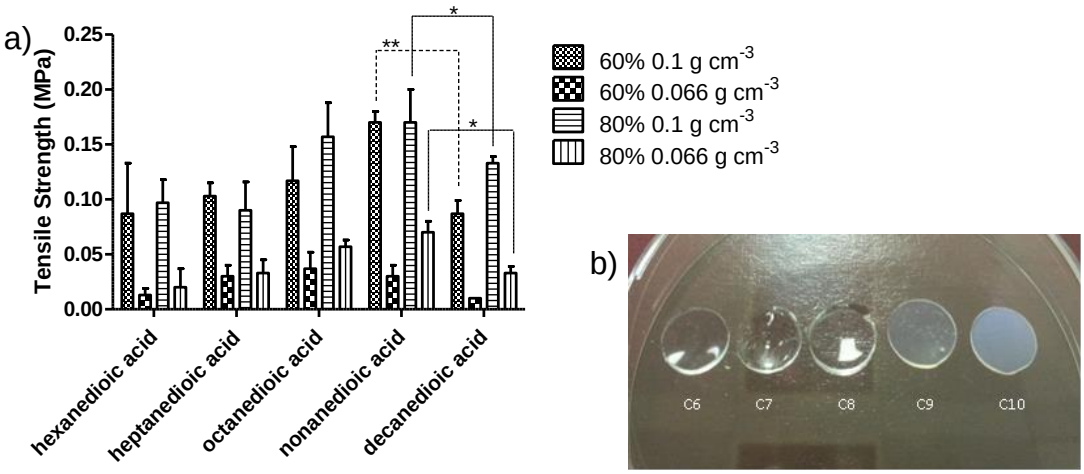

Figure 3.5: a) A comparison of tensile strength of hydrogels cast with differing bis-carboxylic acid cross-linkers and polymer densities -60 mol% cross-linked, 0.1 g cm^{-3} -60 mol% cross-linked, 0.067 g cm^{-3} -80 mol% cross-linked, 0.1 g cm^{-3} -80 mol% cross-linked, 0.067 g cm^{-3}, b) Changes in transparency due to bis-carboxylic acid chain-length. Error bars ±SD, * $p < 0.05$, ** $p < 0.01$ $N = 9$.

The tensile strength of the materials investigated significantly increased as the chain length of the bis-carboxylic acid increased from hexanedioic acid to nonanedioic acid ($p < 0.05$) before significantly reducing again for 3 of the 4 hydrogel compositions with the decanedioic acid cross-linker ($p < 0.05$) (Figure 3.5a). Decanedioic acid was the least soluble of the five bis-carboxylic acids investigated and resulted in the most opaque polymers of each composition. The polymer density had a greater effect on mechanical properties ($p < 0.01$) compared to the degree of cross-linking for each variant with the same bis-carboxylic acid. Minor differences were observed between the varying degrees of cross-linking but these were not statistically significant. These data suggest that the polymer density has a greater effect on polymer strength than the degree of cross-linking. The increase in bis-

carboxylic acid as previously suggested has a negative effect on the transparency of the hydrogel. These data coupled with a visual check for transparency (Figure 3.5b) led to octanedioic acid being chosen as the most appropriate bis-carboxylic acid to cross-link pεK and form the hydrogel.

3.1.3 Optimal hydrogel composition and refractive index:

Further tailoring of the hydrogel properties was investigated with octanedioic acid as the bis-carboxylic acid cross-linker. As expected the ultimate tensile strength increased with an increase in polymer density from 0.067 - 0.077 g cm^{-3} (Figure 3.6a).

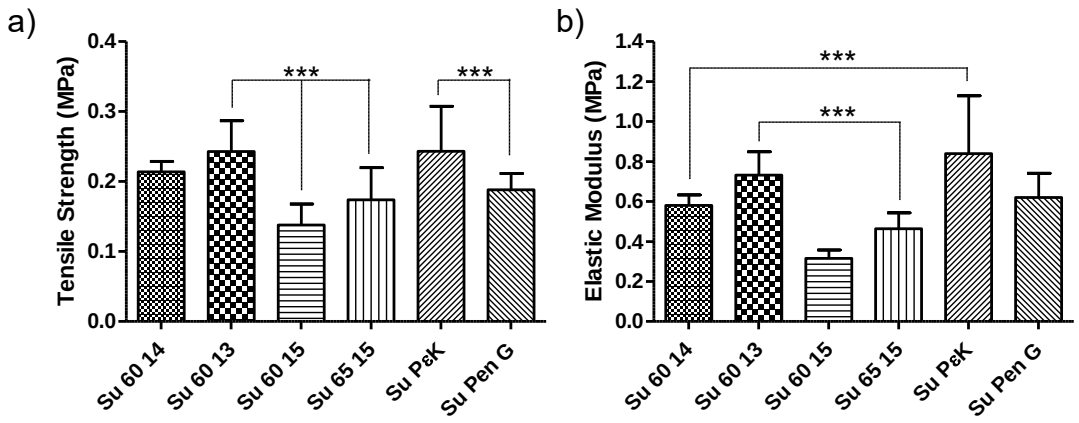

Figure 3.6: a) Comparison of stress between octanedioic acid hydrogel variants, b) comparison of the elastic modulus between octanedioic acid hydrogel variants. A one-way ANOVA with Tukey post-hoc analysis was performed. Error bars ±SD, *** $p < 0.005$ $N = 9$.

The elastic modulus (Figure 3.6b) for hydrogel Su 60 13 (octanedioic acid cross-linker with a density of 0.077 g cm^{-3} and 60 mol% cross-linked) was significantly greater than the other hydrogels tested. However, transparency of this hydrogel was compromised significantly ($p < 0.005$) due to the increased polymer density, resulting in a refractive index (Figure 3.7a) of 1.395 (AR200 digital refractometer (Reichert, New York, USA)). These data were further corroborated with light transmittance data (Figure 3.7b) for hydrogel Su 60 13 (79%) significantly lower than both Su 60 14 (88%) and Su 60 15 (92%). The hydrogel with the next greatest elastic modulus was

hydrogel Su 60 14 (octanedioic acid cross-linker with a density of 0.071 g cm^{-3} and 60 mol% cross-linked) which, despite no significant difference in ultimate tensile strength compared to Su 60 13, was superior to both Su 60 15 (octanedioic acid cross-linker with a density of 0.067 g cm^{-3} and 60 mol% cross-linked) and Su 65 15 (octanedioic acid cross-linker with a density of 0.067 g cm^{-3} and 65 mol% cross-linked).

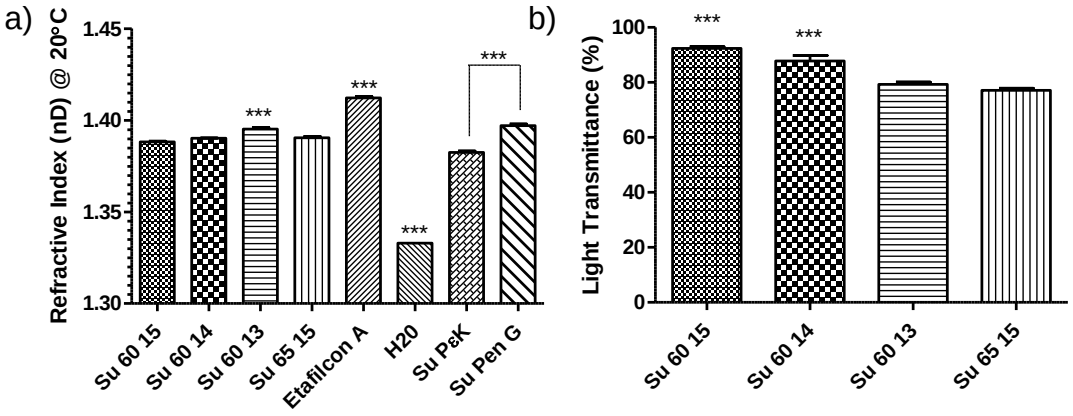

Figure 3.7: a) Refractive index measurements of octanedioic acid hydrogel variants, b) Light transmittance data of four hydrogel variants. A one-way ANOVA with Tukey post-hoc analysis was performed. Error bars ±SD, *** $p < 0.005$ $N = 9$.

Hydrogel Su 60 14 possessed a refractive index of 1.390 making it closely associated with the 1.380 - 1.400 of the human cornea (Kim *et al.*, 2004; Vasudevan, Simpson and Sivak, 2008). All the hydrogels tested had a significantly lower ($p < 0.005$) refractive index than the commercial contact lens etafilcon A at 1.412. Consequently, Su 60 14 was chosen as the hydrogel with superior mechanical properties whilst maintaining an acceptable transparency.

3.1.4 Polymerisation time:

Hydrogel Su 60 14 was polymerised for five different time-points before the polymerisation was stopped and the mechanical properties analysed. The mechanical data were used to identify the optimal polymerisation time for the hydrogel cross-linking to reach completion. The results show a statistically significant increase ($p < 0.05$) in elastic modulus up to 5 h after polymerisation was initiated. The elastic modulus begins to plateau after 5 h (Figure 3.8a) with no significant change observed. These data suggest that after 5 h the polymer has reached a point where cross-linking has ceased.

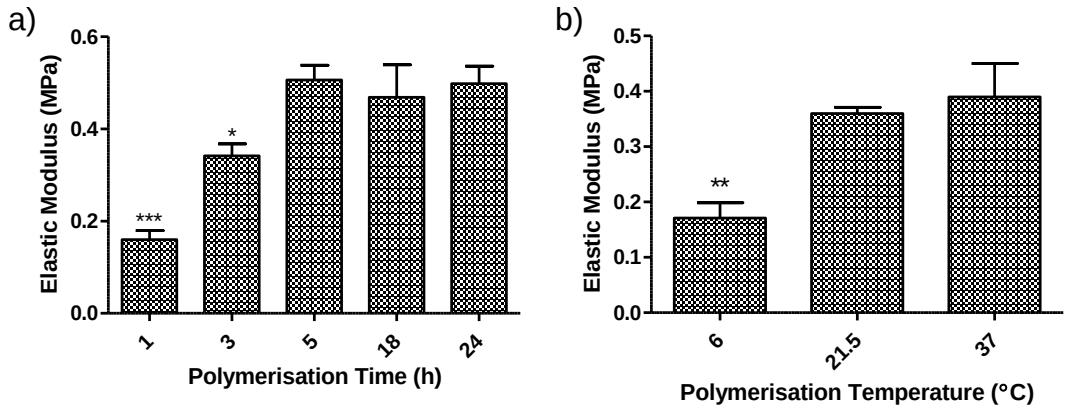

Figure 3.8: Investigation of the optimal polymerisation time (a) and temperature (b) for hydrogel Su 60 14. A one-way ANOVA with Tukey post-hoc analysis was performed. Error bars ±SD, * $p < 0.05$, ** $p < 0.01$, *** $p < 0.005$ $N = 9$.

3.1.5 Polymerisation temperature:

Hydrogel Su 60 14 was polymerised under three different temperatures to analyse the effect of reaction temperature on the final mechanical properties of the hydrogel. The polymerisation temperature data identified that hydrogel Su 60 14 polymerised at room temperature (21.5 °C) and physiological temperature (37 °C) for 5 h had a statistically significant increase ($p < 0.01$) in elastic modulus compared to Su 60 14 polymerised at 6 °C for the same length of time (Figure 3.8b). No significant difference was observed in elastic modulus between Su 60 14 polymerised at 21.5 °C and 37 °C.

3.1.6 Percentage water content:

An important characteristic of a hydrogel is the water content, specifically in the development of contact lens materials where the oxygen permeability is directly associated with the amount of water the hydrogel contains. A gravimetric method was used to determine the volume of water contained within each hydrogel variant. It was discovered that the hydrogels polymerised in this study have a relatively high water content whilst retaining their optimal mechanical properties when compared to a range of commercial contact lens materials (Table 3.3). The water content of all the hydrogel variants tested are within the 67 - 73% range whilst the elastic modulus covers a greater range of the values noted for commercial contact lens materials (0.31 - 0.84 MPa).

A comparison of methods (Figure 3.9) used to determine the water content of the hydrogels confirmed the data obtained via the gravimetric method. No statistically significant difference was observed between the methods tested.

Material	% Water Content	Elastic Modulus (MPa)
Hydroxyethyl methacrylate / methacrylic acid	70	**0.77** (+/- 0.11)
Su 60 13 (60 mol% cross-linked, 0.077 g cm^{-3} polymer density)	67 (+/- 3.4)	**0.73** (+/- 0.12)
Su 60 14 (60 mol% cross-linked, 0.071 g cm^{-3} polymer density)	69 (+/- 0.8)	**0.61** (+/- 0.07)
Vinyl pyrrolidone / methyl methacrylate	70	**0.49** (+/- 0.09)
Su 65 15 (65 mol% cross-linked, 0.067 g cm^{-3} polymer density)	71 (+/- 1.6)	**0.46** (+/- 0.08)
Hydroxyethyl methacrylate / vinyl pyrrolidone	55	**0.36** (+/- 0.07)
Su 60 15 (60 mol% cross-linked, 0.067 g cm^{-3} polymer density)	70 (+/- 1.7)	**0.31** (+/- 0.04)
Su PεK (Su 60 14 with pεK covalently attached)	73 (+/- 0.9)	**0.84** (+/- 0.29)
Su Pen G (Su 60 14 with penicillin G ionically attached)	70 (+/- 0.8)	**0.62** (+/- 0.12)

Table 3.3: Elastic modulus and water content of the hydrogel variants prepared for this report compared to commercial lens materials (Tranoudis and Efron, 2004). ±SD, *N* = 9.

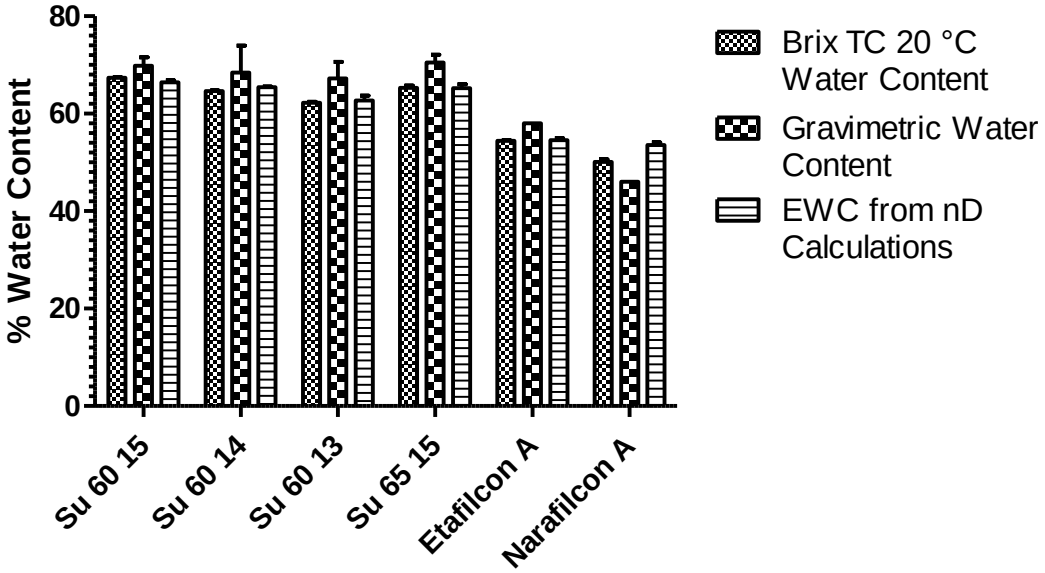

Figure 3.9: Comparison of hydrogel water content determined via different methods. Error bars ±SD, *N* = 9.

3.1.7 Dk values:

Dk values were converted from the previously obtained hydrogel water contents (section 3.1.6) using the formula from section 2.1.7 to create a standard curve (Figure 3.10).

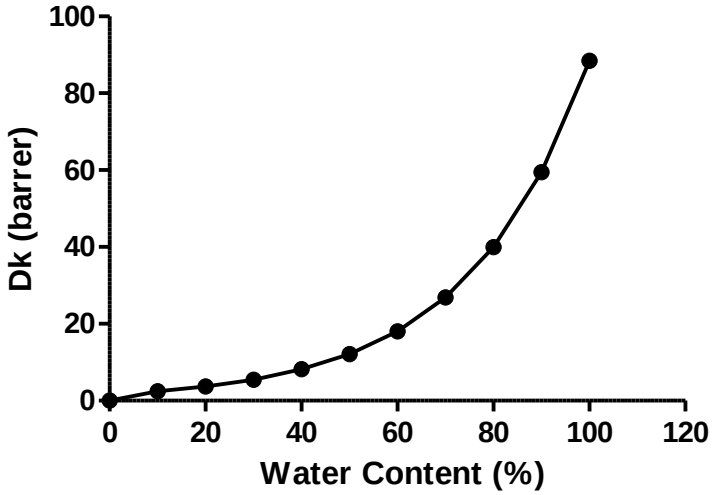

Figure 3.10: Dk values from water content percentage.

The water content obtained for each of the hydrogel variants was compared to the graph to obtain the corresponding Dk value based solely on the water content of the hydrogel.

	Su 60 15	Su 60 14	Su 60 13	Su 65 15	Su PεK	Omafilcon A	Lotrafilcon A
Dk	26.89	25.85	23.87	27.98	30.29	27	140
SD	1.79	1.72	1.91	1.78	1.73	-	-

Table 3.4: Dk values for hydrogel variants. ±SD, *N* = 9.

The Dk values for the hydrogel variants are within a short range (24 - 30 Barrer) and comparable to a conventional hydrogel contact lens (omafilcon A) but much lower than a silicone hydrogel contact lens (lotrafilcon A).

3.1.8 Contact angle analysis:

An investigation of the contact angle of the hydrogel variants was undertaken as a measure of their wettability. This is an important aspect in contact lens design as the more hydrophilic materials allow a greater coverage and recovery of the tear film (Lin and Svitova, 2010). The advancing contact angle was captured and analysed via the sessile drop technique on a Krüss DSA100. The contact angles for the hydrogel variants ranged between 29 - 31 ° with no significant difference observed between them (Figure 3.11). PTFE (96 °) and glass (78 °) had significantly greater ($p < 0.005$) contact angles than any of the hydrogels. These data highlight that the hydrogels have a high degree of wettability.

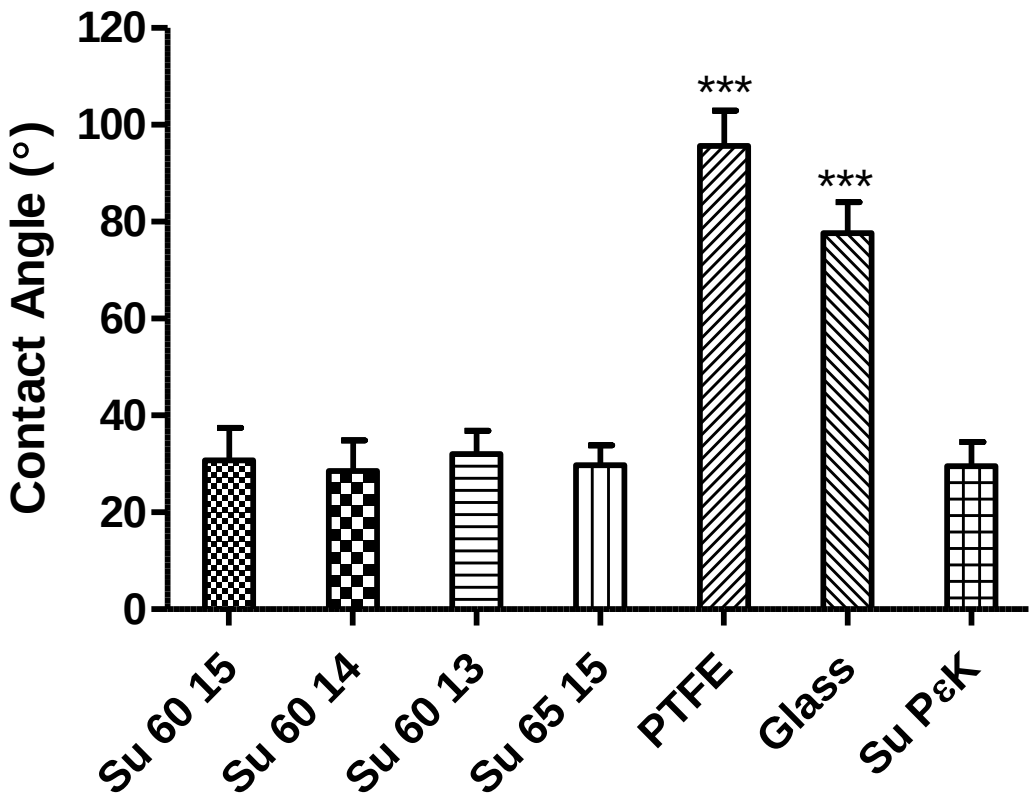

Figure 3.11: Contact angle analysis of the hydrogel variants. A one-way ANOVA with Tukey post-hoc analysis was performed. Error bars ±SD, *** $p < 0.005$ $N = 9$.

3.1.9 Degradation:

Degradation of the hydrogel variants was monitored gravimetrically and with SEM images over a 12 month period.

	Sample	Start Weight	1 Week	1 Month	6 Months	12 Months
PBS	Su 60 15	49.33 ± 4.83	37.53 (76%) ± 10.67	31.93 (65%) ± 3.15	29.87 (61%) ± 4.69	29.67 (60%) ± 4.32
	Su 60 14	50.07 ± 4.91	36.30 (73%) ± 4.30	34.20 (68%) ± 3.10	31.77 (63%) ± 3.13	32.67 (65%) ± 2.66
	Su 60 13	44.03 ± 9.05	31.26 (71%) ± 5.52	30.90 (70%) ± 5.43	29.43 (67%) ± 5.35	29.07 (66%) ± 4.00
	Su 65 15	41.47 ± 7.92	29.93 (72%) ± 5.89	28.93 (70%) ± 5.35	27.06 (65%) ± 5.18	26.97 (65%) ± 5.18
	Su PεK	44.63 ± 2.76	28.10 (63%) ± 0.63	26.50 (59%) ± 1.25	26.00 (58%) ± 0.40	26.63 (60%) ± 1.19
	Etafilcon A	47.9 ± 5.74	39.67 (83%) ± 5.75	30.93 (65%) ± 0.12	30.03 (63%) ± 0.45	30.10 (63%) ± 0.12
	PTFE	31.73 ± 0.58	31.9 (101%) ± 0.17	31.53 (99%) ± 0.47	31.37 (99%) ± 0.59	31.57 (100%) ± 0.06
NaOH	Su 60 15	53.36 ± 10.72	59.66 (112%) ± 13.41	106.97 (200%) ± 24.15		
	Su 60 14	49.56 ± 5.53	57.73 (117%) ± 5.65	103.63 (209%) ± 11.26		
	Su 60 13	43.53 ± 7.36	54.03 (124%) ± 9.25	90.57 (208%) ± 16.73		
	Su 65 15	42.5 ± 5.08	47.43 (112%) ± 7.07	82.87 (195%) ± 11.64		
	Su PεK	46.76 ± 3.54	53.20 (114%) ± 1.44	108.66 (232%) ± 3.41		
	Etafilcon A	41.37 ± 1.00	53.53 (129%) ± 2.00	77.90 (188%) ± 0.17	157.67 (381%) ± 1.53	
	PTFE	30.73 ± 1.16	30.10 (98%) ± 1.05	30.07 (98%) ± 1.06	30.17 (98%) ± 1.38	30.13 (98%) ± 1.27
Trypsin	Su 60 15	51.13 ± 7.85	32.97 (65%) ± 5.60	33.47 (66%) ± 5.73		
	Su 60 14	50.07 ± 4.23	35.23 (70%) ± 3.39	34.20 (68%) ± 3.25		
	Su 60 13	46.67 ± 9.21	29.37 (63%) ± 8.02	32.73 (70%) ± 5.32		
	Su 65 15	42.77 ± 4.74	30.37 (71%) ± 3.21	29.23 (68%) ± 3.69		
	Su PεK	49.30 ± 4.29	29.53 (60%) ± 1.40	28.53 (58%) ± 1.70		
	Etafilcon A	40.13 ± 1.33	30.90 (77%) ± 1.80	29.80 (74%) ± 1.40		
	PTFE	30.00 ± 0.30	29.73 (99%) ± 0.72	29.7 (99%) ± 0.87		

Table 3.5: Degradation sample weights over 12 months (mg) and as a percentage of start weights. ±SD, *N* = 3.

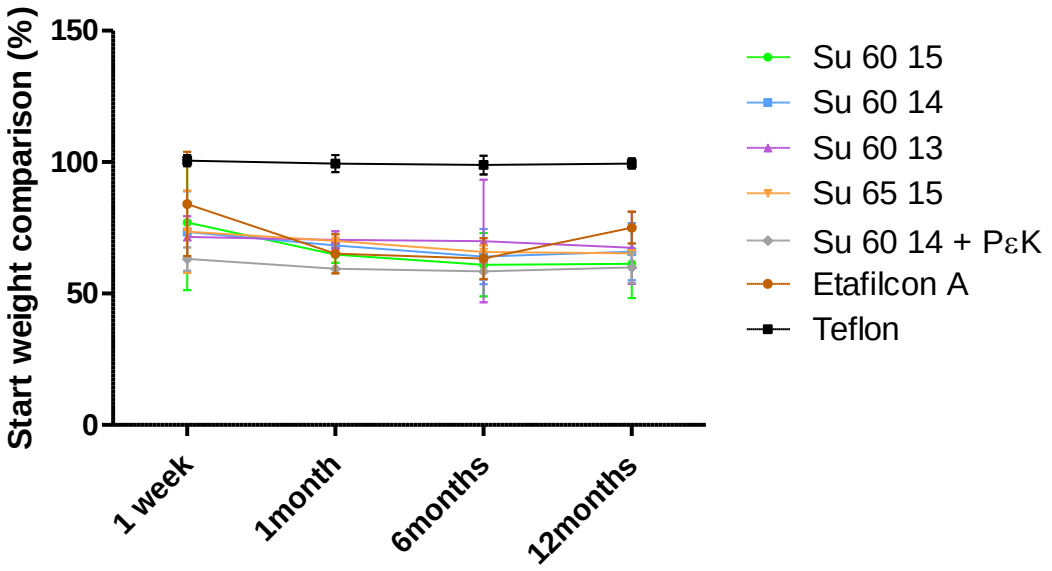

Figure 3.12: Weight loss from hydrogel samples stored in PBS over 12 months as a percentage of start weight. Error bars ±SD, *N* = 9.

Degradation is an important aspect of contact lens wear as long term degradation can lead to discomfort, reduced vision and signs of adverse ocular reactions (Tanner and Efron, 2018). For all the hydrogels stored in PBS or trypsin there was an initial decrease in weight observed after 1 week (Table 3.5). However, for each subsequent time-point there was no significant decrease in weight observed and the hydrogel variants tested followed a similar weight profile as the commercial contact lens material etafilcon A (Figure 3.12). All hydrogel variants stored in NaOH increased in weight until they had completely degraded after 1 month. A visual inspection confirmed that total degradation occurred between 1 - 3 months. Etafilcon A degraded fully after 6 months in NaOH and no degradation was observed from the negative control (PTFE) under any storage conditions. Incubation in trypsin was discontinued after 1 month as no difference was observed between trypsin storage and PBS and the activity of trypsin required daily replenishment.

The SEM images taken at each time-point confirmed the findings from the gravimetric analysis of the hydrogel variants. Obvious signs of degradation were evident for all samples stored in NaOH after 1 month with

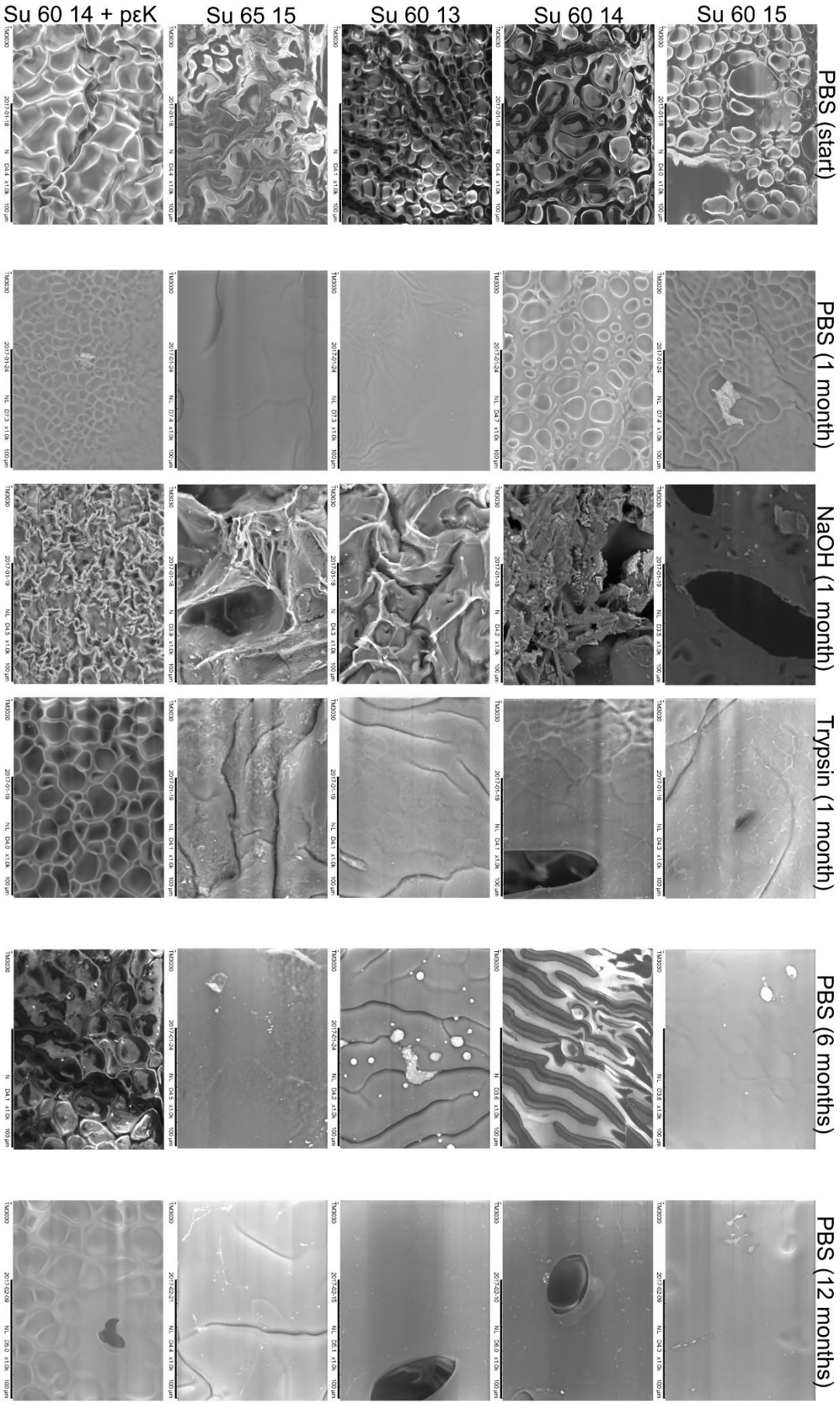

Figure 3.13: SEM images of various time-points of the degradation study. Scale bar is 100 µm

100 µm voids evident in some samples (Su 60 15). However, most voids were smaller but still evident from the SEM images. Hydrogel variants stored in PBS only began to show minor signs of degradation after 12 months but the voids were more random and less ubiquitous than those found in samples stored in NaOH.

3.1.10 Lens formation:

Several attempts were made to cast the hydrogel in the shape of a bandage lens. Spin cast methods resulted in an uneven distribution of the polymer and never resulted in the formation of a viable lens material. The immiscible solvent technique resulted in a formed hydrogel with a curved shape and no obvious signs of trapped gas bubbles, however, it was not lens like nor reproducible (Figure 3.14a).

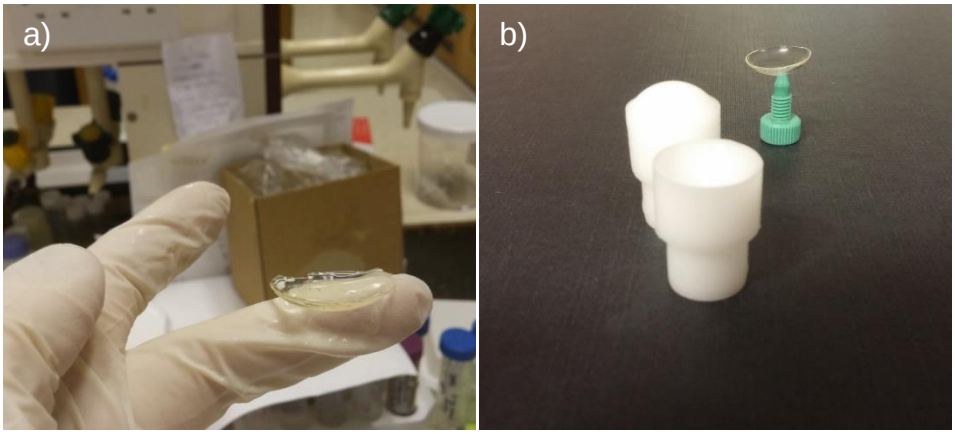

Figure 3.14: Hydrogel casting a) an immiscible solvent technique, b) male/female moulds.

Polymerisation of the standard hydrogel Su 60 14 in a closed vessel male/female mould resulted in the entrapment of gas bubbles within the polymer, resulting in a weakened hydrogel matrix that tore as it polymerised. A reduction in NHS from 0.5 to 0.2 Molar equivalents to the amine groups within the polymer or replacing it with HOBt as the activation agent resulted in the formation of a hydrogel lens (Figure 3.14b).

3.2 Cytocompatibility of HCE-T Cells to Hydrogel Su 60 14

The cytocompatibility of hydrogel Su 60 14 was investigated. A human corneal epithelial cell line (HCE-T) was chosen for in vitro studies because they behave and retain the morphology of primary corneal epithelial cells.

3.2.1 Cytotoxicity:

The cytotoxic response of HCE-T cells to the pεk/bis-carboxylic acid hydrogel material was investigated to determine cell viability. The 8 day growth curve of HCE-T cells cultured in standard media compared to those cultured in media pre-incubated with the pεk/bis-carboxylic acid hydrogel demonstrated there was no significant difference between cell viability at any of the time-points analysed. This result suggests that hydrogel Su 60 14 does not affect HCE-T cell viability when compared to the control (Figure 3.15) and that any leachables from hydrogel Su 60 14 are non-cytotoxic towards the HCE-T cell line.

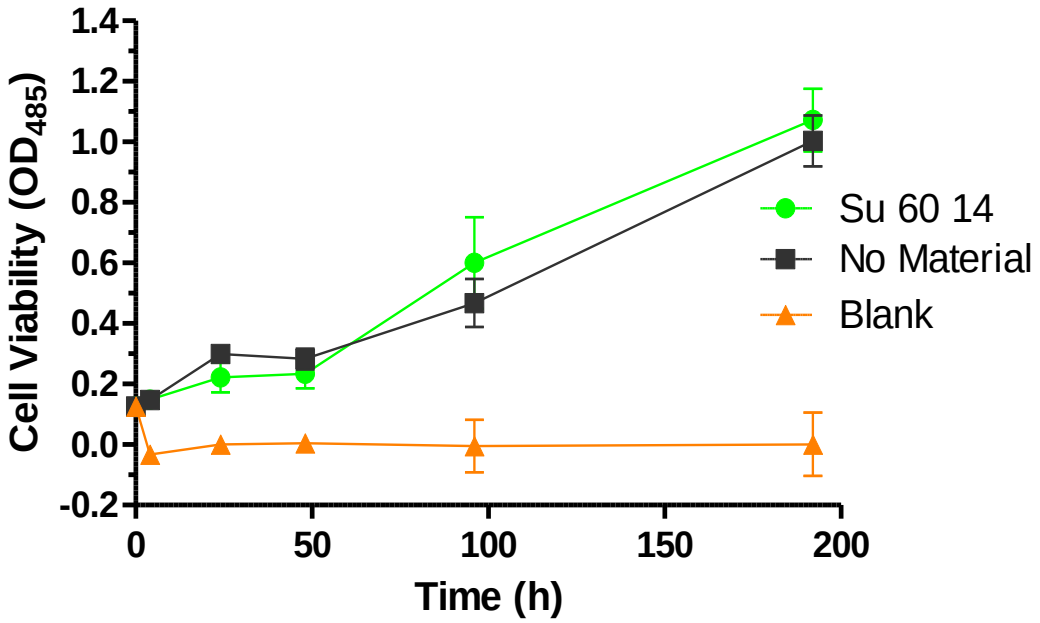

Figure 3.15: Cytotoxicity of leachables from hydrogel Su 60 14 towards the HCE-T cell line. Error bars ±SD, *N* = 9.

3.2.2 Cellular morphology:

A qualitative investigation of cellular morphology when in direct contact with hydrogel Su 60 14 was undertaken to determine any cytotoxicity and complement the quantitative data obtained from the CCK-8 assay. HCE-T cells were seeded either directly underneath or on to the surface of the hydrogel and images were taken and analysed. After seeding HCE-T cells directly on top of hydrogel Su 60 14 very few attached to the surface and those that remained retained a spherical morphology after 48 h (Figure 3.16a). The HCE-T cells cultured on tissue culture plastic directly underneath hydrogel Su 60 14 appear to have a more typical cobblestone morphology after 48 h as expected for this cell type (Figure 3.16b).

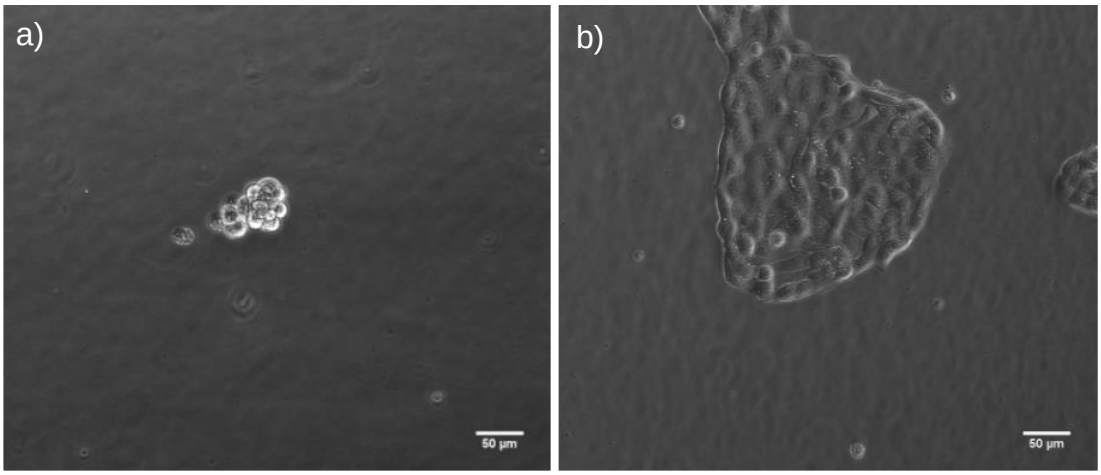

Figure 3.16: HCE-T cell morphology on hydrogel Su 60 14 (a) and TC plastic (b). Scale bar is 50 µm.

A live/dead cell assay was carried out on HCE-T cells cultured directly underneath hydrogel Su 60 14 for 48 h. All the HCE-T cells stain positive for the live cell stain calcein with no ethidium bromide staining evident for dead cells. Cells were counterstained with the nuclear stain Hoechst 33342 (Figure 3.17a). The hydrogel can be observed in the background of the brightfield image (Figure 3.17b).

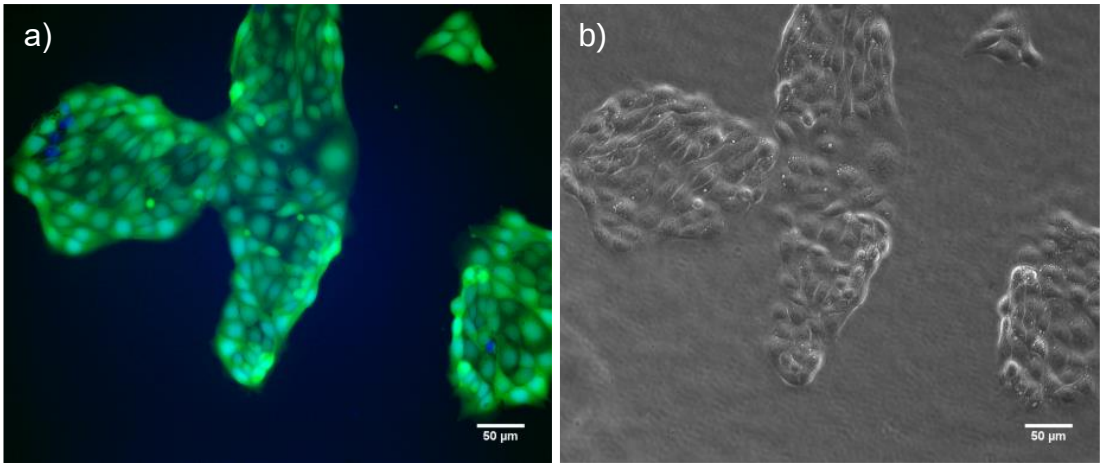

Figure 3.17: Live/Dead assay (a) brightfield image (b) of HCE-T cells cultured directly underneath hydrogel Su 60 14. Scale bar is 50 µm.

These observations suggest that hydrogel Su 60 14 is hydrophilic enough without modification to prevent HCE-T cell attachment but is non-cytotoxic to HCE-T cells when in direct contact.

3.2.3 Scratch assay:

A wound model was set up to investigate if hydrogel Su 60 14 would influence the rate of re-epithelialisation of a scratch wound on a monolayer of HCE-T cells. A confluent monolayer was obtained after 3 days in culture; a linear scratch was made through the monolayer and the hydrogel placed on top of the cells.

The re-epithelialisation of the wound was monitored over a 24 h period, however, no obvious difference was observed between the control and scratch wounds with the hydrogel present. All the scratch wounds closed within 23 h regardless of the hydrogel being present or not (Figure 3.18).

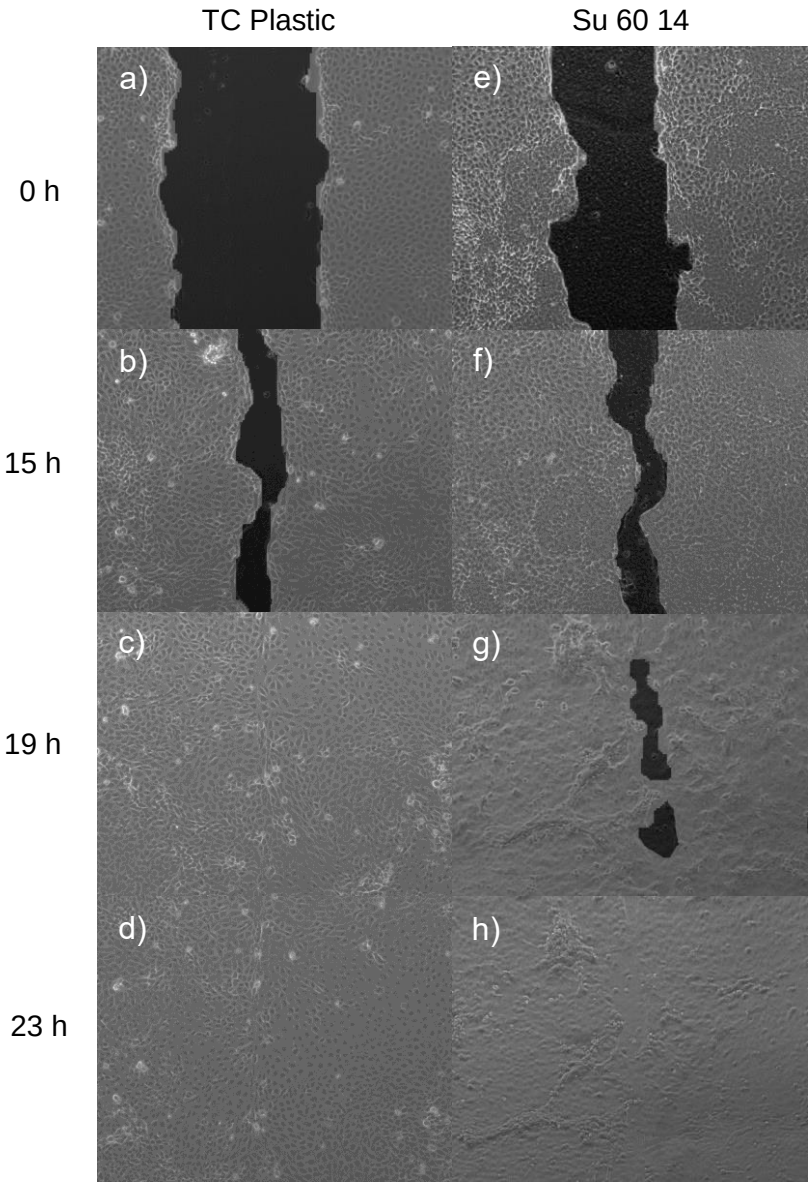

Figure 3.18: Scratch wound closure over 23 h on (a-d) TC plastic and (e-f) hydrogel Su 60 14.

Scratch wound closure was quantified using TScratch software (Figure 3.19) and identified no significant difference in the rate of scratch wound closure with (36% to 1% open area) or without (38% to 0.3% open area) the hydrogel present. These data suggest that the presence of hydrogel Su 60 14 in a HCE-T cell wound environment does not inhibit re-epithelialisation.

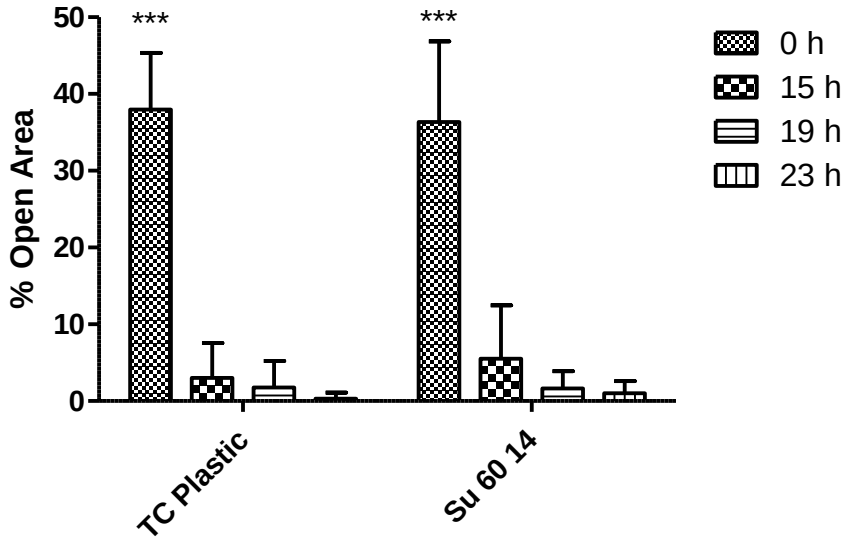

Figure 3.19: Quantification of scratch wound closure. Error bars ±SD, *** $p < 0.005$ $N = 12$.

3.2.4 Monolayer Integrity/Immunocytochemistry:

HCE-T cell monolayers were found to re-epithelialise within 24 h of the initial scratch wound. However, what was not determined was whether there was tight junction formation between cells. To investigate this HCE-T Cells were stained for zona occludens-1 (ZO-1) to identify any defects in the integrity of the monolayer and identify cell to cell contact through their tight junctions. Each of the monolayers appear to be intact and comparable to that of the no hydrogel control. No missing or physically disturbed junctions were observed (Figure 3.20). The results of the ZO-1 staining and the scratch assay suggest that hydrogel Su 60 14 does not inhibit or affect the formation of tight junctions in a HCE-T cell monolayer.

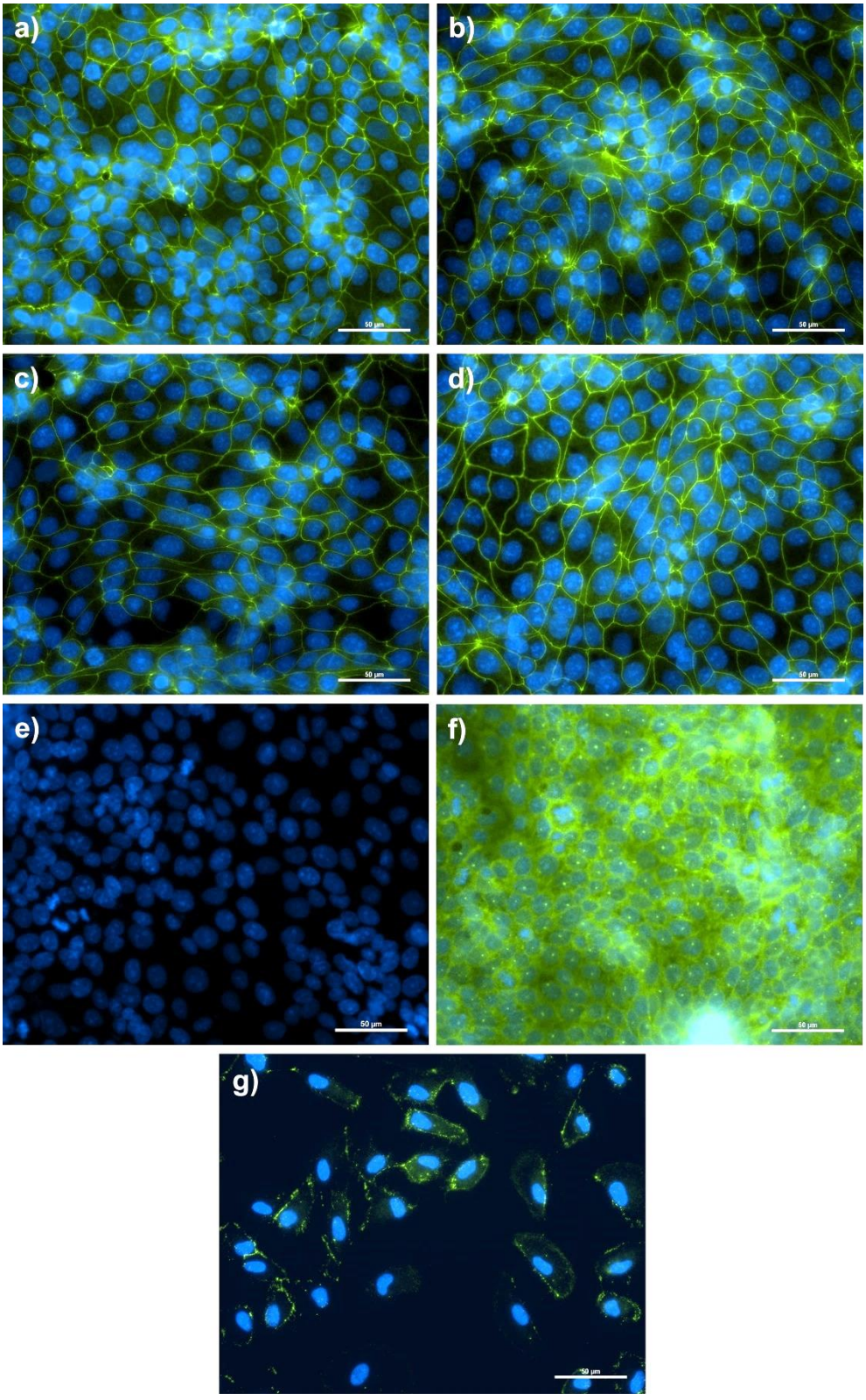

Figure 3.20: ZO-1 staining (green) of HCE-T cells following a 24 h scratch assay. The nuclei are counter-stained with DAPI (blue), a) hydrogel Su 60 14 present with scratch wound, b) no hydrogel present but scratch wound, c) hydrogel Su 60 14 present but no scratch wound, d) no hydrogel present or scratch wound, e) negative control (no primary antibody), f) positive control (IgG instead of primary antibody), g) A19 cell positive control. Scale bar is 50 µm.

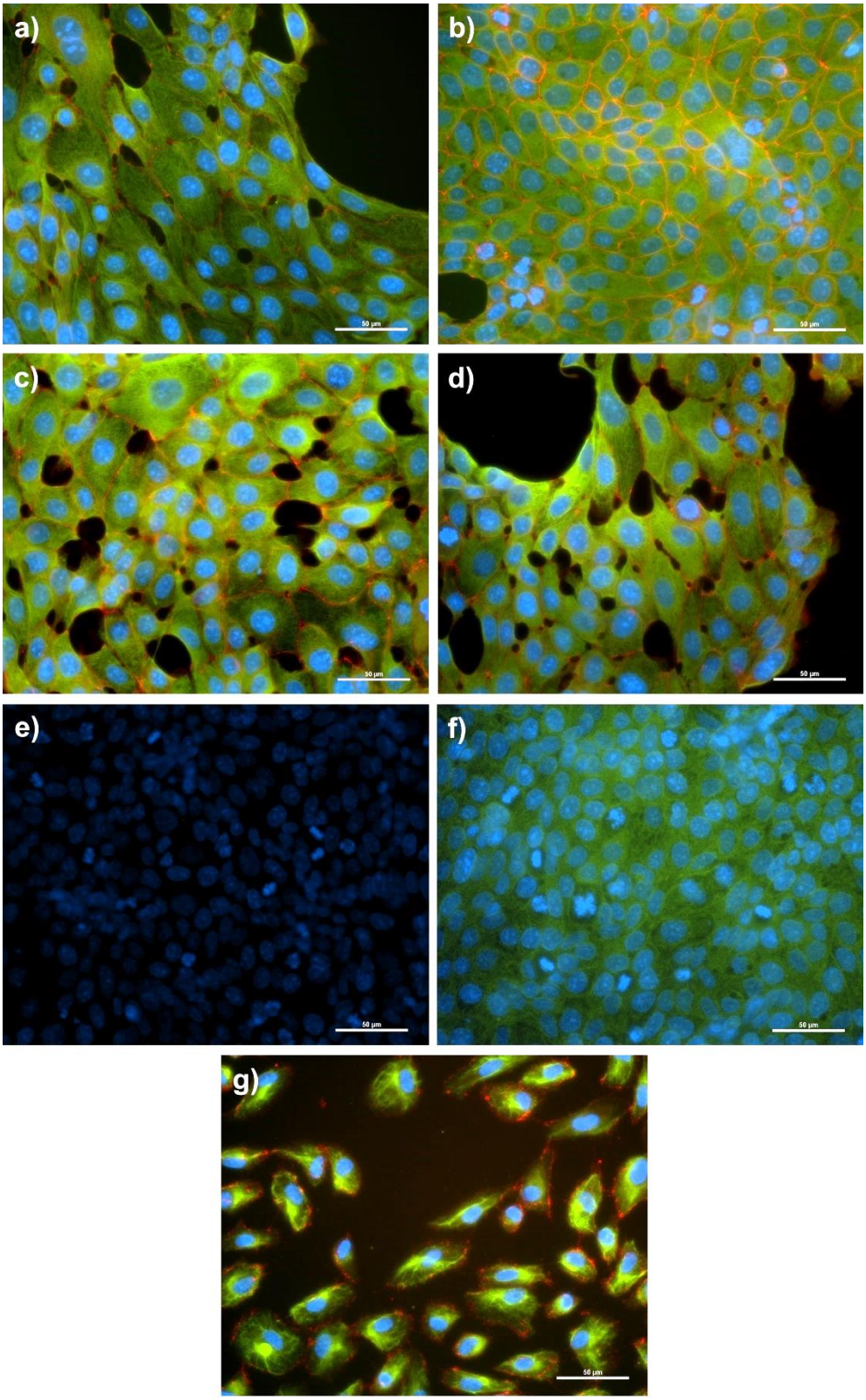

Figure 3.21: ZO-1 (red) and pan cytokeratin (green) staining of HCE-T cells following a 24 h scratch assay. The nuclei are counter-stained with DAPI (blue), a) hydrogel Su 60 14 present with scratch wound, b) no hydrogel present but scratch wound, c) hydrogel Su 60 14 present but no scratch wound, d) no hydrogel present or scratch wound, e) negative control (no primary antibody), f) positive control (IgG instead of primary antibody), g) A19 cell positive control. Scale bar is 50 µm.

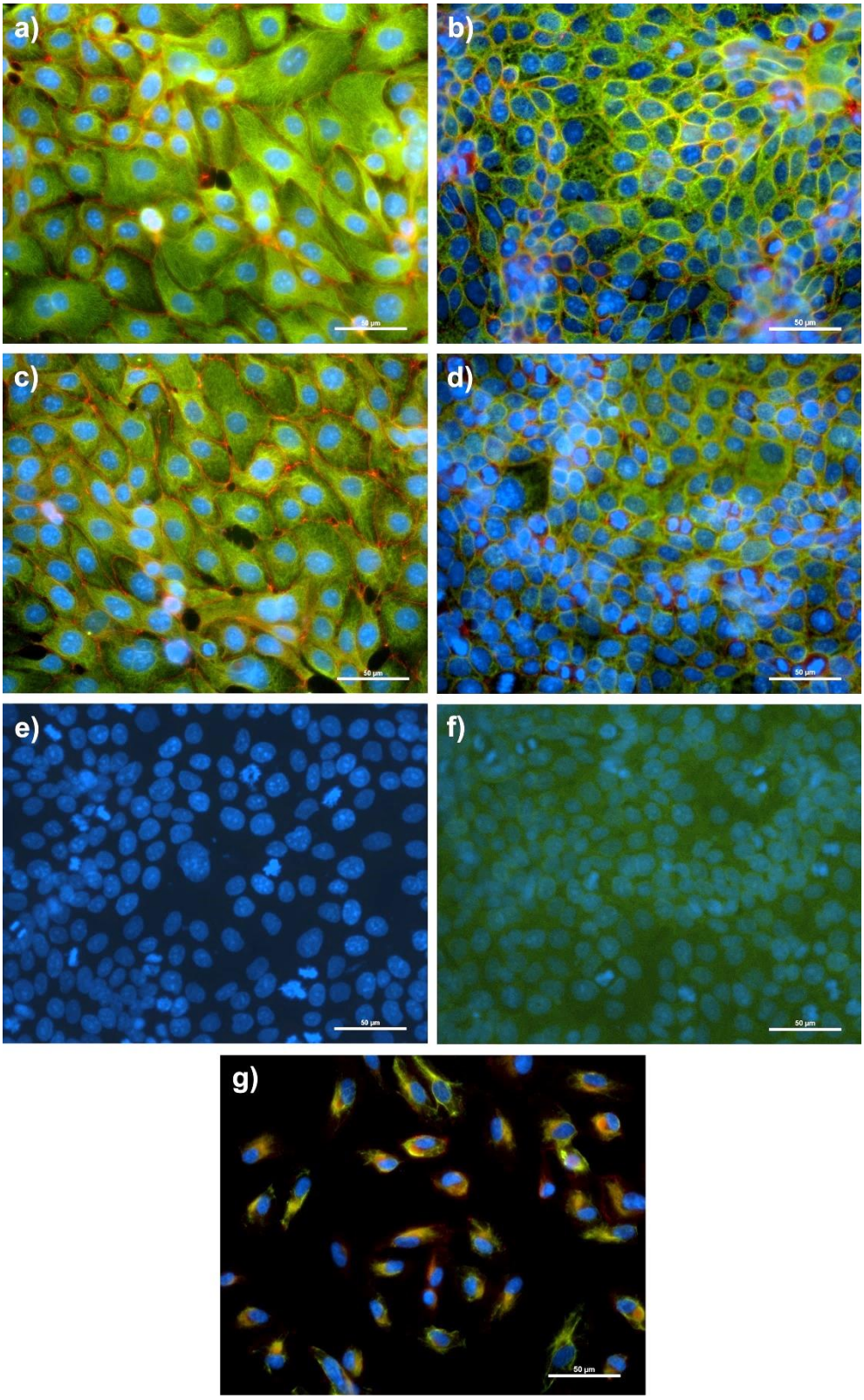

Figure 3.22: Occludin (red) and cytokeratin MNF116 (green) staining of HCE-T cells following a 24 h scratch assay. The nuclei are counter-stained with DAPI (blue), a) hydrogel Su 60 14 present with scratch wound, b) no hydrogel present but scratch wound, c) hydrogel Su 60 14 present but no scratch wound, d) no hydrogel present or scratch wound, e) negative control (no primary antibody), f) positive control (IgG instead of primary antibody), g) A19 cell positive control. Scale bar is 50 µm.

HCE-T cells were also co-stained (Figure 3.21) with ZO-1 and pan cytokeratin to investigate tight junctions as well as staining for keratins specific to epithelial cells. Good tight junction staining was observed as well as positive cytoplasmic staining of keratins. Further analysis of the reformed tight junctions was observed by staining specifically for another tight junction protein, occludin. This was combined with another keratin stain, cytokeratin MNF116. Occludin and cytoplasmic keratin staining was positive in all reformed scratch assay samples confirming the cells were of epithelial cell lineage with tight junction formation between them (Figure 3.22).

3.3 Antibacterial Analysis

A unique characteristic of pεK is its primary function as an antimicrobial compound produced by *Streptomyces* spp. as a defence mechanism. An initial study investigated the antimicrobial activity from several different hydrogel variants against both Gram-positive and Gram-negative bacteria. Further analysis of the hydrogels with the addition of antibacterial biomolecules was investigated to identify the potential of the hydrogel as a drug eluting bandage contact lens.

3.3.1 Antimicrobial activity of hydrogels with different levels of cross-linking:

Hydrogels with varying degrees of cross-linking were monitored over 18 h for any difference in antimicrobial activity. After 4 h resazurin reduction was at approximately 20% for each of the hydrogel variants which was much lower than LB agar (59%). At the 18 h time-point more resazurin was reduced by all hydrogel variants (37%), however, this was still significantly lower than the LB agar control (73%). Across all time-points there was no significant difference in resazurin reduction between the hydrogel variants (Figure 3.23). This result suggests that the alterations in cross-link percentages tested do not change the antimicrobial activity of the hydrogel.

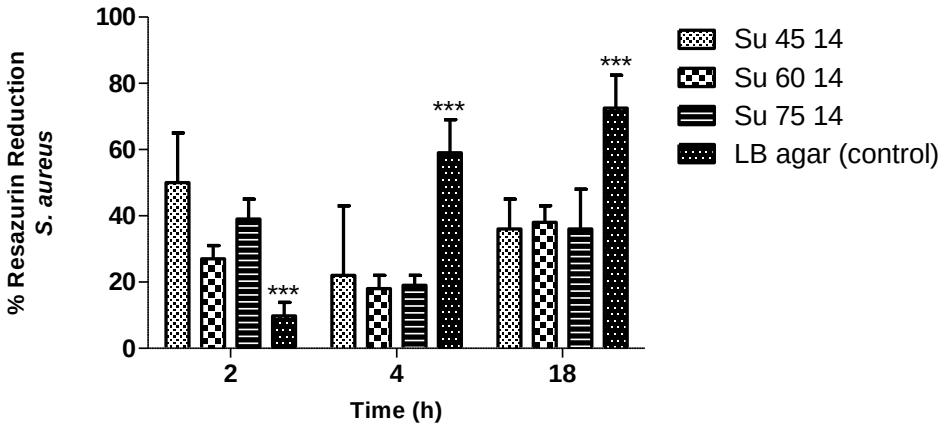

Figure 3.23: Reduction of resazurin by *S. aureus* when cultured in the presence of octanedioic acid hydrogels cross-linked at different percentages. Error bars ±SD, *** $p < 0.005$ $N = 9$.

3.3.2 Biomolecule quantification:

Biomolecule attachment was quantified via different methods depending on the nature of the chemical bond. Covalently bound pεK was quantified using the anionic dye methyl orange and ionically bound penicillin G was quantified by analysing elution rate with RP-HPLC.

3.3.2.1 Methyl orange amine determination:

The anionic dye methyl orange was used to quantify the amount of amine groups available from pεK within the hydrogel. A known concentration of methyl orange was incubated with the hydrogel followed by analysis of the excess solution to quantify how much methyl orange associated with the cationic amine groups of pεK within the hydrogel matrix. This was used to measure both the degree of cross-linking and the increased amount of pεK after re-attachment to the hydrogel post-polymerisation. The amine content for the three cross-link variants of the hydrogel varied between 93 µmol for Su 75 14 to 773 µmol for Su 45 14 with Su 60 14 at 143 µmol (Table 3.6). The addition of pεK greatly enhanced the amount of amine functionality on the polymer to 1660 µmol, a 12-fold increase from the unmodified Su 60 14. The orange anionic dye associated more with Su PεK than any other hydrogel variant (Figure 3.24) These data show that the addition of pεK to the hydrogel post-polymerisation greatly enhances the amine content of the hydrogel compared to an unmodified version.

Hydrogel	Amine (mmol)	A_{465}
Su 60 14	143	1.003
Su PεK	1660	0.184
Su 45 14	773	0.663
Su 75 14	93	1.03

Table 3.6: Methyl orange determination of amino groups available on hydrogel variants. *N* = 3.

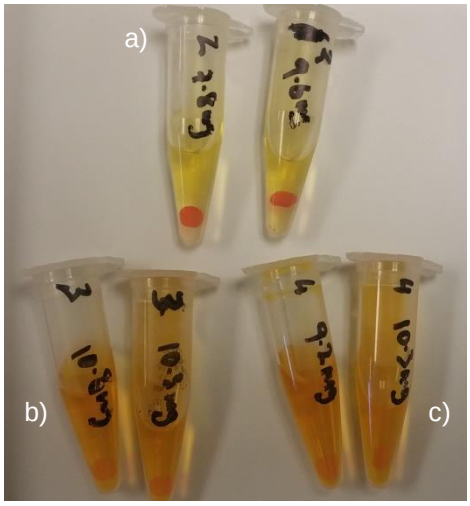

Figure 3.24: Methyl orange assay in duplicate of Su PεK (a), Su 60 14 (b) and Su acetylated (c).

3.3.2.2 Penicillin G elution:

The elution of penicillin G from hydrogel Su Pen G was quantified to investigate how long the antibiotic was associated with the hydrogel and to develop a drug release profile.

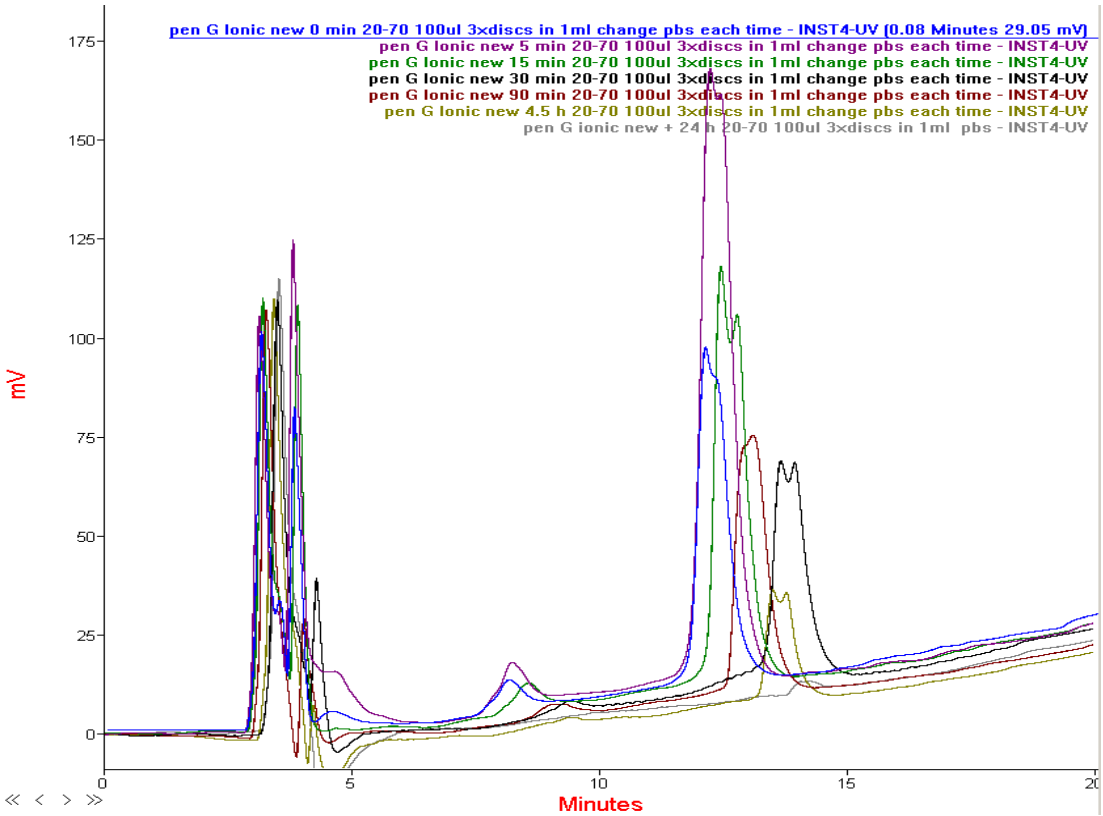

Figure 3.25: Penicillin G elution from Su Pen G was monitored by HPLC over 5 h.

Su Pen G was incubated in PBS at 37 °C for set time-points before the supernatant was removed and analysed by RP-HPLC (Figure 3.25). Results indicate that most of the penicillin G eluted over the initial 30 min of the assay but elution continued for 5 h before the compound became undetectable by HPLC (Figure 3.26).

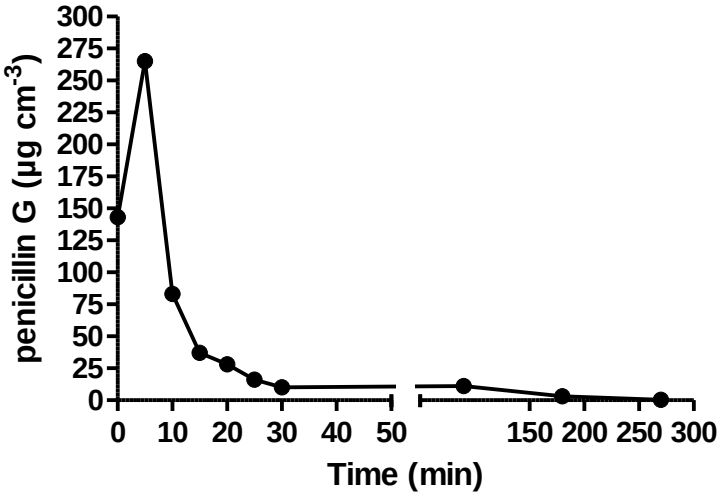

Figure 3.26: Penicillin G elution from Su Pen G.

3.3.3 Antimicrobial activity of hydrogels with biomolecules attached:

A resazurin based cell metabolic activity assay was used as a method to determine microbial cell viability. *S. aureus* and *E. coli* were cultured in the presence of the hydrogel variants for a period of 18 h with resazurin readings taken at time-points in between. The most notable differences were observed after 4 h in culture when for both organisms resazurin reduction was significantly less ($p < 0.005$) when the organisms were cultured in the presence of Su Pen G and Su PεK.

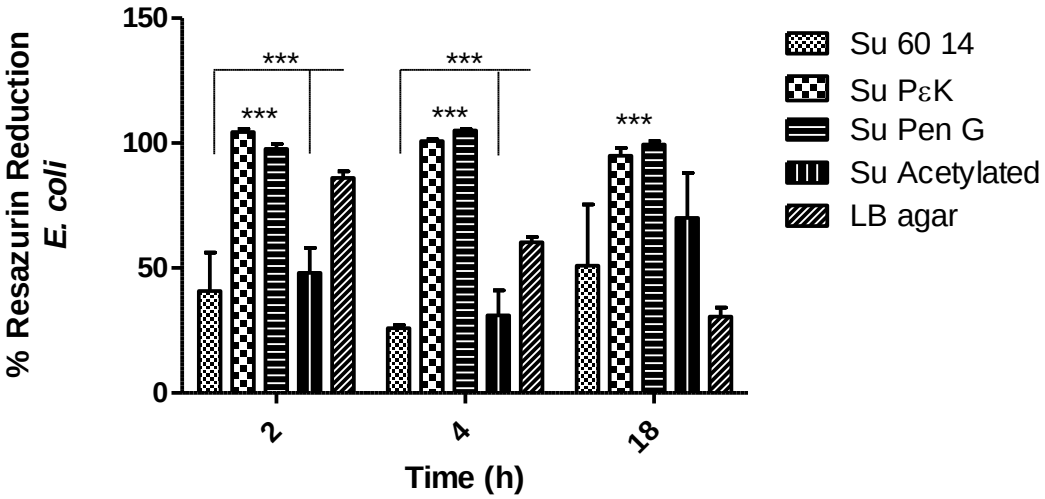

Figure 3.27: Reduction of resazurin by *E. coli* when cultured in the presence of the octanedioic acid hydrogel variants. Error bars ±SD, *** $p < 0.005$ $N = 9$.

After 18 h in culture with *E. coli* resazurin reduction with the Su Pen G (0.7%) and Su PεK (5%) hydrogels present was significantly less ($p < 0.005$) than hydrogels Su 60 14 (49%), Su Acetylated (30%) and the LB agar control (69%). The same trend was observed at the earlier 2 and 4 h time-points, however, significantly less ($p < 0.005$) resazurin reduction was observed for the LB agar control at 2 and 4 h compared to Su 60 14 and Su acetylated. No significant difference was observed between Su PεK and Su Pen G or Su Acetylated and Su 60 14 at any of the time-points investigated (Figure 3.27).

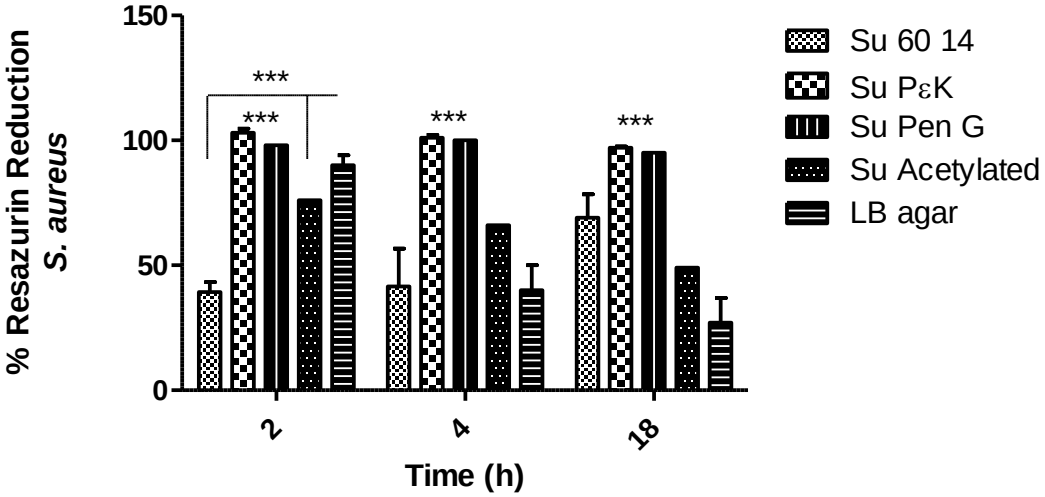

Figure 3.28: Reduction of resazurin by *S. aureus* when cultured in the presence of the octanedioic acid hydrogel variants. Error bars ±SD, *** $p < 0.005$ $N = 9$.

After 18 h in culture with *S. aureus* resazurin reduction with the Su Pen G (5%) and Su PεK (3%) hydrogels present was significantly less ($p < 0.005$) than hydrogels Su 60 14 (31%), Su Acetylated (51%) and the LB agar control (73%). The same trend was observed at the earlier 2 and 4 h time-points, however, significantly less ($p < 0.005$) resazurin reduction was observed for the LB agar control at 2 h compared to Su 60 14 and Su acetylated hydrogels. No significant difference was observed between hydrogels Su PεK or Su Pen G at any time-point (Figure 3.28).

These data suggest that the hydrogels with biomolecules attached (Su Pen G and Su PεK) can reduce the metabolic activity of both organisms tested when compared to LB agar and unmodified hydrogel controls.

3.3.4 Detailed analysis of hydrogel antimicrobial activity towards S. aureus:

After identifying hydrogels Su Pen G and Su PεK as potential antimicrobial materials, a more detailed analysis was undertaken. The efficacy of the hydrogels was tested against both planktonic and attached *S. aureus* and log differences determined by direct cell counts.

Against planktonic *S. aureus* at all time-points a statistically significant ($p < 0.005$) decrease in bacterial cell number was observed when cultured in the presence of the Su Pen G and Su PεK hydrogels. This was most apparent after 18 h when Su Pen G (2.8 log reduction) and Su PεK (1.8 log reduction) were compared to the LB agar control. Su Pen G was also significantly ($p < 0.01$) more effective at reducing planktonic *S. aureus* compared to Su PεK at each time-point. No significant difference in *S. aureus* cell number was observed between Su 60 14 and the process control at any time-point. After 18 h a similar increase in *S. aureus* cell number to the seeding density was observed for Su 60 14 (1.08 log), the process control (1.16 log) and the LB agar control (1.11 log) (Figure 3.29).

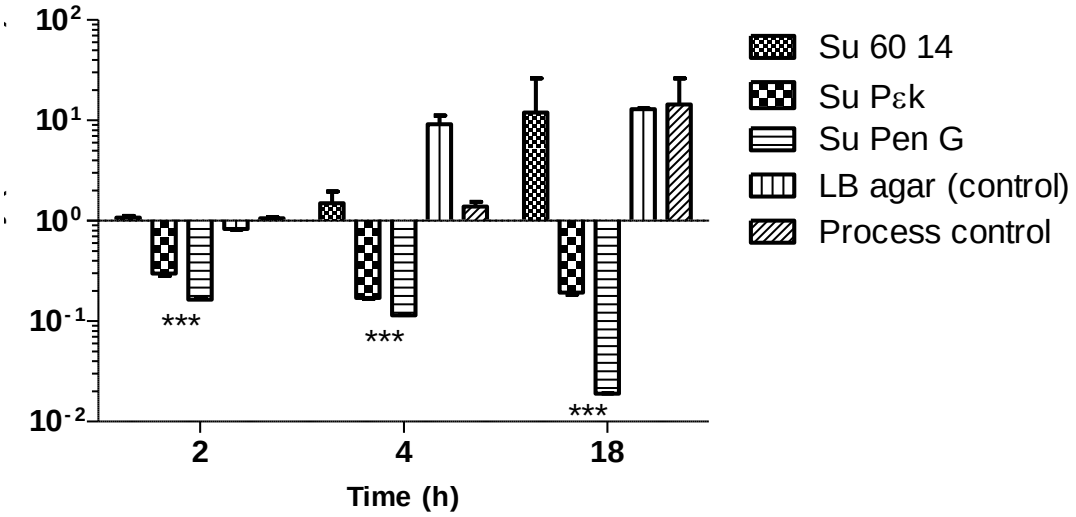

Figure 3.29: Log increase/decrease of planktonic *S. aureus* in the presence of various hydrogel. Error bars ±SD, *** $p < 0.005$ $N = 9$.

Against *S. aureus* attached to the hydrogel a statistically significant ($p < 0.005$) decrease in bacterial cell number was observed with the Su Pen G and Su PεK hydrogels after 18 h. The greatest reduction was observed when Su Pen G (1.1 log reduction) and Su PεK (2.3 log reduction) were compared to the LB agar control. No significant difference in *S. aureus* cell number was observed between Su 60 14 and the process control and both these hydrogels significantly reduced ($p < 0.005$) *S. aureus* cell number compared to the LB agar control (Figure 3.30).

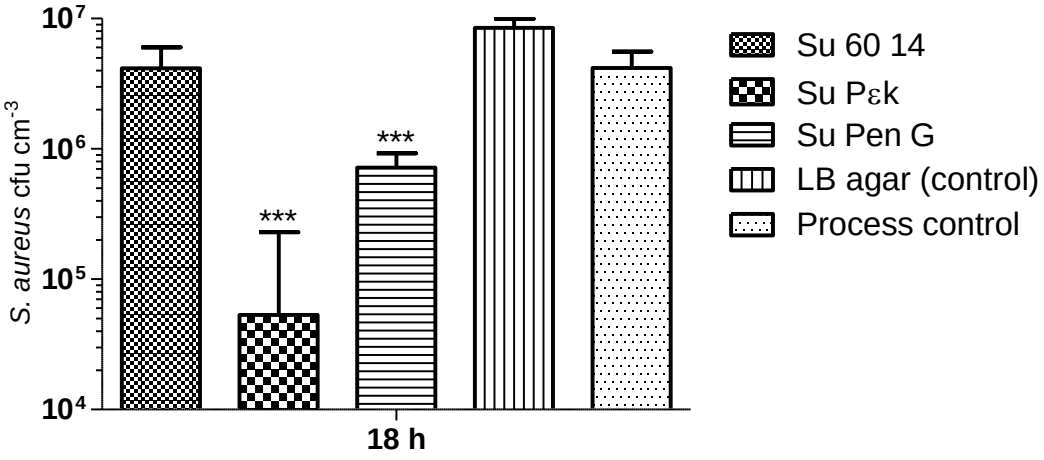

Figure 3.30: Log number of *S. aureus* attached to hydrogel variants after 18 h culture period variants. Error bars ±SD, *** $p < 0.005$ $N = 9$.

These data suggest the hydrogels with biomolecules attached can significantly reduce *S. aureus* cell number on the hydrogel when compared to LB agar and unmodified hydrogel controls.

3.3.5 Bacteria staining:

Bacteria cell staining was used to further analyse *S. aureus* attached to the hydrogels. Propidium iodide was used to stain *S. aureus* in situ on the hydrogel surface whereas a LIVE/DEAD® BacLight™ stain was used to stain live (green) and dead (red) *S. aureus* retrieved from the hydrogels post-culture.

Propidium iodide staining of *S. aureus* attached to the surface of the Su PεK hydrogel revealed that the bacteria were arranged as smaller clusters or possibly singular cocci whereas on the other hydrogel surfaces (Su 60 14 and Su Pen G) their eponymous clustered growth conformation was observed (Figure 3.31 a-c). The conformational differences were confirmed by the LIVE/DEAD® BacLight™ stain as well as identifying differences between the amounts of live or dead *S. aureus* (Figure 3.31 d-f). Both Su Pen G (76%) and Su PεK (74%) kill a significantly greater ($p < 0.005$) number of *S. aureus* compared to the unmodified Su 60 14 hydrogel (10%) after 18 h (Figure 3.32).

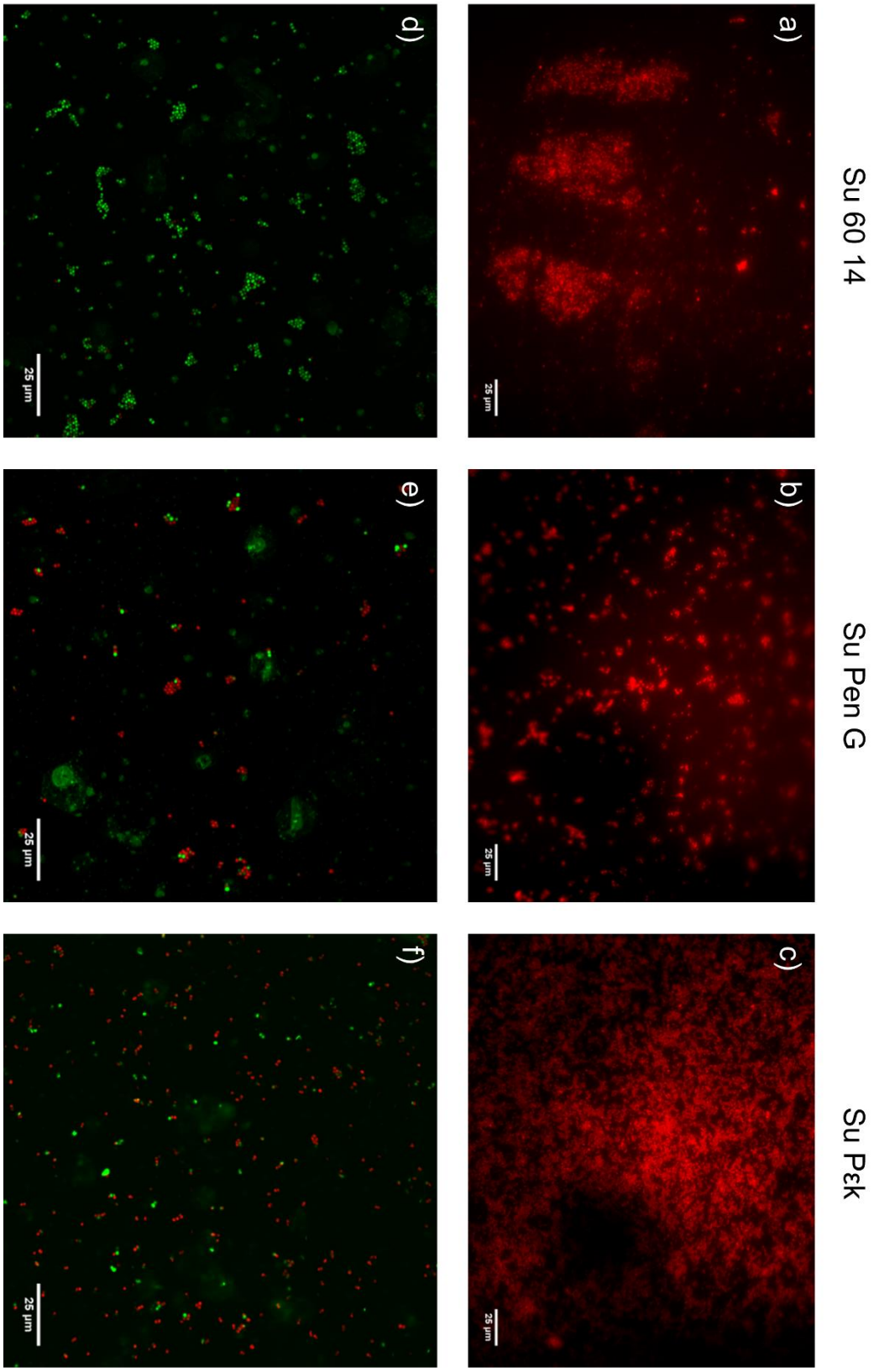

Figure 3.31: a-c) Propidium iodide staining of *S. aureus* on the antimicrobial hydrogels, d-f) LIVE/DEAD® BacLight™ staining of *S. aureus* retrieved from the hydrogel. Scale bar is 25 µm.

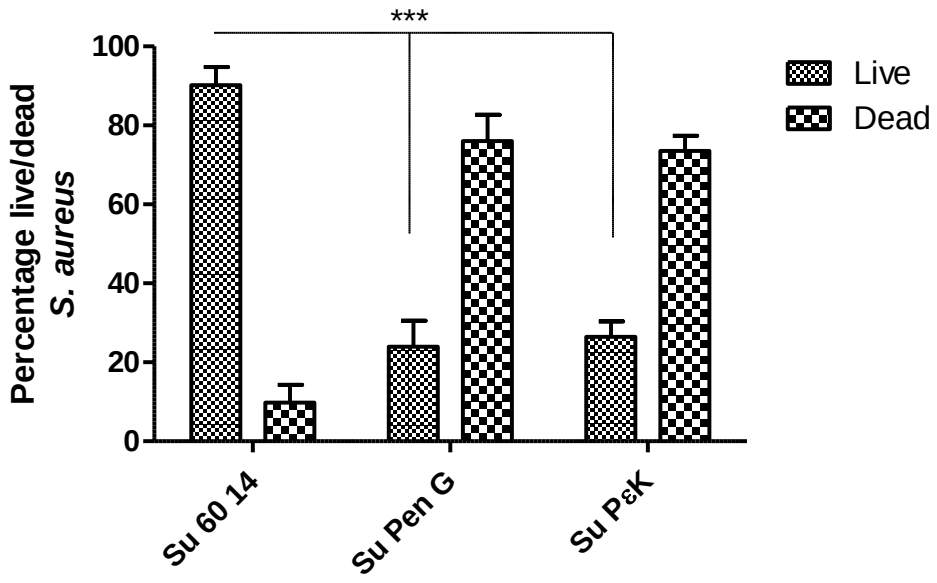

Figure 3.32: Percentage live/dead *S. aureus* retrieved from the hydrogel variants. Error bars ±SD, *** $p < 0.005$ $N = 5$.

These data highlight conformational differences of *S. aureus* attached to the hydrogel variants as well as identifying a greater killing efficacy from the Su Pen G and Su PεK hydrogels compared to hydrogel Su 60 14.

3.3.6 Cytotoxicity:

The cytotoxicity of the antibacterial hydrogel materials to the HCE-T cell line were investigated with a CCK-8 cytotoxicity assay as in section 3.2.1. The 4 day growth curve of HCE-T cells cultured in standard media compared to those cultured in media pre-incubated with the Su Pen G or Su PεK hydrogels resulted in some cytotoxicity becoming significant ($p < 0.005$) after 24 h in culture when compared to the no hydrogel control (Figure 3.33). Leachables from the Su PεK (PO_4) hydrogel showed significantly greater ($p < 0.005$) cytotoxicity towards the HCE-T cell line than any of the other materials tested and this was apparent after 2 h in culture. Leachables from hydrogel Su 60 14, used here as a control, were again non-cytotoxic to the HCE-T cell line. These data suggest that leachables from hydrogel Su Pen G and Su PεK have some cytotoxicity towards the HCE-T cell line after 24 h but it does not result in cell death to the degree of the positive control Su PεK (PO_4).

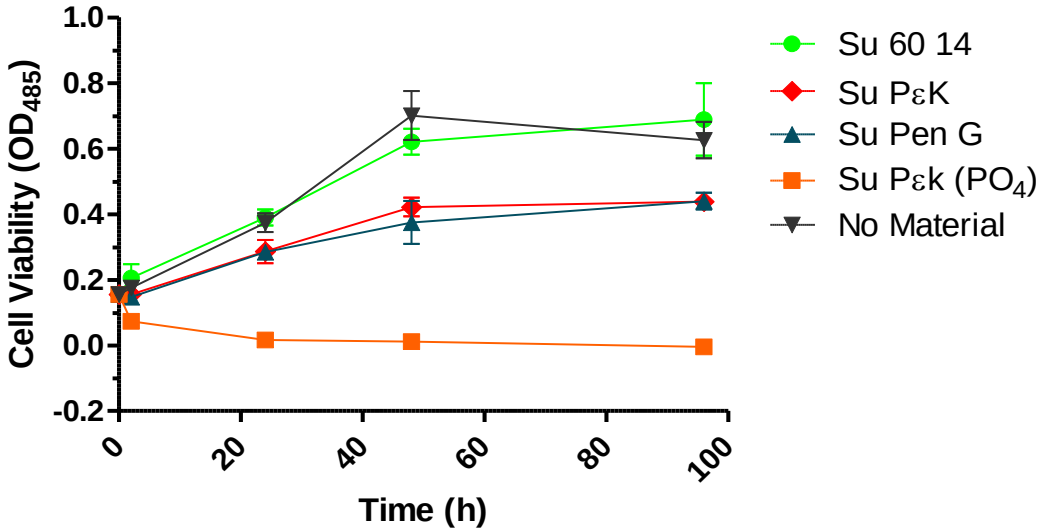

Figure 3.33: Cytotoxicity of leachables from the hydrogel variants towards the HCE-T cell line. Error bars ±SD, *N* = 6.

3.3.7 Scratch assay:

A wound model was again set up as in section 3.2.3 to investigate if hydrogel Su Pen G and Su PεK would influence the rate of re-epithelialisation of a scratch wound on a monolayer HCE-T cells. A confluent monolayer was obtained after 3 days in culture; a linear scratch was made through the monolayer and the hydrogel aligned along the surface.

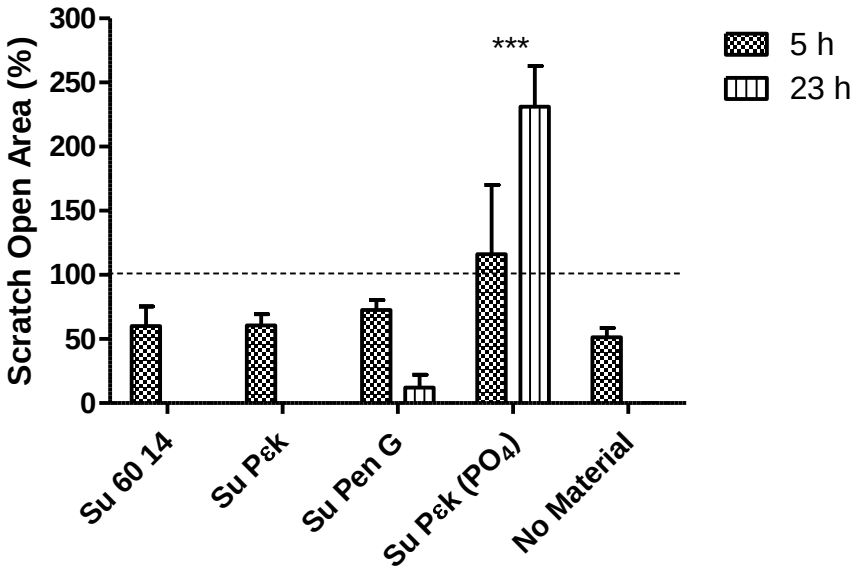

Figure 3.34: Percentage scratch closure with/without hydrogels present at 5 h and 23 h after initial scratch at 0 h ----. Error bars ±SD, *** $p < 0.005$ $N = 9$.

The re-epithelialisation of the wound was monitored over a 23 h period, however, no obvious difference was observed between the no hydrogel control and scratch wounds with Su Pen G and Su PεK present. All the scratch wounds except for hydrogel Su PεK (PO_4) closed within 23 h regardless of the hydrogel being present or not (Figure 3.34). Scratch wound closure was quantified using TScratch software (Figure 3.35) which identified a statistically significant increase ($p < 0.005$) in scratch wound open area with the presence of Su PεK (PO_4) at 5 h (116%) and 23 h (231%) compared to all other hydrogels tested. No significant difference was observed between scratch wound open area for Su Pen G (73%), Su PεK (61%), Su 60 14 (60%) and the no hydrogel control (52%) after 5 h. All the scratch wounds apart from Su Pen G closed after 23 h, however, this was not significant.

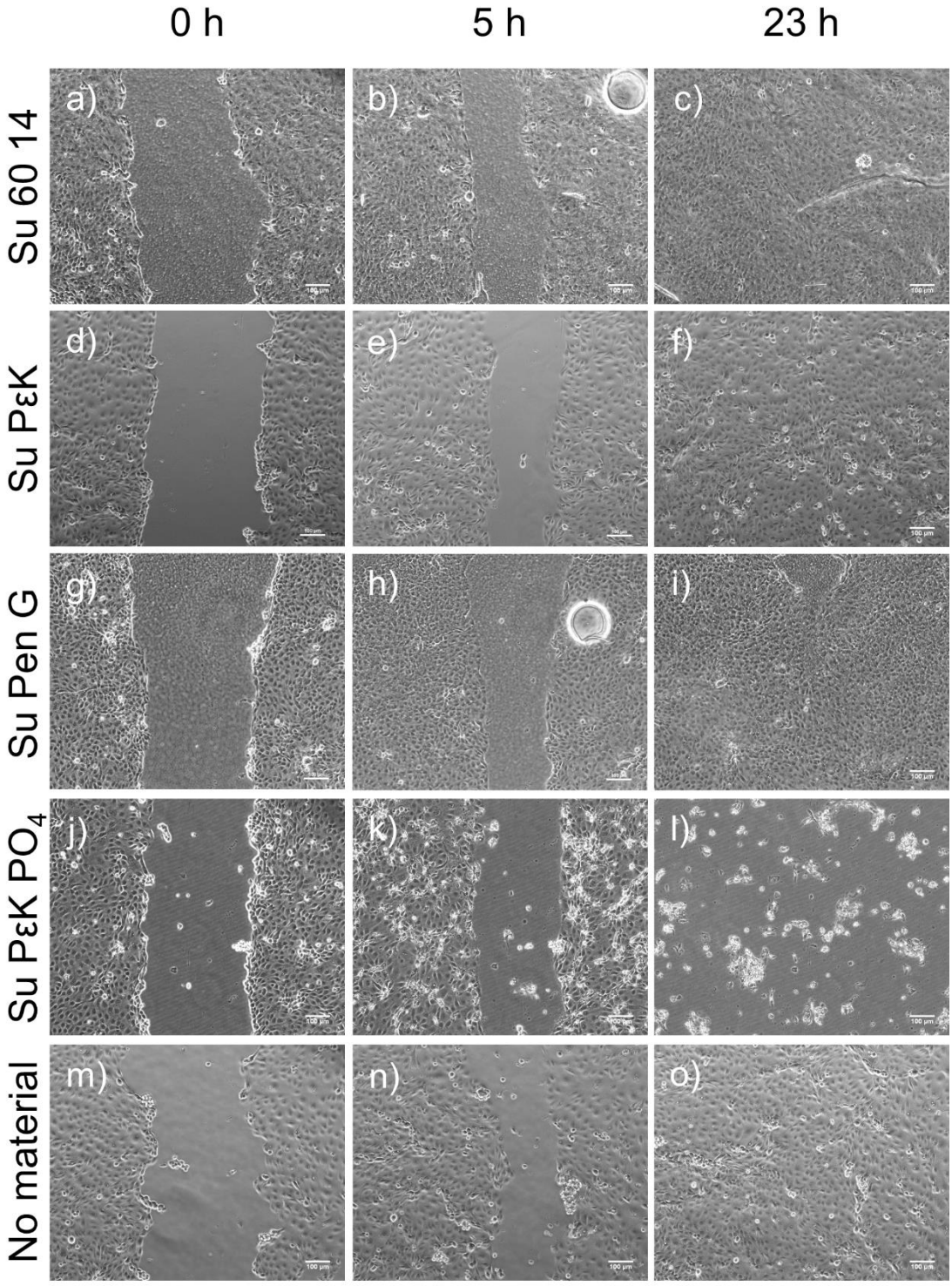

Figure 3.35: Scratch closure of a HCE-T monolayer after 0 h, 5 h and 23 h with hydrogel variants present. Scale bar is 100 µm.

These data suggest that the presence of the Su Pen G and Su PεK hydrogels in a HCE-T cell wound environment does not inhibit re-epithelialisation.

3.3.8 Monolayer integrity:

HCE-T cell monolayers were found to re-epithelialise within 23 h of the initial scratch wound for all materials except Su PεK (PO_4). However, what was not determined was whether tight junctions had reformed within the monolayer. To investigate this HCE-T Cells were stained for zona occludens-1 (ZO-1) to identify any defects in the integrity of the monolayer and identify cell to cell contact through their tight junctions. The monolayers with Su Pen G, Su PεK and Su 60 14 appear to be intact and similar to that of the no hydrogel control. No physically disturbed junctions were observed (Figure 3.36). However, the monolayer with Su PεK (PO_4) present is incomplete with lots of unattached HCE-T cells evident. The results of the ZO-1 staining and the scratch assay suggest that the Su Pen G and Su PεK hydrogels do not physically inhibit or affect the HCE-T cell monolayer.

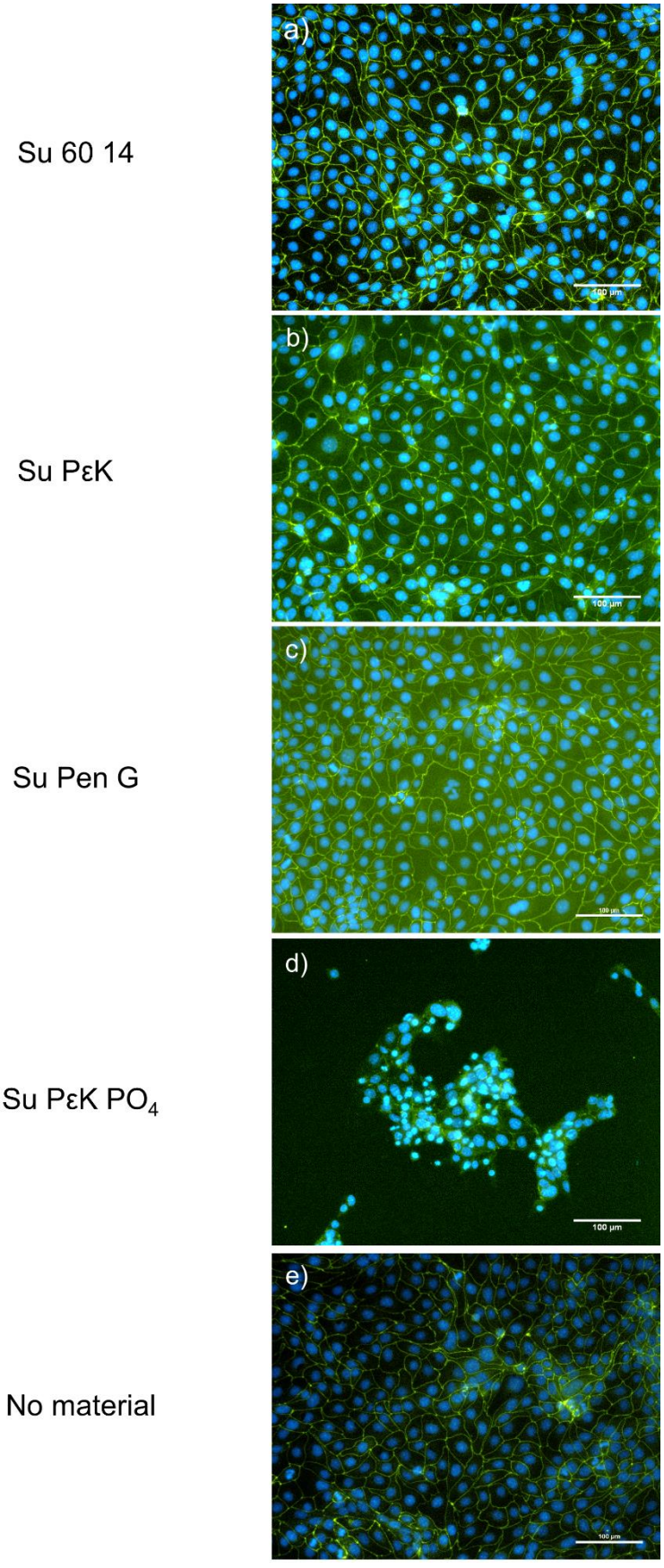

Figure 3.36: ZO-1 staining (green) of HCE-T cells following a 24 h scratch assay in the presence of the hydrogel variants. The nuclei are counter-stained with DAPI (blue). Scale bar is 100 µm.

3.4 Antifungal Analysis

Further analysis of the antimicrobial potential of the hydrogel was investigated with focus on a more clinical application in the fight against fungal keratitis. The hydrogel was investigated for its potential to elute an ionically attached antifungal, AmpB with focus on its killing efficacy, stability and elution rate.

3.4.1 Minimum inhibitory concentration of AmpB against C. albicans:

C. albicans was cultured in PD media or PD media supplemented with 10 v/v% horse serum with a range of concentrations of AmpB. The OD_{600} was measured after 18 h and used to determine the concentration of AmpB that inhibited *C. albicans* growth. The MIC of AmpB that significantly inhibited *C. albicans* growth was found to be between 0.094 and 0.188 µg cm^{-3} for both PD ($p < 0.005$) and PD with 10% horse serum ($p < 0.05$) (Figure 3.37). No significant difference was found in the MIC for *C. albicans* when cultured in PD supplemented with 10 v/v% horse serum compared to PD alone.

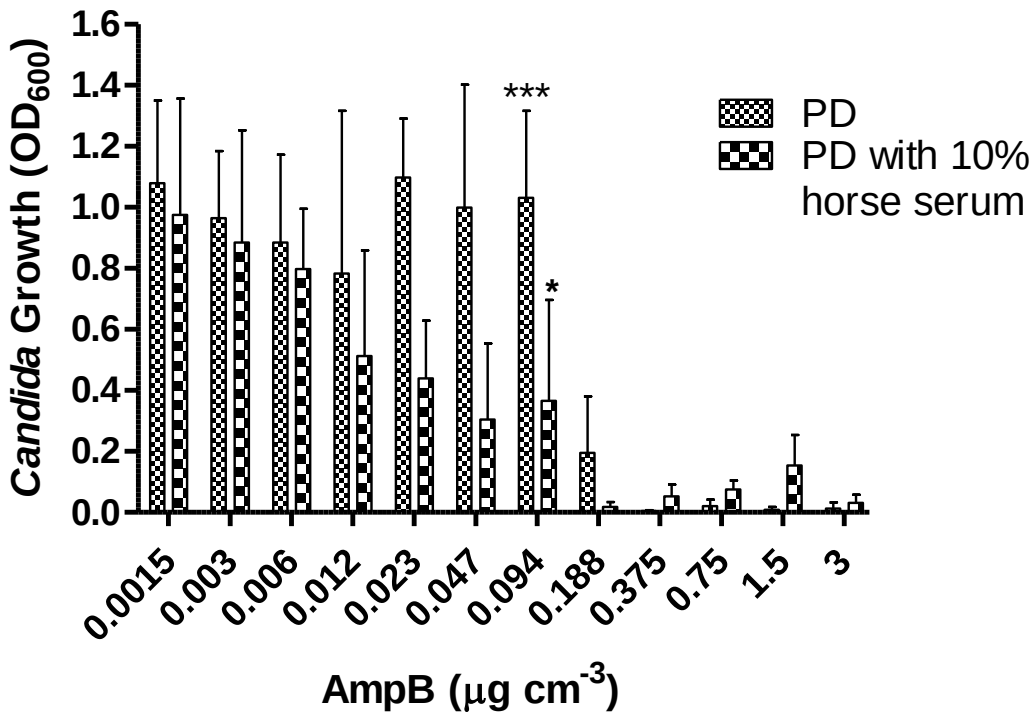

Figure 3.37: MIC for AmpB against *C. albicans* cultured in different growth media, potato dextrose and potato dextrose supplemented with 10% horse serum. Error bars ±SD, * $p < 0.05$, *** $p < 0.005$ $N = 9$.

3.4.2 Fungicidal effects of the -NH_3Cl and -NH_2 hydrogels:

AmpB was loaded onto the hydrogels by soaking them in various concentrations of the drug. The OD_{600} was measured after 18 h and used to determine the efficacy of AmpB eluted from the hydrogels towards *C. albicans.* The loading of AmpB and its release from the hydrogels significantly reduced ($p < 0.005$) the growth of *C. albicans* compared to no AmpB (Figure 3.38). However, there was no statistically significant difference between concentrations of AmpB or between the different materials (i.e -NH_3Cl, -NH_2, -NH_2 hydrogel cultured in PD + 10 v/v% horse serum) when compared across all concentrations. These data suggest that the -NH_3Cl and the -NH_2 hydrogels loaded with all concentrations of AmpB are effective at inhibiting *C. albicans* growth.

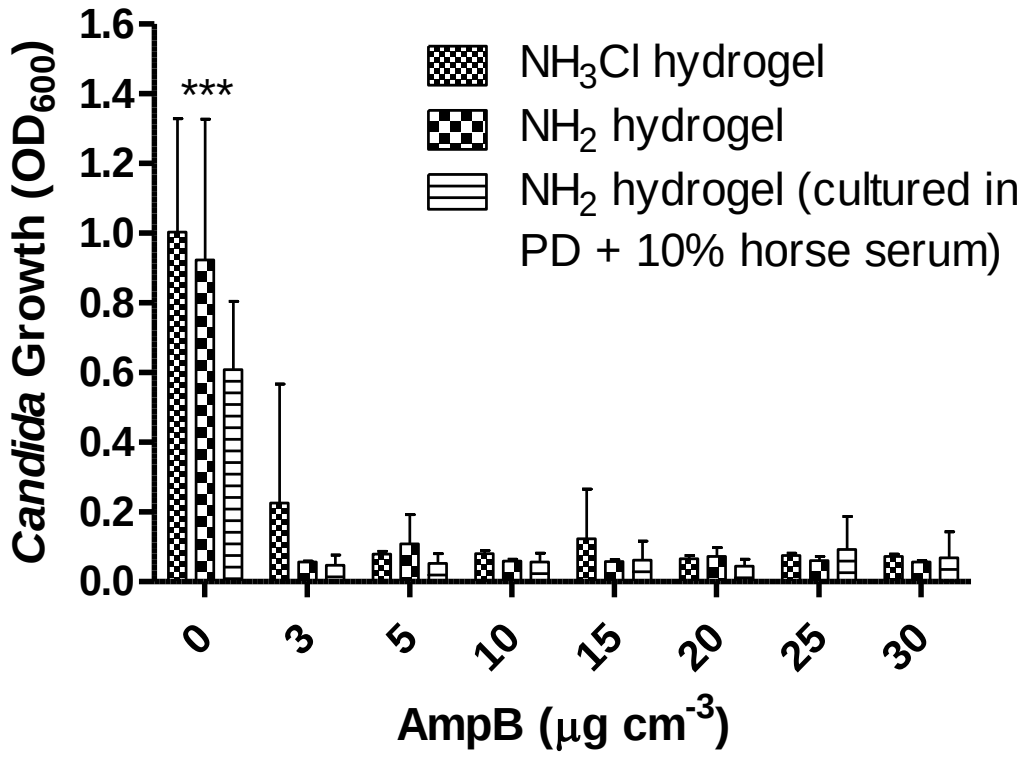

Figure 3.38: Fungicidal effects of hydrogels pre-incubated in various concentrations of AmpB under different growth conditions. Error bars ±SD, *** $p < 0.005$ $N = 9$.

3.4.3 Viability of fungi attached or loosely adhered to the hydrogel:

An investigation of any remaining viable fungi attached or loosely attached to the hydrogel after the antifungal assay was undertaken. After the OD_{600} was measured at the 18 h time-point (section 3.4.2) the -NH_2 and -NH_3Cl hydrogels were compared. Loosely attached viable *C. albicans* were recovered from the wash of the -NH_3Cl hydrogel pre-incubated in 3 µg cm^{-3} AmpB. Whereas, no loosely attached viable fungi were recovered from the -NH_2 hydrogel wash of the same concentration. Similar results were noted with hydrogels placed directly on PD-Agar; no growth was observed on -NH_2 gel with some growth surrounding the -NH_3Cl hydrogel pre-incubated with 3 µg cm^{-3} AmpB (Figure 3.39). Separately, the -NH_2 hydrogels cultured in PD broth and PD broth supplemented with 10% horse serum were removed and washed prior to being plated on PD agar with an aliquot of the wash (Figure 3.40). Almost no growth of *C. albicans* was observed on the -NH_2 hydrogels or the washes across all the pre-incubation concentrations of AmpB. The only visible growth was observed around the -NH_2 hydrogel and wash not pre-incubated with AmpB.

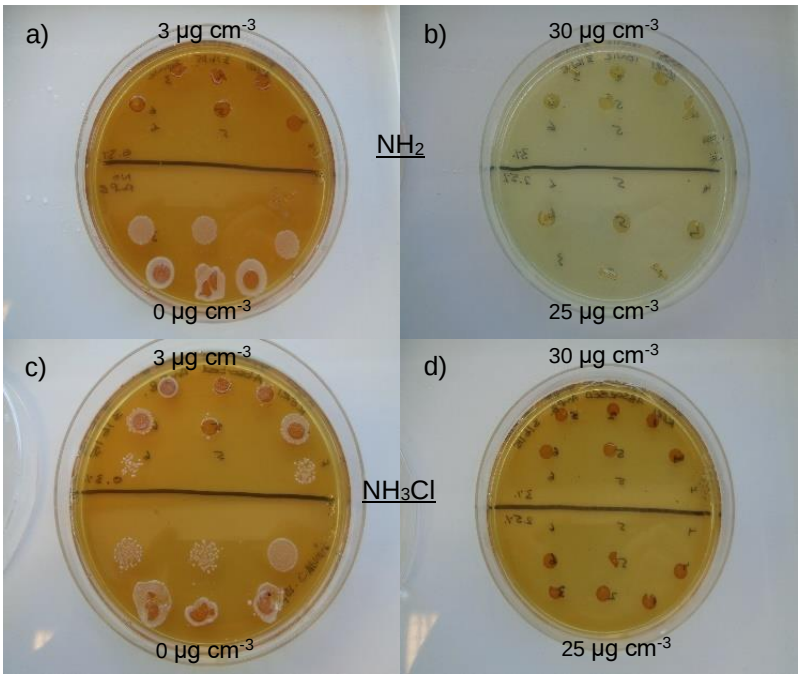

Figure 3.39: **a**) hydrogels and washes plated on PD agar for 0 + 3 µg cm^{-3} AmpB NH_2 hydrogel **b**) hydrogels and washes plated on PD agar for 25 + 30 µg cm^{-3} AmpB NH_2 hydrogel **c**) hydrogels and washes plated on PD agar for 0 + 3 µg cm^{-3} AmpB NH_3Cl hydrogel **d**) hydrogels and washes plated on PD agar for 25 + 30 µg cm^{-3} AmpB NH_3Cl hydrogel.

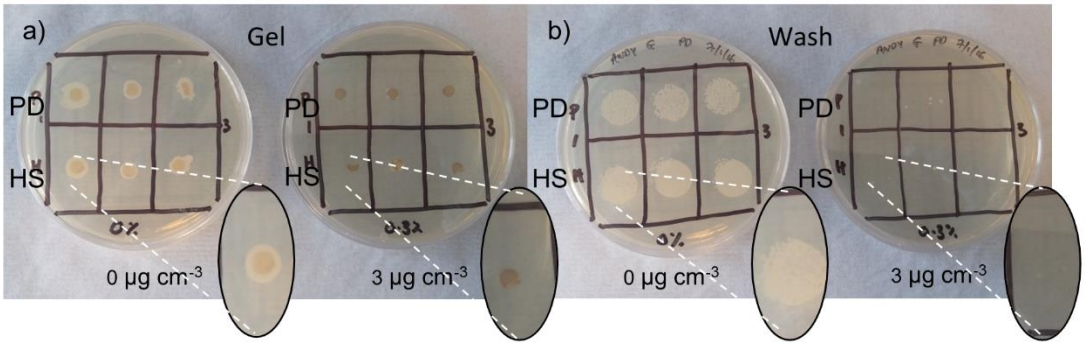

Figure 3.40: a) hydrogels plated on PD agar for 0 + 3 µg cm^{-3} AmpB NH_2 hydrogel cultured in PD broth and PD broth supplemented with 10% horse serum, **b**) washes plated on PD agar for 0 + 3 µg cm^{-3} AmpB NH_2 hydrogel cultured in PD broth and PD broth supplemented with 10% horse serum. PD: hydrogel cultured in PD broth, HS: hydrogel cultured in PD broth supplemented with 10% horse serum.

3.4.4 AmpB elution from the hydrogel:

Elution of AmpB was monitored over 96 h with RP-HPLC immediately after incubation in a solution of AmpB (30 µg cm^{-3}) for 2 h.

The main AmpB peak was obtained after 12 min, however, there was a small peak after 5 min that was also associated with AmpB (Figure 3.41). A standard curve was plotted from AmpB standard concentrations (Figure 3.41c) and used to determine AmpB eluted from the hydrogels at each time-point.

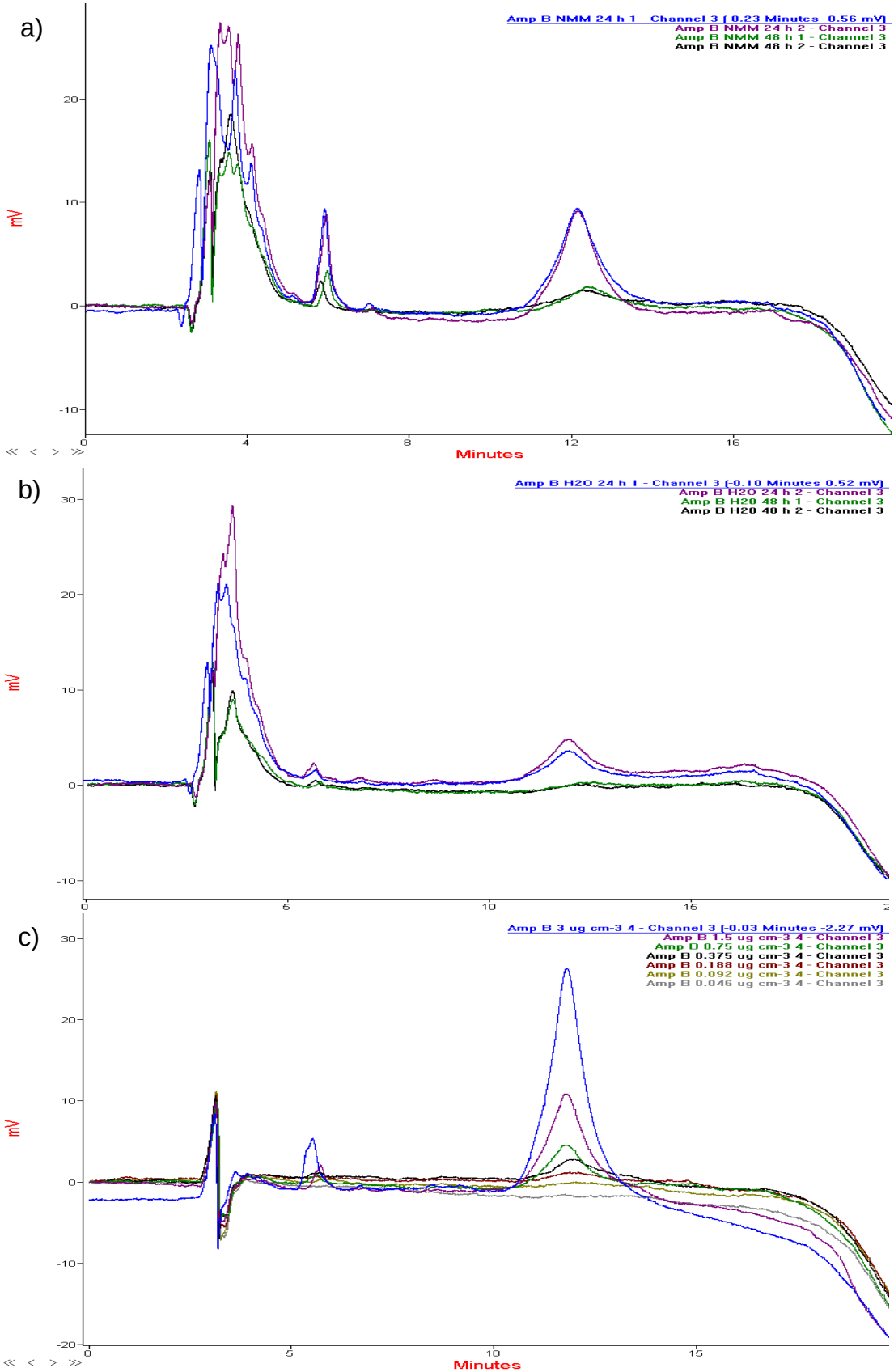

Figure 3.41: a) AmpB elution from -NH_2 hydrogels over a 48 h period, b) AmpB elution from -NH_3Cl hydrogels over a 48 h period, c) AmpB standards of different concentrations.

A therapeutic dose of AmpB (1.058 - 0.185 µg cm^{-3}) eluted from the -NH_2 hydrogel for a period of 72 h with a smaller dose after 96 h (0.134 µg cm^{-3}). The amount of AmpB eluted from the -NH_3Cl hydrogel remained clinically relevant for 48 h (0.436 - 0.175 µg cm^{-3}) before being undetectable after 72 h (Figure 3.42). Significantly ($p < 0.005$) more AmpB was eluted from the -NH_2 hydrogel at all time-points compared to the -NH_3Cl hydrogel. These data suggest more AmpB is associated with the -NH_2 hydrogel compared to the -NH_3Cl hydrogel and releases the drug over a longer period.

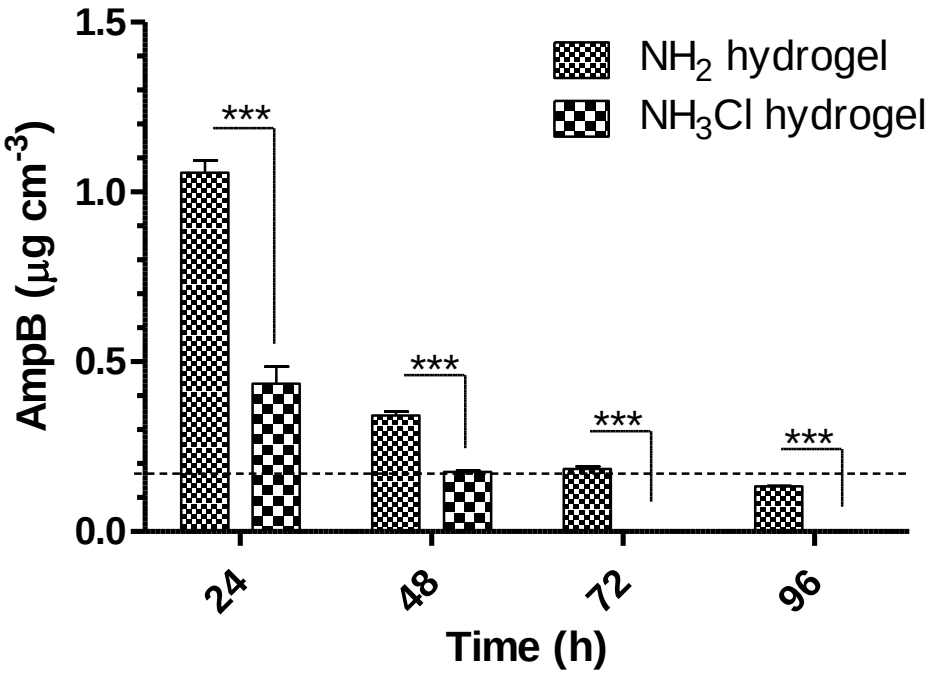

Figure 3.42: AmpB elution from -NH_2 and -NH_3Cl hydrogels over a 96 h period. Line ----- denotes the MIC for *C. albicans* determined in this report. Error bars ±SD, *** $p < 0.005$ $N = 4$.

3.4.5 AmpB stability and efficacy after attachment to the hydrogel:

The -NH_2 hydrogel was incubated with AmpB (30 µg cm^{-3}) for 2 h prior to incubating at 25 °C for various time-points. The -NH_2 hydrogels were then tested for their killing efficacy towards *C. albicans*. AmpB associated with the -NH_2 hydrogel remained stable and produced a killing effect against *C.*

albicans for at least 48 h (Figure 3.43). There appeared to be less *C. albicans* killed at 48 h when compared to the earlier time-points, however this was not statistically significant. There was no difference between the efficacy of the AmpB hydrogels and the 30 μg cm^{-3} AmpB incubation solution at each time-point in terms of the eradication of *C. albicans*. These data suggest that AmpB is stable at 25 °C for at least 48 h after attachment to the -NH_2 hydrogel.

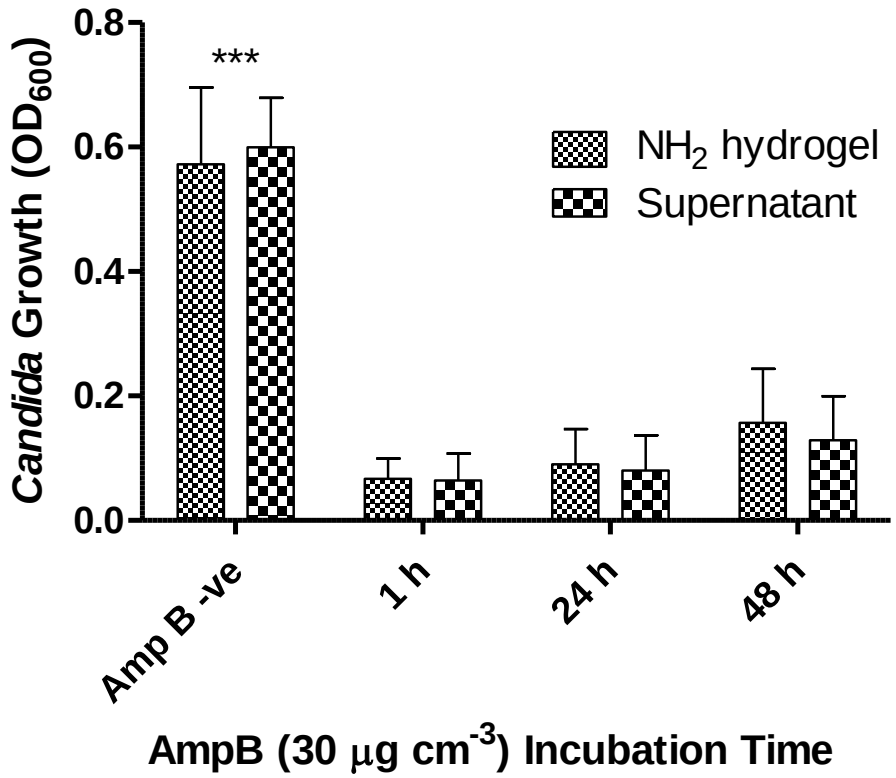

Figure 3.43: Effectiveness of AmpB -NH_2 hydrogel at killing *C. albicans* after pre-incubation for set time-points prior to inoculation with *C. albicans*. Error bars ±SD, *** $p < 0.005$ $N = 6$.

3.4.6 Cytotoxicity of the -NH_2 hydrogel to the HCE-T cell line:

A cytotoxicity study of the leachables from the -NH_3Cl and -NH_2 hydrogels pre-incubated in AmpB (30 µg cm^{-3}) was undertaken. A CCK-8 assay was used as a measure of the metabolic activity of the HCE-T cells. The HCE-T cells were also cultured in standard tissue culture media as a positive control. No significant difference in HCE-T activity was observed at any of the time-points when comparing -NH_2 and -NH_3Cl hydrogels pre-incubated in AmpB to standard cell culture media (Figure 3.44). These data suggest that the -NH_3Cl and -NH_2 hydrogels incubated with the highest concentration of AmpB used in the antifungal study were non-cytotoxic to the HCE-T cell line.

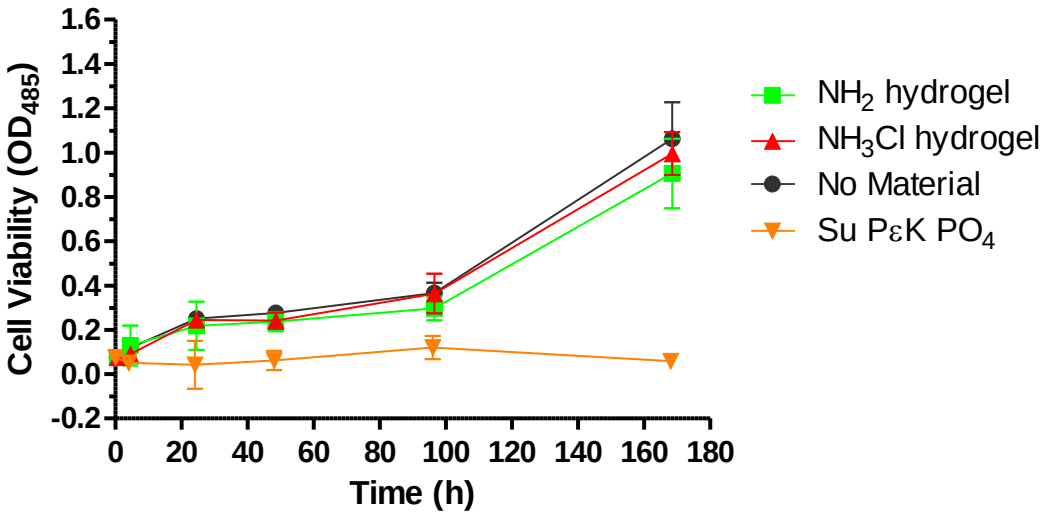

Figure 3.44: Cytotoxicity of AmpB -NH_2 and -NH_3Cl hydrogels towards the HCE-T cell line. Error bars ±SD, *N* = 8.

3.5 Microbial Identification Peptides

The hydrogel bandage contact lens was investigated for its ability to associate other biomolecules for different applications other than antimicrobial activity. Bacterium identifying peptides were associated with the hydrogel to investigate the potential to align the peptide to a site of infection with view to determining whether the pathogen was Gram-positive or Gram-negative. This approach could potentially lead to a quicker diagnosis and more effective treatment of ocular infections especially when combined with more directed and controlled hydrogel release mechanism.

3.5.1 Hydrogel design:

The Su 60 14 hydrogel was polymerised in the same way as 2.1.2 but an anhydride attached to the amine groups to convert it to a carboxyl moiety. The efficacy of the conversion was measured post-modification. A blue positive ninhydrin stain was observed for the unmodified hydrogel; however, a dark yellow colour was obtained for Su 60 14 COOH (Figure 3.45a). This qualitative analysis suggested the conversion to a carboxyl moiety was successful. A methyl orange amine quantification assay was used to confirm the ninhydrin results and give an approximate value of the amount of amine groups still present (Figure 3.45b). It was determined that there was a 60% reduction in amine groups on the Su 60 14 COOH hydrogel (50 µM amine) compared to the unmodified Su 60 14 hydrogel (120 µM amine) (Table 3.7). These data suggest that the amount of amine groups on the modified hydrogel was reduced and replaced by a carboxyl moiety.

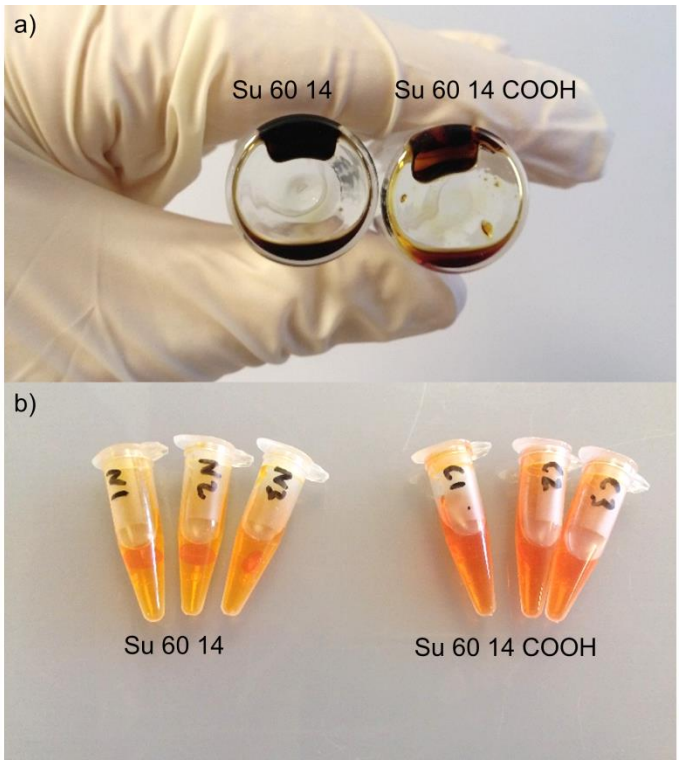

Figure 3.45: Quantification of amine groups present within the hydrogel matrix, a) qualitative evaluation with Kaiser reagent and b) methyl orange amine quantification of the pre (left) and post (right) carboxy functionalised hydrogel.

Hydrogel	Amine (mmol)	A_{465}
Su 60 14	120	1.043
Su 60 14 COOH	50	1.125

Table 3.7: Methyl orange determination of amino groups available on hydrogel variants. *N* = 3.

3.5.2 BAC ONE:

3.5.2.1 Qualitative BAC ONE efficacy analysis:

The BAC ONE peptide was incubated with hydrogel Su 60 14 COOH prior to testing its efficacy at identifying both Gram-positive and Gram-negative bacteria in culture. Nitrobenzodiazole (NBD) fluorescence from the peptide associated with hydrogel Su 60 14 COOH (Figure 3.46a) and from the peptide alone (Figure 3.46b) was observed at incubation concentrations of 5 - 40 μM in the presence of *S. aureus*. However, less fluorescence was obvious from the peptide associated with hydrogel Su 60 14 COOH when incubated with *E. coli* (Figure 3.46c). Fluorescence was only observed at > 20 μM incubation concentration when the peptide alone was incubated with *E. coli* (Figure 3.46d). Some background auto-fluorescence was observed from the hydrogel when present. These data suggest the Su 60 14 COOH hydrogel with BAC ONE can be used to label Gram-positive bacteria without hindering its activity.

3.5.2.2 Quantification of BAC ONE fluorescence:

The fluorescence of the peptide for the range of incubation concentrations was quantified to confirm the observations in section 3.5.2. A microplate reader was used to measure the fluorescence intensity. A statistically significant ($p < 0.005$) increase in fluorescence was observed from the BAC ONE peptide (at 40 μM) associated with hydrogel Su 60 14 COOH in the presence of *S. aureus* when compared to a no microbe control. The BAC ONE peptide incubated with *S. aureus* alone gave the greatest fluorescence signal with statistical significance ($p < 0.005$) over the Su 60 14 COOH hydrogel between 20 - 40 μM incubation concentrations (Figure 3.47). BAC ONE also labelled *E. coli* when associated with the hydrogel and this was statistically greater ($p < 0.05$) than the no microbe control at concentrations of 10 - 40 μM. A much greater fluorescence signal was observed when incubated with *E. coli* with/without the hydrogel present when compared to the corresponding data for *S. aureus*. These data suggest the hydrogel capable of delivering a sufficient quantity of the peptide when pre-incubated in the greater BAC ONE concentration (40 μM).

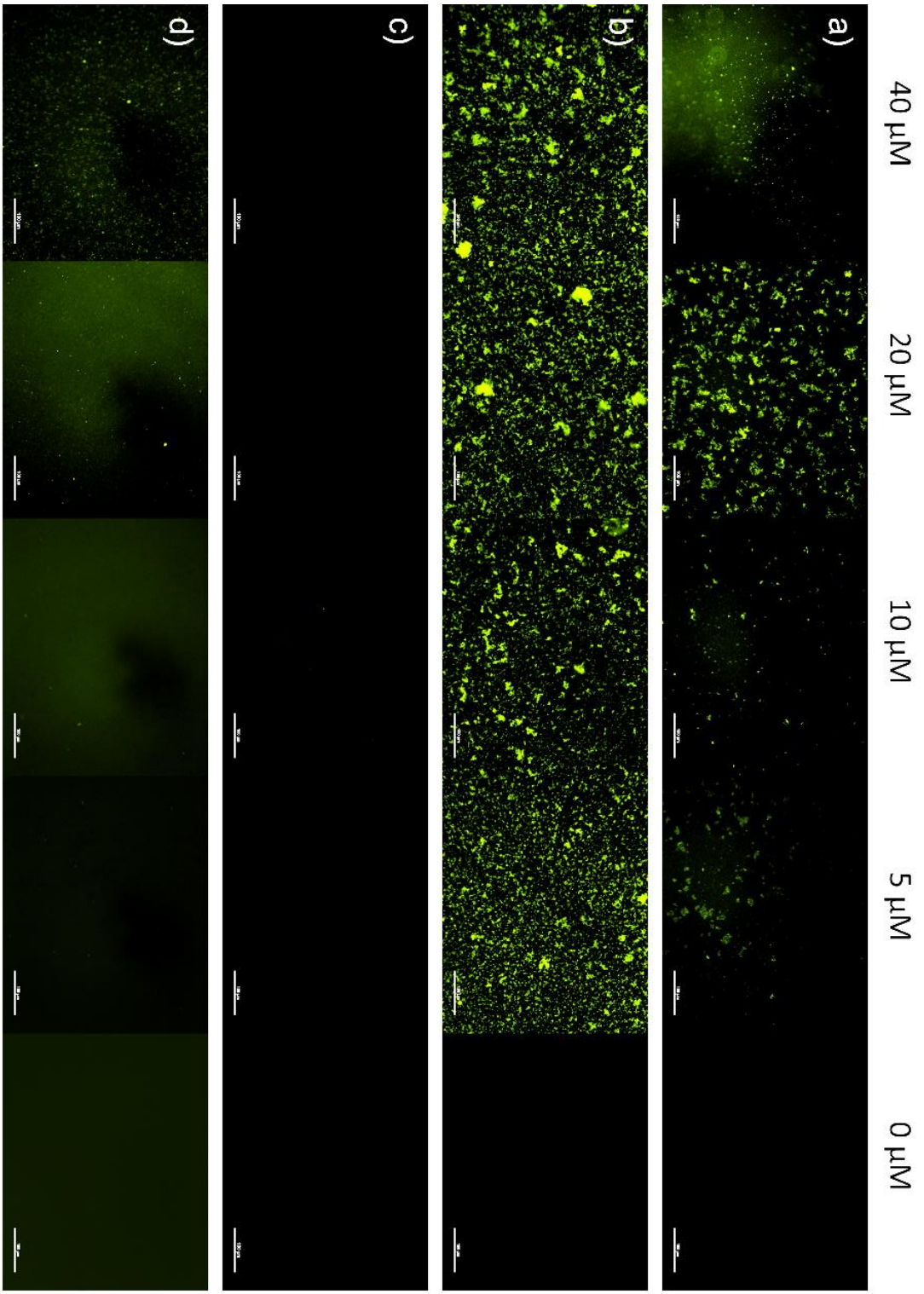

Figure 3.46: Evaluation of BAC ONE efficacy after attaching to hydrogel Su 60 14 COOH with different incubation concentrations, a) Su 60 14 COOH with BAC ONE cultured with *S. aureus* b) BAC ONE cultured with *S. aureus* c) Su 60 14 COOH with BAC ONE cultured with *E. coli* d) BAC ONE cultured with *E. coli.* Scale bar is 100 µM.

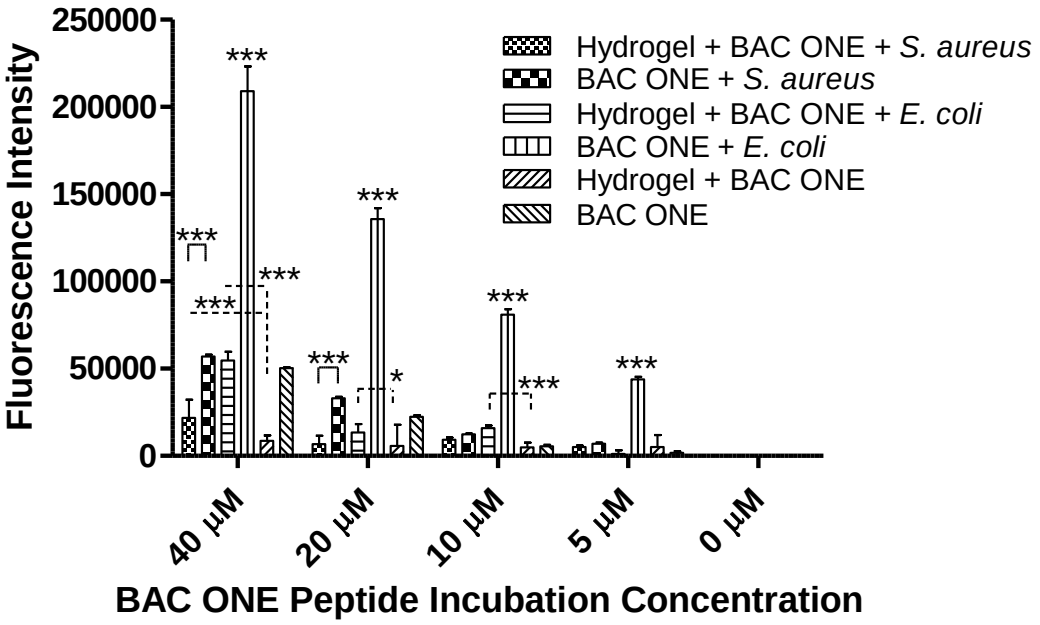

Figure 3.47: Quantification of fluorescence from the BAC ONE peptide attached to hydrogel Su 60 14 COOH. Error bars ±SD, * $p < 0.05$, *** $p < 0.005$ $N = 6$.

3.5.2.3 BAC ONE stability after attachment to the hydrogel:

An investigation of the stability of the peptide after association with the hydrogel was undertaken to determine what time peak fluorescent intensity was observed and when that signal began to deteriorate. The fluorescent signal from the peptide was measured over a 21 h period. It was determined that the BAC ONE peptide associated with the hydrogel was stable across all incubation concentrations for at least 21 h. No significant reduction in fluorescent intensity was observed for any of the incubation concentrations over 21 h (Figure 3.48). These data suggest that optimal fluorescence is maintained for 21 h from initial application.

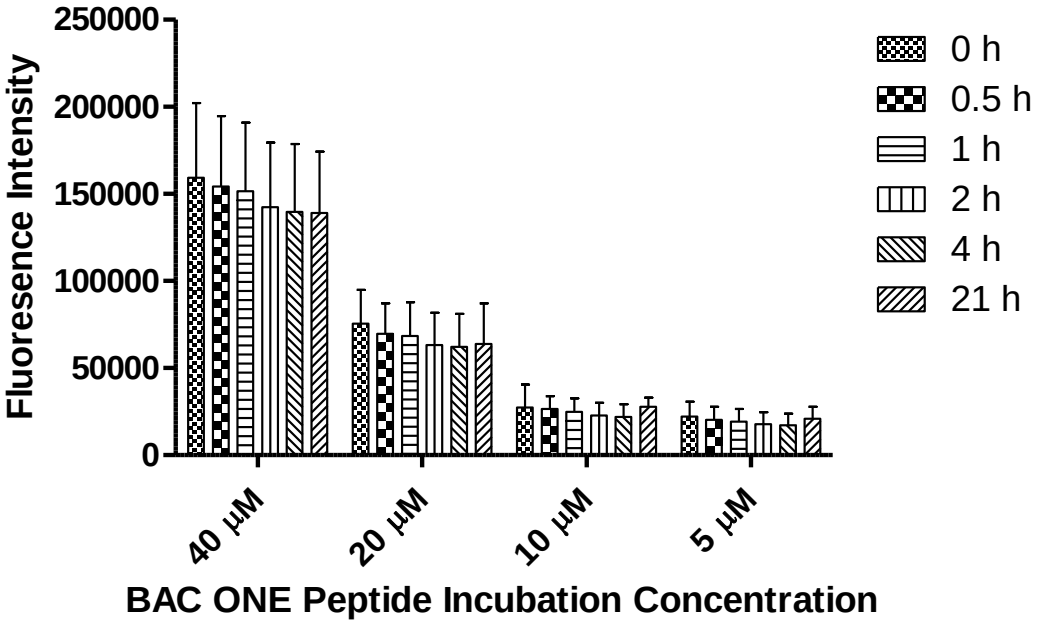

Figure 3.48: Stability of the fluorescent signal from the BAC ONE peptide attached to hydrogel Su 60 14 COOH after 21 h incubation with *S. aureus*. Error bars ±SD, *N* = 6.

3.5.2.4 BAC ONE staining of non-target cells:

A co-culture of HCE-T cells and *S. aureus* or *E. coli* was set up to determine if the BAC ONE peptide would label the mammalian cells. It was identified that BAC ONE associated with hydrogel Su 60 14 COOH successfully labelled *S. aureus* or *E. coli* in a co-culture system but some non-specific labelling of HCE-T cells was evident (Figure 3.49). Although some non-specific staining of HCE-T cells was evident, the bacteria was still identifiable as the fluorescence intensity was greater.

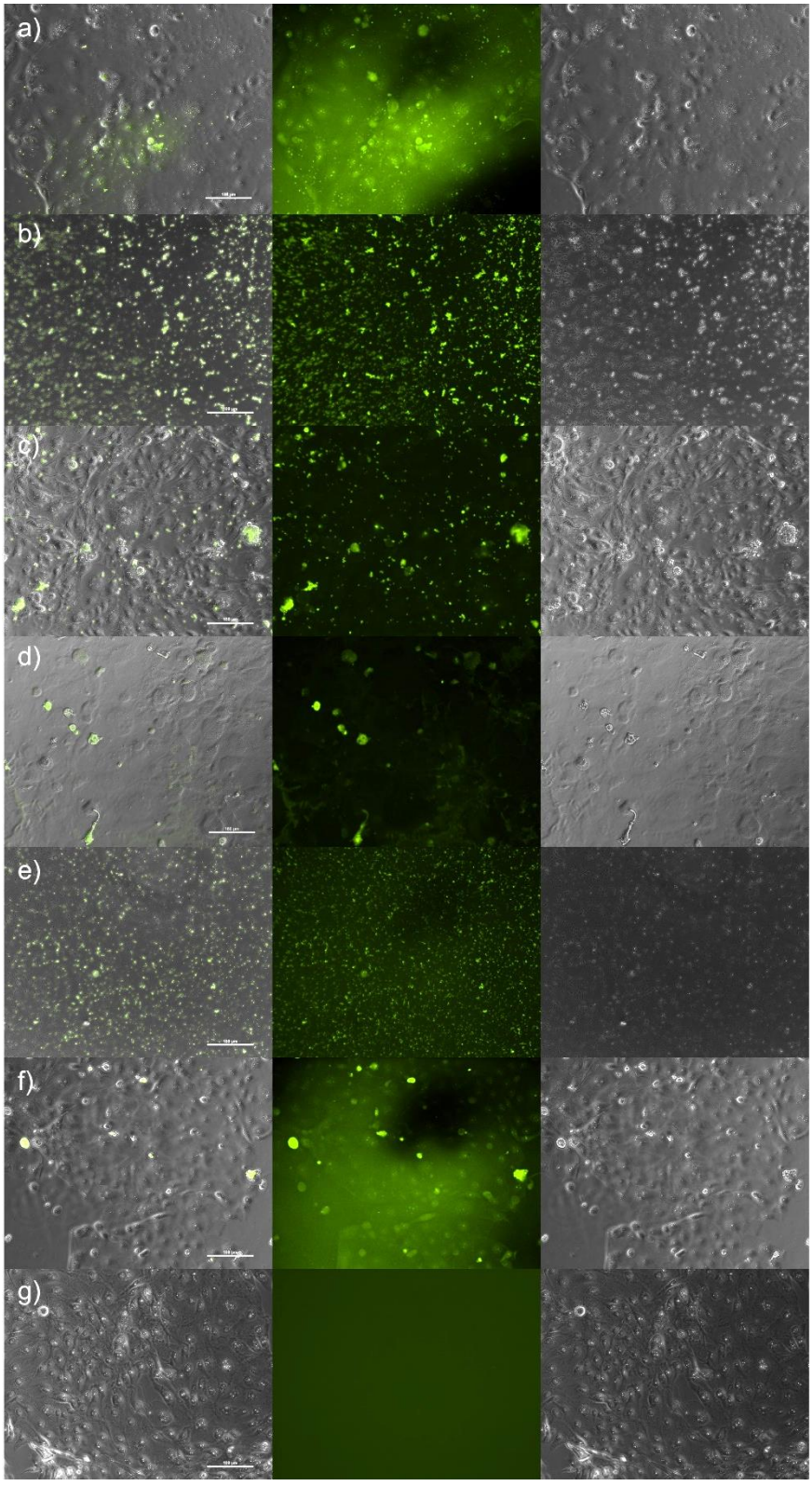

Figure 3.49: Investigation of BAC ONE efficacy in a co-culture of HCE-T cells and *S. aureus* or *E. coli*, a) Su 60 14 COOH with BAC ONE cultured with HCE-T and *S. aureus,* b) BAC ONE cultured with *S. aureus,* c) BAC ONE cultured with HCE-T and *S. aureus,* d) Su 60 14 COOH with BAC ONE cultured with HCE-T and *E. coli,* e) BAC ONE cultured with *E. coli,* f) BAC ONE cultured with HCE-T and *E. coli* g) Su 60 14 COOH with BAC ONE cultured with HCE-T. Scale bar is 100 µm.

3.5.3 BAC TWO:

3.5.3.1 Qualitative BAC TWO efficacy analysis:

The BAC TWO peptide was incubated with hydrogel Su 60 14 COOH prior to testing its efficacy at identifying the Gram-negative *E. coli* in culture. NBD fluorescence from the BAC TWO peptide associated with hydrogel Su 60 14 COOH was observed at incubation concentrations of 10 - 40 μM (Figure 3.50a). Fluorescence was observed across all concentrations of the peptide when it was not associated with the hydrogel (Figure 3.50b). No fluorescence was observed from the peptide in the presence of the Gram-positive organism *S. aureus* (Figure 3.50c). Some background auto-fluorescence was observed from the hydrogel when present. These data suggest the Su 60 14 COOH hydrogel can be used to deliver the BAC TWO peptide without hindering its activity.

3.5.3.2 Quantification of BAC TWO fluorescence:

The fluorescence of the peptide for the range of incubation concentrations was quantified to confirm the observations in section 3.5.3.1. A microplate reader was used to measure the fluorescence intensity. A statistically significant ($p < 0.005$) increase in fluorescence was observed from the BAC TWO peptide (at 40 μM) associated with hydrogel Su 60 14 COOH when compared to a no microbe or *S. aureus* control (Figure 3.51). The peptide incubated with *E. coli* alone gave the greatest fluorescence signal with statistical significance ($p < 0.005$) over the Su 60 14 COOH hydrogel between 10 - 40 μM incubation concentrations. These data suggest the hydrogel capable of delivering a sufficient quantity of the peptide when pre-incubated in the greater BAC TWO concentration (40 μM).

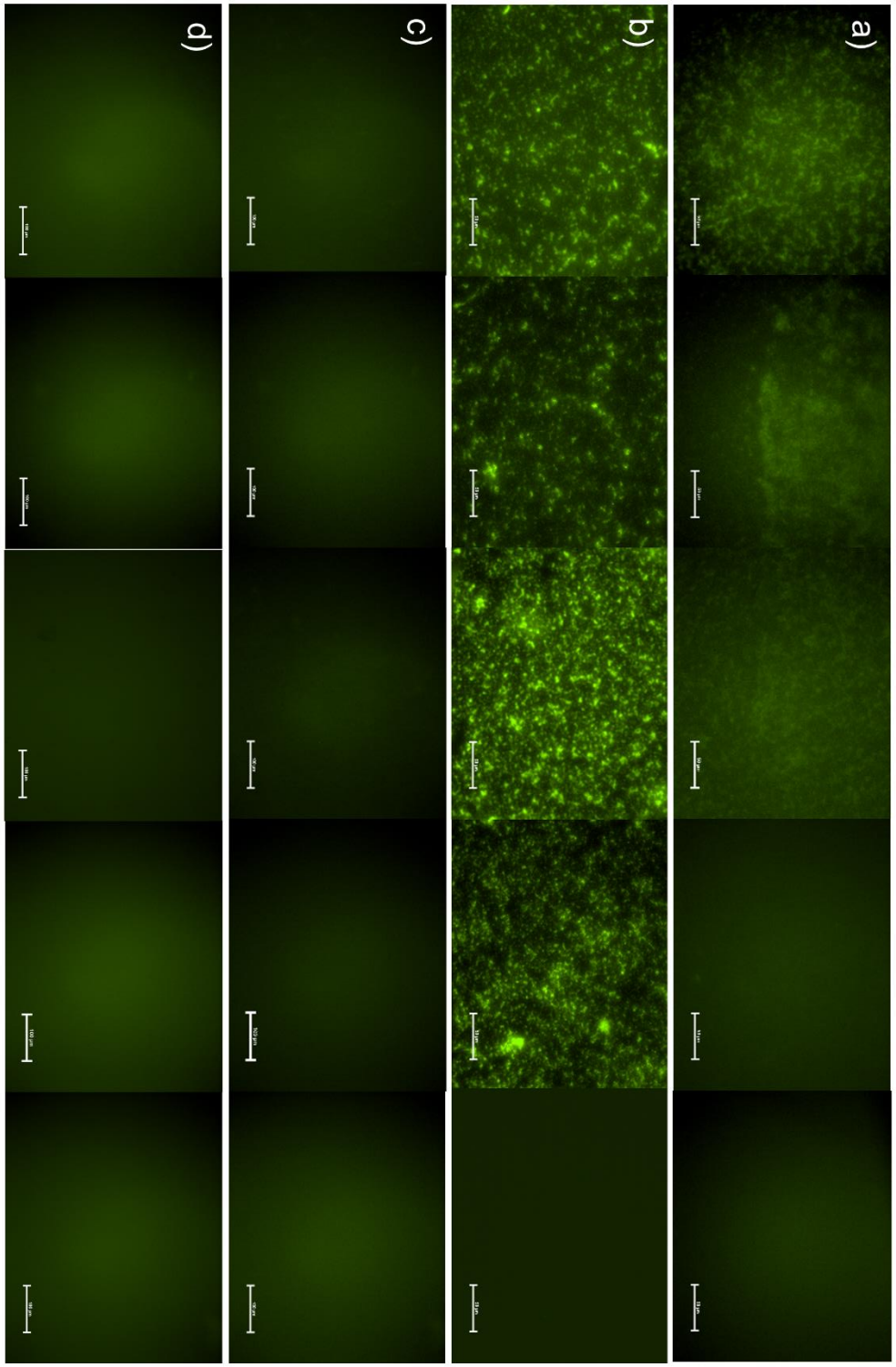

Figure 3.50: Evaluation of BAC TWO efficacy after attaching to hydrogel Su 60 14 COOH with different incubation concentrations, a) Su 60 14 COOH with BAC TWO cultured with *E. coli* b) BAC TWO cultured with *E. coli* c) Su 60 14 COOH with BAC TWO cultured with *S. aureus* d) Su 60 14 COOH with BAC TWO only. Scale bar is 50 µm.

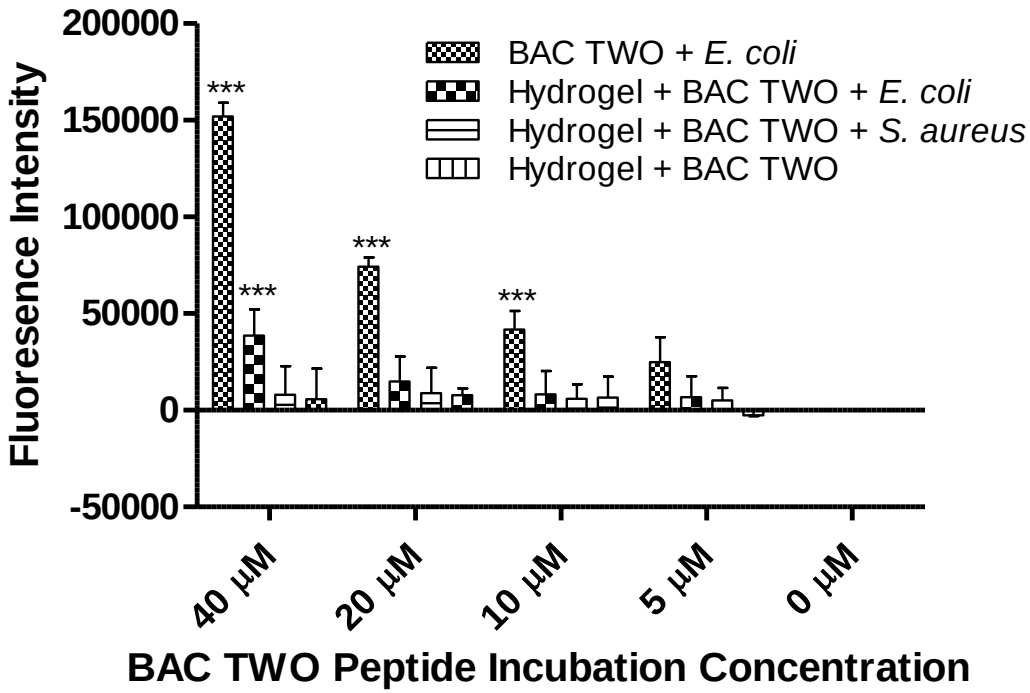

Figure 3.51: Quantification of fluorescence from the BAC TWO peptide attached to hydrogel Su 60 14 COOH. Error bars ±SD, *** $p < 0.005$ $N = 6$.

3.5.3.3 BAC TWO stability after attachment to the hydrogel:

An investigation of the stability of the peptide after association with the hydrogel was undertaken to determine what time peak fluorescent intensity was observed and when that signal began to deteriorate. The fluorescent signal from the peptide was measured over a 21 h period. It was determined that the BAC TWO peptide associated with the hydrogel was stable across all incubation concentrations for at least 4 h. The stability of the peptide was significantly reduced ($p < 0.005$) at 20 and 40 µM incubation concentration after 21 h (Figure 3.52). These data suggest that optimal fluorescence is observed between initial application and 4 h.

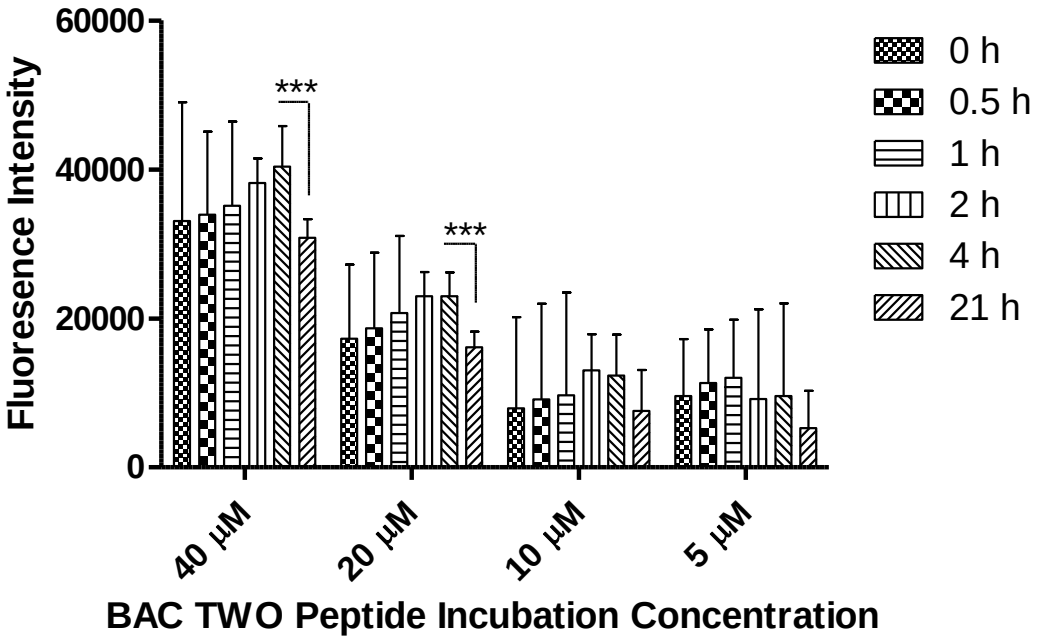

Figure 3.52: Stability of the fluorescent signal from the BAC TWO peptide attached to hydrogel Su 60 14 COOH over 21 h incubation with *E. coli*. Error bars ±SD, *** $p < 0.005$ $N = 6$.

3.5.3.4 BAC TWO staining of non-target cells:

A co-culture of HCE-T cells and *E. coli* was set up to determine if the BAC TWO peptide would label the mammalian cells. It was identified that BAC TWO associated with hydrogel Su 60 14 COOH successfully labelled *E. coli* in a co-culture system with HCE-T cells without labelling the mammalian cells (Figure 3.53). This result suggests that the peptide will not label corneal epithelial cells in a co-culture with *E. coli*.

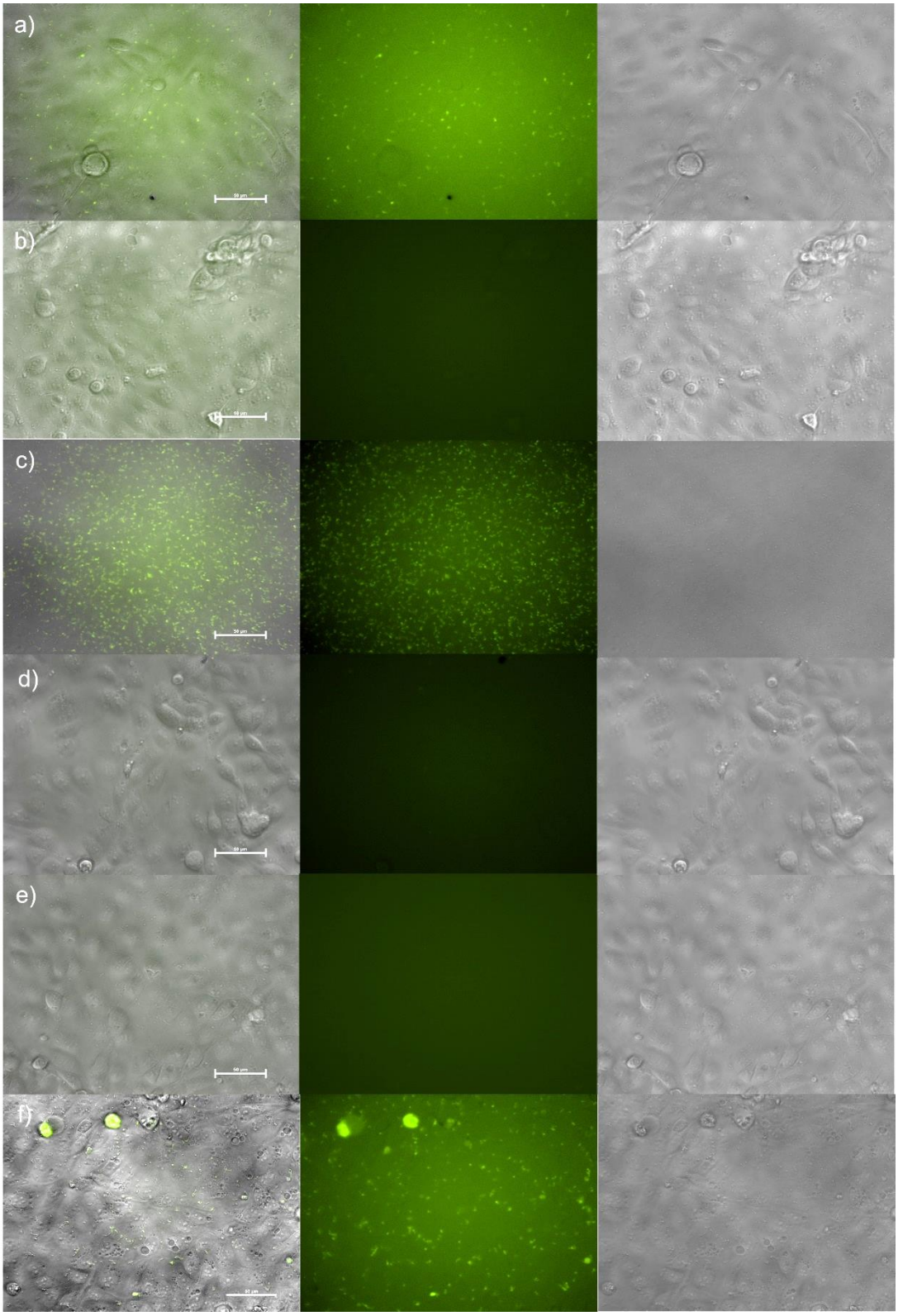

Figure 3.53: Investigation of BAC TWO efficacy in a co-culture of HCE-T cells and *E. coli*, a) Su 60 14 COOH with BAC TWO cultured with HCE-T and *E. coli,* b) Su 60 14 COOH cultured with HCE-T and *E. coli,* c) BAC TWO cultured with *E. coli*, d) Su 60 14 COOH with BAC TWO cultured with HCE-T, e) HCE-T and *E. coli* co-culture, f) BAC TWO cultured with HCE-T and *E. coli.* Scale bar is 50 µm.

3.5.4 Ex vivo bacterial keratitis model:

An ex vivo bacterial keratitis model was setup utilising porcine corneas to test the efficacy of the BAC hydrogel systems in identifying Gram-positive and Gram-negative bacteria (Figure 3.54).

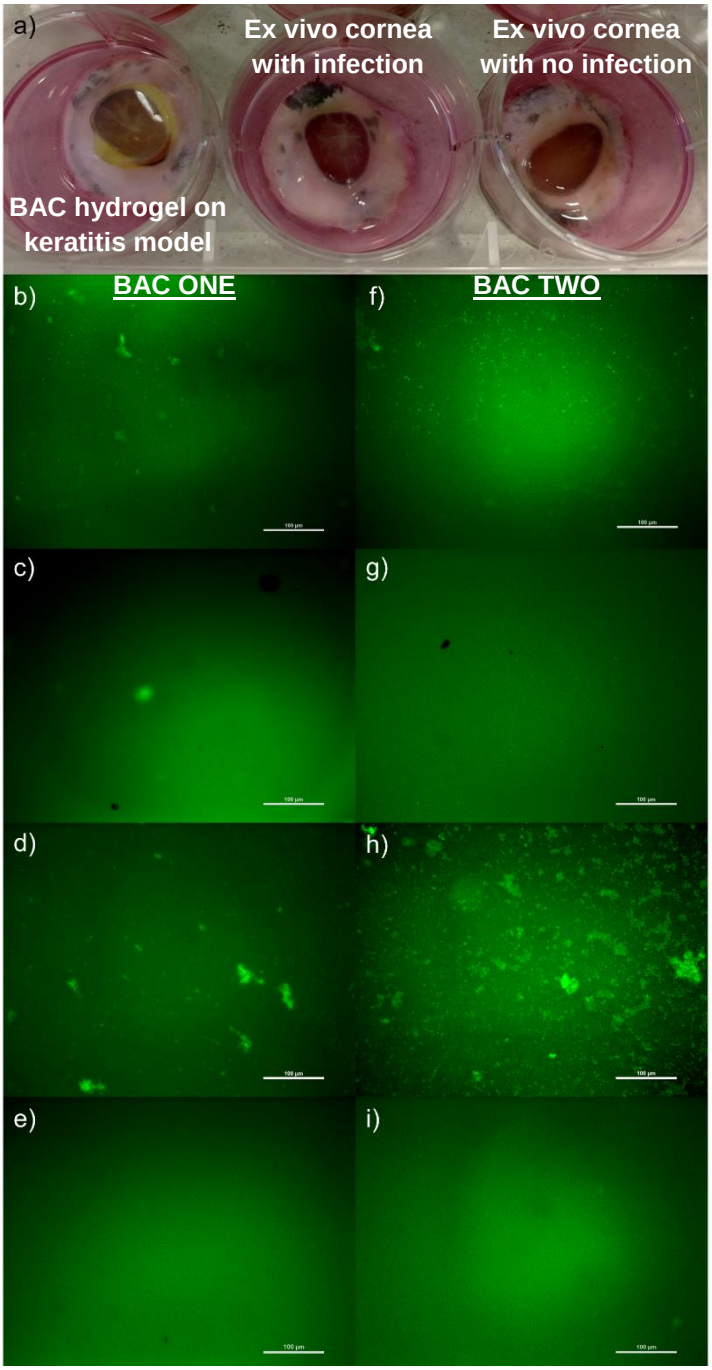

Figure 3.54: Micrographs of bacteria identified by the BAC/hydrogel system in an ex vivo model of bacterial keratitis. Scale bar is 50 µm. (a) Ex vivo corneal model of microbial keratitis, (b) hydrogel and BAC ONE with *E. coli*, (c) Hydrogel and BAC ONE with *S. aureus*, (d) BAC ONE with *E. coli* and (e) Hydrogel and BAC ONE with no infection. (f) Hydrogel and BAC TWO with *S. aureus*, (g) Hydrogel and BAC TWO with *E. coli*, (h) BAC TWO with *E. coli* and (i) Hydrogel and BAC TWO with no infection. Scale bar is 100 µm.

Staining was observed for both *E. coli* and *S. aureus* from BAC ONE associated with the hydrogel, however, it was much more evident for *S. aureus*. BAC ONE peptide alone also stained *S. aureus* in the ex vivo model. Staining was observed for *E. coli* when BAC TWO was associated with the hydrogel, with no staining for *S. aureus* evident. BAC TWO peptide alone also stained *S. aureus* in the ex vivo model.

3.5.5 Cytotoxicity of the BAC hydrogels to the HCE-T cell line:

A cytotoxicity study of the leachables from the modified Su 60 14 COOH hydrogels pre-incubated in BAC ONE or BAC TWO peptide solution (40 µM) was undertaken to investigate BAC peptide cytotoxicity against HCE-T cells. A CCK-8 assay was used as a measure of metabolic activity and HCE-T cells were cultured in standard tissue culture media as a control. No significant difference in HCE-T viability was observed at any of the time-points when comparing the hydrogels with BAC peptides associated to standard cell culture media (Figure 3.55).

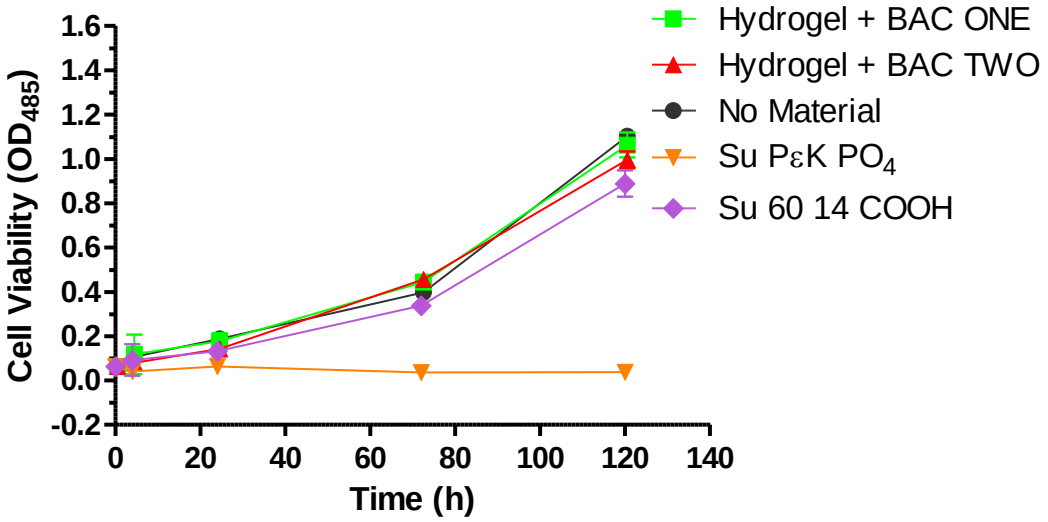

Figure 3.55: Cytotoxicity of the BAC hydrogels towards the HCE-T cell line. Error bars ±SD, *N* = 8.

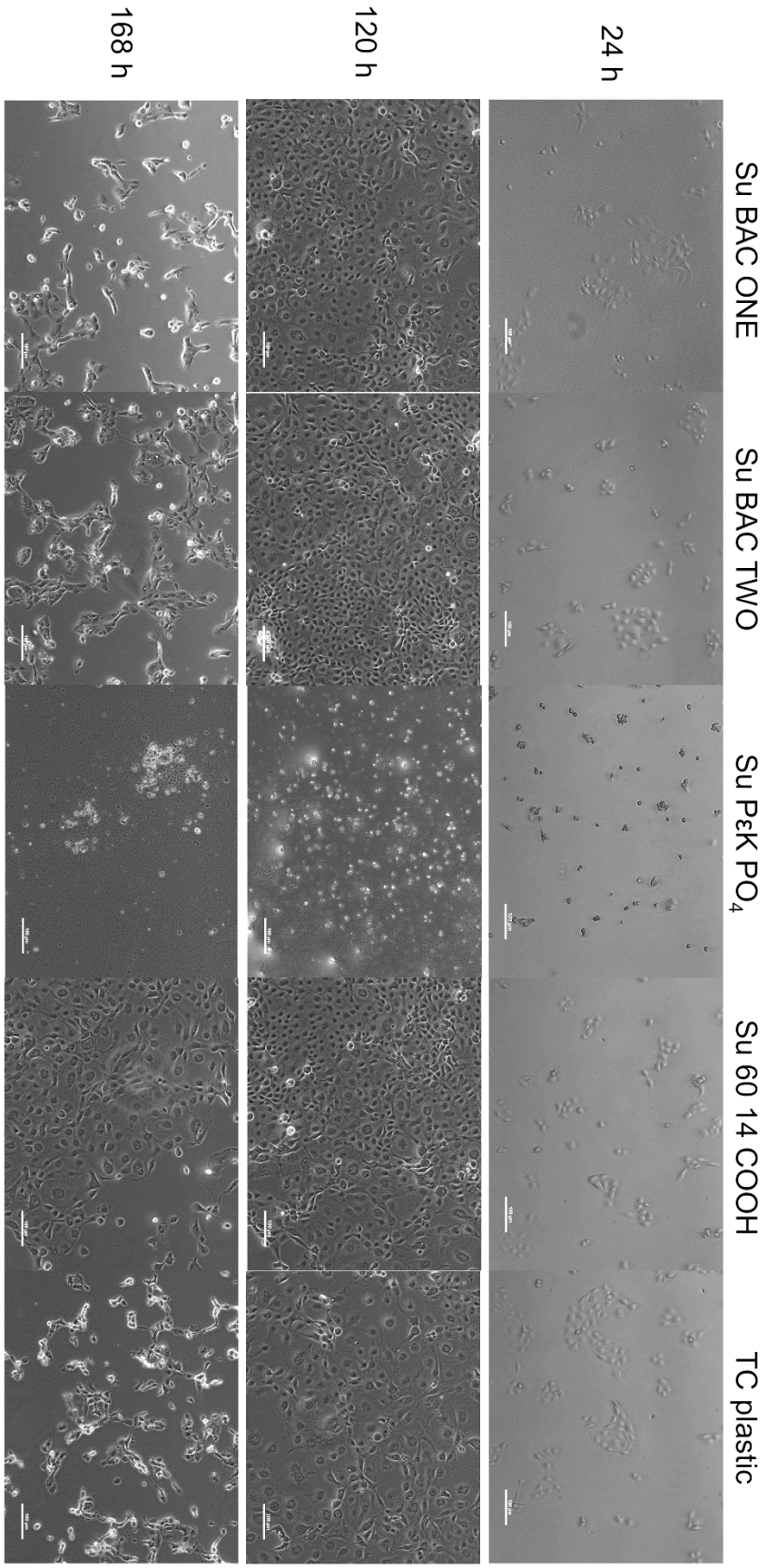

Figure 3.56: Micrographs of HCE-T cells at various intervals during the cytotoxicity study. Scale bar is 100 μm.

Analysis of the micrographs taken at various intervals during the cytotoxicity study confirm the results from the CCK-8 assay (Figure 3.56). A monolayer of HCE-T cells was still visible in those cultured in leachables from the Su 60 14 COOH hydrogel after 168 h.

These data suggest that the Su 60 14 COOH hydrogels incubated with the highest concentration of BAC ONE or TWO were non-cytotoxic to the HCE-T cell line.

4. DISCUSSION

The principle objective of this work was to investigate and optimise the mechanical and physical properties of a pεK/bis-carboxylic acid hydrogel to attain similar values as those already described for commercial contact lens materials. This was followed by detailed investigations of the efficacy of biomolecules attached to the polymer in antibacterial and antifungal activity and the identification of microbes implicated in microbial keratitis. The overarching aim of this study was to develop a novel hydrogel bandage contact lens capable of improving current treatments in the fight against microbial keratitis.

Microbial keratitis is a common condition prevalent in both developed and developing countries and can often result in blindness due to inadequate treatment. The organism implicated in infection varies with geographical location and therefore so does the treatment regimen. Current treatments are, in the most part, inefficient due to minimal absorption of the drug at the site of injury and results in the need for multiple applications of antibiotics to resolve the condition. However, in the developing world, ineffective treatment regimens due to patient non-compliance and proximity to treatment centres can result in disease reoccurrence. This exacerbates the condition and can ultimately result in the need for keratoplasty. In most clinical applications, a bandage lens is applied to provide comfort and protect the wound site. An improvement to current treatments could come in the form of a drug loaded hydrogel bandage lens that could aid the slow release of antimicrobials to the site of injury without the need for the continuous manual administration of the treatment. Therefore, the efficiency of drug delivery may improve and a reduction of patient non-compliance may be observed.

This work has shown that a pεK/bis-carboxylic acid hydrogel can be designed with mechanical and physical properties comparable to commercial contact lens materials. Furthermore, the hydrogel can be loaded with biomolecules covalently, ionically and by simple absorption to provide an antibacterial activity. The model antifungal, AmpB, was ionically associated with the

hydrogel to investigate any antifungal activity. Finally, optical sensing peptides with the environmentally sensitive NBD fluorophore attached were ionically associated with the hydrogel and investigated for their efficacy in labelling Gram-positive and Gram-negative bacteria in vitro and ex vivo as a fast-tracked identification system for bacterial pathogens of microbial keratitis.

4.1 Hydrogel Characterisation

The preliminary stage for the development of an antimicrobial bandage contact lens was to characterise the polymer both physically and mechanically. Firstly, an investigation of the raw materials and how they affect the subsequent polymer was initiated followed by the mechanical and physical investigation of the hydrogel in comparison to commercially available contact lens materials.

4.1.1 PεK characterisation:

PεK is a naturally occurring homopolymer of the amino acid L-lysine that is produced on a multi tonne scale via microbial fermentation, predominantly from *Streptomyces albulus* (Shih, Shen and Van, 2006). All the raw materials for the hydrogels in this report can be acquired from multiple sources with purities of ≥ 99% except for pεK. As a polymer and a product of fermentation, its purity and heterogeneous chain-length distribution can vary from batch to batch so it was imperative to develop analytical procedures for each batch to determine the amine content (mmol g^{-1}) so as calculation adjustments to the polymer mix could be made (Shih, Shen and Van, 2006).

From the literature natural pεK is described as having a high ratio of longer chain oligomers with the majority between 25 - 35 residues in chain length (Shih, Shen and Van, 2006). It has been described that desirable properties of pεK such as its antimicrobial activity or flavour as a food additive may be altered by varying the chain length ratio. PεK with longer chain oligomers have been known to impart more bitterness to the flavour of the substance.

This is of particular importance to the food industry where it is used as an important preservative (Nishikawa and Ogawa, 2006). A way of imparting the vary degrees of oligomer chain lengths on natural pεK is with the use of the pεK degrading enzyme produced naturally by the same organism, *Streptomyces albulus*, as a natural self-defence mechanism against pεK (Yoshida and Nagasawa, 2003). Longer chain oligomers > 10 residues have been identified as having much greater antimicrobial activity as opposed to shorter chain oligomers (Shima *et al.*, 1984).

An RP-HPLC system modified from Hirohara *et al.* 2007 was used to characterise three different batches of pεK that were acquired for this study. It was identified that the ratio of pεK oligomers was different for each batch. The main component of each batch (20 - 35 residues) has a similar pεK profile and elution time; however, each sample also has a varying degree of differing chain length oligomers as identified in the earlier running material. Short chain oligomers (5mer and 10mer) of pεK were synthesised in-house and subsequently used as standards to confirm the representative chain length of each peak on the chromatogram. Furthermore, pεK/bis-carboxylic acid hydrogels were polymerised using the three different batches of pεK. To ensure no other factors could interfere with the cross-linking C, H and N elemental analysis of the three batches was used to determine the amine content (mmol g^{-1}). This ensured the correct amount of reaction components were added to give the same level of cross-linking. The mechanical properties of the hydrogels were compared with no significant difference observed between them. Although no difference in mechanical properties was observed between hydrogels produced from the different batches of pεK it led to the development of an effective analytical process for the quality control (QC) of pεK. The oligomer chain length ratio appears to vary depending on the final application of the pεK product with some companies offering batches of pεK, with oligomers ≥ 20 residues long, as pharmaceutical grade. However, whether there is a correlation between chain-length distribution and the grade offered has not been determined and may solely be a consequence of how the pεK was manufactured and processed.

The RP-HPLC method developed in this study has been optimised to use peak area as an in-house replacement for C, H and N analysis in determining the peptide content, and thereby the amine content of individual pεK batches. It is now a standard operating procedure (SOP, SP0027) used for QC of all pεK batches under SpheriTech's International Organisation for Standardisation (ISO) 9001 quality management system.

4.1.2 Optimal bis-carboxylic acid cross-linker and reaction parameters:

The hydrogel developed in this study is a polymer of pεK cross-linked with a bis-carboxylic acid. The primary constituent of the polymer, pεK, was already established and no alternative sought as this formed the basis of the patents to the polymer. The second major constituent of the polymer, bis-carboxylic acids, were analysed to identify which one would give the final polymer optimal physical and mechanical properties.

Several of the short chain bis-carboxylic acids are produced on a multi tonne scale via the ozonolysis or hydrolysis of unsaturated fatty acids in castor oil (octanedioic acid and decanedioic acid) or oleic acid (nonanedioic acid) and have uses in the production of nylon derivatives as well as plasticisers and lubricants. Heptanedioic acid is produced via the oxidation of unsaturated fatty acid but is the least used bis-carboxylic acid described in this text (Cornils, Lappe and by Staff, 2014). Almost 81% of total hexanedioic acid produced worldwide via the nitric acid oxidation of cyclohexanol is used to make Nylon 6,6 (Musser, 2014). Generally, as the chain-length of the bis-carboxylic increases so too does the cost. The short chain bis-carboxylic acids described here have a low systemic toxicity and are readily β-oxidised by the mitochondria and peroxisomes or eliminated from the body via urine (Fiordeliso, Bron and Kohn, 1995; Grego and Mingrone, 1995). Hexanedioic acid is described as GRAS by the FDA for use as a food additive (Castellan, Bart and Cavallaro, 1991).

An initial hydrogel was polymerised using decanedioic acid to cross-link as this was used as standard for other polymers based on the same constituents (Wellings and Gallagher, 2012). It was clear from the start that

optical clarity was not good enough using decanedioic acid so longer chain bis-carboxylic acids (dodecanedioic acid and tridecanedioic acid) were discounted and shorter chain bis-carboxylic acids (hexanedioic acid, heptanedioic acid, octanedioic acid, nonanedioic acid and decanedioic acid) were investigated. Of the bis-carboxylic acids investigated, decanedioic acid was the least soluble acid due to the longer hydrophobic backbone compared to shorter chain bis-carboxylic acids. A reduction in transparency was observed as the bis-carboxylic acid chain increased and an increase in tensile strength was observed from hexanedioic acid to nonanedioic acid. A significant reduction in tensile strength was noted for most hydrogels with decanedioic acid as the bis-carboxylic acid cross-linker. The increased hydrophobicity possibly results in a less homogenous hydrogel network resulting in a more opaque polymer that contributes to the weakened mechanical properties and lack of transparency when polymerised (Refojo and Yasuda, 1965; Metters and Lin, 2007; Hou *et al.*, 2011). As density of the polymer increases so too does tensile strength. Only marginal differences were observed between the varying degrees of percentage cross-linking when the polymer was a similar density. This suggested that polymer density was more important than degree cross-linking at the levels investigated when trying to improve the polymer strength.

Octanedioic acid provided optimal mechanical properties whilst maintaining transparency and was mid-range when it came to economic considerations. A degree of opacity was observed from nonanedioic acid and decanedioic acid cross-linked hydrogels making them unsuitable and hydrogels with hexanedioic and heptanedioic acid cross-linkers have less desirable mechanical properties. These data led to octanedioic acid being chosen as the bis-carboxylic acid to cross-link pεK within the hydrogel matrix.

Immediately prior to developing the hydrogel further some important reaction parameters were standardised. By controlling these parameters at near optimal conditions the energy consumed can be minimised and the reaction can be as cost and energy efficient as possible. Both the reaction time and temperature are easily controlled with optimal reaction times being as short

as possible and the temperature as close to room temperature as possible to ensure no need for incubation under extreme cold or warm conditions. The hydrogels were polymerised for different lengths of time and separately at different temperatures. Mechanical analysis of the hydrogels made under different conditions was used to indicate the polymerisation end-point. In the optimal polymerisation time study elastic modulus increased gradually from 1 h to 5 h with statistical significance before reaching a plateau that continued to 24 h. The increase in elastic modulus is related to the continuing cross-linking up to the 5 h time-point thereby determining that a polymerisation time of at least 5 h was required to allow cross-linking to reach completion. An increase in the rate of the reaction can lead to the development of cleaner more economical reaction processes (Ameta *et al.*, 2013). During the polymerisation temperature study, no significant difference was found in the elastic modulus between hydrogels incubated at 21.5 °C and 37 °C. Both these hydrogels showed a significant increase in elastic modulus from the hydrogel that was polymerised at 6 °C. This may be directly associated with improved reaction kinetics combined with thermodynamic instability of the reaction. Every 10 °C rise in temperature is associated with two- to threefold increase in rate of reaction (Upadhyay, 2006). This suggests that the reaction had come to completion within 5 h of polymerising at these temperatures. It was determined from these data that the most reproducible mechanical properties were obtained when hydrogel Su 60 14 was polymerised at room temperature. An incubator was setup to keep polymerisation temperature constant. The manufacturer's recommendation was a running temperature of 3 °C above room temperature so the incubator was set to 25 °C and all subsequent hydrogels polymerised at that temperature.

4.1.3 Optimal mechanical and physical properties of the hydrogel:

Following optimisation of the reaction parameters and the bis-carboxylic acid cross-linker several hydrogel variants were investigated as potential candidates for bandage contact lenses. Su 60 15 (pεK 60 mol% cross-linked with octanedioic acid and a density of 0.067 g cm^{-3}), Su 60 14 (pεK 60 mol% cross-linked with octanedioic acid and a density of 0.071 g cm^{-3}), Su 60 13 (pεK 60 mol% cross-linked with octanedioic acid and a density of 0.077 g cm^{-}

^{3}) and Su 65 15 (pεK 65 mol% cross-linked with octanedioic acid and a density of 0.067 g cm^{-3}) were investigated for their mechanical and physical properties.

The elastic modulus for hydrogel Su 60 13 was significantly greater than the other hydrogels tested. However, optical clarity of this hydrogel was compromised as the increased polymer density results in a refractive index of 1.395. The hydrogel with the next greatest elastic modulus was hydrogel Su 60 14 which had no significant difference in stress or strain compared to Su 60 13. It also had a refractive index of 1.390 more closely associated to the 1.380 of the human cornea (Kim *et al.*, 2004). Similarly, light transmittance data measured at 544 nm for Su 60 13 (79%) was much lower than that obtained for Su 60 14 (88%) and Su 60 15 (92%) which were more closely aligned to the human cornea (90%) (Beems and Van Best, 1990). Hydrogel Su 60 14 was chosen as the hydrogel with the greatest mechanical properties whilst maintaining an acceptable optical clarity. The elastic modulus for all the hydrogels were in the range of 0.31 - 0.73 MPa comparable to commercial lens materials whilst maintaining a relatively high water content of between 67 - 73% regardless of the polymer composition. This may be extremely beneficial in that the mechanical properties may be tailored without significantly reducing the water content of the lens. This characteristic is important for both oxygen permeability and comfort of the lens to the wearer (Guzman-Aranguez, Colligris and Pintor, 2013). Another interesting finding was the difference in both water content and refractive index of the antimicrobial hydrogels. Su PεK had a higher water content and lower refractive index compared to Su Pen G. This may correspond with the increased water absorption capacity of Su PεK due to the increased amounts of hydrophilic amino groups allowing for an increase in water molecule absorption (Leeder and Watt, 1965).

The measurement of oxygen permeability of contact lens materials has become more important in recent years with the advent of extended wear silicone contact lenses through which silicone becomes the main oxygen carrier over water of conventional contact lenses (Efron *et al.*, 2007). An

increased understanding of the implications of a decreased oxygen supply to the avascular cornea such as hypoxia that can lead to oedema or microbial keratitis has also increased the importance of Dk values (Holden and Mertz, 1984; French, 2005). As the hydrogels in this study were not modified in any way to increase oxygen permeability the water content was therefore used to determine their Dk values. This may not be the optimal method as there are two ISO standard methods for the determination of oxygen permeability of contact lens materials (ISO 18369-4:2006). The measurements are taken via a polarographic method or the coulometric method. The polarographic method was developed by Fatt in the 1970s and is most applicable for the measurement of hydrogel lenses with a Dk between 0 - 145 Barrer. The coulometric method was developed in the advent of the development of high oxygen permeable silicone lenses (Morgan and Efron, 1998; Morgan, Brennan and Alvord, 2001).

Realistically, all hydrogel lenses induce some degree of hypoxia to the cornea. Hydrogel lenses with lower Dk values (≤ 20 Barrer) cause increased oedema and vascularisation with higher Dk value (≥ 20 Barrer) lenses causing minimal changes to the cornea (Brennan and Morgan, 2009). The theoretical maximum Dk of hydrogels based on a water content of 100% is 88. However, the hydrogels described in this report have Dk values of between 24 - 30 Barrer and are comparable to conventional hydrogel lens materials such as omafilcon A (27 Barrer) and lidofilcon A (32 Barrer) (Blackmore, 2010).

Wettability measurements are used as a measure of the comfort of a contact lens material and is mainly determined by measuring the contact angle via the sessile drop, captive bubble or Wilhelmy plate methods (Campbell, Carnell and Eden, 2013). Improving wettability has become more important in recent years with the increased usage of more hydrophobic silicone lenses. These have been improved with the addition of hydrophilic monomers such as NVP. The hydrogels described in this report have an average contact angle of 30 ° making them highly hydrophilic. A hydrophilic contact lens

material ensures tear film stability, improved optical quality and comfort (Ketelson, Meadows and Stone, 2005; Keir and Jones, 2013).

4.2 Cytocompatibility of Hydrogel Variants In Vitro

The HCE-T cell line was chosen as the ideal candidate for the in vitro analysis of cytotoxicity from the hydrogels. A measure of the cytotoxicity was important to ensure the hydrogel variants were cytocompatible to human corneal epithelial cells in vitro. The HCE-T cell line displays excellent morphological and molecular similarities to corneal epithelial cells in vivo (Rönkkö *et al.*, 2016). However, as with all cell lines variations in gene expression and general cell biology have been observed. Gene expression can be either up or down regulated when compared to primary corneal epithelial cells with some keratins only expressed by the cell line (Huhtala *et al.*, 2003; Rönkkö *et al.*, 2016).

An initial investigation of the interaction of HCE-T cells with hydrogel Su 60 14 determined there was no negative impact of direct contact on cells cultured directly underneath the hydrogel. However, when HCE-T cells were seeded on top of the hydrogel they remained spherical and failed to adhere. The hydrogels described in this report have an average contact angle of 30 ° making them too hydrophilic for optimal cell attachment. A material that does not promote cell adhesion may be more suitable as a bandage lens applied to a healing corneal epithelium. An optimal contact angle for cell adhesion has been suggested to be between 40 - 70 ° for a range of cell types with materials outside this range generally too hydrophobic or too hydrophilic (Figure 4.1) to allow optimal cell adherence (Wachem *et al.*, 1987; Tamada and Ikada, 1993; Dowling *et al.*, 2011). ECM protein deposition on hydrophilic materials results in loosely attached proteins due to the polar and highly charged surface of the material and protein attraction to the surrounding water molecules. Hydrophobic surfaces are more favourable to protein deposition via hydrophobic interactions, however, the attractions can be irreversible resulting in the denaturation and loss of bioactivity of the protein

that ultimately results in less cell adhesion (Guney *et al.*, 2013). Many other factors affect cell adhesion to materials including surface functionality, surface topography, mechanical properties and the behaviour of the particular cell type investigated, however, material hydrophilicity is still identified as the most prominent factor (Chang and Wang, 2011).

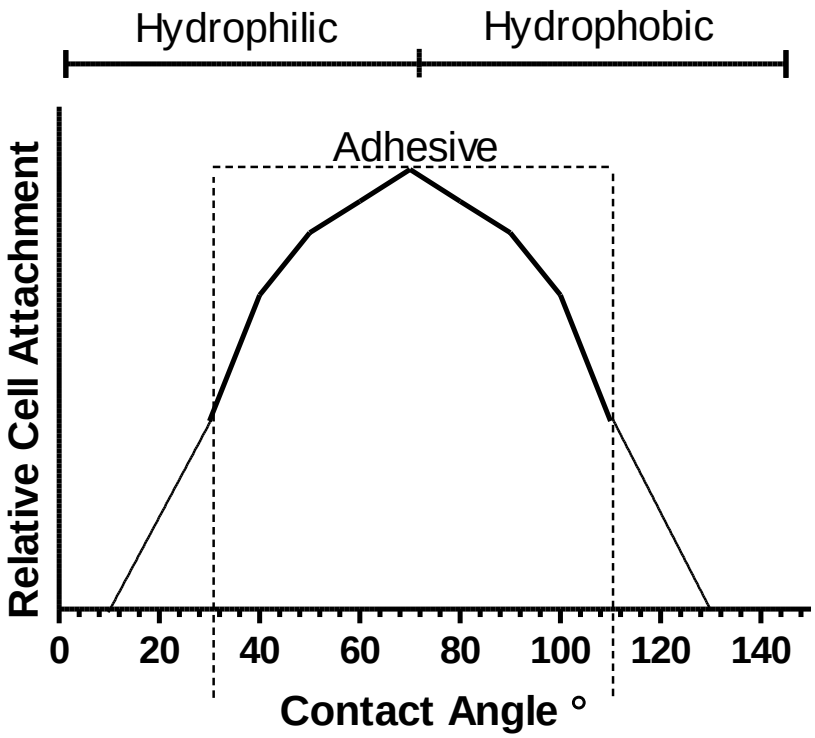

Figure 4.1: A general representation of mammalian cell adherence in relation to the contact angle of a material.

4.2.1 Unmodified hydrogel Su 60 14:

An indirect cytotoxicity assay was carried out to determine if any leachable from the hydrogel Su 60 14 influenced HCE-T cells in vitro. Over the period of an 8 day culture no significant effects to cell viability was observed when compared to the control. This suggests that leachables from the hydrogel are non-cytotoxic to the HCE-T cell line and provided the initiative to investigate what effects direct contact may have on HCE-T cell behaviour.

A scratch assay was used to determine the rate of re-epithelialisation of a HCE-T cell monolayer when in direct contact underneath the hydrogel material. Most scratch wounds with the hydrogel present had closed by 23 h. This was also true of the control and no significant difference was observed in scratch wound closure rates when quantified with TScratch software. The scratch wound closure rate is comparable with HCE-T cell scratch wound closure rates of 24 h stated in the literature (Movahedan *et al.*, 2012; Hou *et al.*, 2013). This suggests the Su 60 14 hydrogel does not inhibit HCE-T cell re-epithelialisation when in direct contact. The rate of wound healing is of great importance when considering a bandage lens material ensuring an unhindered healing process and less discomfort for the patient from the protective barrier it provides (Grentzelos *et al.*, 2009).

A more in-depth investigation of the closed scratch assays via immunofluorescence staining was undertaken. A reformed epithelial monolayer should stain positive for tight junction proteins between cells. Tight junction proteins are made up of a family of transmembrane and membrane associated proteins that regulate cell to cell contact and the functioning of the epithelial barrier (Figure 4.2). ZO-1 is a 220 kDa cytoplasmic protein that is associated with the membrane and involved in the formation of tight junctions that are expressed around the cell membrane when a cell monolayer is intact and the epithelial barrier functioning. ZO-1 is located within the superficial layer of the corneal epithelium and has also been implicated in cell signalling during proliferation and differentiation (Ko, Yanai and Nishida, 2009; Chen *et al.*, 2012). Occludin is a 65 kDa transmembrane protein and along with claudin and junction adhesion molecules is directly involved in the formation of tight junctions. Short adhesive strands of the proteins help form the paracellular barrier and mediate the transfer of ions and small molecules (Ryeom, Paul and Goodenough, 2000; Cummins, 2012; Fanning and Anderson, 2013). A compromised corneal epithelial barrier may result in a route of infection. Specifically staining for these tight junction proteins identifies whether the epithelial barrier function of the reformed monolayers are physically compromised in any way (Chen *et al.*, 2012). Strong ZO-1 and occludin fluorescence signals were obtained for each of the different samples

of closed scratch wounds. This suggested that the presence of the hydrogel had no adverse effect on the reformation of a HCE-T cell monolayer.

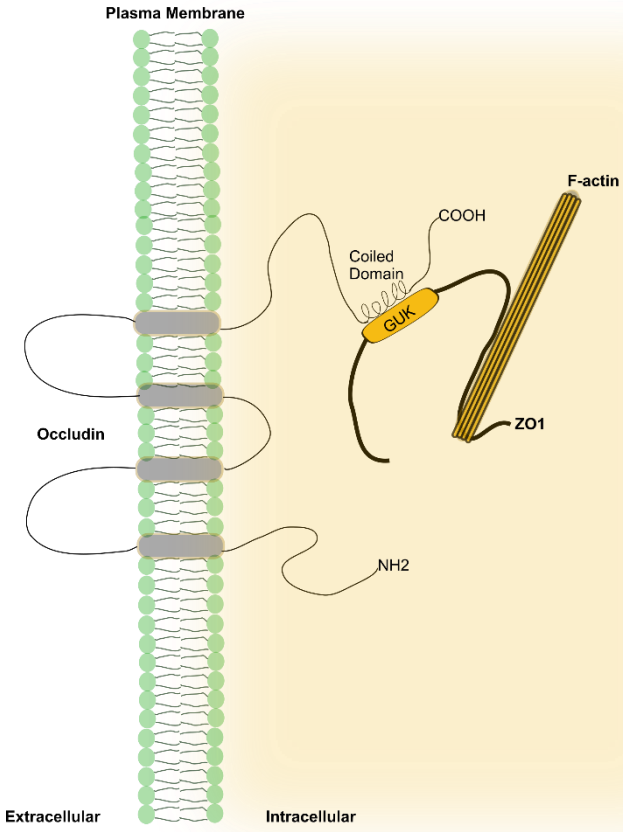

Figure 4.2: Location and interaction of cell adhesion proteins investigated with immunofluorescence staining on HCE-T cells.

Keratins are water insoluble proteins that form intermediate filaments in most epithelial cells. Staining for keratins is often used as an epithelial cell marker. The 10 nm diameter intermediate filaments provide the structural framework to the cell cytoplasm of mammalian cells. Over 50 keratins have been discovered in the last 30 years and are divided into two groups, type I (acidic) and type II (basic) (Schermer and Galvin, 1986; Karantza, 2011; Merjava *et al.*, 2011). Of these, keratin 3 and 12 are specific to the cornea and often found as a dimer (Huhtala *et al.*, 2003; Coutinho *et al.*, 2011). In a previous study the HCE-T cell line was found to express keratins 3, 7, 8, 18 and 19. Keratins 7, 8 and 19 not normally found in the cornea and more specific to

simple epithelial cells were also identified in the HCE-T cell line (Huhtala *et al.*, 2003). In this study keratins 8 and 18 were identified by staining with the antibodies pan cytokeratin (anti-keratins 4, 5, 6, 8, 10, 13 and 18) and cytokeratin MNF116 (anti-keratins 1, 2, 3, 4, 5, 6, 7 and 8) and confirmed the identity of the cells in this report as cells of an epithelial lineage.

These data coupled with data for scratch wound closure and cytotoxicity suggest that the hydrogel has no negative effects on HCE-T cells in vitro, suggesting it is cytocompatible with this cell type. However, conventional bandage lens materials are evolving and more research is focussing on the inclusion of a drug delivery capacity to help prevent or aid the treatment of ocular infections.

4.2.2 Hydrogels with biomolecules associated:

A repeat of the cytocompatibility tests on the hydrogels after the association of antimicrobials highlighted several novel insights. Minor cytotoxicity arising from the covalent attachment of pεK (Su Pεk) and the ionic association of penicillin G (Su Pen G) to the hydrogels was observed after 24 h in culture and may be due to pH changes in the media from biomolecule elution or insufficient neutralisation of salts associated with the hydrogels. To highlight this, a hydrogel soaked in x10 PBS (Su PεK PO_4) to associate phosphate salt with the amine groups showed the most cytotoxicity and was evident after only 2 h. This toxicity was most likely due to the phosphate salt leaching from the hydrogel into cell culture media. Consideration of the effect of hydrogel-associated molecules may be necessary with extra neutralisation steps a possible requirement prior to cell culture. A repeat of the HCE-T scratch assay and ZO-1 staining found no difference in re-epithelialisation when Su PεK and Su Pen G hydrogels were present compared with the Su 60 14 hydrogel and tissue culture plastic control. ZO-1 staining was evident for all the hydrogels, except with Su PεK PO_4 where no monolayer was present and almost all cells were detached after 23 h. The toxicity observed after 24 h from Su PεK and Su Pen G hydrogels may not have a negative impact in vivo as the natural flushing mechanism associated with blinking would maintain

the tear film turnover surrounding the cornea epithelium (Wong, Wan and Kaye, 2002).

The non-covalent association of AmpB with hydrogel Su 65 15 and the BAC peptides with hydrogel Su 60 14 COOH were investigated for cytotoxicity to the HCE-T cell line. All the modified hydrogels were non-cytotoxic towards the HCE-T cell line compared to the no material control. Further investigation (scratch assay or antibody staining) of these hydrogels was deemed unnecessary as no negative impact on HCE-T cell viability was observed and the cytocompatibility of the unmodified Su 60 14 and Su PεK and Su Pen G were already well characterised.

4.3 Efficacy of Hydrogel Variants against a Model of Bacterial Keratitis

Model strains of both Gram-positive (*S. aureus* Newman) and Gram-negative (*E. coli* MC1061) bacteria were chosen as candidates to examine the antibacterial affect from the hydrogels as wild type strains of both organisms are implicated in bacterial keratitis (Rhem *et al.*, 2000; Ferrari *et al.*, 2009; Karsten, Watson and Foster, 2012). However, the prevalent organism implicated in bacterial keratitis can vary over time and depending on geographical location (Orlans, Hornby and Bowler, 2011). Both organisms are identified as susceptible to the model antibiotic used in this part of the study, penicillin G (Korsak, Liebscher and Vollmer, 2005; Baba *et al.*, 2008). PεK is well documented as having an efficacy against a broad range of microbes due to the polycationic nature of the molecule with an MIC of 12.5 μg cm^{-3} against both *E. coli* and *S. aureus* (Shima *et al.*, 1984; Hyldgaard *et al.*, 2014; Li *et al.*, 2014).

4.3.1 Antimicrobial activity from hydrogel cross-link variants:

An investigation of antibacterial activity from hydrogels with varying amounts of amine groups available in the polymer backbone was undertaken. The cross-link density of the hydrogel (Su 60 14) was either increased to 75% (Su 75 14) or reduced to 45% (Su 45 14) to change the number of free amine

functional groups that contribute towards antimicrobial activity. The metabolic activity of the *S. aureus* was measured with a resazurin assay. There was approximately 40% less resazurin reduction for all hydrogels after 4 h and 18 h when compared with the LB agar control. However, there was no significant difference in resazurin reduction when comparing hydrogels of different cross-link densities. These data suggest there may not be enough difference between the amounts of free amino group's side-by-side within the polymer backbone to make a significant difference to antimicrobial activity evident between the three hydrogels with differing cross-link densities. This outcome may correlate with the 100-fold decrease in antimicrobial activity that pεK, with < 9 lysine residues has when compared with longer chain oligomers (Shima *et al.*, 1984; Yoshida and Nagasawa, 2003).

4.3.2 Antimicrobial activity from hydrogels with biomolecules:

PεK was covalently attached to the hydrogel post-polymerisation as longer chains to test the hypothesis that longer chain oligomers of pεK would have a greater antimicrobial activity than shorter chain oligomers found in the polymer backbone of the hydrogel cross-link variants. Following a methyl orange assay, it was determined that a 12-fold increase in amine groups was achieved after pεK attachment. Minimal reduction of resazurin was observed for both *S. aureus* and *E. coli* in the presence of the Su PεK hydrogel at the 2 h and 4 h time-points and only a minor resazurin reduction at the 18 h time-point for both *S. aureus* (3%) and *E. coli* (5%). The unmodified hydrogel performed marginally better than the LB agar control at the 2 h and 4 h time-points with both bacteria. After 18 h the resazurin reduction by both bacteria in the presence of Su PεK was approximately half of that of the LB agar control. These data suggest that the increased amount of amine groups have a positive impact on the antibacterial activity of the hydrogel.

A more detailed investigation into improving the antimicrobial activity of the hydrogel by either the ionic attachment of penicillin G or the covalent attachment of pεK was undertaken with focus on *S. aureus* as the model pathogen. Immediately after penicillin G attachment an elution study determined that release from hydrogel Su Pen G occurred over 5 h but an

initial burst release profile (Figure 4.3) was observed over the first 30 min. The burst release of compounds from drug delivery hydrogels is a common phenomenon when no specific modifications are made to control drug release (Huang and Brazel, 2001; Hoare and Kohane, 2008). However, a burst release is not ideal due to possible toxic concentrations of drugs released immediately followed by less than therapeutic amounts. Commercial considerations are also commonly involved as wastage of valuable drugs is not commercially viable and a lack of controlled release may result in performance inconsistencies that could result in regulatory problems (Omidian *et al.*, 2012). Some examples of methods used to control drug release include a layer by layer technique to incorporate ciprofloxacin in a pHEMA hydrogel and resulted in zero order release of the drug over 4 weeks or the incorporation of nanoparticles loaded with lidocaine incorporated into a pHEMA hydrogel that resulted in controlled release of the drug over a few days (Gulsen and Chauhan, 2004; Ciolino *et al.*, 2009). Possibilities to control drug release from hydrogel Su Pen G could include penicillin G loaded microparticles of the hydrogel that could be incorporated into the polymer mix prior to polymerisation. These may provide a two-stage release of the drug with a slower release of penicillin G from the microparticles following the initial burst release from the hydrogel matrix. Another example could include multiple dosing of the hydrogel by adding topical drops of the drug to the hydrogel at set time-points. The difficulty with this method is that the drug may reach below therapeutic levels during the dosing regimen coupled with spikes in drug concentrations following replenishing the hydrogel with topical drops (Omidian *et al.*, 2012).

The subsequent antimicrobial activity was assessed against both planktonic and attached *S. aureus* on the Su PεK and Su Pen G hydrogels. The assay of planktonic *S. aureus* revealed the greatest log reduction of 2.8 was observed from Su Pen G which may be explained from the fact that penicillin G was attached ionically and therefore becomes more bioavailable in the culture media when it's released from the hydrogel thereby having a greater effect than Su PεK on planktonic bacteria. Activity towards *S. aureus* attached to hydrogel Su PεK revealed the greatest log reduction of 2.3. This

may be due to the covalent attachment of cationic pεK to the hydrogel promoting interaction with the net negative charge of *S. aureus* at the hydrogel surface. The covalent attachment of antimicrobial components to biomaterials for the prevention of biofilm formation and increased antibacterial activity has been well described. These range from synthetic and natural coatings such as pHEMA and chitosan to AMPs such as melimine (Rasul *et al.*, 2010; Costa *et al.*, 2011; Dutta *et al.*, 2013).

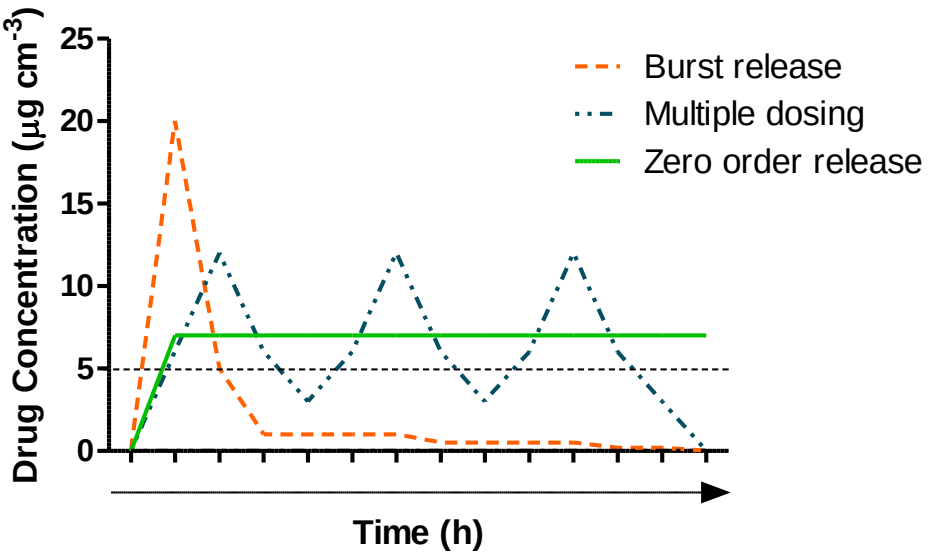

Figure 4.3: Typical drug release profiles observed from drug delivery devices. Line ----- denotes the therapeutic dose for the drug.

4.3.3 Bacteria viability and morphology:

Propidium iodide staining of *S. aureus* attached to the surface of the hydrogels revealed that the bacteria were arranged as singular cocci where they were attached to Su PεK as opposed to the other hydrogel surfaces where their eponymous clustered growth conformation was observed. The expected electrostatic interaction between the negatively-charged *S. aureus* surface and the highly cationic Su PεK hydrogel may be strong enough with this species to disrupt growth compared with other microbes (Haaber *et al.*, 2012). This interaction disrupts aggregation, biofilm formation and disrupts the integrity of the cell wall leaving the microbes more susceptible to antimicrobial agents (Figure 4.4) (Hall-Stoodley, Costerton and Stoodley,

2004; Hyldgaard *et al.*, 2014). Further staining with LIVE/DEAD® BacLight™ of *S. aureus* retrieved from the hydrogel supports the conformational differences previously observed with the propidium iodide staining. There was also confirmation of significantly greater *S. aureus* death when in contact with both the Su PεK and Su Pen G hydrogels compared with the unmodified Su 60 14 hydrogel, underpinning an increased antimicrobial activity after biomolecule attachment.

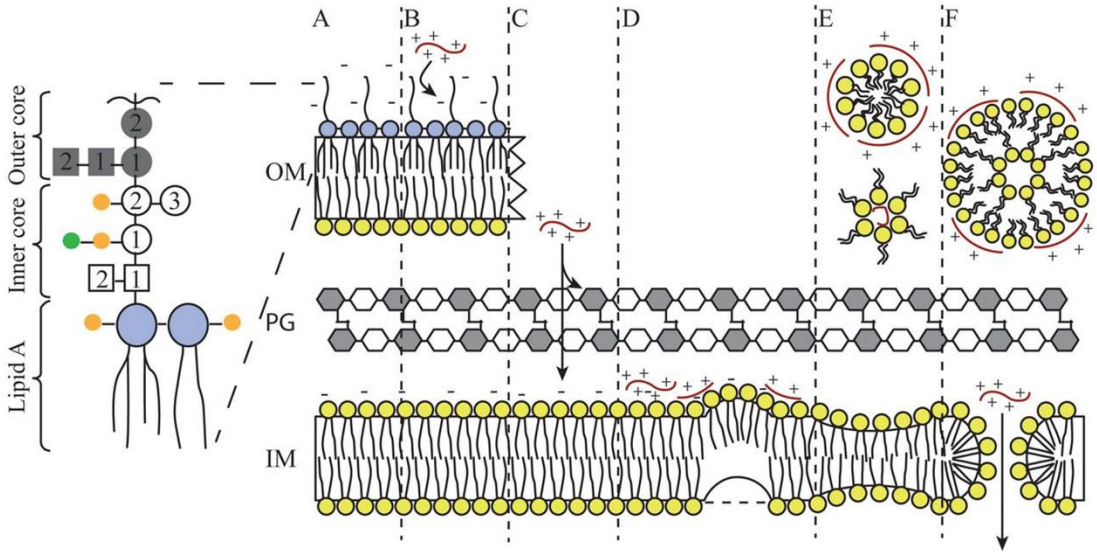

Figure 4.4: Schematic illustration of the proposed mechanism of action of pεK against bacteria. (A) Untreated cell wall with intact outer membrane (OM), peptidoglycan layer (PG), and inner membrane (IM), (B) electrostatic forces between pεK and LPS results in LPS layer removal, (C) pεK could interact with the peptidoglycan layer or move through the peptidoglycan layer and interact electrostatically with the inner membrane, thereby initiating the nonspecific carpet-like mechanism, (D) when pεK reaches a threshold concentration on the inner membrane, it enforces the negative curvature of one (dashed line at lower leaflet) or both (solid line at lower leaflet) leaflets of the membrane, (E) pεK thins the membrane, (F) a hole in the inner membrane allows pεK access to the cytoplasm where it can cause further damage. Figure adapted from Hyldgaard *et al.*, 2014 and reproduced with permission from the American Society of Microbiology.

This study demonstrates the effectiveness of antimicrobials that can either be attached via covalent bonding or electrostatic attachment to the amine groups and therefore should work for other more clinically relevant

antimicrobials with these properties. Other agents may possibly be incorporated and released via dissolution in the aqueous phase of the hydrogel.

4.4 Efficacy of AmpB Loaded Hydrogels against a Fungal Keratitis Model

Wild-type *C. albicans* strain SC5314 was used to model a fungal keratitis infection as it is the most prevalent fungus in temperate climates and the particular strain is the most well studied strain of *Candida* (Thomas and Kaliamurthy, 2013). A hydrogel lens material was produced with a 60% cross-link density and a polymer density of 0.07 g cm^{-3} (Su 60 15). Like hydrogel Su 60 14 it has a positive charge due to the remaining uncross-linked amine groups within the polymer matrix. After synthesis, the amine groups were associated with Cl^- ions that could hinder their interaction with potential drug molecules. It was demonstrated that a post-synthesis treatment with NMM removed the Cl^- ions via neutralisation. AmpB was used as the antifungal agent given that it is the first-line choice against *C. albicans* (Singh, 2015) and has a carboxyl group which can promote attachment of the drug molecule to the free amine groups on hydrogel Su 60 15 (Baginski and Czub, 2009).

4.4.1 Antifungal capacity of the AmpB loaded hydrogel:

An MIC was obtained for AmpB to determine its efficacy against *C. albicans* SC5314 in vitro. The MIC was found to be between 0.094 and 0.188 µg cm^{-3} against *C. albicans* cultured in both PD and PD with 10% horse serum and correlates with MIC data for ocular isolates from the literature of 0.06 - 1 µg cm^{-3} (Monte Mascaro *et al.*, 2003; Therese *et al.*, 2006). A concentration of AmpB well above the MIC is necessary to ensure adequate dosing to the cornea considering that ≤ 7% reaches the target tissues. Using serial dilutions of the stock AmpB solution we demonstrated that AmpB incorporated into the hydrogels significantly reduced the growth of *C. albicans* compared to no AmpB independent of the solution concentration

over 18 h. Generally, both -NH_3Cl and -NH_2 hydrogels pre-incubated in Amp B and cultured under both normal growth conditions and when the PD was supplemented with 10% horse serum had a similar efficacy to *C. albicans*. When the hydrogels themselves were evaluated it was clear that there were no viable fungi on the -NH_2 hydrogels or removed by the washing step whereas, viable fungi could be recovered from -NH_3Cl hydrogels. This suggests, as anticipated more AmpB attaches to -NH_2 hydrogels than the -NH_3Cl hydrogels confirming that the removal of hydrochloride via neutralisation allows more AmpB to interact electrostatically with the free amine groups of the hydrogel. Once the hydrogels had been removed from the wells it was important to evaluate if any fungi remaining could proliferate even if growth was low when the hydrogels were present. This could model the situation where the medicated lens was removed from the eye without knowing if all the infection had been removed. Over the subsequent 24 h very little fungal growth was observed in the well that had contained the -NH_2 hydrogels whereas the few fungi remaining after removal of the -NH_3Cl hydrogels could proliferate. These data show that the concentration of AmpB attached to, and released from, the -NH_2 hydrogels is fungicidal, whereas the amount of AmpB delivered from the -NH_3Cl hydrogels is fungistatic.

4.4.2 Elution and stability of AmpB:

It is important to evaluate how much AmpB diffuses out of the hydrogels over time to help optimize the drug loading regime. It was determined that after storage for all time-points the -NH_2 hydrogel released a clinically relevant dose of AmpB for 72 h, only falling below the MIC after 96 h. The -NH_3Cl hydrogel released a clinically relevant dose for the first 24 h but reduced to the MIC threshold after 48 h. The -NH_2 hydrogel released a significantly greater dose than the -NH_3Cl hydrogel at each time-point analysed. These data demonstrate that the -NH_2 hydrogels are more effective at delivering a clinically relevant dose of AmpB than the -NH_3Cl hydrogels. Furthermore, it was demonstrated that the dose of AmpB delivered by the -NH_2 hydrogel was stable enough after 48 h storage to kill *C. albicans* with a similar efficacy as a hydrogel used immediately after pre-incubation in AmpB. Effective treatment of fungal keratitis will require the bandage contact lens to maintain

the level of AmpB against the cornea at a therapeutic level to promote penetration of the drug into the corneal stroma. These data suggest that the -NH_2 hydrogel may be more effective at this than the -NH_3Cl hydrogel.

4.5 Early Detection of Pathogens Implicated in Microbial Keratitis

Development of a bandage contact lens that can distinguish between Gram-positive and Gram-negative bacteria by fluorescent labelling could provide a vital rapid detection tool for keratitis and improve early diagnosis. It would allow for a more accurate determination of which class of antibiotic may be required for treatment without having to wait several days for the culture analysis from corneal scrapes to become available. Hydrogel Su 60 14 was modified to change the amine functionality of the polymer backbone to a carboxyl moiety (Su 60 14 COOH) enabling attachment of amine functional AMPs. The AMPs (BAC ONE and BAC TWO) have an NBD fluorophore attached that is environmentally sensitive and fluoresces in hydrophobic environments such as cell membranes (Figure 4.5). The carboxyl modification of the hydrogel was confirmed both qualitatively by ninhydrin staining for primary amine groups followed by a quantitative analysis of amine functional groups via a methyl orange assay. It was determined that there were 60% more amine groups on the unmodified Su 60 14 hydrogel compared to the modified Su 60 14 COOH hydrogel. The reduction in amine groups is a direct consequence of the reaction of glutaric anhydride with the amine functional group in the polymer backbone resulting in a carboxyl moiety.

4.5.1 Hydrogel/BAC peptide evaluation:

The BAC ONE peptide is based on a fragment (residues 29 - 41) of the 59-residue cytoplasmic peptide ubiquicidin and has an affinity for both Gram-positive and Gram-negative organisms due to its cationic nature. Ubiquicidin binds non-specifically to both anionic lipids (Gram-negative) and teichoic acids (Gram-positive) allowing the NBD fluorophore to label both types of

bacteria (Akhtar *et al.*, 2005; Wiesner and Vilcinskas, 2010; Akram *et al.*, 2015).

The modified hydrogel was incubated with a range of concentrations (0 - 40 μM) of BAC ONE peptide to test its efficacy when associated with the hydrogel. The result of the fluorescence intensity assay suggests that at the greatest incubation concentration (40 μM) a statistically greater signal was obtained from the hydrogel and BAC ONE when cultured with either *E. coli* or *S. aureus* compared to the hydrogel and BAC ONE alone. A similar result was observed with the BAC ONE peptide alone present. These data suggest that the fluorescence obtained is directly related to the bacteria in the assay that have been labelled with BAC ONE. The fluorescent intensity obtained for *E. coli* was much greater than that obtained for *S. aureus* when incubated with the hydrogel and BAC ONE or BAC ONE alone. This is in direct contradiction to the FITC images where *E. coli* was much harder to detect than *S. aureus.* One possibility for this is in the difference in planktonic growth characteristics of both organisms. *S. aureus* are cocci and tend to form grape-like clusters of 5 - 20 cells whereas *E. coli* are generally non-cluster forming bacteria unless under conditions of stress (Koyama, Yamada and Matsuhashi, 1977; Novo *et al.*, 1995; Mittal *et al.*, 2003; Haaber *et al.*, 2012). The larger clusters of *S. aureus* may make fluorescence more obvious from micrographs and singular but more ubiquitous *E. coli* harder to distinguish from background fluorescence. The fluorescence intensity data confirmed that BAC ONE associated with the hydrogel labels both Gram-positive and Gram-negative organisms used in this study. However, this was not confirmed by the FITC fluorescent images. The use of a confocal microscope to observe fluorescence may help to minimise any background fluorescence and allow *E. coli* to be more easily observed.

The BAC TWO peptide used in this study is a derivative of polymyxin B. Polymyxin B is a pentacationic cyclic lipopeptide AMP that has been found to be nephrotoxic. Several derivatives of polymyxin B have been designed, such as BAC TWO, which replace some of the cationic groups on the linear part of the peptide with neutral compounds. These derivatives have been

found to be less nephrotoxic and more suitable candidates as antimicrobial agents (Mingeot-Leclercq *et al.*, 2012; Vaara, 2013). Polymyxin B binds specifically to lipid A of LPS found in the outer membrane of Gram-negative bacteria forming a stable complex that is stoichiometric with one molecule of polymyxin B binding to one molecule of lipid A (Morrison and Jacobs, 1976).

The modified hydrogel was incubated with a range of concentrations (0 - 40 μM) of BAC TWO peptide to test its efficacy when associated with the hydrogel. The fluorescence quantification results showed that at the greater incubation concentration (40 μM) a statistically greater fluorescent signal was obtained from labelled *E. coli* when compared to the *S. aureus* and no peptide controls. This was confirmed with the FITC fluorescent images as more labelled *E. coli* were observed at the greater incubation concentration (40 μM) as well as some labelling at 20 and 10 μM when incubated with the hydrogel and BAC TWO. No fluorescence was observed when the hydrogel and BAC TWO was incubated with *S. aureus* or with no organism present across all the incubation concentrations tested. This result highlights the specific affinity of BAC TWO for Gram-negative organisms with both the fluorescence intensity data and FITC images confirming it.

A direct comparison between the BAC peptides associated with the hydrogel and BAC peptides alone when incubated with bacteria is, however, not a like for like comparison. The BAC peptide concentration used in this study was the actual concentration of the peptide solution whereas the concentration of BAC peptide associated with the hydrogel was not determined and only the concentration of the incubation solution to which the hydrogel was immersed was used. The actual concentration of BAC peptides associated with the hydrogels may be lower and this appears to be reflected in the fluorescent intensity results. The BAC peptide alone gives a greater fluorescent result over any of the hydrogels with BAC peptide associated. However, other factors such as peptide hindrance within the hydrogel matrix may prevent optimal fluorescent signals being obtained.

The stability of the fluorescence from the NBD fluorophore was investigated as it may become a limiting factor in the length of time the hydrogel and BAC peptide system can be applied to the cornea for appropriate detection of microbial pathogens. The BAC ONE peptide associated with the hydrogel was stable for at least 21 h of incubation with *S. aureus* at 37 °C across all incubation concentrations investigated. Therefore, the stability of the BAC ONE peptide in situ for 21 h should be more than sufficient to allow for maximum labelling of bacterial pathogens in ocular disease. The BAC TWO peptide associated with the hydrogel was less stable than BAC ONE. It was stable for up to 4 h incubation with *E. coli* at 37 °C but at 21 h the fluorescence was significantly reduced at 20 and 40 μM incubation concentrations. The stability of the BAC TWO peptide in situ for 4 h and the fact a signal was observed < 30 min from incubation should still be sufficient to allow for maximum labelling of bacterial pathogens in ocular disease as part of a rapid detection system.

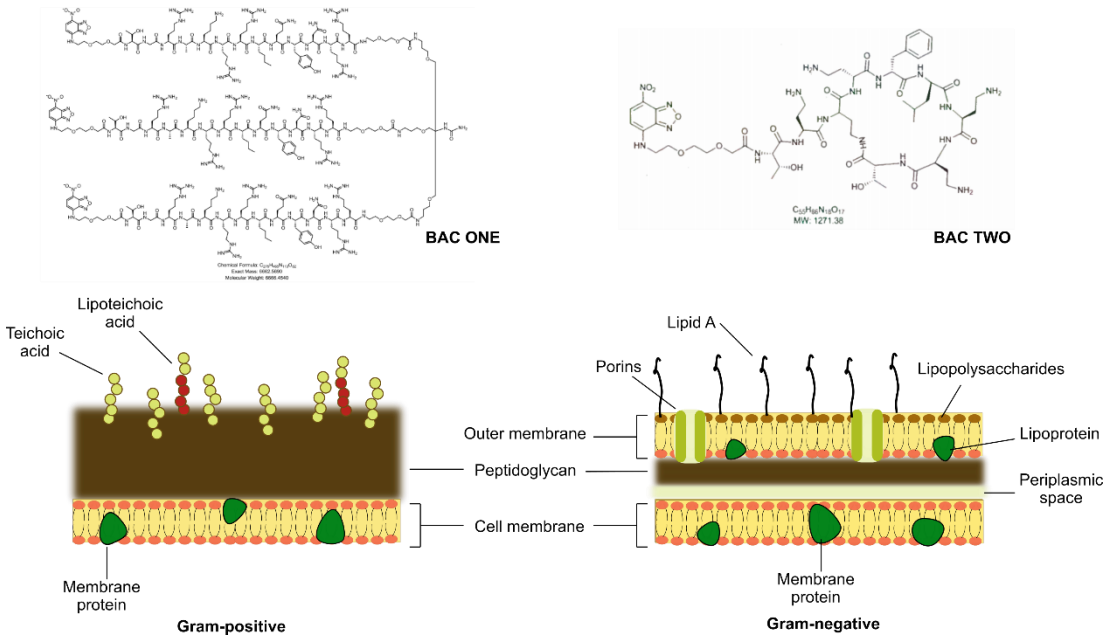

Figure 4.5: Bacteria outer membrane composition with targets for BAC peptides highlighted.

4.5.2 Investigation of mammalian cell staining from BAC peptides:

The labelling of non-specific cell types may not be optimal as a tool in the identification of specific pathogens involved in microbial keratitis. An emphasis was placed on the non-specific labelling of HCE-T cells in a co-culture with bacteria. There was evidence of some non-specific staining of HCE-T cells when the hydrogel and BAC ONE were incubated in the co-culture system. However, the fluorescence observed from *S. aureus* was prominent enough to be able to identify the pathogen in the co-culture. When the BAC TWO peptide modified hydrogels were incubated with a confluent culture of human corneal epithelial cells there was no evidence of fluorescent labelling of mammalian cells. A fluorescent signal was observed immediately upon addition of *E. coli* to the cell culture. The signal was directly associated with the microbes and gave confidence of the specificity of BAC TWO peptides towards *E. coli* when in contact corneal epithelial cells. Cationic AMPs such as BAC ONE and BAC TWO are initially attracted to the acidic phospholipids and teichoic acids on the bacterial cell wall. They then penetrate the wall with a hydrophobic tail resulting in the activation of the NBD fluorescence due to the hydrophobicity of the surrounding environment. The membrane surrounding mammalian cells have zwitterionic phospholipids present with no net negative charge that help to repel cationic molecules and as a result prevent toxicity (LaRock and Nizet, 2015). However, the presence of some anionic groups such as sialic acid, acidic amino acids and phosphate or sulphate groups present on the mammalian cell membrane may still promote non-specific binding as may have been the case for the less specific binding arrangement of BAC ONE against HCE-T cells (Crawford, 1987).

4.5.3 Efficacy of hydrogel/BAC peptide system against an ex vivo model of bacterial keratitis:

The ex vivo model was setup to try and replicate the in vitro results in a more appropriate model of bacterial keratitis. No unexpected results were observed from both BAC ONE and BAC TWO when associated with the hydrogel compared to the in vitro testing of the same materials. The hydrogel and BAC ONE and BAC ONE alone labelled *S. aureus* whilst the hydrogel

and BAC TWO and BAC TWO alone labelled *E. coli*. The only major difference observed from the in vitro testing was the conformation of bacteria on the hydrogel after removal from the ex vivo model. More clumped material was retrieved, possibly due to biofilm formation on the ex vivo model compared to the culture of planktonic bacteria in vitro. Staining was still evident but less was observed from clumps of bacteria in the ex vivo model compared to the more unicellular and ubiquitous bacteria in vitro. This provides further evidence of the efficacy of the peptides in identifying Gram-positive and Gram-negative bacteria when associated with Su 60 14 COOH and may lead to testing the BAC peptide/hydrogel systems in an in vivo animal model.

The BAC peptide/hydrogel system described here can be used to identify Gram-positive and Gram-negative organisms both microscopically and spectrophotometrically almost immediately after incubation with minimal toxicity observed in in vitro studies. This could provide a rapid, cost effective and less invasive technique to current methods that require corneal scrapes to retrieve culture specimens and long culture times to confirm pathogen identity. This technology may be of most use in developing countries where proximity to treatment centres and patient compliance are barriers to delivering the correct treatment regimen (Yoltan, 2001).

A possible application of this system could involve a combination of both peptides associated with the hydrogel with different fluorophores and placed on an infected cornea. If isolates only stain for BAC TWO it would indicate only Gram-negative organisms are present. If both BAC ONE and BAC TWO fluorophores are excited, it would suggest a mixed colony of Gram-negative and Gram-positive organisms or only Gram-positive organisms are present. If no fluorescence is detected from either BAC peptide, then the indications could suggest that the keratitis is not of bacterial origin. This may be followed by a quick microscopic evaluation of the optically transparent hydrogel or periodic acid Schiff or Gomori methenamine silver staining techniques to identify evidence of fungal keratitis (Thomas, 2003). As is the case with most infections a mix of isolates are often present and can account for up to a third

of total cases of keratitis, in which case a measure of the fluorescence may determine the most prominent organism and treatment could be directed per the results (Tuft, 2006; Al-Mujaini *et al.*, 2009). This may be followed with soaking the hydrogel in the most appropriate or in some cases of misdiagnosis, the correct antibiotic and applying it to the cornea thereby allowing patients to return to their communities and continue treatment at home with good compliance. All of this may be possible in the field, with specific reference to primary eye care centres in India, as only minimal equipment such as a microscope with fluorescent filters for direct observation of BAC peptides or a spectrophotometer for fluorescence quantification would be required.

4.6 Adherence to the Principles of Green Chemistry:

Some of the fundamental principles that underlie research and development of the hydrogel include the need for the process to be economical, the materials are non-animal derived and the principles of green chemistry are adhered to as much as possible. These principles are to ensure any product is commercially viable for SpheriTech Ltd.

The relatively new field of green chemistry was developed in the 1990s with focus on designing chemical processes that minimise the production of harmful by-products and reduce the carbon footprint whilst maintaining an economical process. The primary motivation for the development of green chemistry was the increasing inefficiency of large scale industrial processes. The amount of chemical waste from these processes can be 5 - 100 times greater than the chemical or pharmaceutical end-products (Li and Trost, 2008). Green chemistry is based on 12 principles and 11 of which have been addressed by the hydrogel polymerisation process in this report with number 11 deemed unnecessary due to the lack of hazardous substance formation (Table 4.1). The design of the polymer reaction ensures all reactants are completely used and minimal waste is generated apart from non-toxic by-products such as urea which is regarded as GRAS by the FDA and

reconstituted NHS (Anastas and Kirchhoff, 2002; Andersen, 2005; Hermanson, 2013b; Klykov and Weller, 2015).

1.	**Prevention:** It is better to prevent waste than to treat or clean up waste after it is formed
2.	**Atom economy:** Synthetic methods should be designed to maximize the incorporation of all materials used in the process into the final product
3.	**Less hazardous chemical synthesis:** Wherever practicable, synthetic methods should be designed to use and generate substances that possess little or no toxicity to human health and the environment
4.	**Designing safer chemicals:** Chemical products should be designed to affect their desired function while minimising their toxicity
5.	**Safer solvents and auxiliaries:** The use of auxiliary substances (e.g., solvents, separation agents, etc.) should be made unnecessary wherever possible and innocuous when used
6.	**Design for energy efficiency:** Energy requirements of chemical processes should be recognised for their environmental and economic impacts and should be minimised. If possible, synthetic methods should be conducted at ambient temperature and pressure
7.	**Use of renewable feedstocks:** A raw material or feedstock should be renewable rather than depleting whenever technically and economically practicable
8.	**Reduce derivatives:** Unnecessary derivatization (use of blocking groups, protection/deprotection, temporary modification of physical/chemical processes) should be minimised or avoided if possible, because such steps require additional reagents and can generate waste
9.	**Catalysis:** Catalytic reagents (as selective as possible) are superior to stoichiometric reagents
10.	**Design for degradation:** Chemical products should be designed so that at the end of their function they break down into innocuous degradation products and do not persist in the environment
11.	**Real-time analysis for pollution prevention:** Analytical methodologies need to be further developed to allow for real-time, in-process monitoring and control prior to the formation of hazardous substances
12.	**Inherently safer chemistry for accident prevention:** Substances and the form of a substance used in a chemical process should be chosen to minimise the potential for chemical accidents, including releases, explosions, and fires

Table 4.1: The 12 principles of green chemistry. Adapted from Anastas and Eghbali, 2010.

Short reaction times at room temperature combined with the use of a renewable feedstock such as pεK from microbial fermentation and bis-carboxylic acids from plants help to reduce the energy impacts of the process. Currently, heat or UV sources are required to create free radicals for

addition polymerisation used in the contact lens industry which have an environmental and economic impact (Maldonado-Codina, 2018). The polymerisation of pεK is carried out in water at room temperature. Water is the solvent used in the subsequent washing process for the hydrogels investigated in this study and is optimal due to the reduced environmental impact. Currently, hydrogel lens manufacture requires an extraction step with organic solvents to remove unreacted monomers which increases production costs and decreases efficiency (Ashton Acton, 2013). The use of NHS as the activation agent instead of explosive reagents such as HOBt also help to reduce risk (Anastas and Kirchhoff, 2002; Anastas and Eghbali, 2010). These hydrogels can be manufactured reproducibly and in an environmentally friendly way since they gel from aqueous solutions at room temperature requiring no harsh solvents such as those used in the production of silicone hydrogel contact lenses.

Another aspect of green chemistry focusses on the degradation products and their potential environmental impact. Degradation has already been described as an important aspect of contact lens wear as long term degradation can lead to discomfort, reduced vision and signs of adverse ocular reactions (Tanner and Efron, 2018). The results of the degradation study in this report suggest that the hydrogel when stored under optimal conditions in storage media remains stable for at least 12 months with minimal physical signs of degradation. However, once degradation occurs it would result in the breakup of the polymer into lysine, pεK, bis-carboxylic acids or a mixture of both depending upon the affinity of proteolytic enzymes to cleaving the amide within pεK itself or the amide between pεK and bis-carboxylic acids. Trypsin, secreted from the pancreas is one proteolytic enzyme known to have a specific affinity for cleaving the C-terminal of both lysine and arginine (Inagami and Mitsuda, 1964; Olsen, Ong and Mann, 2004). However, to date the only known protease to cleave pεK is found in microbes that produce pεK as a defence mechanism with no studies on the degradation of pεK in vivo recorded. Hypothetically and based upon the mechanism of the pεK degrading enzyme, further proteolytic degradation of pεK would result in cleavage of individual molecules of the essential amino

acid L-lysine resulting in its absorption or excretion from the body (Yoshida and Nagasawa, 2003; Yamanaka *et al.*, 2010; Yoshida, 2010). Bis-carboxylic acids are β-oxidised by the mitochondria and peroxisomes or pass through the body and are excreted in urine (Kølvraa and Gregersen, 1986; Jin and Tserng, 1990; Grego and Mingrone, 1995; Houten *et al.*, 2012). The final degradation products (pεK/L-lysine and bis-carboxylic acids) are non-toxic, however, whether the process of degradation of the hydrogel in this study invokes an inflammatory response, foreign body reaction or injury as observed for other biomaterials is unknown (Anderson, 2001).

Control of the rate of degradation could occur by the addition of other molecules that change the nature of the hydrogel cross-linking. This may be used to increase or decrease the rate of degradation. An example of this may be the addition of L-cysteine to the polymerisation which may result in the formation of the dimer molecule cystine and the introduction of weak disulphide bridges within the polymer backbone. These disulphide bridges readily reduce to cysteine and may result in an increase in the rate of degradation that's controllable via the ratio of disulphide bridges to covalent bonds. This mechanism has been described for albumin where disulphide bridges and ionic bonds make it a readily degradable biopolymer for medical applications (Nair and Laurencin, 2007). The solubility of keratins is also facilitated by the oxidation and reduction of the main stabilising bonds, disulphide bridges. The cystine content can be as high as 18% in keratins (Kasperova, Kunert and Raska, 2013).

All the aspects identified above ensure the polymerisation process for the hydrogel described in this study adheres to all the principles required for a green chemistry process and should allow for an industrially viable process.

4.7 Further Hydrogel Optimisation

Further optimisation of the hydrogel was undertaken to optimise the polymerisation process with particular reference to creating a reproducible

lens material. Previously, a reproducible hydrogel was polymerised as 1 mm thick sheets in trays, however, when the same polymer was cast in male/female contact lens moulds a build-up of CO_2 gas from the reaction resulted in the break-up of the polymer. An investigation of methods to overcome this problem was undertaken and focussed on the polymerisation method and composition of the polymer.

An initial emphasis focussed on using other polymerisation methods or vessels. Numerous attempts were made at creating a viable lens from the traditional mould methods with NHS as the activation agent but the formation of CO_2 led to bubbles getting trapped within the polymer resulting in the deterioration of the hydrogel. The immiscible solvent technique was also tried and resulted in an uneven and non-reproducible polymer. A spin cast technique resulted in small hydrogel blobs that did not resemble contact lens materials. Spin casting may still provide a potential route with further development of the reaction parameters as an open vessel polymerisation would allow for the escape of any CO_2 produced negating the need to replace NHS as the activation agent.

NHS upon reaction with EDCI to form an activated ester intermediate and the subsequent stable bis-carboxylic acid ester can also result in the formation of β-alanine (Wilchek and Miron, 1987; Hermanson, 2013a). The β-alanine side product can be incorporated into the polymer backbone and influence the polymer mechanical properties. To overcome this and create a lens via this method NHS was replaced with other activating agents and the reactions monitored to identify suitable alternatives (Appendix 8.2, 8.3.2 and 8.4.2). HOBt was identified as the most suitable alternative to NHS as no gas was formed during the polymerisation and a viable lens was retrieved, however, the mechanical properties were negatively affected.

A recent amino acid analysis (Alta Bioscience Ltd., Birmingham, England) of a polymer with 0.1, 0.25, 0.5, 0.75 and 1 equivalents of NHS to the total amino groups of pεK found an incremental increase in the incorporation of the β-alanine side-product as the level of NHS increased (4.2, 9.8, 21.9, 34.7

and 58.9% of the total amino acid content of the hydrogel). It is unknown at this point how much the mechanical properties are reliant on β-alanine incorporation or the efficiency of NHS as the optimal activation reagent or a mixture of both. These data follow the literature where it is stated that three molecules of NHS are required to create and incorporate one β-alanine residue into the polymer, so when increasing amounts of NHS are available in the reaction it results in an increase in β-alanine incorporation into the polymer.

The addition of different levels of decanedioic and tridecanedioic acid with octanedioic acid was investigated to improve mechanical properties with a reduction in the amount of NHS used in the polymerisation. This was to try and get similar mechanical properties to Su 60 14 but with 0.2 equivalents of NHS as opposed to 0.5 equivalents and thereby reduce β-alanine and CO_2 production. A subsequent investigation of the mechanical properties, water content, contact angle and light transmittance was undertaken (Appendix 8.3.3 and 8.4.3). An array of hydrogels with differing mechanical and physical properties were obtained but none were comparable to Su 60 14 with 0.5 equivalents of NHS used in the polymerisation.

The protein sorption capacity of the hydrogel variants was also investigated to determine the potential for biofouling. The depletion of IgG, BSA and trypsin in the supernatant was used to determine the amount of protein absorbed onto the hydrogel variants (Appendix 8.3.4 and 8.4.4). Almost all the BSA had adsorbed onto all the hydrogel variants after 18 h with no significance between them. Interestingly minimal BSA had adsorbed on any of the control materials. This may be explained by BSA's greater affinity for hydrophilic surfaces compared to hydrophobic surfaces, although some adsorption onto hydrophobic surfaces would still be expected (Jeyachandran *et al.*, 2009). Less than 10% of the total IgG had adsorbed onto any of the materials tested after 120 h possibly due to the denaturation and aggregation of the antibody molecule observed when it is incubated at elevated temperatures (Vermeer and Norde, 2000). Significantly more trypsin had adsorbed onto all the polymer variants after 120 h than the hydrophobic

material controls which is an unexpected result. However, this may be due again to the nature of the polymer backbone and as already suggested (section 4.1.2) the affinity of trypsin to cleave at the carboxyl end of lysine which is the major constituent of the hydrogel variants (Koutsopoulos *et al.*, 2007).

4.8 Other Applications

The polymer investigated in this report has already shown a diverse range of mechanical and physical properties which have been optimised for the development of a bandage contact lens. These modifiable properties could allow the hydrogel to be tailored for a range of other applications. So far, we have investigated Su 60 14 for its antibacterial, antifungal and ability to carry biomolecules for bacterial cell labelling. Additional procedures to complement the work already undertaken as well as some other possible applications are described below.

As a substrate for tissue engineering in the cornea, current researchers within our group are seeking to use a thin layer of the gel to support corneal endothelial cell growth and proliferation. It is envisaged that a monolayer of corneal endothelial cells attached to the hydrogel could be placed on a damaged endothelium and left in situ to allow regeneration of the endothelium and a return of the pumping mechanism required to maintain a healthy functioning cornea. Part of this work will look to alter the hydrophilicity of the hydrogel to allow cell adherence. This may be achieved with the addition of long chain fatty acids such as hexanoic acid, octanoic acid or decanoic acid to increase hydrophobicity that may promote cell adherence. The covalent attachment of cell adhesion peptides such as RGD may also be an option to aid cell adhesion.

As a side note, the above monoacids are also antimicrobial and may be incorporated into the hydrogel in the same way as extra pεK was added to Su PεK. Many other antimicrobial compounds could be incorporated in the same

way such as the vast array of AMPs. The functionality of the polymer could be changed to introduce new functional groups similar to the conversion of amine to a carboxyl functionality with the addition of glutaric anhydride. One possibility could be to incorporate molecules via ester linkages or the formation of disulphide bridges between a cysteine in the hydrogel network and a cysteine within an AMP as a means of controlling drug elution. As well as being able to change the release profile of attached drugs ester linkages and disulphide bridges within the hydrogel network could also provide a means of changing the degradation rate where necessary.

Microparticles are another promising tool in the area of drug release and the incorporation of drug loaded microparticles into the hydrogel network during polymerisation may provide a dual release mechanism. First, the drug within the hydrogel network would have a burst release profile followed by slower elution of the drug within the microparticles into the hydrogel network and subsequent elution from the polymer. This may provide a method to change a drug release profile from the undesirable burst release profile. SpheriTech have developed microparticles (SpheriSomes®) that have shown promise in the incorporation and release of an array of compounds and may be a possible candidate for this mechanism.

A suggestion for increasing the oxygen permeability of the hydrogel without introducing silicone was to introduce other oxygen absorbing molecules during polymerisation. Haem and pyrogallol were two of the compounds mentioned, however, it is unclear whether these compounds would release any absorbed oxygen and allow it to pass through the lens or just capture it in situ. A more simplistic approach may be the formation of a microporous hydrogel via the incorporation of water extractable porosigens that can be completely removed post polymerisation to leave voids that would allow oxygen to permeate through the hydrogel more freely (Tighe and Mann, 2016).

Other compounds such as smart probes could also be introduced, for example, to monitor the pH of wounds and relay information to monitor the wound for infection. This could allow for less disturbance to the wound bed

area when looking for visible signs of infection and allow for a quicker response if infection has been detected. Wound healing compounds such as perlecan and decorin could potentially be incorporated to increase the rate of wound healing for chronic wounds.

The range of different applications for this hydrogel are vast and leaves a lot of scope for study of this material within many different areas.

5. CONCLUSIONS

This study identified the potential of pεK/bis-caboxylic acid hydrogels as suitable materials for drug delivery bandage contact lenses with potential use in a range of ocular applications. This work clearly identified hydrogels with mechanical and physical properties comparable to commercial contact lens materials. Furthermore, the hydrogels could be loaded with clinically relevant doses of biomolecules and used to identify microbial pathogens and reduce the microbial burden of known ocular pathogens. These hydrogel bandage lenses may lead to successful identification and treatment of ocular infections with particular emphasis on microbial keratitis.

Mechanical and physical characterisation of the hydrogels:

- A range of hydrogels with tailorable mechanical properties can be polymerised with pεK and a range of saturated bis-carboxylic acids.
- A variety of pεK/octanedioic acid hydrogels were synthesised with a range of elastic moduli whilst maintaining a relatively high water content (70%).
- A hydrogel (Su 60 14) was synthesised that has comparable mechanical and physical properties to commercial contact lens materials.

Hydrogel cytotoxicity:

- The hydrogel (Su 60 14) was non-cytotoxic to the HCE-T cell line and did not impede re-epithelialisation from the subsequent scratch assay.
- The reformed monolayer had good tight junction formation identified via ZO-1 and occludin staining with expression of epithelial cell specific keratins also evident.
- The addition of biomolecules did not substantially increase cytotoxicity although some was observed after 24 h for hydrogels Su PεK and Su Pen G.

Antibacterial activity:

- The unmodified hydrogel (Su 60 14) had a minimal antibacterial activity and this did not change with differences in the cross-link percentage of the hydrogels tested.
- The surface attachment of pεK to the hydrogel post-polymerisation (Su PεK) resulted in a 12-fold increase in amine functional groups and was most effective against *S. aureus* attached to the hydrogel.
- The penicillin G loaded hydrogel (Su Pen G) was most effective against planktonic *S. aureus*. Penicillin G elution was detected for 5 h after initial incubation of the hydrogel.

Antifungal activity:

- The hydrogel (Su 60 15) was successfully modified to increase AmpB loading as determined via RP-HPLC.
- Both AmpB loaded hydrogels can kill *C. albicans*, however, the -NH_2 hydrogel had the greatest killing affect.
- A therapeutic dose of AmpB eluted from both hydrogels for at least 48 h and up to 72 h for the -NH_2 hydrogel. The AmpB eluted from the hydrogels remained stable for at least 48 h.

Microbe detection peptide:

- Both BAC peptides were successfully associated with a modified Su 60 14 hydrogel (Su 60 14 COOH).
- Gram-positive and Gram-negative bacteria were identified by a BAC ONE loaded hydrogel (40 μM optimal incubation concentration).
- A Gram-negative organism was identified by a BAC TWO loaded hydrogel (40 μM optimal incubation concentration). The peptide had no affinity for Gram-positive organisms.
- Some non-specific staining of HCE-T cells was evident from the hydrogel with BAC ONE associated whilst only microbial cells were labelled from the hydrogels with BAC TWO associated in a co-culture of *S. aureus* or *E. coli* and HCE-T cells.
- In vitro results were replicated in an ex vivo bacterial keratitis model.

6. FUTURE DIRECTION

The work completed as part of this thesis has formed the basis of a successful MRC grant application (MR/R006334/1) to continue the work and bring a bandage contact lens to market. Some of the work necessary to bring a viable lens to market as well as additional complementary work is detailed below.

In this thesis, a reproducible hydrogel was described and well characterised physically and mechanically. However, it was later identified that the most appropriate casting method (male/female mould) was unsuitable due to the chemistry involved in polymerisation. During NHS/EDCI mediated cross-linking several side reactions occur with β-alanine and CO_2 produced. This has a detrimental effect on the polymer when it is cast in a closed vessel as CO_2 becomes trapped within the matrix. An initial fix was to replace NHS with HOBt which minimises β-alanine and CO_2 production. This allowed a lens material to be cast from the hydrogel; however, the mechanical properties were reduced. Several changes were made to get around the problem such as the addition of mono acids or a mix of bis-carboxylic acids, a change in the activating agent and alterations to the levels of NHS used with a mix of results. However, significantly more work must be done to overcome this issue with some notable hurdles such as a lack of water soluble alternatives to NHS as the activating agent. An alternative open vessel polymerisation method may negate the need to replace NHS completely; however, this may need to be designed specifically for this polymer. Also, it appears β-alanine incorporation may be necessary to obtain optimal mechanical properties so addition of β-alanine, or other amino acids combined with HOBt activation may provide a way forward.

The ex vivo cornea model described in this thesis could be adapted to investigate the antimicrobial activity of the hydrogels and complement the findings of the in vitro bacterial and fungal keratitis studies. Clinical isolates of *S. aureus* and *C. albicans* could be used with the more clinically relevant *P. aeruginosa* replacing *E. coli* as the model Gram-negative organism. More

clinically relevant antibiotics could also be used with meropenem replacing penicillin G as the model broad spectrum β-lactam antibiotic. Natamycin is the model antifungal drug for filamentous fungal infections so an investigation of *Fusarium* clinical isolates with natamycin associated with the hydrogel via its carboxyl moiety may also be of interest (Müller, Kara-José and De Castro, 2013).

7. REFERENCES

Acheson, J. F., Joseph, J. and Spalton, D. J. (1987) 'Use of soft contact lenses in an eye casualty department for the primary treatment of traumatic corneal abrasions.', *The British Journal of Ophthalmology*, 71(4), pp. 285–289.

Achiron, A. and Hamiel, U. (2014) 'Call for caution in the use of ocular steroidal medications - Risk for fungal keratitis', *European Geriatric Medicine*, 5(6), p. 426.

Acker, H. Van, Dijck, P. Van and Coenye, T. (2014) 'Molecular mechanisms of antimicrobial tolerance and resistance in bacterial and fungal biofilms', *Trends in Microbiology*, 22(6), pp. 326–333.

Akhtar, M. S., Qaisar, A., Irfanullah, J., Iqbal, J., Khan, B., Jehangir, M., Nadeem, M. A. and Imran, M. B. (2005) 'Antimicrobial peptide 99mTc-ubiquicidin 29–41 as human infection-imaging agent : Clinical trial', *Journal of Nuclear Medicine*, 46(4), pp. 567–573.

Akpek, E. K. and Gottsch, J. D. (2003) 'Immune defense at the ocular surface.', *Eye*, 17(8), pp. 949–956.

Akram, A. R., Avlonitis, N., Lilienkampf, A., Perez-Lopez, A. M., McDonald, N., Chankeshwara, S. V., Scholefield, E., Haslett, C., Bradley, M. and Dhaliwal, K. (2015) 'A labelled-ubiquicidin antimicrobial peptide for immediate in situ optical detection of live bacteria in human alveolar lung tissue', *Chemical Science*, 6(12), pp. 6971–6979.

Al-Mujaini, A., Al-Kharusi, N., Thakral, A. and Wali, U. K. (2009) 'Bacterial keratitis: Perspective on epidemiology, clinico-pathogenesis, diagnosis and treatment.', *Sultan Qaboos University Medical Journal*, 9(2), pp. 184–195.

Alfonso, E. C., Miller, D., Cantu-Dibildox, J., O'Brien, T. P. and Schein, O. D. (2006) 'Fungal keratitis associated with non-therapeutic soft contact lenses', *American Journal of Ophthalmology*, 142(1), pp. 154–155.

Ali, M. and Byrne, M. E. (2009) 'Controlled release of high molecular weight hyaluronic acid from molecularly imprinted hydrogel contact lenses', *Pharmaceutical Research*, 26(3), pp. 714–726.

Ali, M. and Murphy, C. J. (2016) 'Biomechanical relationships between the corneal endothelium and Descemet's membrane', *Experimental Eye Research*, 152(November), pp. 57–70.

Alvarez-Lorenzo, C., Yanez, F. and Concheiro, A. (2010) 'Ocular drug delivery from molecularly-imprinted contact lenses', *Journal of Drug Delivery Science and Technology*, 20(4), pp. 237–248.

Amescua, G., Miller, D. and Alfonso, E. C. (2012) 'What is causing the corneal ulcer? Management strategies for unresponsive corneal ulceration', *Eye*, 26(2), pp. 228–236.

Ameta, C., Ameta, K. L., Sharma, B. K. and Ameta, R. (2013) 'Microwave assisted organic synthesis: A need of the day', in Ameta, S. . and Ameta, R. (eds) *Green Chemistry: Fundamentals and Applications*. Ontario, Canada: Apple Academic Press Inc., pp. 284–309.

Ananthi, S., Chitra, T., Bini, R., Prajna, N. V, Lalitha, P. and Dharmalingam, K. (2008) 'Comparative analysis of the tear protein profile in mycotic keratitis patients', *Molecular Vision*, 14(July 2007), pp. 500–507.

Anastas, P. and Eghbali, N. (2010) 'Green chemistry: Principles and practice', *Chemical Society Reviews*, 39(1), pp. 301–312.

Anastas, P. T. and Kirchhoff, M. M. (2002) 'Origins, current status, and future challenges of green chemistry', *Accounts of Chemical Research*, 35(9), pp. 686–694.

Andersen, F. A. (2005) 'Final report of the safety assessment of urea', *International Journal of Toxicology*, 24(3), pp. 1–56.

Anderson, J. M. (2001) 'Biological responses to materials', *Annual Review of Materials Research*, 31(1), pp. 81–110.

Andrade-Vivero, P., Fernandez-Gabriel, E., Alvarez-Lorenzo, C. and Concheiro, A. (2007) 'Improving the Loading and Release of NSAIDs from pHEMA Hydrogels by Copolymerization with Functionalized Monomers', *Journal of Pharmaceutical Sciences*, 96(4), pp. 802–813.

Araki-sasaki, K., Ohashi, Y., Sasabe, T., Hayashi, K., Watanabe, H., Tano, Y. and Handa, H. (1995) 'An SV40-immortalized human corneal epithelial cell line and its characterization', *Investigative Ophthalmology & Visual Science*, 36(3), pp. 614–621.

Ashton Acton, Q. (2013) *Ethylene Glycols—Advances in Research and Application: 2013 Edition*. Edited by Q. Ashton Acton. Atlanta, GA: Scholarly Editions.

Azuara-Blanco, A., Pillai, C. T. and Dua, H. S. (1999) 'Amniotic membrane transplantation for ocular surface reconstruction', *British Journal of Ophthalmology*, 83(4), pp. 399–402.

Baba, T., Bae, T., Schneewind, O., Takeuchi, F. and Hiramatsu, K. (2008) 'Genome sequence of Staphylococcus aureus strain newman and comparative analysis of staphylococcal genomes: Polymorphism and evolution of two major pathogenicity islands', *Journal of Bacteriology*, 190(1), pp. 300–310.

Baenninger, P. B. (2014) 'Survey on bandage contact lens practice in the United Kingdom', *Journal of Clinical & Experimental Ophthalmology*, 5(1), pp. 1–4.

Baginski, M. and Czub, J. (2009) ‘Amphotericin B and its new derivatives - mode of action.’, *Current drug metabolism*, 10(5), pp. 459–469.

Bankar, S. B. and Singhal, R. S. (2013) ‘Panorama of poly-ε-lysine’, *RSC Advances*, 3(23), pp. 8586–8603.

Beems, E. . and Van Best, J. . (1990) ‘Light transmission of the cornea in whole human eyes’, *Experimental Eye Research*, 50(4), pp. 393–395.

Bhamra, T. S. and Tighe, B. J. (2017) ‘Mechanical properties of contact lenses: The contribution of measurement techniques and clinical feedback to 50 years of materials development.’, *Contact Lens and Anterior Eye*, 40(2), pp. 70–81.

Bispo, P. J. M., Haas, W. and Gilmore, M. S. (2015) ‘Biofilms in infections of the eye’, *Pathogens*, 4(1), pp. 111–136.

Blackmore, S. J. (2010) ‘The use of contact lenses in the treatment of persistent epithelial defects’, *Contact Lens and Anterior Eye*, 33(5), pp. 239–244.

Blankenship, J. R., Wormley, F. L., Boyce, M. K., Schell, W. A., Filler, S. G., Perfect, J. R. and Heitman, J. (2003) ‘Calcineurin Is Essential for *Candida albicans* Survival in Serum and Virulence’, *Eukatyotic Cell*, 2(3), pp. 422–430.

Bourcier, T., Thomas, F., Borderie, V., Chaumeil, C. and Laroche, L. (2003) ‘Bacterial keratitis: predisposing factors, clinical and microbiological review of 300 cases.’, *The British Journal of Ophthalmology*, 87(7), pp. 834–838.

Bourne, W. M. (2003) ‘Biology of the corneal endothelium in health and disease.’, *Eye*, 17(8), pp. 912–918.

Bourne, W. M. and McLaren, J. W. (2004) ‘Clinical responses of the corneal endothelium’, *Experimental Eye Research*, 78(3), pp. 561–572.

Brennan, N. and Morgan, P. B. (2009) ‘Clinical highs and lows of Dk/t’, *Optician*, (July), pp. 16–20.

Bron, a J. (2001) ‘The architecture of the corneal stroma’, *The British Journal of Ophthalmology*, 85(4), pp. 379–381.

Buglisi, J. a, Knoop, K. J., Levsky, M. E. and Euwema, M. (2007) ‘Experience with bandage contact lenses for the treatment of corneal abrasions in a combat environment.’, *Military Medicine*, 172(4), pp. 411–413.

Bunya, V. Y., Hammersmith, K. M., Rapuano, C. J., Ayres, B. D. and Cohen, E. J. (2007)

'Topical and oral voriconazole in the treatment of fungal keratitis', *American Journal of Ophthalmology*, 143(1), pp. 151–153.

Campbell, D., Carnell, S. M. and Eden, R. J. (2013) 'Applicability of contact angle techniques used in the analysis of contact lenses, part 1', *Eye & Contact Lens: Science & Clinical Practice*, 39(3), pp. 254–262.

Castellan, A., Bart, J. C. J. and Cavallaro, S. (1991) 'Industrial production and use of adipic acid', *Catalysis Today*, 9(3), pp. 237–254.

Chak, V., Kumar, D. and Visht, S. (2013) 'A review on collagen based drug delivery systems', *International Journal of Pharmacy Teaching & Practices*, 4(4), pp. 811–820.

Chang, H. and Wang, Y. (2011) 'Cell responses to surface and architecture of tissue engineering scaffolds', in Eberli, D. (ed.) *Regenerative Medicine and Tissue Engineering - Cells and Biomaterials*. Rijeka, Croatia: InTech, pp. 569–588.

Chauhan, A. (2015) 'Ocular drug delivery role of contact lenses', *Delhi Journal of Ophthalmology*, 26(2), pp. 131–135.

Chen, S., Mienaltowski, M. J. and Birk, D. E. (2015) 'Regulation of corneal stroma extracellular matrix assembly', *Experimental Eye Research*, 133(April), pp. 69–80.

Chen, W., Hu, J., Zhang, Z., Chen, L., Xie, H., Dong, N., Chen, Y. and Liu, Z. (2012) 'Localization and expression of zonula occludins-1 in the rabbit corneal epithelium following exposure to benzalkonium chloride', *PLoS ONE*, 7(7), pp. 1–9.

Ciolino, J. B. (2009) 'General considerations in designing a drug-eluting contact lens', *Behavioral Health Management*, 4(6), pp. 569–571.

Ciolino, J. B., Hoare, T. R., Iwata, N. G., Behlau, I., Dohlman, C. H., Langer, R. and Kohane, D. S. (2009) 'A drug-eluting contact lens', *Investigative Ophthalmology and Visual Science*, 50(7), pp. 3346–3352.

Ciolino, J. B., Hudson, S. P., Mobbs, A. N., Hoare, T. R., Iwata, N. G., Fink, G. R. and Kohane, D. S. (2011) 'A prototype antifungal contact lens', *Investigative Ophthalmology and Visual Science*, 52(9), pp. 6286–6291.

Ciolino, J. B., Stefanescu, C. F., Ross, A. E., Salvador-Culla, B., Cortez, P., Ford, E. M., Wymbs, K. A., Sprague, S. L., Mascoop, D. R., Rudina, S. S., Trauger, S. A., Cade, F. and Kohane, D. S. (2014) 'In vivo performance of a drug-eluting contact lens to treat glaucoma for a month', *Biomaterials*, 35(1), pp. 432–439.

Cornils, B., Lappe, P. and by Staff, U. (2014) 'Dicarboxylic acids, aliphatic', in Elvers, B. (ed.)

Ullmann's Encyclopedia of Industrial Chemistry. 7th edn. Weinheim, Germany, Germany: Wiley-VCH Verlag GmbH & Co. KGaA, pp. 1–18.

Costa, F., Carvalho, I. F., Montelaro, R. C., Gomes, P. and Martins, M. C. L. (2011) 'Covalent immobilization of antimicrobial peptides (AMPs) onto biomaterial surfaces', *Acta Biomaterialia*, 7(4), pp. 1431–1440.

Coutinho, A. B., De Freitas, D., Filho, J. P. D. S., Corrêa, Z. M. S., Odashiro, A. N. and Burnier, M. N. (2011) 'Cytokeratin expression in corneal dystrophies', *Arquivos Brasileiros de Oftalmologia*, 74(2), pp. 118–122.

Craig, J. P., Tomlinson, A. and McCann, L. (2010) 'Tear Film', in Dartt, D. A., Besharse, J. C., and Dana, R. (eds) *Encyclopedia of the Eye*. USA: Elsevier, pp. 254–262.

Crawford, N. (1987) 'Electrokinetic aspects of cell surfaces', in Crawford, N. and Taylor, D. (eds) *Interactions of Cells with Natural or Foreign Surfaces*. New York. Plenum Press, pp. 11–20.

Cummins, P. M. (2012) 'Occludin: One protein, many forms', *Molecular and Cellular Biology*, 32(2), pp. 242–250.

Cwiklik, L. (2016) 'Tear film lipid layer: A molecular level view', *Biochimica et Biophysica Acta - Biomembranes*, 1858(10), pp. 2421–2430.

Dartt, D. A. (2004) 'Control of mucin production by ocular surface epithelial cells', *Experimental Eye Research*, 78(2), pp. 173–185.

Dartt, D. A. and Willcox, M. D. P. (2013) 'Complexity of the tear film: Importance in homeostasis and dysfunction during disease', *Experimental Eye Research*, 117, pp. 1–3.

Davies, D. (2003) 'Understanding biofilm resistance to antibacterial agents', *Nature Reviews*, 2(2), pp. 114–122.

Dell, S. J., Hovanesian, J. A., Raizman, M. B., Crandall, A. S., Doane, J., Snyder, M., Masket, S., Lane, S. and Fram, N. (2011) 'Randomized comparison of postoperative use of hydrogel ocular bandage and collagen corneal shield for wound protection and patient tolerability after cataract surgery', *Journal of Cataract and Refractive Surgery*, 37(1), pp. 113–121.

Desai, J. V, Mitchell, A. P. and Andes, D. R. (2014) 'Fungal biofilms, drug resistance, and recurrent infection', *Cold Spring Harbor Perspectives in Medicine*, 4(10), pp. 1–18.

Dóczi, I., Gyetvai, T., Kredics, L. and Nagy, E. (2004) 'Involvement of *Fusarium* spp. in fungal keratitis', *Clinical Microbiology and Infection*, 10(9), pp. 773–776.

Dowling, D. P., Miller, I. S., Ardhaoui, M. and Gallagher, W. M. (2011) 'Effect of surface wettability and topography on the adhesion of osteosarcoma cells on plasma-modified polystyrene', *Journal of Biomaterials Applications*, 26(3), pp. 327–347.

Dua, H. S., Gomes, J. A. P., King, A. J. and Maharajan, V. S. (2004) 'The amniotic membrane in ophthalmology', *Survey of Ophthalmology*, 49(1), pp. 51–77.

Dutta, D., Cole, N., Kumar, N. and Willcox, M. D. P. (2013) 'Broad spectrum antimicrobial activity of melimine covalently bound to contact lenses', *Investigative Ophthalmology and Visual Science*, 54(1), pp. 175–182.

Edelstein, S. L., Akduman, L., Durham, B. H., Fothergill, A. W. and Hsu, H. Y. (2012) 'Resistant *Fusarium* keratitis progressing to endophthalmitis.', *Eye & Contact Lens*, 38(5), pp. 331–335.

Edwards, J. D., Bower, K. S., Sediq, D. A., Burka, J. M., Stutzman, R. D., VanRoekel, C. R., Kuzmowych, C. P. and Eaddy, J. B. (2008) 'Effects of lotrafilcon A and omafilcon A bandage contact lenses on visual outcomes after photorefractive keratectomy', *Journal of Cataract and Refractive Surgery*, 34(8), pp. 1288–1294.

Efron, N., Morgan, P. B., Cameron, L. D., Brennan, N. A. and Goodwin, M. (2007) 'Oxygen permeability and water content of silicone hydrogel contact lens materials', *Optometry and Vision Science*, 84(4), pp. 328–333.

Eghrari, A.O., Riazuddin, S.A. and Gottsch, J. D. (2015) 'Overview of the cornea: structure, function and development', in Hejtmancik, J. F. and Nickerson, J. M. (eds) *Progress in Molecular Biology and Translational Science: Molecular Biology of Eye Disease*. USA: Elsevier, pp. 7–23.

Fanning, A. S. and Anderson, J. M. (2013) 'Zonula occludens-1 and -2 are cytosolic scaffolds that regulate the assembly of cellular junctions', *Annals of the New York Academy of Sciences*, 5(1165), pp. 113–120.

Ferrari, T. M., Leozappa, M., Lorusso, M., Epifani, E. and Ferrari, L. M. (2009) 'Escherichia coli keratitis treated with ultraviolet A/riboflavin corneal cross-linking: A case report', *European Journal of Ophthalmology*, 19(2), pp. 295–297.

Filipe, H. P., Henriques, J., Reis, P., Silva, P. C., Quadrado, M. J. and Serro, A. P. (2016) 'Contact lenses as drug controlled release systems: A narrative review', *Revista Brasileira de Oftalmologia*, 75(3), pp. 241–247.

Fiordeliso, J., Bron, S. and Kohn, J. (1995) 'Design, synthesis and preliminary characterisation of tyrosine-containing polyarylates: New biomaterials for medical

applications', in Cooper, S. L., Bamford, C. H., and Tsuruta, T. (eds) *Polymer Biomaterials in Solution, as Interfaces and as Solids*. Utrecht, The Netherlands, The Netherlands: VSP, pp. 695–708.

Fish, R. and Davidson, R. S. (2010) 'Management of ocular thermal and chemical injuries, including amniotic membrane therapy.', *Current Opinion in Ophthalmology*, 21(4), pp. 317–321.

Fleiszig, S. M. (2006) 'The Glenn A. Fry award lecture 2005. The pathogenesis of contact lens-related keratitis', *Optometry and Vision Science*, 83(12), pp. 866–873.

Fleiszig, S. M. J. and Evans, D. J. (2002) 'The pathogenesis of bacterial keratitis: Studies with Pseudomonas aeruginosa', *Clinical and Experimental Optometry*, 85(5), pp. 271–278.

Fleiszig, S. M. J., Kwong, M. S. F. and Evans, D. J. (2003) 'Modification of *Pseudomonas aeruginosa* interactions with corneal epithelial cells by human tear fluid', *Infection and Immunity*, 71(7), pp. 3866–3874.

Forrester, J. V, Dick, A. D., McMenamin, P. . and Roberts, F. (2008) *The Eye: Basic Sciences in Practice*. 3rd edn. USA: Elsevier Saunders.

Fraunfelder, F. W. and Cabezas, M. (2011) 'Treatment of recurrent corneal erosion by extended-wear bandage contact lens.', *Cornea*, 30(2), pp. 164–166.

French, K. (2005) 'Contact lens material properties', *Optitican*, 230(6022), pp. 20–28.

Friedberg, M. L., Pleyer, U. and Mondino, B. J. (1991) 'Device drug delivery to the eye. Collagen shields, iontophoresis, and pumps.', *Ophthalmology*, 98(5), pp. 725–732.

Gandhi, S. and Jain, S. (2015) 'The anatomy and physiology of cornea', in Cortina, M. S. and de la Cruz, J. (eds) *Keratoprostheses and Artificial Corneas*. Berlin: Springer-Verlag, pp. 19–25.

Garhwal, R., Shady, S. F., Ellis, E. J., Ellis, J. Y., Leahy, C. D., Mccarthy, S. P., Crawford, K. S. and Gaines, P. (2012) 'Sustained ocular delivery of ciprofloxacin using nanospheres and conventional contact lens materials', *Investigative Ophthalmology and Visual Science*, 53(3), pp. 1341–1352.

Gaudana, R., Ananthula, H. K., Parenky, A. and Mitra, A. K. (2010) 'Ocular Drug Delivery', *The AAPS Jounal*, 12(3), pp. 348–360.

Ghate, D. and Edelhauser, H. F. (2008) 'Barriers to glaucoma drug delivery.', *Journal of Glaucoma*, 17(2), pp. 147–156.

Gheorghe, A., Pop, M., Burcea, M. and Serban, M. (2016) ‘New clinical application of amniotic membrane transplant for ocular surface disease’, *Journal of Medicine and Life*, 9(2), pp. 177–179.

Gipson, I. K. (2004) ‘Distribution of mucins at the ocular surface’, *Experimental Eye Research*, 78(3), pp. 379–388.

Gipson, I. K. and Argüeso, P. (2003) ‘Role of mucins in the function of the corneal and conjunctival epithelia’, *International Review of Cytology*, 231, pp. 1–49.

Govindarajan, B. and Gipson, I. K. (2010) ‘Membrane-tethered mucins have multiple functions on the ocular surface’, *Experimental Eye Research*, 90(6), pp. 655–663.

Gower, E. W., Keay, L. J., Oechsler, R. A., Iovieno, A., Alfonso, E. C., Jones, D. B., Colby, K., Tuli, S. S., Patel, S. R., Lee, S. M., Irvine, J., Stulting, R. D., Mauger, T. F. and Schein, O. D. (2010) ‘Trends in Fungal keratitis in the United States, 2001 to 2007’, *Ophthalmology*, 117(12), pp. 2263–2267.

Grabarek, Z. and Gergely, J. (1990) ‘Zero-lenght crosslinking procedure with the use of acetyl esters’, *Analytical Biochemistry*, 185, pp. 131–135.

Green, M., Apel, A. and Stapleton, F. (2008) ‘Risk factors and causative organisms in microbial keratitis.’, *Cornea*, 27(1), pp. 22–27.

Greenwald, Y. and Kleinmann, G. (2008) ‘Use of collagen shields for ocular-surface drug delivery’, *Expert Review of Ophthalmology*, 3(6), pp. 627–633.

Grego, A. V. and Mingrone, G. (1995) ‘Dicarboxylic acids, an alternate fuel substrate in parenteral nutrition: an update’, *Clinical Nutrition*, 14(3), pp. 143–148.

Grentzelos, M. A., Plainis, S., Astyrakakis, N. I., Diakonis, V. F., Kymionis, G. D., Kallinikos, P. and Pallikaris, I. G. (2009) ‘Efficacy of 2 types of silicone hydrogel bandage contact lenses after photorefractive keratectomy’, *Journal of Cataract and Refractive Surgery*, 35(12), pp. 2103–2108.

Gulsen, D. and Chauhan, A. (2004) ‘Ophthalmic drug delivery through contact lenses.’, *Investigative Ophthalmology & Visual Science*, 45(7), pp. 2342–2347.

Guney, A., Kara, F., Ozgen, O., Aksoy, E., Hasirci, V. and Hasirci, N. (2013) ‘Surface modification of polymeric biomaterials’, in Taubert, A., Mano, J. F., and Rodríguez-Cabello, J. C. (eds) *Biomaterials Surface Science*. Weinheim, Germany: Wiley-VCH Verlag GmbH & Co. KGaA, pp. 92–95.

Guzman-Aranguez, A. and Argüeso, P. (2010) ‘Structure and biological roles of mucin-type

O-glycans at the ocular surface.', *The Ocular Surface*, 8(1), pp. 8–17.

Guzman-Aranguez, A., Colligris, B. and Pintor, J. (2013) 'Contact lenses: promising devices for ocular drug delivery.', *Journal of Ocular Pharmacology and Therapeutics*, 29(2), pp. 189–199.

Haaber, J., Cohn, M. T., Frees, D., Andersen, T. J. and Ingmer, H. (2012) 'Planktonic aggregates of *Staphylococcus aureus* protect against common antibiotics', *PLoS ONE*, 7(7), pp. 1–12.

Hadassah, J., Prakash, D., Sehgal, P. K., Agarwal, A. and Bhuvaneshwari, N. (2008) 'Clinical evaluation of succinylated collagen bandage lenses for ophthalmic applications', *Ophthalmic Research*, 40(5), pp. 257–266.

Hall-Stoodley, L., Costerton, J. W. and Stoodley, P. (2004) 'Bacterial biofilms: from the natural environment to infectious diseases', *Nature Reviews*, 2(2), pp. 95–108.

Hamrah, P. and Sahin, A. (2013) 'Limbus and corneal epithelium', in Holland, E. J., Mannis, M. J., and Lee, W. B. (eds) *Ocular Surface Disease: Cornea, Conjunctiva and Tear Film*. USA: Elsevier Saunders, pp. 29–33.

Hanada, K., Shimazaki, J., Shimmura, S. and Tsubota, K. (2001) 'Multilayered amniotic membrane transplantation for severe ulceration of the cornea and sclera', *American Journal of Ophthalmology*, 131(3), pp. 324–331.

Hazlett, L. D. (2010) 'Immunopathogenesis of *Pseudomonas* keratitis', in Dartt, D. A., Besharse, J. C., and Dana, R. (eds) *Encyclopedia of the Eye*. USA: Elsevier, pp. 311–317.

Hermanson, G. T. (2013a) 'Chapter 15 – Immobilization of Ligands on Chromatography Supports', in *Bioconjugate Techniques*, pp. 589–740.

Hermanson, G. T. (2013b) 'Chapter 4 – Zero-Length Crosslinkers', in *Bioconjugate Techniques*, pp. 259–273.

Hiratani, H., Fujiwara, A., Tamiya, Y., Mizutani, Y. and Alvarez-Lorenzo, C. (2005) 'Ocular release of timolol from molecularly imprinted soft contact lenses', *Biomaterials*, 26(11), pp. 1293–1298.

Hirohara, H., Saimura, M., Takehara, M., Miyamoto, M. and Ikezaki, A. (2007) 'Substantially monodispersed poly(epsilon-l-lysine)s frequently occurred in newly isolated strains of Streptomyces sp.', *Applied Microbiology and Biotechnology*, 76(5), pp. 1009–1016.

Hoare, T. R. and Kohane, D. S. (2008) 'Hydrogels in drug delivery: Progress and challenges', *Polymer*, 49(8), pp. 1993–2007.

Hodges, R. R. and Dartt, D. A. (2013) ‘Tear film mucins: Front line defenders of the ocular surface; comparison with airway and gastrointestinal tract mucins’, *Experimental Eye Research*, 117, pp. 62–78.

Høiby, N., Bjarnsholt, T., Givskov, M., Molin, S. and Ciofu, O. (2010) ‘Antibiotic resistance of bacterial biofilms’, *International Journal of Antimicrobial Agents*, 35(4), pp. 322–332.

Holden, B. A. and Mertz, G. W. (1984) ‘Critical oxygen levels to avoid corneal edema for daily and extended wear contact lenses’, *Investigative Ophthalmology and Visual Science*, 25(10), pp. 1161–1167.

Hong, J., Xu, J., Hua, J. and Sun, X. (2013) ‘Bacterial keratitis in Shanghai’, *Ophthalmology*, 120(3), p. 647.

Hou, A., Toh, L. X., Gan, K. H., Lee, K. J. R., Manser, E. and Tong, L. (2013) ‘Rho GTPases and regulation of cell migration and polarization in human corneal epithelial cells’, *PLoS ONE*, 8(10), pp. 1–11.

Hou, Y., Fei, R., Burkes, J. C., Lee, S. D., Munoz-Pinto, D., Hahn, M. S. and Grunlan, M. A. (2011) ‘Thermoresponsive nanocomposite hydrogels: transparency, rapid deswelling and cell release’, *Journal of Biomaterials and Tissue Engineering*, 1(1), pp. 93–100.

Houten, S. M., Denis, S., Argmann, C. A., Jia, Y., Ferdinandusse, S., Reddy, J. K. and Wanders, R. J. A. (2012) ‘Peroxisomal L-bifunctional enzyme (Ehhadh) is essential for the production of medium-chain dicarboxylic acids.’, *Journal of Lipid Research*, 53(7), pp. 1296–1303.

Huang, X. and Brazel, C. S. (2001) ‘On the importance and mechanisms of burst release in matrix-controlled drug delivery systems’, *Journal of Controlled Release*, 73(2–3), pp. 121–136.

Huhtala, A., Nurmi, S. K., Tahti, H., Salminen, L., Alajuuma, P., Rantala, I., Helin, H. and Uusitalo, H. (2003) ‘The immunohistochemical characterisation of an SV40-immortalised human corneal epithelial cell line’, *ATLA Alternatives to Laboratory Animals*, 31(4), pp. 409–417.

Hyldgaard, M., Mygind, T., Vad, B. S., Stenvang, M., Otzen, D. E. and Meyer, R. L. (2014) ‘The antimicrobial mechanism of action of epsilon-poly-L-lysine’, *Applied and Environmental Microbiology*, 80(24), pp. 7758–7770.

Imamura, Y., Chandra, J., Mukherjee, P. K., Lattif, A. A., Szczotka-flynn, L. B., Pearlman, E., Lass, J. H., Donnell, K. O. and Ghannoum, M. A. (2008) ‘*Fusarium* and *Candida albicans* biofilms on soft contact lenses : Model development , influence of lens type , and

susceptibility to lens care solutions', *Antimicrobial Agents and Chemotherapy*, 52(1), pp. 171–182.

Inagami, T. and Mitsuda, H. (1964) 'The mechanism of the specificity of trypsin catalysis.', *The Journal of Biological Chemistry*, 239(5), pp. 1388–1394.

Itzhaki, R. F. (1972) 'Calorimetric method for estimating polylysine and polyarginine', *Analytical Biochemistry*, 50(2), pp. 569–74.

Jad, Y. E., Khattab, S. N., de la Torre, B. G., Govender, T., Kruger, H. G., El-Faham, A. and Albericio, F. (2014) 'Oxyma-B, an excellent racemization suppressor for peptide synthesis', *Organic & Biomolecular Chemistry*, 12(42), pp. 8379–8385.

Järvinen, K., Järvinen, T. and Urtti, A. (1995) 'Ocular absorption following topical delivery', *Advanced Drug Delivery Reviews*, 16(1), pp. 3–19.

Jeyachandran, Y. L., Mielczarski, E., Rai, B. and Mielczarski, J. A. (2009) 'Quantitative and qualitative evaluation of adsorption/desorption of bovine serum albumin on hydrophilic and hydrophobic surfaces', *Langmuir*, 25(19), pp. 11614–11620.

Jin, S. J. and Tserng, K. Y. (1990) 'Metabolic origins of urinary unsaturated dicarboxylic acids.', *Biochemistry*, 29(37), pp. 8540–8547.

Johns, K. J. and O'Day, D. M. (1988) 'Pharmacologic management of keratomycoses.', *Survey of Ophthalmology*, 33(3), pp. 178–188.

Johnson, M. E. and Murphy, P. J. (2004) 'Changes in the tear film and ocular surface from dry eye syndrome', *Progress in Retinal and Eye Research*, 23(4), pp. 449–474.

Joyce, N. C. (2012) 'Proliferative capacity of corneal endothelial cells', *Experimental Eye Research*, 95(1), pp. 16–23.

Kakisu, K., Matsunaga, T., Kobayakawa, S., Sato, T. and Tochikubo, T. (2013) 'Development and efficacy of a drug-releasing soft contact lens', *Investigative Ophthalmology and Visual Science*, 54(4), pp. 2551–2561.

Karantza, V. (2011) 'Keratins in health and cancer: more than mere epithelial cell markers', *Oncogene*, 30(2), pp. 127–138.

Karsten, E., Watson, S. L. and Foster, L. J. R. (2012) 'Diversity of microbial species implicated in keratitis: a review.', *The Open Ophthalmology Journal*, 6, pp. 110–124.

Kasperova, A., Kunert, J. and Raska, M. (2013) 'The possible role of dermatophyte cysteine dioxygenase in keratin degradation', *Medical Mycology*, 51(5), pp. 449–454.

Kaye, S. B., Rao, P. G., Smith, G., Scott, J. A., Hoyles, S., Morton, C. E., Willoughby, C., Batterbury, M. and Harvey, G. (2003) 'Simplifying collection of corneal specimens in cases of suspected bacterial keratitis', *Journal of Clinical Microbiology*, 41(7), pp. 3192–3197.

Kaye, S., Tuft, S., Neal, T., Tole, D., Leeming, J., Figueiredo, F., Armstrong, M., McDonnell, P., Tullo, A. and Parry, C. (2010) 'Bacterial susceptibility to topical antimicrobials and clinical outcome in bacterial keratitis', *Investigative Ophthalmology and Visual Science*, 51(1), pp. 362–368.

Kearns, V. R. and Williams, R. L. (2009) 'Drug delivery systems for the eye.', *Expert Review of Medical Devices*, 6(3), pp. 277–290.

Keay, L., Edwards, K., Naduvilath, T., Taylor, H. R., Snibson, G. R., Forde, K. and Stapleton, F. (2006) 'Microbial keratitis: Predisposing factors and morbidity', *Ophthalmology*, 113(1), pp. 109–116.

Keir, N. and Jones, L. (2013) 'Wettability and silicone hydrogel lenses', *Eye & Contact Lens: Science & Clinical Practice*, 39(1), pp. 99–107.

Ketelson, H. A., Meadows, D. L. and Stone, R. P. (2005) 'Dynamic wettability properties of a soft contact lens hydrogel', *Colloids and Surfaces B: Biointerfaces*, 40(1), pp. 1–9.

Kim, Y. L., Walsh, J. T., Goldstick, T. K. and Glucksberg, M. R. (2004) 'Variation of corneal refractive index with hydration.', *Physics in Medicine and bBology*, 49(5), pp. 859–868.

Kleinmann, G., Larson, S., Hunter, B., Stevens, S., Mamalis, N. and Olson, R. J. (2006) 'Collagen shields as a drug delivery system for the fourth-generation fluoroquinolones', *Ophthalmologica*, 221(1), pp. 51–56.

Klykov, O. and Weller, M. G. (2015) 'Quantification of N-hydroxysuccinimide and N-hydroxysulfosuccinimide by hydrophilic interaction chromatography (HILIC)', *Analytical Methods*, 7(15), pp. 6443–6448.

Ko, J.-A., Yanai, R. and Nishida, T. (2009) 'Up-regulation of ZO-1 expression and barrier function in cultured human corneal epithelial cells by substance P.', *FEBS letters*, 583(12), pp. 2148–2153.

Kølvraa, S. and Gregersen, N. (1986) 'In vitro studies on the oxidation of medium-chain dicarboxylic acids in rat liver.', *Biochimica et Biophysica Acta*, 876(3), pp. 515–525.

Korsak, D., Liebscher, S. and Vollmer, W. (2005) 'Susceptibility to antibiotics and B-lactamase induction in murein hydrolase mutants of Escherichia coli', *Antimicrobial Agents and Chemotherapy*, 49(4), pp. 1404–1409.

Koutsopoulos, S., Patzsch, K., Bosker, W. T. E. and Norde, W. (2007) 'Adsorption of trypsin on hydrophilic and hydrophobic surfaces', *Langmuir*, 23(4), pp. 2000–2006.

Koyama, T., Yamada, M. and Matsuhashi, M. (1977) 'Formation of regular packets of Staphylococcus aureus cells', *Journal of Bacteriology*, 129(3), pp. 1518–1523.

Kruse, F. E., Rohrschneider, K. and Völcker, H. E. (1999) 'Multilayer amniotic membrane transplantation for reconstruction of deep corneal ulcers', *Ophthalmology*, 106(8), pp. 1504–1511.

Kulagina, N. V., Lassman, M. E., Ligler, F. S. and Taitt, C. R. (2005) 'Antimicrobial peptides for detection of bacteria in biosensor assays', *Analytical Chemistry*, 77(19), pp. 6504–6508.

Lagali, N., Germundsson, J. and Fagerholm, P. (2009) 'The role of Bowman's layer in corneal regeneration after phototherapeutic keratectomy: A prospective study using in vivo confocal microscopy', *Investigative Ophthalmology & Visual Science*, 50(9), pp. 4192–4198.

Lalitha, P., Prajna, N. V., Kabra, A., Mahadevan, K. and Srinivasan, M. (2006) 'Risk factors for treatment outcome in Fungal keratitis', *Ophthalmology*, 113(4), pp. 526–530.

LaRock, C. N. and Nizet, V. (2015) 'Cationic antimicrobial peptide resistance mechanisms of streptococcal pathogens', *Biochimica et Biophysica Acta (BBA) - Biomembranes*, 1848(11), pp. 3047–3054.

Leal, S. M., Cowden, S., Hsia, Y. C., Ghannoum, M. A., Momany, M. and Pearlman, E. (2010) 'Distinct roles for Dectin-1 and TLR4 in the pathogenesis of Aspergillus fumigatus keratitis', *PLoS Pathogens*, 6(7), pp. 1–16.

Leck, A. (2015) 'Taking a corneal scrape and making a diagnosis', *Community Eye Health Journal*, 28(89), pp. 8–9.

Lee, R. and Manche, E. E. (2016) 'Trends and associations in hospitalizations due to corneal ulcers in the United States, 2002-2012', *Ophthalmic Epidemiology*, 23(4), pp. 257–263.

Leeder, J. D. and Watt, I. C. (1965) 'The role of amino groups in water absorption by keratin.', *The Journal of Physical chemistryhysical Chemistry*, 69(10), pp. 3280–3284.

Li, C.-J. and Trost, B. M. (2008) 'Green chemistry for chemical synthesis.', *Proceedings of the National Academy of Sciences of the United States of America*, 105(36), pp. 13197–13202.

Li, Y.-Q., Han, Q., Feng, J.-L., Tian, W.-L. and Mo, H.-Z. (2014) 'Antibacterial characteristics and mechanisms of ε-poly-lysine against Escherichia coli and Staphylococcus aureus', *Food Control*, 43, pp. 22–27.

Lichtinger, A., Yeung, S. N., Kim, P., Amiran, M. D., Iovieno, A., Elbaz, U., Ku, J. Y. F., Wolff, R., Rootman, D. S. and Slomovic, A. R. (2012) 'Shifting trends in bacterial keratitis in Toronto: An 11-year review', *Ophthalmology*, 119(9), pp. 1785–1790.

Lin, M. C. and Svitova, T. F. (2010) 'Contact lenses wettability in vitro: effect of surface-active ingredients', *Optometry and Vision Science*, 87(6), pp. 440–447.

Liu, J., Sheha, H. and Fu, Y. (2010) 'Update on amniotic membrane transplantation', *Expert Review of Ophthalmology*, 5(5), pp. 645–661.

Lu, L., Reinach, P. S. and Kao, W. W. (2001) 'Corneal epithelial wound healing.', *Experimental Biology and Medicine*, 226(7), pp. 653–664.

Maldonado-Codina, C. (2017) 'Soft Lens Materials', in Efron, N. (ed.) *Contact Lens Practice*. 3rd edn. Amsterdam: Elsevier Ltd, pp. 45–59.

Maldonado-Codina, C. and Efron, N. (2003) 'Hydrogel lenses – materials and manufacture: A review.', *Optometry in Practice*, 4(2), pp. 101–113.

Mannoor, M. S., Zhang, S., Link, A. J. and McAlpine, M. C. (2010) 'Electrical detection of pathogenic bacteria via immobilized antimicrobial peptides', *Proceedings of the National Academy of Sciences*, 107(45), pp. 19207–19212.

Manzouri, B., Vafidis, G. C. and Wyse, R. K. (2001) 'Pharmacotherapy of fungal eye infections.', *Expert Opinion on Pharmacotherapy*, 2(11), pp. 1849–1857.

Martin, M. V (1978) 'Germ-tube formation by oral strains of *Candida tropicalis'*, *Jounal of Medical Microbiology*, 12(7), pp. 187–193.

Mather, R., Karenchak, L. M., Romanowski, E. G. and Kowalski, R. P. (2002) 'Fourth generation fluoroquinolones: new weapons in the arsenal of ophthalmic antibiotics', *American Journal of Ophthalmology*, 133(4), pp. 463–466.

Maulvi, F. A., Soni, T. G. and Shah, D. O. (2015) 'Extended release of hyaluronic acid from hydrogel contact lenses for dry eye syndrome', *Journal of Biomaterials Science, Polymer Edition*, 26(15), pp. 1035–1050.

Maulvi, F. A., Soni, T. G. and Shah, D. O. (2016) 'A review on therapeutic contact lenses for ocular drug delivery', *Drug Delivery*, 7544(February), pp. 1–10.

McCulley, J. P. and Shine, W. E. (2001) 'The lipid layer: The outer surface of the ocular surface tear film', *Bioscience Reports*, 21(4), pp. 407–418.

McDermott, A. M. (2013) 'Antimicrobial compounds in tears', *Experimental Eye Research*,

117, pp. 53–61.

McLaughlin-Borlace, L., Stapleton, F., Matheson, M. and Dart, J. K. (1998) ‘Bacterial biofilm on contact lenses and lens storage cases in wearers with microbial keratitis.’, *Journal of Applied Microbiology*, 84(5), pp. 827–838.

McMahon, T. T. and Zadnik, K. (2000) ‘Twenty-five years of contact lenses: the impact on the cornea and ophthalmic practice’, *Cornea*, 19(5), pp. 730–740.

Meek, K. M. and Boote, C. (2004) ‘The organization of collagen in the corneal stroma’, *Experimental Eye Research*, 78(3), pp. 503–512.

Meek, K. M., Leonard, D. W., Connon, C. J., Dennis, S. and Khan, S. (2003) ‘Transparency, swelling and scarring in the corneal stroma’, *Eye*, 17(8), pp. 927–936.

Merjava, S., Neuwirth, A., Tanzerova, M. and Jirsova, K. (2011) ‘The spectrum of cytokeratins expressed in the adult human cornea, limbus and perilimbal conjunctiva’, *Histology and Histopathology*, 26(3), pp. 323–331.

Metters, A. T. and Lin, C.-C. (2007) ‘Biodegradable hydrogels: Tailoring properties and function through chemistry and structure’, in Wong, J. Y. and Bronzino, J. D. (eds) *Biomaterials*. Boca Raton: CRC Press, pp. 5–1.

Millar, T. J. and Schuett, B. S. (2015) ‘The real reason for having a meibomian lipid layer covering the outer surface of the tear film - A review’, *Experimental Eye Research*, 137, pp. 125–138.

Mingeot-Leclercq, M. P., Tulkens, P. M., Denamur, S., Vaara, T. and Vaara, M. (2012) ‘Novel polymyxin derivatives are less cytotoxic than polymyxin B to renal proximal tubular cells’, *Peptides*, 35(2), pp. 248–252.

Mitchell, B. M. and Wilhelmus, K. R. (2005) ‘Inflammatory response to fungal keratitis’, *Ocular Surface*, 3(4 Suppl), pp. S152-3.

Mittal, N., Budrene, E. O., Brenner, M. P. and van Oudenaarden, A. (2003) ‘Motility of *Escherichia coli* cells in clusters formed by chemotactic aggregation’, *Proceedings of the National Academy of Sciences*, 100(23), pp. 13259–13263.

Mohammadpour, M., Amouzegar, A., Hashemi, H., Jabbarvand, M., Kordbacheh, H., Rahimi, F. and Hashemian, M. N. (2015) ‘Comparison of Lotrafilcon B and Balafilcon A silicone hydrogel bandage contact lenses in reducing pain and discomfort after photorefractive keratectomy: A contralateral eye study’, *Contact Lens and Anterior Eye*. British Contact Lens Association, 38(3), pp. 211–214.

Monte Mascaro, V. L. D., Höfling-lima, A. L., Gompertz, O. F., Yu, M. C. Z., da Matta, D. A., Colombo, A. L., Mascaro, V. L. D. M., Höfling-lima, A. L., Gompertz, O. F., Yu, M. C. Z., Matta, D. A. da and Colombo, A. L. (2003) 'Antifungal susceptibility testing of yeast isolated from corneal infections', *Arquivos Brasileiros de Oftalmologia*, 66(5), pp. 647–652.

Morgan, C., Brennan, N. and Alvord, L. (2001) 'Comparison of the coulometric and polarographic measurement of a high-Dk hydrogel.', *Optometry and Vision Science*, 78(1), pp. 19–29.

Morgan, P. B. and Efron, N. (1998) 'The oxygen performance of contemporary hydrogel contact lenses.', *Contact lens & anterior eye*, 21(1), pp. 3–6.

Morrison, D. C. and Jacobs, D. M. (1976) 'Binding of polymyxin B to the lipid A portion of bacterial lipopolysaccharides', *Immunochemistry*, 13(10), pp. 813–818.

Morrison, P. W. and Khutoryanskiy, V. V (2014) 'Advances in ophthalmic drug delivery', *Therapeutic Delivery*, 5(12), pp. 1297–1315.

Movahedan, A., Majdi, M., Afsharkhamseh, N., Sagha, H. M., Saadat, N. S., Shalileh, K., Milani, B. Y., Ying, H. and Djalilian, A. R. (2012) 'Notch inhibition during corneal epithelial wound healing promotes migration', *Investigative Ophthalmology and Visual Science*, 53(12), pp. 7476–7483.

Mukherjee, P. K., Chandra, J., Yu, C., Sun, Y., Pearlman, E. and Ghannoum, M. A. (2012) 'Characterization of Fusarium Keratitis Outbreak Isolates: Contribution of Biofilms to Antimicrobial Resistance and Pathogenesis', *Investigative Ophthalmology and Visual Science*, 53(8), pp. 4450–4457.

Müller, G. G., Kara-José, N. and De Castro, R. S. (2013) 'Antifungals in eye infections: Drugs and routes of administration', *Revista Brasileira de Oftalmologia*, 72(2), pp. 132–141.

Musser, M. T. (2014) 'Adipic acid', in Elvers, B. (ed.) *Ullmann's Encyclopedia of Industrial Chemistry*. 7th edn. Weinheim, Germany, Germany: Wiley-VCH Verlag GmbH & Co. KGaA, pp. 1–11.

Naiker, S. and Odhav, B. (2004) 'Mycotic keratitis: profile of *Fusarium* species and their mycotoxins. Mykotische Keratitis: Profil von Fusarium-Arten und ihren Mykotoxinen', *Mycoses*, 47(1–2), pp. 50–56.

Nair, L. S. and Laurencin, C. T. (2007) 'Biodegradable polymers as biomaterials', *Progress in Polymer Science*, 32(8–9), pp. 762–798.

Najafi, F. and Sarbolouki, M. N. (2003) 'Biodegradable micelles/polymersomes from fumaric/sebacic acids and poly(ethylene glycol).', *Biomaterials*, 24(7), pp. 1175–1182.

Nakajima, N. and Ikada, Y. (1995) ‘Mechanism of amide formation by carbodiimide for bioconjugation in aqueous media.’, *Bioconjugate Chemistry*, 6(1), pp. 123–130.

Neoh, C. F., Daniell, M., Chen, S. C. A., Stewart, K. and Kong, D. C. M. (2014) ‘Clinical utility of caspofungin eye drops in fungal keratitis’, *International Journal of Antimicrobial Agents*, 44(2), pp. 96–104.

Nicolson, P. C. and Vogt, J. (2008) ‘Contact Lenses: Silicone Hydrogels’, in Wnek, G. E. and Bowlin, G. L. (eds) *Encyclopedia of Biomaterials and Biomedical Engineering*. 2nd edn. Boca Raton, FL: CRC Press, pp. 715–728.

Nishikawa, M. and Ogawa, K. (2006) ‘Inhibition of epsilon-poly-L-lysine biosynthesis in Streptomycetaceae bacteria by short-chain polyols’, *Applied and Environmental Microbiology*, 72(4), pp. 2306–2312.

Novo, N. F., Barbosa, H. R., Rodrigues, M. F. A., Campos, C. C., Chaves, M. E., Nunes, I. and Juliano, Y. (1995) ‘Counting of viable cluster-forning and non cluster-forning bacteria: a comparison between the drop and the spread methods.’, *Journal of Microbiological Methods*, 22, pp. 39–50.

O’Brien, T. P. (2003) ‘Management of bacterial keratitis: Beyond exorcism towards consideration of organism and host factors.’, *Eye*, 17(8), pp. 957–974.

O’Day, D. M., Ray, W. A., Head, W. S. and Robinson, R. D. (1984) ‘Influence of the corneal epithelium on the efficacy of topical antifungal agents.’, *Investigative Ophthalmology & Visual Science*, 25(7), pp. 855–859.

Olsen, J. V, Ong, S.-E. and Mann, M. (2004) ‘Trypsin cleaves exclusively C-terminal to arginine and lysine residues.’, *Molecular & Cellular Proteomics*, 3(6), pp. 608–614.

Omidian, H., Park, K., Siegel, R. A. and Rathbone, M. J. (2012) ‘Fundamentals and applications of controlled release drug delivery’, *Society*, pp. 75–105.

Orlans, H. O., Hornby, S. J. and Bowler, I. C. J. W. (2011) ‘In vitro antibiotic susceptibility patterns of bacterial keratitis isolates in Oxford, UK: a 10-year review.’, *Eye*, 25(4), pp. 489–493.

Ou, J. I. and Acharya, N. R. (2007) ‘Epidemiology and treatment of fungal corneal ulcers.’, *International Ophthalmology Clinics*, 47(3), pp. 7–16.

Panda, A. and Sudan, R. (2003) ‘Collagen corneal shields’, *Survey of Ophthalmology*, 48(2), p. 241.

Papp-Wallace, K. M., Endimiani, A., Taracila, M. A. and Bonomo, R. A. (2011)

‘Carbapenems: Past, present, and future’, *Antimicrobial Agents and Chemotherapy*, 55(11), pp. 4943–4960.

Parekh, M., Graceffa, V., Bertolin, M., Elbadawy, H., Salvalaio, G., Ruzza, A., Camposampiero, D., Gomez, D. A., Barbaro, V., Ferrari, B., Breda, C., Ponzin, D. and Ferrari, S. (2013) ‘Reconstruction and regeneration of corneal endothelium: a review on current methods and future aspects’, *Journal of Cell Science & Therapy*, 4(3), pp. 1–8.

Passi, S., Nazzaro-Porro, M., Picardo, M., Mingrone, G. and Fasella, P. (1983) ‘Metabolism of straight saturated medium chain length (C9 to C12) dicarboxylic acids.’, *Journal of Lipid Research*, 24(9), pp. 1140–1147.

Paulsen, F. P. and Berry, M. S. (2006) ‘Mucins and TFF peptides of the tear film and lacrimal apparatus’, *Progress in Histochemistry and Cytochemistry*, 41(1), pp. 1–53.

Pavelka, M. and Roth, J. (2010) *Functional Ultrastructure*. Vienna: Springer Vienna.

Pearlman, E., Leal, S., Tarabishy, A., Sun, Y., Szczotka-Flynn, L., Imamura, Y., Mukherjee, P., Chandra, J., Momany, M., Hastings-Cowden, S. and Ghannoum, M. (2010) ‘Pathogenesis of Fungal keratitis’, in Dartt, D. A., Besharse, J. C., and Dana, R. (eds) *Encyclopedia of the Eye*. USA: Elsevier, pp. 268–272.

Pettit, R. K., Weber, C. A. and Pettit, G. R. (2009) ‘Application of a high throughput Alamar blue biofilm susceptibility assay to *Staphylococcus aureus* biofilms’, *Annals of Clinical Microbiology and Antimicrobials*, 8(28), pp. 1–7.

Prajna, N. V., O’Brien, K. S., Acharya, N. R. and Lietman, T. M. (2013) ‘Voriconazole for fungal keratitis’, *Ophthalmology*, 120(9), pp. 62–63.

Pratoomsoot, C., Tanioka, H., Hori, K., Kawasaki, S., Kinoshita, S., Tighe, P. J., Dua, H., Shakesheff, K. M. and Rose, F. R. A. J. (2008) ‘A thermoreversible hydrogel as a biosynthetic bandage for corneal wound repair’, *Biomaterials*, 29(3), pp. 272–281.

Pratt, L. A. and Kolter, R. (1998) ‘Genetic analysis of Escherichia coli biofilm formation: Roles of flagella, motility, chemotaxis and type I pili’, *Molecular Microbiology*, 30(2), pp. 285–293.

Rasul, R., Cole, N., Balasubramanian, D., Chen, R., Kumar, N. and Willcox, M. D. P. (2010) ‘Interaction of the antimicrobial peptide melimine with bacterial membranes’, *International Journal of Antimicrobial Agents*, 35(6), pp. 566–572.

Refojo, M. F. and Yasuda, H. (1965) ‘Hydrogels from 2-hydroxyethyl methacrylate and propylene glycol monoacrylate’, *Journal of Applied Polymer Science*, 9(7), pp. 2425–2435.

Rhem, M. N., Lech, E. M., Patti, J. M., McDevitt, D., Höök, M., Jones, D. B. and Wilhelmus, K. R. (2000) 'The collagen-binding adhesin is a virulence factor in *Staphylococcus aureus* keratitis', *Infection and Immunity*, 68(6), pp. 3776–3779.

Rönkkö, S., Vellonen, K.-S., Järvinen, K., Toropainen, E. and Urtti, A. (2016) 'Human corneal cell culture models for drug toxicity studies', *Drug Delivery and Translational Research*, 6(6), pp. 660–675.

Ruben, M. and Watkins, R. (1975) 'Pilocarpine dispensation for the soft hydrophilic contact lens.', *British Journal of Ophthalmology*, 59(8), pp. 455–458.

Ryeom, S. W., Paul, D. and Goodenough, D. A. (2000) 'Truncation mutants of the tight junction protein ZO-1 disrupt corneal epithelial cell morphology.', *Molecular Biology of the Cell*, 11(5), pp. 1687–1696.

Saini, A., Rapuano, C. J., Laibson, P. R., Cohen, E. J. and Hammersmith, K. M. (2013) 'Episodes of microbial keratitis with therapeutic silicone hydrogel bandage soft contact lenses', *Eye & Contact Lens*, 39(5), pp. 324–328.

Saraswathi, P. and Beuerman, R. W. (2015) 'Corneal Biofilms: From Planktonic to Microcolony Formation in an Experimental Keratitis Infection with *Pseudomonas Aeruginosa'*, *Ocular Surface*, 13(4), pp. 331–345.

Sardi, J. C. O., Scorzoni, L., Bernardi, T., Fusco-Almeida, A. M. and Giannini, M. J. S. M. (2013) 'Candida species : current epidemiology , pathogenicity , biofilm formation , natural antifungal products and new therapeutic options', *Journal of Medical Microbiology*, 62, pp. 10–24.

Saw, V. P. J., Minassian, D., Dart, J. K. G., Ramsay, A., Henderson, H., Poniatowski, S., Warwick, R. M. and Cabral, S. (2007) 'Amniotic membrane transplantation for ocular disease: a review of the first 233 cases from the UK user group', *British Journal of Ophthalmology*, 91(8), pp. 1042–1047.

Schaefer, F., Bruttin, O., Zografos, L. and Guex-Crosier, Y. (2001) 'Bacterial keratitis: a prospective clinical and microbiological study', *British Journal of Ophthalmology*, 85(7), pp. 842–847.

Schermer, A. and Galvin, S. (1986) 'Differentiation-related expression of a major 64K corneal keratin in vivo and in culture suggests limbal location of corneal epithelial stem cells', *The Journal of Cell Biology*, 103(1), pp. 49–62.

Sengupta, J., Saha, S., Khetan, A., Sarkar, S. K. and Mandal, S. M. (2012) 'Effects of lactoferricin B against keratitis-associated fungal biofilms', *Journal of Infection and*

Chemotherapy, 18(5), pp. 698–703.

Shah, S., Chatterjee, A., Mathai, M., Kelly, S. P., Kwartz, J., Henson, D. and McLeod, D. (1999) 'Relationship between corneal thickness and measured intraocular pressure in a general ophthalmology clinic.', *Ophthalmology*, 106(11), pp. 2154–2160.

Shalchi, Z., Gurbaxani, A., Baker, M. and Nash, J. (2011) 'Antibiotic resistance in microbial keratitis: Ten-year experience of corneal scrapes in the United Kingdom', *Ophthalmology*, 118(11), pp. 2161–2165.

Sheha, H., Liang, L., Li, J. and Tseng, S. C. G. (2009) 'Sutureless amniotic membrane transplantation for severe bacterial keratitis', *Cornea*, 28(10), pp. 1118–1123.

Shell, J. W. (1982) 'Pharmacokinetics of topically applied ophthalmic drugs.', *Survey of Ophthalmology*, 26(4), pp. 207–218.

Shi, W., Wang, T., Xie, L., Li, S., Gao, H., Liu, J. and Li, H. (2010) 'Risk factors, clinical features, and outcomes of recurrent fungal keratitis after corneal transplantation', *Ophthalmology*, 117(5), pp. 890–896.

Shi, Y., Lv, H., Fu, Y., Lu, Q., Zhong, J., Ma, D., Huang, Y. and Xue, W. (2013) 'Preparation and characterization of a hydrogel carrier to deliver gatifloxacin and its application as a therapeutic contact lens for bacterial keratitis therapy.', *Biomedical Materials*, 8(5), p. 55007.

Shih, I. L., Shen, M. H. and Van, Y. T. (2006) 'Microbial synthesis of poly(epsilon-lysine) and its various applications', *Bioresource Technology*, 97(9), pp. 1148–1159.

Shima, S., Matsuoka, H., Iwamoto, T. and Sakai, H. (1984) 'Antimicrobial action of epsilon-poly-L-lysine.', *The Journal of Antibiotics*, 37(11), pp. 1449–1455.

Shima, S. and Sakai, H. (1977) 'Polylysine produced by *Streptomyces'*, *Agriculture and Biological Chemistry*, 41(9), pp. 1807–1809.

Shoham, S. (2015) 'Host/pathogen interactions in Fungal keratitis', *Current Fungal Infection Reports*, 9(1), pp. 52–56.

Singh, D. (2015) *Fungal keratitis treatment and management*, *Medscape*. Available at: http://emedicine.medscape.com/article/1194167-treatment (Accessed: 12 July 2015).

Stapleton, F. and Carnt, N. (2012) 'Contact lens-related microbial keratitis: how have epidemiology and genetics helped us with pathogenesis and prophylaxis.', *Eye*, 26(2), pp. 185–93.

Stein, H. A. (2008) 'The history of contact lenses: Part 2', *Eye Care Review*, 2(4), pp. 14–15.

Stepp, M. A. (2010) 'Corneal epithelium: cell biology and basic science', in Dartt, D. A., Besharse, J. C., and Dana, R. (eds) *Encyclopedia of the Eye*. USA: Elsevier, pp. 435–441.

Sueke, H., Kaye, S., Neal, T., Murphy, C., Hall, A., Whittaker, D., Tuft, S. and Parry, C. (2010) 'Minimum inhibitory concentrations of standard and novel antimicrobials for isolates from bacterial keratitis', *Investigative Ophthalmology & Visual Science*, 51(5), pp. 2519–2524.

Sueke, H., Kaye, S., Wilkinson, M. C., Kennedy, S., Kearns, V., Zheng, Y., Roberts, P., Tuft, S. and Neal, T. (2015) 'Pharmacokinetics of Meropenem for Use in Bacterial Keratitis.', *Investigative Ophthalmology & Visual Science*, 56(10), pp. 5731–5738.

Sun, R. L., Jones, D. B. and Wilhelmus, K. R. (2007) 'Clinical characteristics and outcome of *Candida* keratitis', *American Journal of Ophthalmology*, 143(6), pp. 1043–1045.

Suri, K., Kosker, M., Raber, I. M., Hammersmith, K. M., Nagra, P. K., Ayres, B. D., Halfpenny, C. P. and Rapuano, C. J. (2013) 'Sutureless amniotic membrane ProKera for ocular surface disorders: Short-term results.', *Eye & Contact Lens*, 39(5), pp. 341–347.

Szczotka-Flynn, L., Lass, J. H., Sethi, A., Debanne, S., Benetz, B. A., Albright, M., Gillespie, B., Kuo, J., Jacobs, M. R. and Rimm, A. (2010) 'Risk factors for corneal infiltrative events during continuous wear of silicone hydrogel contact lenses', *Investigative Ophthalmology and Visual Science*, 51(11), pp. 5421–5430.

Szliter-Berger, E. A. and Hazlett, L. D. (2010) 'Corneal epithelium: response to infection', in Dartt, D. A., Besharse, J. C., and Dana, R. (eds) *Encyclopedia of the Eye*. USA: Elsevier, pp. 442–448.

Tamada, Y. and Ikada, Y. (1993) 'Cell adhesion to plasma-treated polymer surfaces', *Polymer*, 34(10), pp. 2208–2212.

Tanner, J. and Efron, N. (2018) 'Reusable Soft Lenses', in Efron, N. (ed.) *Contact Lens Practice*. 3rd edn. Amsterdam: Elsevier Ltd, pp. 175–186.

Tashakori-Sabzevar, F. and Mohajeri, S. A. (2015) 'Development of ocular drug delivery systems using molecularly imprinted soft contact lenses', *Drug Development and Industrial Pharmacy*, 41(5), pp. 703–713.

Thatte, S. (2011) 'Amniotic membrane transplantation: An option for ocular surface disorders.', *Oman Journal of Ophthalmology*, 4(2), pp. 67–72.

Therese, K. L., Bagyalakshmi, R., Madhavan, H. N. and Deepa, P. (2006) 'In-vitro susceptibility testing by agar dilution method to determine the minimum inhibitory concentrations of amphotericin B, fluconazole and ketoconazole against ocular fungal

isolates', *Indian Journal of Medical Microbiology*, 24(4), pp. 273–279.

Thomas, P. A. (2003) 'Fungal infections of the cornea.', *Eye*, 17(8), pp. 852–862.

Thomas, P. A. and Kaliamurthy, J. (2013) 'Mycotic keratitis : epidemiology , diagnosis and management', *Clinical Microbiology and Infection*, 19(3), pp. 210–220.

Tieppo, A., White, C. J., Paine, A. C., Voyles, M. L., McBride, M. K. and Byrne, M. E. (2012) 'Sustained in vivo release from imprinted therapeutic contact lenses', *Journal of Controlled Release*, 157(3), pp. 391–397.

Tighe, B. J. (2013) 'A Decade of silicone hydrogel development: Surface properties, mechanical properties, and ocular compatibility', *Eye & Contact Lens*, 39(1), pp. 4–12.

Tighe, B. J. and Mann, A. (2016) 'Physicochemical properties of hydrogels for use in ophthalmology', in Chirila, T. V and Harkin, D. G. (eds) *Biomaterials and Regenerative Medicine in Ophthalmology*. 2nd edn. London: woodhead, pp. 75–100.

Togo, Y., Takahashi, K., Saito, K., Kiso, H., Huang, B., Tsukamoto, H., Hyon, S. H. and Bessho, K. (2013) 'Aldehyded dextran and ε -poly(L-lysine) hydrogel as nonviral gene carrier', *Stem Cells International*, 2013(634379), pp. 3–7.

Tranoudis, I. and Efron, N. (2004) 'Tensile properties of soft contact lens materials', *Contact Lens and Anterior Eye*, 27(4), pp. 177–191.

Trattler, B. W. B. (2012) 'Promoting corneal wound healing', *Cataract & Refractive Surgery Today*, (July), pp. 1–4.

Tuft, S. (2006) 'Polymicrobial infection and the eye', *British Journal of Ophthalmology*, 90(3), pp. 257–258.

Tuft, S. J. and Matheson, M. (2000) 'In vitro antibiotic resistance in bacterial keratitis in London', *The British Journal of Ophthalmology*, 84(7), pp. 687–691.

Uchino, M. and Tsubota, K. (2010) 'Tear Film Overview', in Dartt, D. A., Besharse, J. C., and Dana, R. (eds) *Encyclopedia of the Eye*. USA: Elsevier, pp. 263–268.

Upadhyay, M. P., Srinivasan, J. P. and Whitcher, J. P. (2007) 'Microbial keratitis in the developing world: Does prevention work?', *International Ophthalmology Clinics*, 47(3), pp. 17–25.

Upadhyay, S. (2006) 'Temperature effect on raction rate', in Upadhyay, S. (ed.) *Chemical Kinetics and Reaction Dynamics*. New York: Springer, pp. 46–54.

Vaara, M. (2013) 'Novel derivatives of polymyxins', *Journal of Antimicrobial Chemotherapy*,

68(6), pp. 1213–1218.

Vasudevan, B., Simpson, T. L. and Sivak, J. G. (2008) 'Regional Variation in the Refractive-Index of the Bovine and Human Cornea', *Optometry and Vision Science*, 85(10), pp. 977–981.

Vazirani, J., Wurity, S. and Ali, M. H. (2015) 'Multidrug-resistant *Pseudomonas aeruginosa* keratitis: Risk factors, clinical characteristics, and outcomes', *Ophthalmology*, 122(10), pp. 2110–2114.

Vermeer, A. W. P. and Norde, W. (2000) 'The thermal stability of immunoglobulin : Unfolding and aggregation of a multi-domain protein', *Biophysical Journal*, 78(1), pp. 394–404.

Volkman, J. K. (2006) 'Lipid markers for marine organic matter', in Hutzinger, O. (ed.) *The Handbook of Environmental Chemistry*. Berlin: Springer-Verlag, pp. 27–70.

Wachem, P. B. Van, Hogt, A. H., Beugeling, T., Feijen, J., Bantjes, A., Detmers, J. P. and Aken, W. Van (1987) 'Adhesion of cultured human endothelial cells onto methacrylate polymers with varying surface wettability and charge', *Biomaterials*, 8(5), pp. 323–328.

Wang, J., Morton, M. J., Elliott, C. T., Karoonuthaisiri, N., Segatori, L. and Biswal, S. L. (2014) 'Rapid detection of pathogenic bacteria and screening of phage- derived peptides using microcantilevers', *Analytical Chemistry*, 86(3), pp. 1671–1678.

Wedge, C. I. and Rootman, D. S. (1992) 'Collagen shields: efficacy, safety and comfort in the treatment of human traumatic corneal abrasion and effect on vision in healthy eyes.', *Canadian Journal of Ophthalmology. Journal Canadien d'Ophtalmologie*, 27(6), pp. 295–298.

Wellings, D. A. and Gallagher, A. G. (2012) 'Three-dimensional scaffolds for tissue culture and regenerative medicine', *International Pharmaceutical Industry*, 4(2), pp. 44–46.

Whitcher, J. P., Srinivasan, M. and Upadhyay, M. P. (2001) 'Corneal blindness: a global perspective', *Bulletin of the World Health Organisation*, 79(3), pp. 214–221.

Whitcher, J. P., Srinivasan, M. and Upadhyay, M. P. (2002) 'Prevention of corneal ulceration in the developing world.', *International Ophthalmology Clinics*, 42(1), pp. 71–77.

Wiesner, J. and Vilcinskas, A. (2010) 'Antimicrobial peptides: The ancient arm of the human immune system', *Virulence*, 1(5), pp. 440–464.

Wilchek, M. and Miron, T. (1987) 'Limitations of N-hydroxysuccinimide esters in affinity chromatography and protein immobilization.', *Biochemistry*, 26(8), pp. 2155–2161.

Willcox, M. D. P. (2013) ‘Microbial adhesion to silicone hydrogel lenses : A review’, *Eye & contact lens*, 39(1), pp. 61–66.

Willcox, M. D. P., Harmis, N., Cowell, B. A., Williams, T. and Holden, B. A. (2001) ‘Bacterial interactions with contact lenses ; effects of lens material , lens wear and microbial physiology’, *Biomaterials*, 22(24), pp. 3235–3247.

Willcox, M. D. P., Hume, E. B. H., Aliwarga, Y., Kumar, N. and Cole, N. (2008) ‘A novel cationic-peptide coating for the prevention of microbial colonization on contact lenses’, *Journal of Applied Microbiology*, 105(6), pp. 1817–1825.

Williams, R. L. and Wong, D. (2009) ‘Ophthalmic Biomaterials’, in Narayan, R. (ed.) *Biomedical Materials*. Boston, MA, MA: Springer US, pp. 327–347.

Willoughby, C. E., Batterbury, M. and Kaye, S. B. (2002) ‘Collagen corneal shields’, *Survey of Ophthalmology*, 47(2), pp. 955–964.

Wilson, S. E. and Hong, J. W. (2000) ‘Bowman’s layer structure and function: critical or dispensable to corneal function? A hypothesis.’, *Cornea*, 19(4), pp. 417–420.

Winterton, L. C. and Su, K. C. (2005) ‘Hydrogel Contact Lens Application, Care and Evaluation’, in Bennett, E. S. and Weissman, B. A. (eds) *Clinical Contact Lens Practice*. 1st edn. Philadelphia, PA: Lippincott, Williams and Wilkins, pp. 355–379.

Wong, K. K. W., Wan, W. Y. and Kaye, S. B. (2002) ‘Blinking and operating: cognition versus vision’, *British Journal of Ophthalmology*, 86(4), p. 479.

Wong, R. L. M., Gangwani, R. A., Yu, L. W. H. and Lai, J. S. M. (2012) ‘New treatments for bacterial keratitis’, *Journal of Ophthalmology*, 2012(831502).

Wulff, G. (1995) ‘Molecular imprinting in cross-linked materials with the aid of molecular templates— a way towards artificial antibodies’, *Angewandte Chemie International Edition in English*, 34(17), pp. 1812–1832.

Xinming, L., Yingde, C., Lloyd, A. W., Mikhalovsky, S. V., Sandeman, S. R., Howel, C. A. and Liewen, L. (2008) ‘Polymeric hydrogels for novel contact lens-based ophthalmic drug delivery systems: A review’, *Contact Lens and Anterior Eye*, 31(2), pp. 57–64.

Yamanaka, K., Kito, N., Imokawa, Y., Maruyama, C., Utagawa, T. and Hamano, Y. (2010) ‘Mechanism of epsilon-poly-L-lysine production and accumulation revealed by identification and analysis of an epsilon-poly-L-lysine-degrading enzyme’, *Applied and Environmental Microbiology*, 76(17), pp. 5669–5675.

Ye, R., Xu, H. H., Wan, C., Peng, S., Wang, L., Xu, H. H., Aguilar, Z. P., Xiong, Y., Zeng, Z.

and Wei, H. (2013) ‘Antibacterial activity and mechanism of action of ε-poly-l-lysine’, *Biochemical and Biophysical Research Communications*, 439(1), pp. 148–153.

Yoltan, D. P. (2001) ‘Anti-infective drugs’, in Bartlett, J. D. and Jaanus, S. D. (eds) *Clinical Ocular Pharmacology*. 4th edn. Oxford: Butterworth-Heinmann, pp. 219–264.

Yoshida, T. (2010) ‘Biochemistry and enzymology of poly-epsilon-l-lysine degradation’, in Hamano, Y. (ed.) *Amino-Acid Homopolymers Occurring in Nature*. Berlin: Springer Berlin Heidelberg, pp. 45–59.

Yoshida, T. and Nagasawa, T. (2003) ‘epsilon-poly-L-lysine: Microbial production, biodegradation and application potential’, *Applied Microbiology and Biotechnology*, 62(1), pp. 21–26.

Yuan, X. and Wilhelmus, K. R. (2010) ‘Toll-like receptors involved in the pathogenesis of experimental *Candida albicans* keratitis.’, *Investigative Ophthalmology & Visual Science*, 51(4), pp. 2094–2100.

Zegans, M. E., Becker, H. I., Budzik, J. and O’Toole, G. (2002) ‘The role of bacterial biofilms in ocular infections.’, *DNA and Cell Biology*, 21(5–6), pp. 415–420.

Zegans, M. E., Shanks, R. M. Q. and O’Toole, G. a (2005) ‘Bacterial biofilms and ocular infections.’, *The Ocular Surface*, 3(2), pp. 73–80.

Zhang, X., Sun, X., Wang, Z., Zhang, Y. and Hou, W. (2017) ‘Keratitis-associated fungi form biofilms with reduced antifungal drug susceptibility’, *Investigative Ophthalmology & Visual Science*, 53(12), pp. 7774–7778.

Zhou, C., Li, P., Qi, X., Sharif, A. R. M., Poon, Y. F., Cao, Y., Chang, M. W., Leong, S. S. J. and Chan-Park, M. B. (2011) ‘A photopolymerized antimicrobial hydrogel coating derived from epsilon-poly-l-lysine’, *Biomaterials*, 32(11), pp. 2704–2712.

8. APPENDIX

8.1 Hydrogel Composition

An Excel spreadsheet used to work out the polymer composition of each of the hydrogel variants is described below (Figure 8.1). The spreadsheet was developed by Dean Simpkin and further optimised by Andrew Gallagher of SpheriTech Ltd.

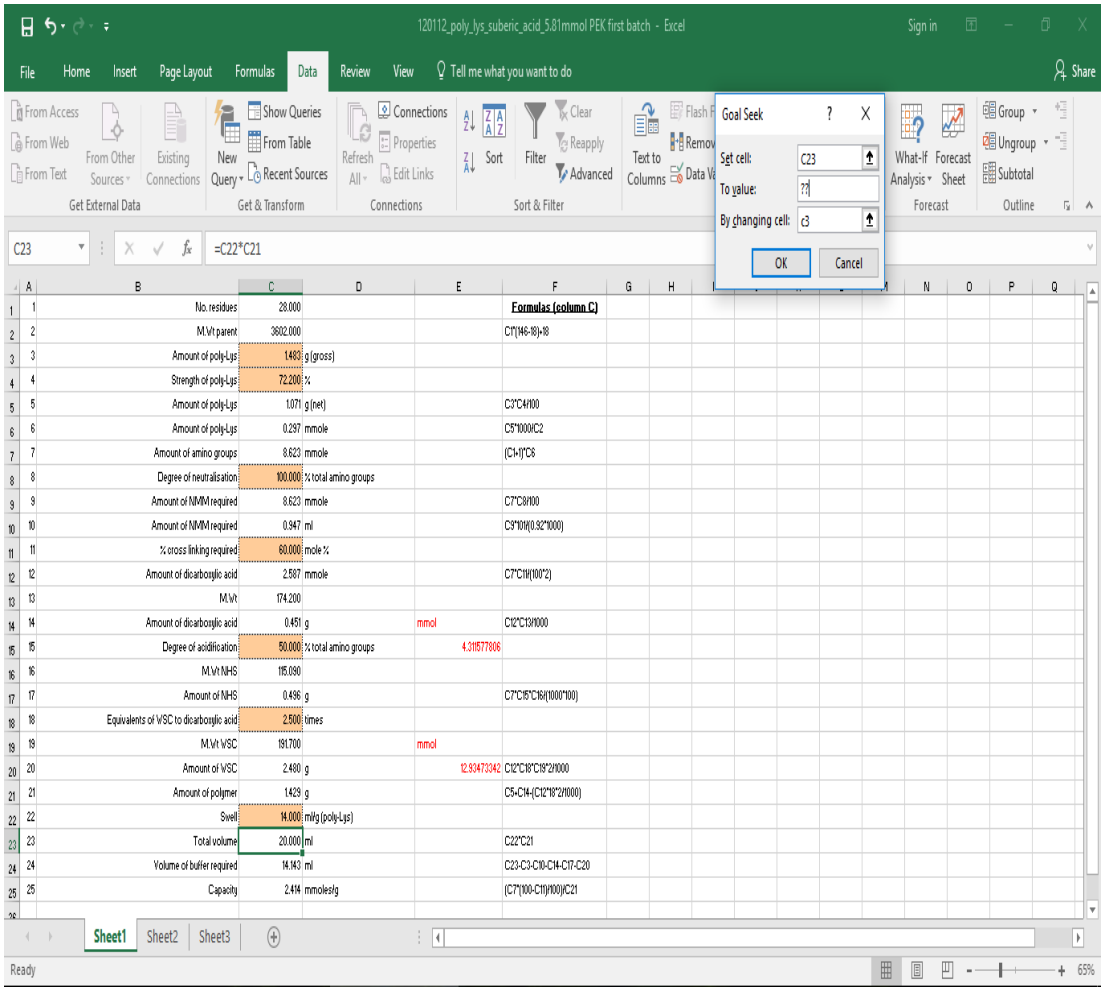

Figure 8.1: Excel spreadsheet for determining hydrogel composition.

The shaded boxes are parameters that can be changed and once they are filled in a goal seek analysis is run. The total volume of polymer solution required is inputted and cell C3 changed. This gives the polymer composition for the required final volume.

8.2 Activation Agent

Reagent	PεK / octanedioic acid hydrogels				
	(Su 60 14) NHS	(Su 60 14) HOBt	(Su 60 14) Oxyma	(Su 60 14) Oxyma B	(Su 60 14) 4-nitrophenol
PεK	1.48 g (8.62 mmol)	1.48 g (8.62 mmol)	1.48 g (8.62 mmol)	1.48 g (8.62 mmol)	1.48 g (8.62 mmol)
Octanedioic acid	0.45 g (2.59 mmol)	0.45 g (2.59 mmol)	0.45 g (2.59 mmol)	0.45 g (2.59 mmol)	0.45 g (2.59 mmol)
NMM	0.95 cm^3	0.95 cm^3	0.95 cm^3	0.95 cm^3	0.95 cm^3
EDCI	2.48 g (12.94 mmol)	2.48 g (12.94 mmol)	2.48 g (12.94 mmol)	2.48 g (12.94 mmol)	2.48 g (12.94 mmol)
Activation agent	0.50 g (4.34 mmol)	0.66 g (4.34 mmol)	0.62 g (4.34 mmol)	0.80 g (4.34 mmol)	0.60 g (4.34 mmol)

Table 8.1: Su 60 14 with various activation reagents.

8.3 Further Hydrogel Optimisation - Methods

Hydrogel reagents were supplied from the same sources as in section 2.1. The following raw materials were used in this part of the study; **hexadecanoic acid** B20322 and **trypsin** J60402 (Alfa Aesar, Haverhill, MA, USA), **oxyma** FE04090 (CMS Chemicals Ltd., Berkshire, England), **1,3-dimethylbarbituric acid** 8.42116.0100 (Merck Millipore Ltd., Watford, England), **sodium nitrite**, **hexanoic acid** 153745, **BSA** A7906 and **IgG** 18640 (Sigma-Aldrich, St Louis, MO, USA), **octanoic acid** O0027 (TCI Europe, Zwijndrecht, Belgium), **acetic acid** 20104.334, **NaOH** 28244.364, **toluene** 28675.465 and **MeOH** (VWR International Ltd., Lutterworth, England), **tridecanedioic acid** (Shanghai Worldyang Chemical Co., Ltd., Shanghai, China). All other equipment and reagents were supplied by SpheriTech Ltd. unless otherwise stated.

8.3.1 Optimisation of hydrogel washing protocol:

Reaction by-products such as the isourea and NHS as well as unreacted pεK and bis-carboxylic acid can remain associated with the hydrogel post-polymerisation. The pεK is also supplied as the hydrochloride salt and this can remain associated with the amine functional groups of the hydrogel post-polymerisation, potentially hindering biomolecule association. It is therefore vital that an optimal wash protocol is implemented post-polymerisation.

In the first instance a comparison was made between Su 60 15, Su 60 14, Su 60 13 and Su 65 15 either washed in 13 x H_2O (50 cm^3) or with a previously established washing system which consists of 1 x H_2O, 3 x NaOH (0.25 mol dm^{-3}), 3 x H_2O, 3 x HCl (0.25 mol dm^{-3}) and 3 x H_2O. Each wash protocol was followed up with another H_2O wash after 4 days. Samples of specified washes were monitored with a Cecil CE292 UV spectrophotometer (Cecil Instruments Ltd., Cambridge, England) at 230 nm to determine any leachables eluted from the hydrogels and compared to the initial wash.

A continuation of this study investigated the mechanical properties of Su 60 14 washed in three different ways. The wash system was either 10 x H_2O or

1 x H_2O, 2 x NaOH (0.25 mol dm^{-3}), 2 x H_2O, 2 x HCl (0.25 mol dm^{-3}) and 4 x H_2O or 5 x 10 v/v% aqueous NMM and 5 x H_2O. All washes were 50 cm^3 and the samples were again monitored with a Cecil CE292 UV spectrophotometer (Cecil Instruments Ltd., Cambridge, England) at 230 nm. The mechanical properties of the samples were monitored as in section 2.1.3 over a period of one month.

8.3.2 Activation agent:

The cross-linking activation agents were altered for hydrogel Su 60 14 by reducing their amounts or changing the compound completely. This was to try and minimise the effects of the CO_2 gas that forms during cross-linking and negate its effect on the hydrogel in closed vessels (i.e. contact lens moulds). The hydrogel was then renamed depending on the amount or activation compound used.

The hydrogel was polymerised following the protocol in section 2.1.2 with the following adjustments; the amount of NHS was reduced to 50, 25, 20, 15 and 12.5% of the original amount or NHS was replaced with either HOBt, oxyma, oxyma B or 4-nitrophenol (Table 8.1). The hydrogels (2 x 10 cm^3 aliquots) were poured separately into 10 cm^2 square Petri dishes (Thermo Scientific, Waltham, WA, USA). The remaining solution (30 cm^3) was left in the 50 cm^3 Falcon tube with the lid sealed and left to polymerise.

The shrinkage and colour of the polymer, gas formation and polymerisation time were all recorded.

8.3.2.1 Oxyma B synthesis:

The following protocol was adapted from the original protocol (Jad *et al.*, 2014). 1,3-dimethylbarbituric acid (2.5 mmol, 3.9 g) was dissolved in NaOH (2.5 M, 15 cm^3). MeOH (2.5 cm^3) was added to the transparent solution. Sodium nitrite (0.0275 mol, 1.9 g) was dissolved in water (7.5 cm^3) and added to the 1,3-dimethylbarbituric acid solution and stirred at 45 °C for 2 - 3 min to keep the solute in solution. The mixture was cooled to 10 °C to form a precipitate before adding acetic acid (7.5 mmol, 4.5 g) dropwise. The mixture

was kept at 25 °C for 1 h. The reaction was acidified with the addition of concentrated HCl (6.25 cm^3) followed by stirring for 10 min. The precipitate was filtered using a water vacuum and washed with 50 v/v% aqueous MeOH followed by a water wash. The product was recrystallised from aqueous MeOH (2:1) to obtain white crystals of oxyma B.

8.3.3 Additional molecules – bis-carboxylic acids:

The composition of hydrogel Su 60 14 was altered with the addition of differing ratios of decanedioic and tridecanedioic bis-carboxylic acids to change the mechanical properties without changing the cross-linking and the density of the polymer. The hydrogel was then renamed depending bis-carboxylic acids used.

PεK (3.71 g) was added to a 50 cm^3 Falcon tube with water (15 cm^3) and placed on a roller to dissolve. Filtered 5 v/v% aqueous Tween 80 (250 mm^3) was added. The bis-carboxylic acids supplied as solids were dissolved in water (5 cm^3) with NMM (2.37 cm^3) and sonicated until dissolved. The remaining bis-carboxylic acids supplied as liquids were mixed with the other bis-carboxylic acid solution as soon as a clear solution was obtained. The bis-carboxylic acid solution was added to the pεK solution and made up to 25 cm^3 with water. NHS (1.24 g) and EDCI (6.2 g) were measured into a 50 cm^3 Falcon tube and dissolved in water (15 cm^3) before making up to 25 cm^3. All solutions were filtered to 0.45 µm using a syringe filter. EDCI and NHS were mixed and immediately added to the pεK/octanedioic acid solution. This was inverted five times. An aliquot of the polymer solution (10 cm^3) was poured into each 10 cm^2 square Petri dish (Thermo Scientific, Waltham, WA, USA). These were incubated for at least 5 h at room temperature until the hydrogel had polymerised. The hydrogel was then covered with water to prevent dehydration. The hydrogels were washed 5 x H_2O before the resulting analysis.

Mechanical properties (section 2.1.3), refractive index (section 2.1.5), gravimetric water content (section 2.1.7) and contact angle (section 2.1.9) were all measured as in the relevant previous sections.

8.3.4 Protein sorption study:

An investigation of biofouling was undertaken to determine the rate at which different proteins become absorbed onto the hydrogel variants. Hydrogels Su 60 15, Su 60 14, Su 60 13 and Su 65 15 were polymerised as already described in section 2.1.2.

A 1 mg cm^{-3} aqueous solution (10 cm^3) of each protein (trypsin, BSA and IgG) was prepared. Hydrogel discs were cut (0.785 cm^2) and incubated at 5 discs in a 7 cm^3 vial with each protein solution (5 cm^3) at 37 °C for set time-points over 18 h. At each time-point supernatant was removed (3 cm^3) and the absorbance read at 280 nm with a Cecil CE292 UV spectrophotometer (Cecil Instruments Ltd., Cambridge, England) against the starting concentration of the corresponding protein solution. A standard curve of each protein concentration against absorbance was composed using 1, 0.5, 0.25, 0.125 and 0.0625 mg cm^{-3} protein solutions against a water blank at 280 nm.

8.4 Further Hydrogel Optimisation - Results

8.4.1 Hydrogel wash optimisation:

An investigation of the hydrogel wash procedure post-polymerisation was undertaken to determine the most efficient method.

Wash protocol	Su 60 15	Su 60 14	Su 60 13	Su 65 15	Wash protocol	Su 60 15	Su 60 14	Su 60 13	Su 65 15
	Mean % of first wash					Mean % of first wash			
H_2O	100.0	100.0	100.0	100.0	H_2O	100.0	100.0	100.0	100.0
H_2O	13.0 +/- 1.3	69.2 +/- 1.6	17.6 +/- 0.4	15.2 +/- 3.0	NaOH	118.4 +/- 6.4	120.9 +/- 2.8	120.5 +/- 5.9	177.7 +/- 23.8
H_2O					NaOH				
H_2O	25.9 +/- 0.9	5.4 +/- 0.6	29.7 +/- 0.7	0.9 +/- 0.3	NaOH	23.0 +/- 3.1	25.1 +/- 0.7	35.0 +/- 2.1	49.6 +/- 5.4
H_2O					H_2O				
H_2O	4.6 +/- 0.3	5.5 +/- 0.2	4.0 +/- 0.3	0.5 +/- 0.3	H_2O	0.1 +/- 0.1	0.0 +/- 0.1	0.3 +/- 0.2	0.5 +/- 0.3
H_2O					H_2O				
H_2O	2.8 +/- 0.3	6.0 +/- 0.8	2.3 +/- 1.3	0.5 +/- 0.4	HCl	-0.6 +/- 0.2	-0.6 +/- 0.2	-0.7 +/- 0.3	-1.0 +/- 0.2
H_2O					HCl				
H_2O	0.9 +/- 0.2	4.2 +/- 0.3	3.7 +/- 0.4	1.5 +/- 0.1	HCl	-0.3 +/- 0.1	-0.2 +/- 0.2	-0.3 +/- 0.2	-0.7 +/- 0.0
H_2O					H_2O				
H_2O					H_2O				
H_2O	0.5 +/- 0.2	1.7 +/- 0.2	1.5 +/- 0.1	0.3 +/- 0.2	H_2O	0.4 +/- 0.3	15.9 +/- 12.7	-0.4 +/- 0.1	-0.8 +/- 0.2
4d H_2O	76.2 +/- 1.8	80.1 +/- 3.0	82.0 +/- 5.0	113.6 +/- 3.4	4d H_2O	-0.1 +/- 0.1	-0.1 +/- 0.1	0.0 +/- 0.0	-0.2 +/- 0.1

Table 8.2: Absorbance of wash components against original wash.

Figure 8.2: Freeze dried hydrogel after water washes (left) or NMM washes (right).

The wash supernatant from four hydrogel variants (Su 60 15, Su 60 14, Su 60 13 and Su 65 15) was monitored via a spectrophotometer and the absorbance obtained was converted to a percentage of the absorbance from the first wash (Table 8.2). At the end of each wash procedure < 2% of leachables were still present for most the hydrogels except for Su 60 14 after the HCl/NaOH wash (15.9% ± 12.7%). However, there was a large margin of error associated with this value.

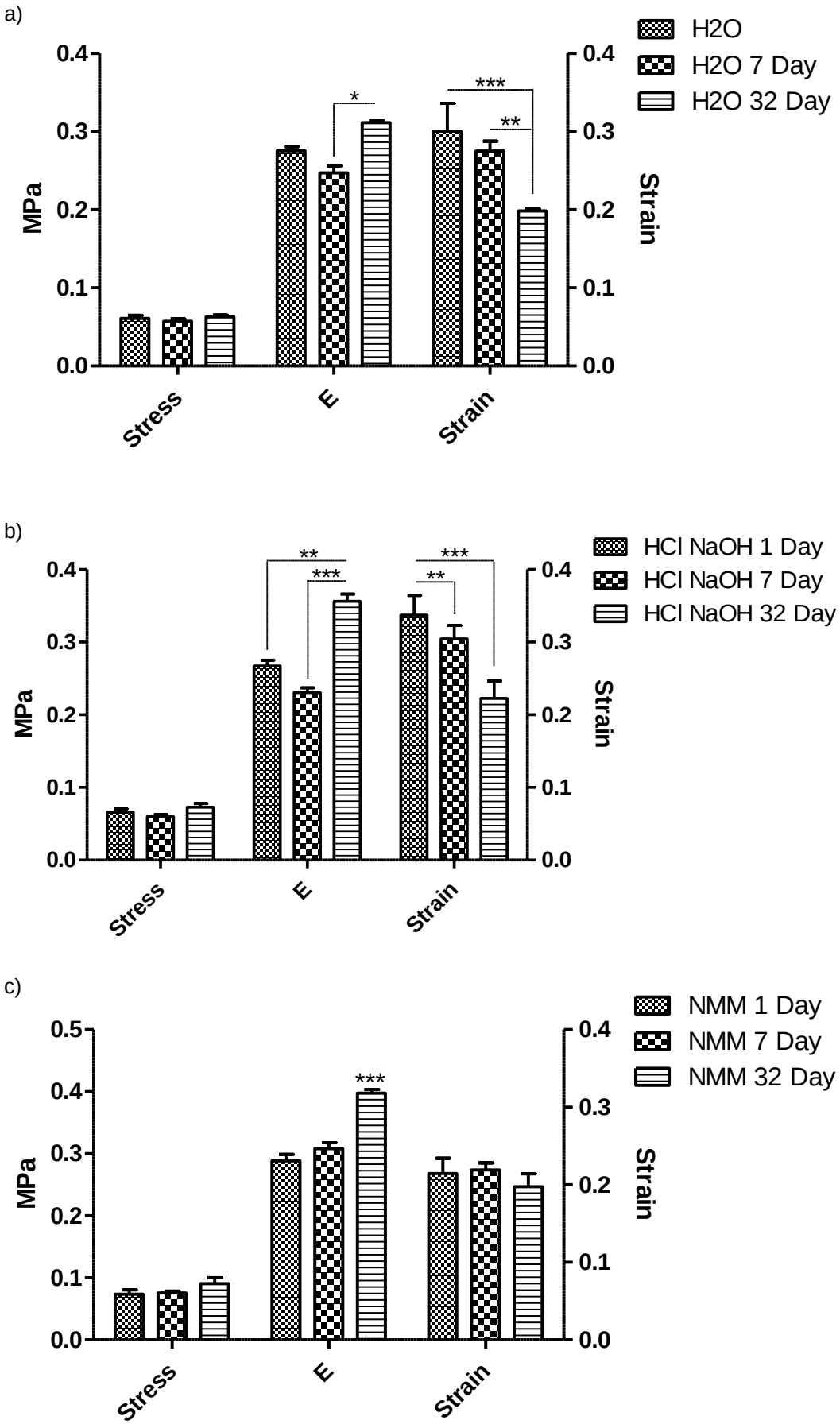

Figure 8.3: Mechanical properties of Su 60 14 after a) H_2O washes, b) acid/base washes and c) NMM washes. Error bars ±SD, * $p < 0.05$ ** $p < 0.01$ *** $p < 0.005$ $N = 4$.

The NMM wash was more efficient at removing the hydrochloride salt associated with the hydrogel than the H_2O wash (Figure 8.2). Mechanical property analysis over 32 days showed a statistically significant ($p < 0.005$) decrease in strain and increase in elastic modulus was obtained when hydrogel Su 60 14 was washed in H_2O or HCl/NaOH (Figure 8.3). In contrast, there was no significant change in strain when the hydrogel was washed in NMM.

8.4.2 Activation agent:

An investigation of different activation agents with view to replacing NHS was undertaken. This was to potentially reduce gas formation during polymerisation. Four out of five of the hydrogels polymerised, with nitrophenol excluded as a potential activation agent due to the lack of hydrogel formation (Figure 8.4). Of the remaining hydrogels, NHS resulted in the fastest polymerisation time (7 min) and a clear polymer, however, gas was formed (Table 8.3). The addition of HOBt resulted in a clear hydrogel with no gas formation. The hydrogel also swelled upon washing and had a relatively long polymerisation time (29 min). Oxyma and oxyma B resulted in coloured hydrogels and gas was formed with oxyma B.

Su 60 14	Polymerised Size (cm^2)	Washed Size (cm^2)	Polymerisation Time (min)	Colour	Gas
NHS	7.37 +/- 0.1	7.17 +/- 0.1	7.00 +/- 0.0	Clear	Y
HOBt	8.83 +/- 0.2	9.97 +/- 0.1	29 +/- 1.0	Clear	N
Oxyma B	8.23 +/- 0.1	8.2 +/- 0.0	10 +/- 0.0	Light Orange	Y
Oxyma	7.7 +/- 0.1	8.1 +/- 0.1	21 +/- 1.0	Orange	N
Nitrophenol	–	–	–	–	–

Table 8.3: Characteristics of hydrogel Su 60 14 when polymerised using different activation agents. *N* = 3.

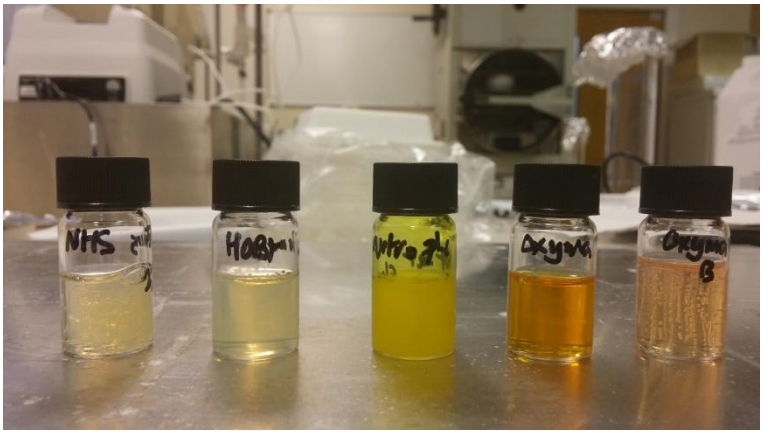

Figure 8.4: Hydrogel Su 60 14 with different activation agents.

8.4.2.1 Oxyma B synthesis:

A white crystalline solid was obtained (3.5 g) with a yield of 76%. Once dissolved the solid turns to a purple/red colour.

As 0.025 mol of 1,3-dimethylbarbituric acid was used and an equivalent of oxyma B can be expected as the end-product if a 100% yield is achieved. Therefore, an equivalent (0.025 mol) of oxyma B (MW: 185 g mol^{-1}) is 4.625 g.

3.5 / 4.625 x 100 = 76%

8.4.3 Additional molecules:

The physical and mechanical properties of the hydrogel were monitored with the addition of decanedioic and tridecanedioic as a combination of bis-carboxylic acid cross-linker with octanedioic acid. The same properties were monitored with varying levels of NHS added as the activating agent.

8.4.3.1 Mechanical properties:

The mechanical properties were measured as in section 2.1.3 and used to compare the effect of different levels of octanedioic/decanedioic acid, octanedioic/tridecanedioic acid and NHS have on the polymerised hydrogel.

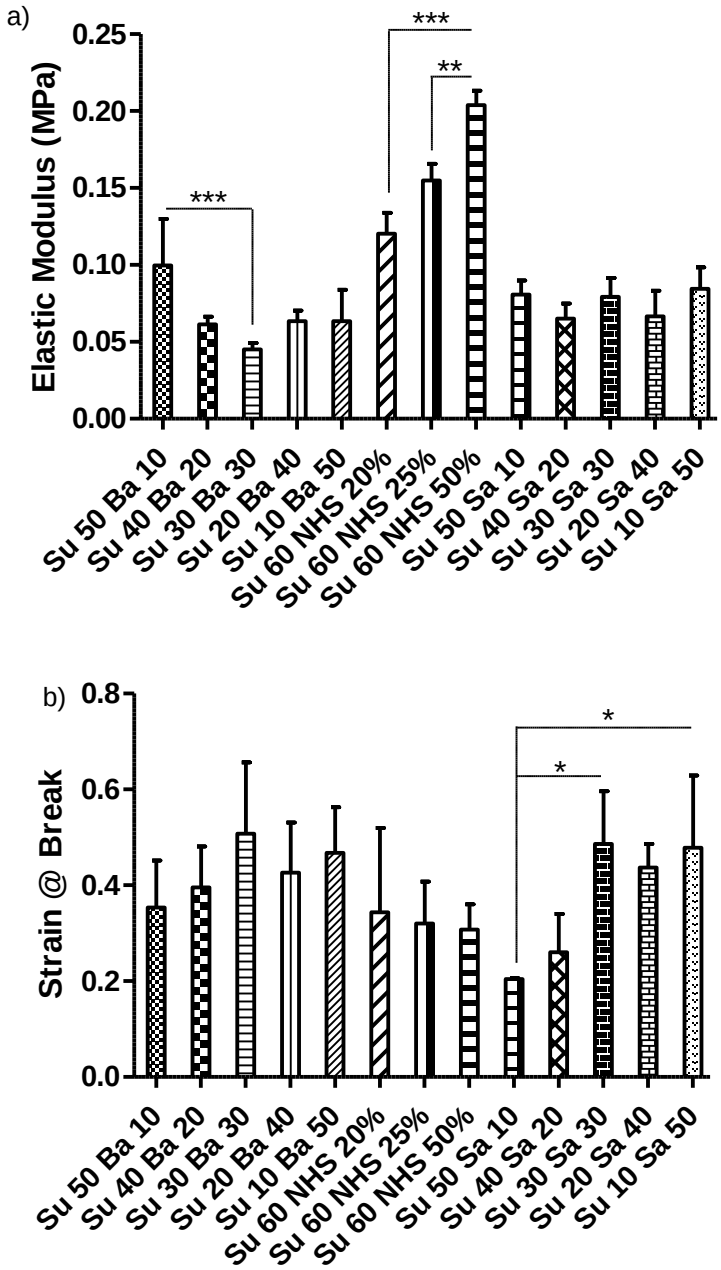

Figure 8.5: Elastic modulus (a) and strain (b) of hydrogel variants with altered bis-carboxylic acid and NHS compositions. Error bars ±SD, * $p < 0.05$ ** $p < 0.01$ *** $p < 0.005$ $N = 4$.

8.4.3.2 Water content:

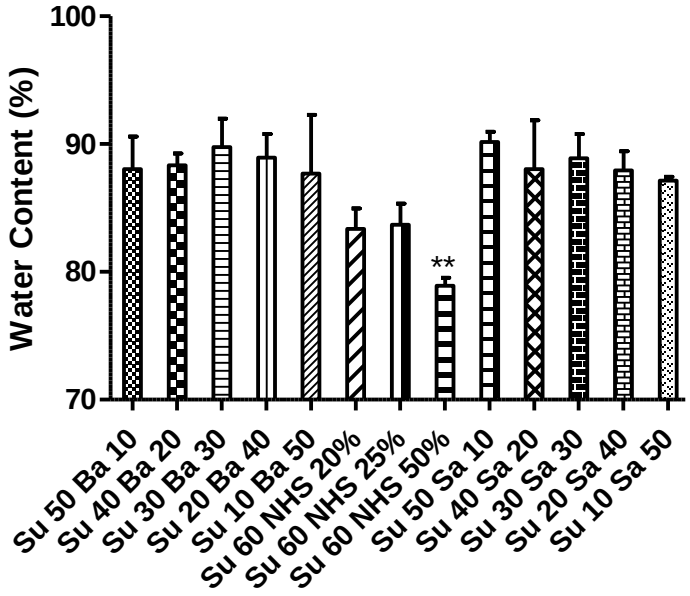

Figure 8.6: Water content of hydrogel variants with altered bis-carboxylic acid and NHS compositions. Error bars ±SD, ** p < 0.01 *N* = 4.

8.4.3.3 Contact angle:

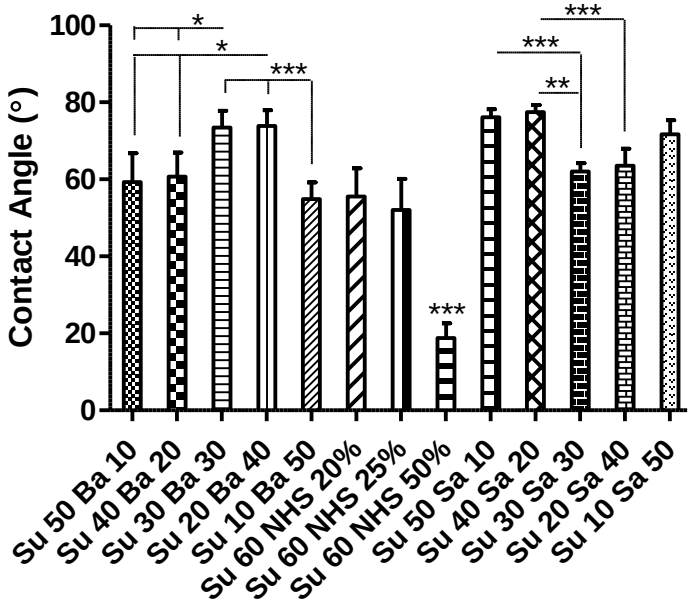

Figure 8.7: Contact angle of hydrogel variants with altered bis-carboxylic acid and NHS compositions. Error bars ±SD, * p < 0.05 ** p < 0.01 *** *p* < 0.005 *N* = 4.

8.4.3.4 Light transmittance:

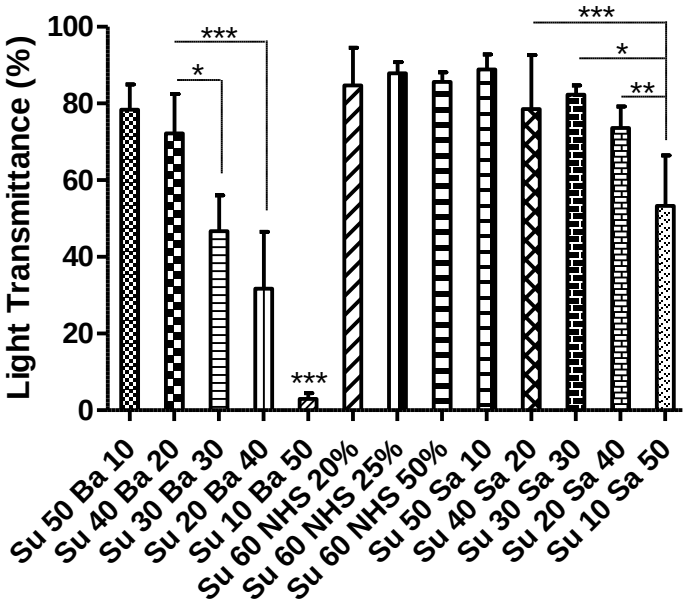

Figure 8.8: Light transmittance of hydrogel variants with altered bis-carboxylic acid and NHS compositions. Error bars ±SD, * $p < 0.05$ ** $p < 0.01$ *** $p < 0.005$ $N = 4$.

8.4.4 Protein sorption:

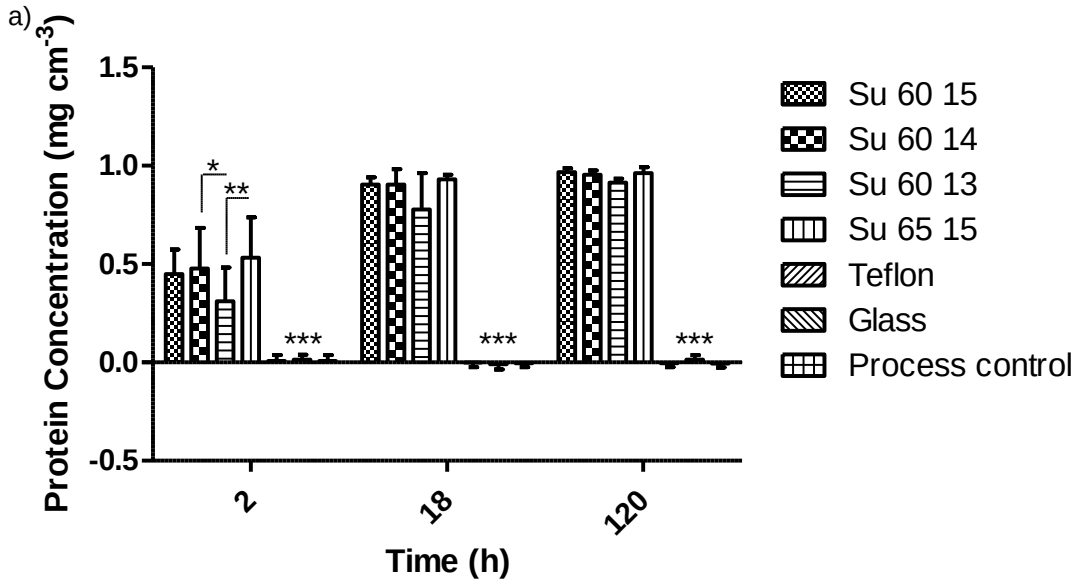

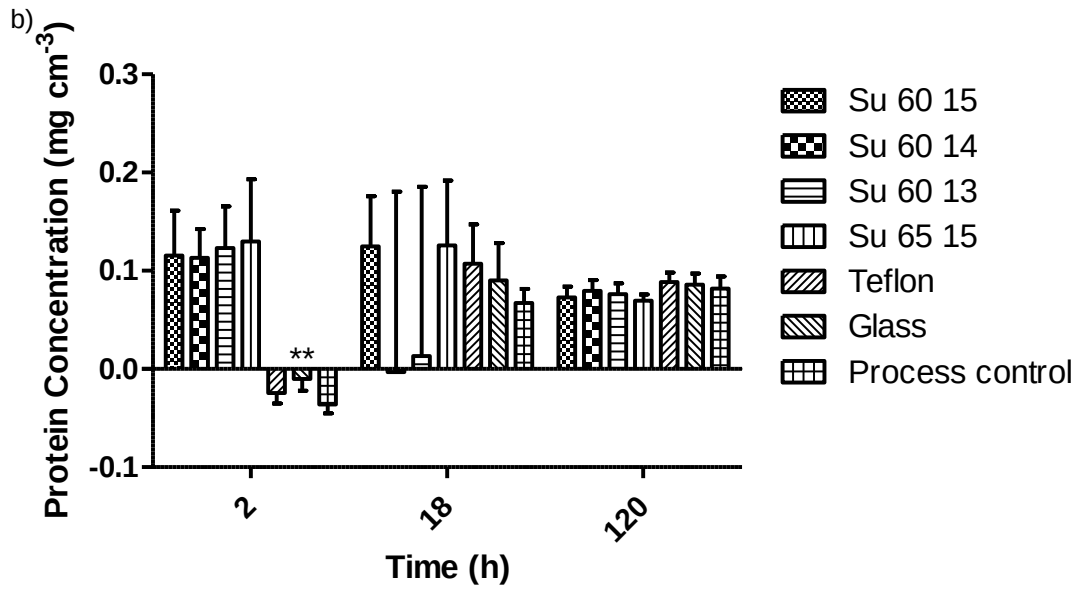

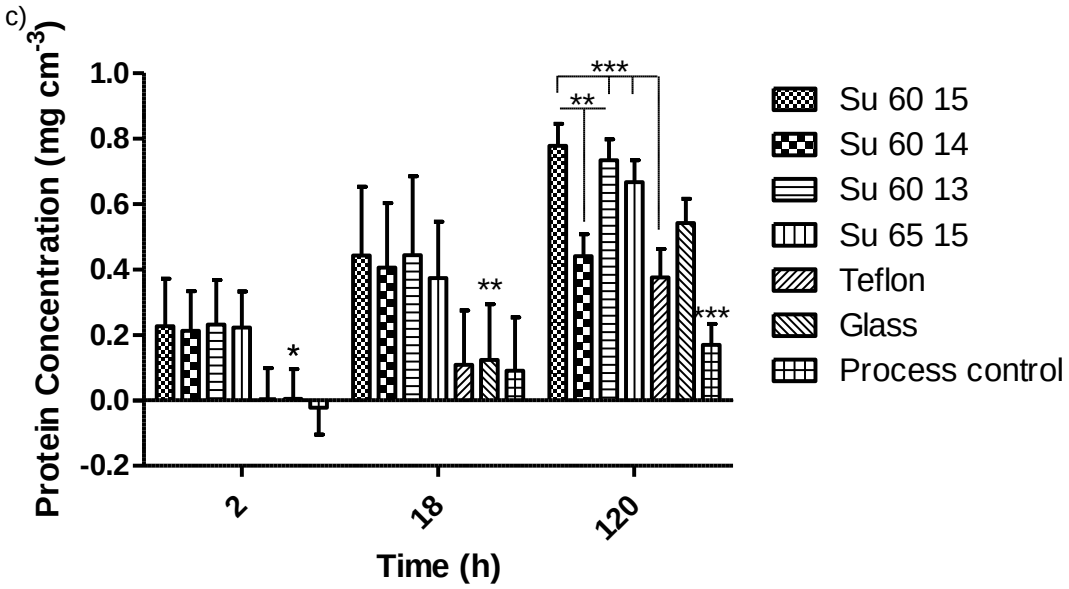

Figure 8.9: Sorption of BSA (a), IgG (b) and trypsin (c) onto the hydrogel variants. Error bars ±SD, * p < 0.05 ** p < 0.01 *** *p* < 0.005 *N* = 4.

SUPPORTING PAPERS